# SANDIA REPORT

SAND2016-0231
Unlimited Release
January 2016

Supplements SAND2004-0730
dated February 2006

# DRSPALL: Impact of the Modification of the Numerical Spallings Model on Waste Isolation Pilot Plant Performance Assessment

Dwayne C. Kicker, Courtney G. Herrick, Todd R. Zeitler, Bwalya Malama,
David K. Rudeen, and Amy P. Gilkey

Prepared by
Sandia National Laboratories
Albuquerque, New Mexico 87185 and Livermore, California 94550

Sandia National Laboratories is a multi-program laboratory managed and operated by Sandia Corporation, a wholly owned subsidiary of Lockheed Martin Corporation, for the U.S. Department of Energy's National Nuclear Security Administration under contract DE-AC04-94AL85000. This research is funded by WIPP programs administered by the Office of Environmental Management (EM) of the U.S Department of Energy.



Issued by Sandia National Laboratories, operated for the United States Department of Energy by Sandia Corporation.



Available to DOE and DOE contractors from
U.S. Department of Energy
Office of Scientific and Technical Information
P.O. Box 62
Oak Ridge, TN 37831

Telephone: (865) 576-8401
Facsimile: (865) 576-5728
E-Mail: reports@osti.gov
Online ordering: http://www.osti.gov/scitech

Available to the public from
U.S. Department of Commerce
National Technical Information Service
5301 Shawnee Rd
Alexandria, VA 22312

Telephone: (800) 553-6847
Facsimile: (703) 605-6900
E-Mail: orders@ntis.gov
Online order: http://www.ntis.gov/search

SAND2016-0231
Unlimited Release
January 2016

Supplements SAND2004-0730
dated February 2006

# DRSPALL: Impact of the Modification of the Numerical Spallings Model on Waste Isolation Pilot Plant Performance Assessment

Dwayne C. Kicker[1], Courtney G. Herrick[2], Todd R. Zeitler[2], Bwalya Malama[3], David K. Rudeen[4], and Amy P. Gilkey[4]

Defense Waste Management Programs
Sandia National Laboratories
4100 National Parks Highway, Building A
Carlsbad, New Mexico 88220

**Abstract**

The numerical code DRSPALL (from ***d***irect ***r***elease ***spall***ings) is written to calculate the volume of Waste Isolation Pilot Plant (WIPP) solid waste subject to material failure and transport to the surface as a result of a hypothetical future inadvertent drilling intrusion. An error in the implementation of the DRSPALL finite difference equations was discovered as documented in Software Problem Report (SPR) 13-001. The modifications to DRSPALL to correct the finite difference equations are detailed, and verification and validation testing has been completed for the modified DRSPALL code. The complementary cumulative distribution function (CCDF) of spallings releases obtained using the modified DRSPALL is higher compared to that found in previous WIPP performance assessment (PA) calculations. Compared to previous PAs, there was an increase in the number of vectors that result in a nonzero spallings volume, which generally translates to an increase in spallings releases. The overall mean CCDFs for total releases using the modified DRSPALL are virtually unchanged, thus the modification to DRSPALL did not impact WIPP PA calculation results.

[1] Stoller Newport News Nuclear, Inc. (SN3), a wholly owned subsidiary of Huntington Ingalls Industries, Inc., Carlsbad, New Mexico 88220, Sandia Contract No. 1018118.
[2] Sandia National Laboratories, Carlsbad, New Mexico 88220.
[3] Presently with Natural Resources Management & Environmental Sciences Department, California Polytechnic State University, San Luis Obispo, California 93407. The work described in this report was performed while employed by Sandia National Laboratories.
[4] GRAM, Inc., Albuquerque, New Mexico 87112, Sandia Contract No. 1557789.

*This page is intentionally left blank.*

# CONTENTS

# CONTENTS (Continued)

## CONTENTS (Continued)

# FIGURES

## FIGURES (Continued)

## FIGURES (Continued)

## TABLES

## TABLES (Continued)

## TABLES (Continued)



## NOMENCLATURE

| | |
|---|---|
| CCDF | complementary cumulative distribution function |
| CRA-2004 | 2004 Compliance Recertification Application |
| CRA-2004 PABC | 2004 Compliance Recertification Application Performance Assessment Baseline Calculation |
| CRA-2014 | 2014 Compliance Recertification Application |
| CVS | Code Versions System |
| DBR | direct brine release |
| DDZ | drilling damaged zone |

## NOMENCLATURE (Continued)

| | |
|---|---|
| DPS | DRSPALL pressure scenario |
| DRZ | disturbed rock zone |
| EPA | U.S. Environmental Protection Agency |
| LHS | Latin hypercube sampling |
| PA | performance assessment |
| PABC-2009 | 2009 Compliance Recertification Application Performance Assessment Baseline Calculation |
| SCMS | Software Configuration Management System |
| SPR | software problem report |
| WIPP | Waste Isolation Pilot Plant |

# 1. INTRODUCTION

Software Problem Report (SPR) 13-001 (WIPP PA 2013a) identifies an error in the implementation of the finite difference equations contained in DRSPALL source code file *wasteflowcalc.f90*[1]. This report describes the modifications to DRSPALL implemented in Version 1.22 to correct the finite difference equations and determines the impact of these modifications on Waste Isolation Pilot Plant (WIPP) performance assessment (PA) calculations. This report supplements SAND2004-0730, *DRSPALL: Spallings Model for the Waste Isolation Pilot Plant 2004 Recertification* (Lord et at. 2006).

A range of spallings volumes initially calculated using DRSPALL Version 1.10 (Vugrin 2005, Appendix D) has been used in PA calculations beginning with the 2004 Compliance Recertification Application Performance Assessment Baseline Calculation (CRA-2004 PABC) and continuing through the 2014 Compliance Recertification Application (CRA-2014). An impact assessment (Kicker, Herrick, and Zeitler 2015) establishes a new range of spallings volumes (Appendix C) that will be used in future WIPP PA calculations and documents the impact of applying the new spallings volumes (developed using DRSPALL Version 1.22) to previous WIPP PA calculations.

The conceptual model for spallings as documented by Lord et al. (2006, Section 3) has not changed. This conceptual model is implemented in the numerical Fortran code DRSPALL (from ***d***irect ***r***elease ***spall***ings). DRSPALL is written to calculate the volume of WIPP spallings, which are defined as solid waste material subject to tensile stresses leading to mechanical failure and transport to the surface as a result of a hypothetical future inadvertent drilling intrusion. The code calculates coupled repository and wellbore transient mixed-phase compressible fluid flow before, during, and after the drilling intrusion process. Mathematical models are included of bit penetration, mixed-phase (mud, salt, waste, and gas) fluid flow in the well, fluid expulsion at the surface, coupling of the well and the drilled repository, repository spalling (tensile) failure, fluidized bed transport of failed waste, and repository internal gas flow. The wellbore model is one-dimensional with linear flow, while the repository model is one-dimensional with either spherical or cylindrical radial flow (see Section 4.2).

A description of the PA process, including the recent migration of PA codes to a new operating platform, is provided in Section 2. The modifications to the DRSPALL code are described in Section 3. In response to the modifications, a zone size sensitivity study was conducted to determine the optimal zone size to implement the finite different equations (Section 4). The verification and validation testing of the modified DRSPALL code is documented in Section 5. The impact to WIPP PA calculations as a result of the DRSPALL modifications is provided in Section 6.

[1] Prior to Version 1.21, the DRSPALL source code file names contained the prefix "DRS_". This prefix was removed from all source code file names in Version 1.21 and is not used in this document.

*This page is intentionally left blank.*

# 2. THE PERFORMANCE ASSESSMENT PROCESS

WIPP PA calculations estimate the probability and consequence of potential radionuclide releases from the repository to the accessible environment for a regulatory period of 10,000 years after facility closure. The PA models are updated with new information as part of a recertification process that occurs at five-year intervals following the receipt of the first waste shipment at the site in 1999. A new PA baseline was established by the 2009 Performance Assessment Baseline Calculation (PABC-2009) with recertification of the WIPP by the U.S. Environmental Protection Agency (EPA) in November 2010. The 2014 Compliance Recertification Application (CRA-2014) PA has been submitted to the EPA and is currently under review.

## 2.1. Treatment of Uncertainty

A significant amount of uncertainty is associated with characterizing the physical properties of geologic materials that influence potential releases. The WIPP PA methodology accommodates both aleatory (i.e., stochastic) and epistemic (i.e., subjective) uncertainty in its constituent models. Aleatory uncertainty pertains to unknowable future events such as intrusion times and locations that may affect repository performance. It is accounted for by the generation of random sequences of future events. Epistemic uncertainty concerns parameter values that are assumed to be constants, but the exact parameter values are uncertain due to a lack of knowledge about the system. An example of a parameter with epistemic uncertainty is the permeability of a material. Epistemic uncertainty is accounted for by sampling parameter values from assigned distributions. One set of sampled values required to run a WIPP PA calculation is termed a vector. In a performance assessment, models are executed for three replicates of 100 vectors, each vector providing model realizations resulting from a particular set of parameter values. Parameter values sampled in each PA were also used in the corresponding DRSPALL impact assessment (Section 4), and are documented by Kirchner (2010 and 2013). A sample size of 10,000 possible sequences of future events is used in PA calculations to address aleatory uncertainty. The releases for each of 10,000 possible sequences of future events are tabulated for each of the 300 vectors, totaling 3,000,000 possible futures.

For a random variable, the complementary cumulative distribution function (CCDF) provides the probability of the variable being greater than a particular value. By regulation, PA results are presented as a distribution of CCDFs of releases (EPA 1996). Each individual CCDF summarizes the likelihood of releases across all futures for one vector of parameter values. The uncertainty in parameter values results in a distribution of CCDFs.

## 2.2. Determination of Radionuclide Releases

Releases are quantified in terms of "EPA units". Each radionuclide has a release limit prescribed to it. This limit is defined as the maximum allowable release (in curies) of that radionuclide per a waste amount containing $1\times10^6$ curies of alpha-emitting transuranic radionuclides with half-lives greater than 20 years. Releases in EPA units result from a normalization by radionuclide and the total inventory. For each radionuclide, the ratio of its 10,000 year cumulative release (in curies) to its release limit is calculated. The sum of these ratios is calculated across the set of radionuclides and normalized by the transuranic inventory (in curies) of α-emitters with half-

lives greater than 20 years, as specified by regulation. Mathematically, the formula used to calculate releases in terms of EPA units is

$$R = \frac{1 \times 10^6 \, curies}{C} \sum_i \frac{Q_i}{L_i} \tag{2-1}$$

where $R$ is the normalized release in EPA units. Quantity $Q_i$ is the 10,000 year cumulative release (in curies) of radionuclide $i$. Quantity $L_i$ is the release limit for radionuclide $i$, and $C$ is the total transuranic inventory (in curies) of α-emitters with half-lives greater than 20 years. Note that the definition of the release limit $L_i$ results in a constant value of $1 \times 10^6$ curies being factored out of the summation.

## 2.3. Migration of the WIPP Performance Assessment Codes

The original DRSPALL results were developed for the CRA-2004 PABC on an Alpha OpenVMS platform using DRSPALL Version 1.10. These results were used for all subsequent PAs continuing through the CRA-2014. These are referred to as "VMS" results (Figure 2-1).

After submittal of the CRA-2014, PA codes have been migrated to a Sun Solaris Blade Server using a UNIX operating system as part of a planned update to an aging operating system. The migration process includes qualifying PA codes on the new platform. The version of DRSPALL that was implemented and qualified on the Solaris platform is Version 1.21. It is referred to as the "migrated" version (Figure 2-1).

As part of the migration, both the PABC-2009 calculations (Clayton et al. 2010) and the CRA-2014 calculations (Camphouse et al. 2013), which were originally run on the VMS platform, were rerun on the Solaris platform and the releases projected from analyses on the two platforms were compared (Kirchner, Gilkey, and Long 2013). While slight differences in spallings volumes exist between the VMS DRSPALL (Version 1.10) and the migrated DRSPALL (Version 1.21), the cumulative distributions are essentially indistinguishable as presented in Section 4 (see Sections 4.1.2.2, 4.1.2.3, and 4.1.2.4). The PA calculations performed on the Solaris platform using DRSPALL Version 1.21 are referred to as migrated PABC-2009 (Revision 0) and migrated CRA-2014 (Revision 0).

The modifications to DRSPALL described in this document were applied to the migrated DRSPALL Version 1.21 to create DRSPALL Version 1.22, which is subsequently referred to as the "modified" version (Figure 2-1). The modified DRSPALL Version 1.22 was run solely on the Solaris platform. The impact assessment presented in Section 4 uses a new set of spallings results using DRSPALL Version 1.22 that have been applied to both the PABC-2009 and CRA-2014 PAs to produce the updated PABC-2009 (Revision 1) and the updated CRA-2014 (Revision 1) PA results (Kirchner, Gilkey, and Long 2015). The updated PAs (Revisions 1) are compared to the current baseline (i.e., the VMS PABC-2009), the migrated PABC-2009 (Revision 0), the VMS CRA-2014, and the migrated CRA-2014 (Revision 0) to assess the impact of modified spallings data on PA results.

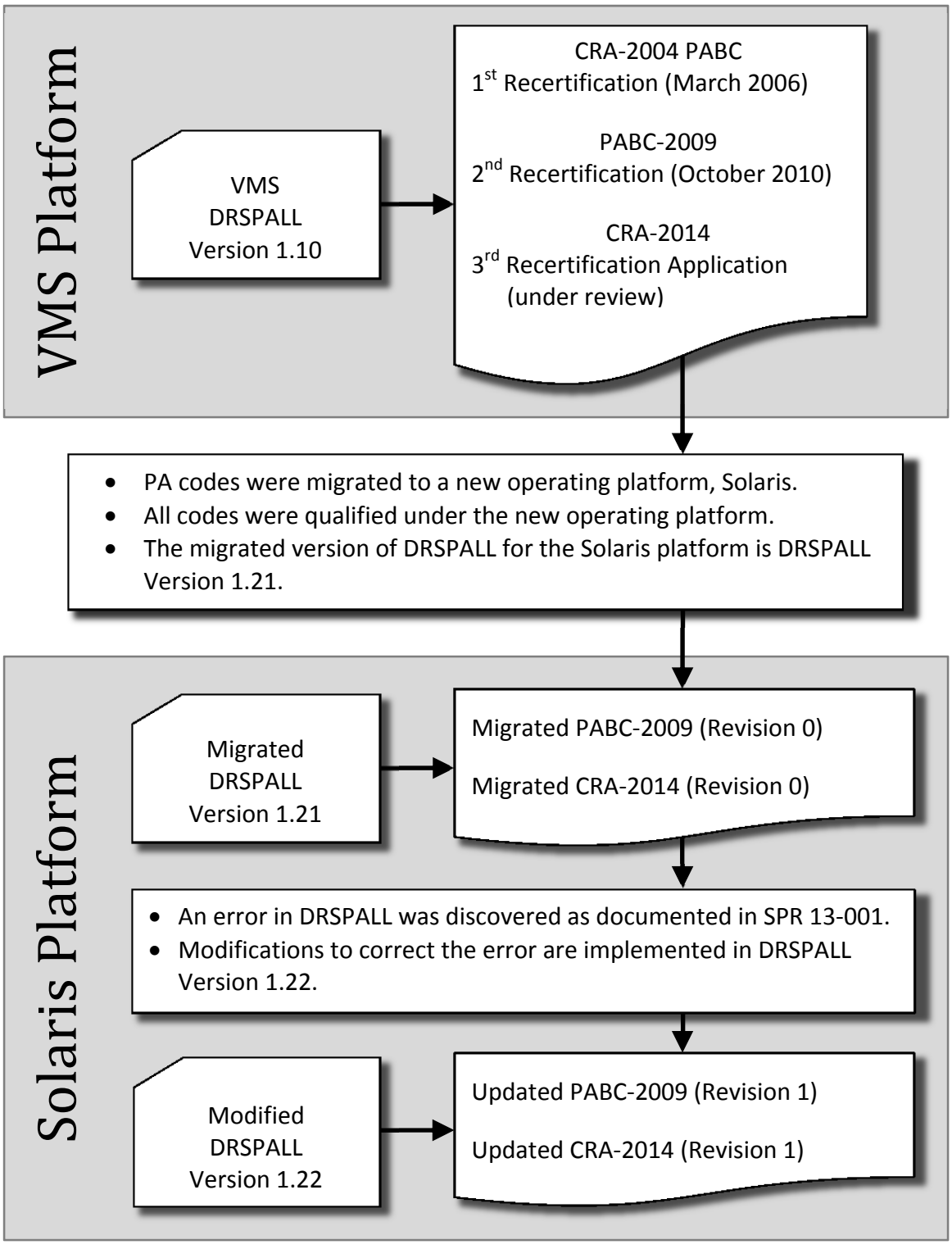


**Figure 2-1. Flowchart of the Migration of WIPP PA Codes and DRSPALL Modifications.**

*This page is intentionally left blank.*

# 3. MODIFICATIONS TO THE DRSPALL CODE

SPR 13-001 (WIPP PA 2013a) states that the DRSPALL source code file *wasteflowcalc.f90* contains an error in the implementation of the finite difference equations. DRSPALL uses the Darcy flow equation with a Forchheimer correction to account for high gas flow rates (WIPP PA 2015a, Section 4.3.1), which is defined using the variable 'Forchterm'. The *wasteflowcalc.f90* source code file contains three 'Forchterm' equations (for the first cell, the interior cells, and the last cell), with each equation as follows:

$$Forchterm = \frac{k'(i+1) - k'(i)}{4k'(i)\Delta r(i)} \tag{3-1}$$

where $k'$ = velocity-dependent permeability ($m^2$), and
$\Delta r$ = repository zone size (m).

However, in accordance with the previous version of the DRSPALL design document (WIPP PA 2004a; WIPP PA 2013b), which is based on a centered-difference discretization, the correct equation should be:

$$Forchterm = \frac{k'(i+1) - k'(i-1)}{4k'(i)\Delta r(i)}. \tag{3-2}$$

In response to SPR 13-001, the finite difference solution to the DRSPALL waste flow equation was evaluated (Appendix A). In addition to the error identified in SPR 13-001, it was found that the derivation of the constant zone size equations was also incorrect. The derivation of Equation 4.6.2 in the previous design document (WIPP PA 2004a) was incorrect because $k'$ was treated as a constant in the denominator, despite it being a variable in the numerator. The approach for modifying the DRSPALL code was to start from design document Equation 4.3.10 (WIPP PA 2015a, Section 4.3), which is equivalent to Equation A-1, and clarify the original design document Equation 4.6.1 (WIPP PA 2004a, Section 4.6), shown by Equation A-5. This essentially results in a simplification of the original Equation 4.6.1 to include a natural log term, as shown in Equation A-5. The original Equation 4.6.2 in the previous design document (WIPP PA 2004a, Section 4.6) was re-derived as shown by Equation A-6.

The finite difference discretization is then performed for zones of constant size. Appendix A provides a simplified version of the final derivation (Equation A-7), which is in fact identical to the previous design document Equation 4.6.3 (WIPP PA 2004a, Section 4.6), except that the coefficient terms $\alpha_1$ and $\alpha_2$ are different due to the correction for the spatial variability of $k'$, which produced a modified 'Forchterm' that uses the natural log.

A variable zone size implementation was described based on the previous DRSPALL design document (WIPP PA 2004a, Section 4.6; WIPP PA 2013b). However, this was done incorrectly, as a simple substitution of variable zone sizes into the equation derived for a constant zone size is not valid. The derivation of an equation similar to Equation A-6 for a variable zone size would require a complete re-derivation, which was determined unnecessary because current computing resources allow for reasonably fast computational times even for a greater number of zones, such

that an increasing zone size is not needed. So it was decided to run DRSPALL exclusively with a constant zone size. DRSPALL Version 1.22 will display an error message if a growth rate other than 1.0 is input.

These changes are made in the CalculateWasteFlowImplicit routine of the source code file *wasteflowcalc.f90* in the calculation of 'Forchterm' for first, interior, and last cell coefficients. In correcting the calculation of 'Forchterm', the indexing of the second permeability() term was also corrected to be 'i-1' instead of 'i'. The coefficients for the last cell (i=numReposZones) have changed: aa(i) has been changed from '-alpha1' to '-alpha1-alpha2' and bb(i) has been changed from '1.0+alpha1' to '1.0+alpha1+alpha2'.

It should be noted that since a constant zone size is used exclusively, values for both 'reposDR(i)' (distance between zone edges) and 'reposDRH(i)' (distance between zone centers) will now be the same.

## 3.1. Boundary Conditions

In the CalculateWasteFlowImplicit routine of *wasteflowcalc.f90*, the index of the "first cell coefficients" (i) has been changed from 'firstIntactZone' to 'firstIntactZone+1', since any values for the boundary ('firstIntactZone') would be constant and fixed by the specified pressure (Dirichlet) boundary condition in the cavity. That is, the boundary nodes are not included in the coefficient matrix, so there should be no aa(i), bb(i), cc(i) coefficients for 'firstIntactZone'. The effect of the boundary node (firstIntactZone) is included in the b-vector of the linear system of equations. Consequently, the indexing for the "interior cell coefficients" now begins at 'firstIntactZone+2' instead of 'firstIntactZone+1'. Also, as a consequence of this, the indexing of the matrix inversion has changed (lines 230-245). The boundary pressure is now assigned to 'reposPres(firstIntactZone)' instead of 'reposPres(0)'. Because of that, 'exitPoreVelocity' is now calculated using a centered-difference approximation, which leads to 'reposPres(firstIntactZone+1)' being used instead of 'reposPres(firstIntactZone)'.

Previously, the permeability of the 'firstIntactZone-1' zone was set to the value of the 'firstIntactZone'. This was changed by eliminating that assignment (line 32 of *wasteflowcalc.f90*) because the permeability of the 'firstIntactZone-1' is no longer used. Also, where previously the array element 'psi(firstIntactZone-1)' was calculated from the gas viscosity and boundary pressure, this assignment has been made applicable to 'psi(firstIntactZone)' (line 37 of *wasteflowcalc.f90*), since the 'firstIntactZone' is the boundary.

## 3.2. Summary of Code Changes

A summary of the changes to the source code files for DRSPALL Version 1.22 is described in Appendix B along with source code excerpts from DRSPALL Versions 1.21 and 1.22 showing the change. Changes were made in the following DRSPALL source code files:

- *A1main_drspall.f90*
- *globals.F90*
- *maincalc.f90*
- *parameters.f90*

- *setupcalc.f90*
- *vmsfilewrite.f90*
- *wasteflowcalc.f90*
- *wastestresscalc.f90*
- *wellborecalc.f90*.

Source code files *cdbcontrol.f90*, *cdbglobals.F90*, and *vmsoutputcontrol.f90* were not modified in DRSPALL Version 1.22.

*This page is intentionally left blank.*

# 4. ZONE SIZE SENSITIVITY STUDY

In response to the modifications to the DRSPALL code, a zone size sensitivity study was conducted to determine the optimal zone size to implement the finite different equations (Kicker 2015). The zone size sensitivity study is an update to the original analyses and documentation prepared in support of the WIPP 2004 Compliance Recertification Application (Lord et al. 2006, Section 5).

## 4.1. Objective

The objective of the study is to demonstrate the effect of repository zone size, $\Delta r$, characteristic tensile failure length, $L_t$, and wellbore zone size, $\Delta z$, on the spall release as a result of modifications to the DRSPALL code (Version 1.22). The dependence of spall release on a combination of mechanisms (stress, failure, and fluidization) requires that stress and failure be examined explicitly, in addition to spall release, in order to gain a meaningful understanding of the impacts of zone size on the DRSPALL model performance. The wellbore provides the inner pressure boundary condition to the repository by accurately modeling the transport of mud, injected gas, and mobilized waste to the surface. Repository zone size is discussed in detail and the wellbore zone size effect is briefly demonstrated. The results from this study facilitate selection of an appropriate set of DRSPALL zone size parameters and justify the values recommended for WIPP performance assessment (PA) spalling release calculations.

## 4.2. Background

DRSPALL has the capability to model the repository in two different ways. When the user specifies the cylindrical model, the repository and cavity are modeled as a cylinder of constant height equal to the repository thickness. The radius of the cylindrical cavity, CAVRAD, increases with drilling time and as spalling occurs. When the user specifies the spherical model, the repository and cavity are hemispherical where the cavity radius, CAVRAD, is also a function of time and increases for the same reasons.

The origin for the cylindrical geometry is a line down the center of the borehole denoting the axis of symmetry (Figure 4-1). The origin for the spherical repository domain is the point where the axis of the drill bit first touches the top of the repository. The three primary radial variables in DRSPALL output are the drill cuttings radius (CUTRAD), cavity radius (CAVRAD), and the tensile-failed radius (TENSRAD). The relationship among these three is demonstrated in Figure 4-1. The cuttings radius represents the position of the drill-bit face in the repository. Typically drilling is the only mechanism that expands the cavity radius, so the drill radius and cavity radius will overlay. In the event of spallings, however, the cavity radius may grow larger than the drilled radius. A third radial variable, tensile-failed radius, identifies solid material that has failed due to the stress state, but has not mobilized into the flow stream. This may or may not be larger than the cavity radius, but it can never be smaller. A thorough discussion of the DRSPALL spallings model is provided by Lord et al. (2006) and the updated DRSPALL design document (WIPP PA 2015a).

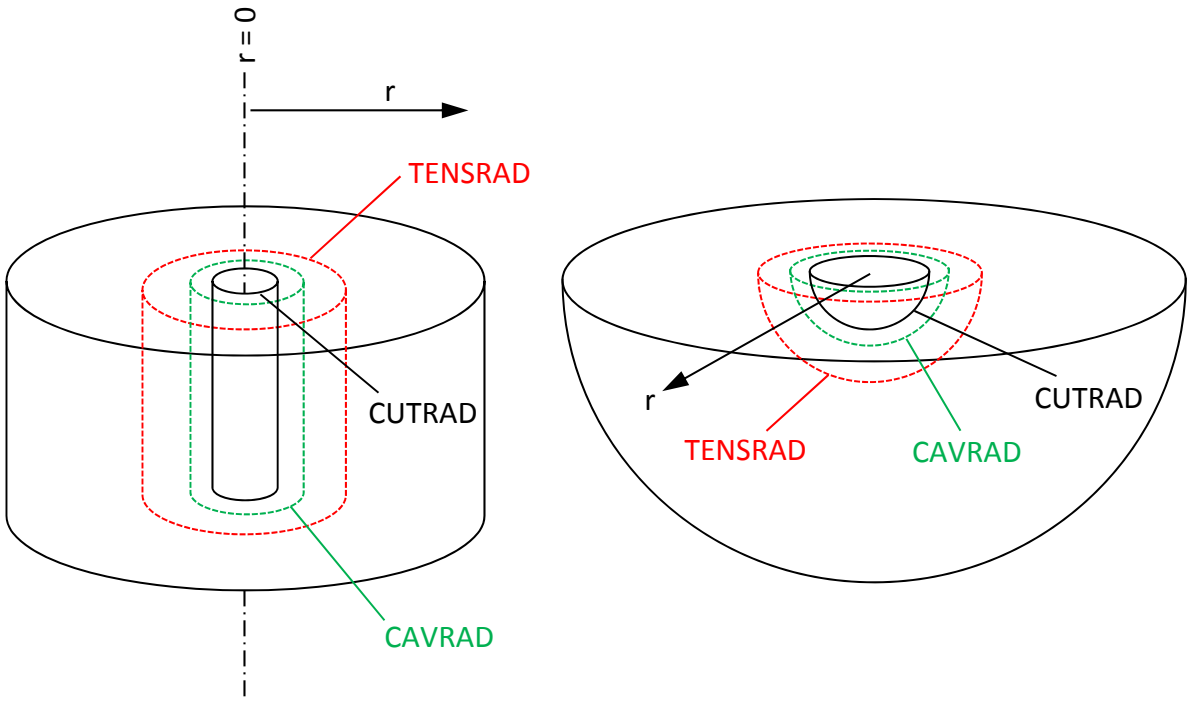


**Figure 4-1. Radial Variables in Cylindrical Geometry and Spherical Geometry.**

The characteristic tensile failure length, herein referred to as characteristic length, is the distance from the wellbore interface over which radial effective stress is averaged and then compared to a tensile cutoff in order to determine material failure from spalling (Lord et al. 2006, Section 3.5.5.1). This characteristic length is used to allow failure of a shell of material next to the wellbore to occur, as material failure is always at some finite distance into the solid. This situation occurs because the radial effective stress is always zero at the boundary between the wellbore and repository where both the radial elastic stress and pore pressure are equal to the bottomhole pressure, and the seepage stress is zero. This implies that the cell-centered radial effective stress will decrease toward zero near the wellbore boundary, and that this stress always will be less than the tensile cutoff at the boundary zone for some sufficiently small zone size. These small zones near the boundary will never fail, leading to the conclusion that grid refinement always leads to zero spalling under the assumption that failure propagates into the waste from the cavity interface. The use of a characteristic length over which failure is evaluated allows an internal failure to lead to failure of a shell of material. This is, in fact, a realistic approach, since solid material next to a wellbore does not tend to fail continuously from the wellbore boundary into the waste on a particulate scale. Instead, discrete chunks will fail whose size is determined by the characteristics of the waste, such as the type of waste material, its original size, its degree of compaction at the time of the borehole intrusion, and its tensile strength. Failure of material close to the wellbore will therefore lead to loss of strength of the shell between this failure point and the wellbore, provided the thickness of the shell is not too large.

The average radial effective stress over the characteristic length therefore is used to evaluate tensile failure in DRSPALL. With the characteristic length, grid refinement leads to a "converged" radial effective stress profile, resulting in similar tensile failure behavior for different zone sizes. The theoretical background for the stress model discussed above is presented in detail by Lord et al. (2006, Section 3.5.2).

## 4.3. Approach

The problem parameters used to evaluate the effects of the zone size and characteristic tensile failure length were chosen to be within the typical sampling range for WIPP intrusion analyses. To ensure an effective evaluation of DRSPALL zone size sensitivities, a set of input parameters was selected such that the resulting DRSPALL output produced a range of spall release volumes. The input values for this zone size study are listed in Table 4-1. The parameters that are varied in this sensitivity study are shaded in the table.

Eighteen spherical DRSPALL configurations were compared to determine the sensitivity of cavity radius, pore pressure, and solid stress profiles to various combinations of zone sizes and characteristic lengths. The suite of test case configurations is outlined in Table 4-2, which also provides the nomenclature used to identify the runs in the figures presented below. All other material and problem specification parameters remained the same. Two of the cases (8-8-1 and 8-8-2) were used to evaluate wellbore zone size effect on bottomhole pressure. Four of the cases (2-4-2, 4-4-2, 8-4-2, 16-4-2) were run a second time with a large tensile failure limit in order to analyze the development of the radial tensile stress profiles without the complication of failure and fluidization. The same four cases were repeated a third time using the cylindrical geometry. The cavity radius was chosen as a basis for evaluation because it is directly related to tensile failure and fluidization (Section 4.4.1). Pore pressure and radial stress profiles are also compared because they are the primary numerical solution variables (Section 4.4.2). Spallings volumes are also compared using a sampling approach to account for uncertainty (Section 4.4.3). Lastly, the effect of wellbore zone size is demonstrated in Section 4.5. DRSPALL input and output files along with an Excel calculation file for post processing are located in Code Versions System (CVS) repositories contained in */nfs/data/CVSLIB/WIPP_SPECIAL_ANALYSES/DRSPALL_122_ ZONE_SIZE_SENSITIVITY*.

## 4.4. Repository Zone Size

### 4.4.1. Cavity Radius History

The cavity radius provides a global measure of zone size convergence because it is the final result from tensile failure and fluidization of the waste. Cavity radius (CAVRAD) histories are provided in this section for the spherical geometry. The drill radius (DRILLRAD) history is also included as a reference curve. DRILLRAD varies over time as is bounded by the drill cuttings radius, CUTRAD, shown in Figure 4-1. CUTRAD represents the maximum drill cuttings radius. The DRILLRAD history is constant regardless of material failure and thus provides a baseline minimum radius for comparison to CAVRAD. Any difference between a test case cavity history and the drill history, i.e. when CAVRAD > DRILLRAD, is due to tensile failure and fluidization and will be referred to as the spall radius.

**Table 4-1. Input Values for the Zone Size Sensitivity Study, Case 4-2-2.** Input values for case 4-2-2 are echoed in output file, *drs_r1_p4_v050-04-02Lt-02.xdbg*, located in Files/Output module of CVS repository, */nfs/data/CVSLIB/WIPP_SPECIAL_ANALYSES / DRSPALL_V122_ZONE_SIZE_SENSITIVITY / test5-individualRuns*. The parameters that are varied in other test cases are shaded.

| | | | |
|---|---|---|---|
| REPOSITORY | | | |
| Land Elevation | (m) | : | 1.0373E+03 |
| Repository top | (m) | : | 3.8470E+02 |
| Total Thickness | (m) | : | 0.0000E+00 |
| DRZ Thickness | (m) | : | 8.5000E–01 |
| DRZ Permeability | (m^2) | : | 1.0000E–15 |
| Outer Radius | (m) | : | 1.9200E+01 |
| Initial Gas Pressure | (m) | : | 1.4800E+07 |
| Far-Field In-Situ Stress | (m) | : | 1.4900E+07 |
| WASTE | | | |
| Porosity[2] | (-) | : | 6.1090E–01 |
| Permeability[2] | (m^2) | : | 1.0673E–12 |
| Forchheimer Beta | (-) | : | 1.1500E–06 |
| Biot Beta | (-) | : | 1.0000E+00 |
| Poisson's Ratio | (-) | : | 3.8000E–01 |
| Cohesion | (Pa) | : | 1.4000E+05 |
| Friction Angle | (deg) | : | 4.5800E+01 |
| Tensile Strength[2] | (Pa) | : | 1.4379E+05 |
| Tensile Failure Characteristic Length[1] | (m) | : | 2.0000E–02 |
| Particle Diameter[2] | (m) | : | 3.4622E–02 |
| Gas Viscosity | (Pa-s) | : | 8.9339E–06 |
| MUD | | | |
| Density | (kg/m^3) | : | 1.2100E+03 |
| Viscosity | (Pa-s) | : | 9.1700E–03 |
| Wall Roughness Pipe | (m) | : | 5.0000E–05 |
| Wall Roughness Annulus | (m) | : | 5.0000E–05 |
| Max Solids Vol. Fraction | (Pa-s) | : | 6.1500E–01 |
| Solids Viscosity Exponent | (Pa-s) | : | –1.5000E+00 |
| WELLBORE/DRILLING | | | |
| Bit Diameter | (m) | : | 3.1115E–01 |
| Pipe Diameter | (m) | : | 1.1430E–01 |
| Collar Diameter | (m) | : | 2.0320E–01 |
| Pipe Inside Diameter | (m) | : | 9.7180E–02 |
| Collar Length | (m) | : | 1.8288E+02 |
| Exit Pipe Length | (m) | : | 0.0000E+00 |
| Exit Pipe Diameter | (m) | : | 2.0320E–01 |
| Drilling Rate | (m/s) | : | 4.4450E–03 |
| Bit Above Repository | (m) | : | 1.5000E–01 |
| Mud Pump Rate | (m^3/s) | : | 2.0181E–02 |

**Table 4-1. Input Values for the Zone Size Sensitivity Study, Case 4-2-2. (Continued)** Input values for case 4-2-2 are echoed in output file, *drs_r1_p4_v050-04-02Lt-02.xdbg*, located in the Files/Output module of CVS repository, */nfs/data/CVSLIB/WIPP_SPECIAL_ANALYSES / DRSPALL_V122_ZONE_SIZE_SENSITIVITY / test5-individualRuns*. The parameters that are varied in other test cases are shaded.

| | | | |
|---|---|---|---|
| WELLBORE/DRILLING (continued) | | | |
| Max Pump Pressure | (Pa) | : | 2.7500E+07 |
| DDZ Thickness | (m) | : | 1.6000E–01 |
| DDZ Permeability | (m^2) | : | 1.0000E–14 |
| Stop Drilling Exit Vol. Rate | (m^3/s) | : | 1.0000E+03 |
| Stop Pumping Exit Vol. Rate | (m^3/s) | : | 1.0000E+03 |
| Stop Drilling Time | (s) | : | 1.0000E+03 |
| COMPUTATIONAL | | | |
| Spherical/Cylindrical | (S/C) | : | S |
| Allow Fluidization | (Y/N) | : | Y |
| Max Run Time | (s) | : | 6.0000E+02 |
| Repository Cell Length[1] | (m) | : | 4.0000E–03 |
| Radius, Growth Rate | (m,-) | : | 0.500, 1.000 |
| Wellbore Cell Length[1] | (m) | : | 2.0000E+00 |
| Wellbore Cell Growth Rate | (-) | : | 1.0000E+00 |
| First Wellbore Zone | (-) | : | 1.0000E+01 |
| Well Stability factor | (-) | : | 5.0000E–02 |
| Repository Stability factor | (-) | : | 5.0000E+00 |
| Mass Diffusion factor | (-) | : | 1.0000E–04 |
| Momentum Diffusion factor | (-) | : | 1.0000E–02 |
| PARAMETERS | | | |
| Pi | (-) | : | 3.1416E+00 |
| Atmospheric Pressure | (Pa) | : | 1.0177E+05 |
| gravity | (m/s^2) | : | 9.8067E+00 |
| Gas Constant | (J/kg K) | : | 4.1160E+03 |
| Repository Temperature | (K) | : | 3.0000E+02 |
| Water Compressibility | (1/Pa) | : | 3.1000E–10 |
| Waste Density | (kg/m^3) | : | 2.6500E+03 |
| Salt Density | (kg/m^3) | : | 2.1800E+03 |
| Shape Factor | (-) | : | 1.0000E–01 |
| Tensile Velocity | (m/s) | : | 1.0000E+03 |
| Bit Nozzle Number | (-) | : | 3.0000E+00 |
| Bit Nozzle Diameter | (m) | : | 1.1112E–02 |
| Choke Efficiency | (-) | : | 9.0000E–01 |

NOTES: [1]Variable parameter modified in the zone size sensitivity study (see Table 4-2).
[2]Uncertain parameter that is varied in Section 4.4.3.

**Table 4-2. Description of Test Cases for the Zone Size Sensitivity Study.**

| Case | Description |
|---|---|
| 4-1-2 | $\Delta r$ = 0.004 m; $L_t$ = 0.01 m, $\Delta z$ = 2 m |
| 8-2-2 | $\Delta r$ = 0.008 m; $L_t$ = 0.02 m, $\Delta z$ = 2 m |
| 16-4-2 | $\Delta r$ = 0.016 m; $L_t$ = 0.04 m, $\Delta z$ = 2 m |
| 2-1-2 | $\Delta r$ = 0.002 m; $L_t$ = 0.01 m, $\Delta z$ = 2 m |
| 4-2-2 | $\Delta r$ = 0.004 m; $L_t$ = 0.02 m, $\Delta z$ = 2 m |
| 8-4-2 | $\Delta r$ = 0.008 m; $L_t$ = 0.04 m, $\Delta z$ = 2 m |
| 16-8-2 | $\Delta r$ = 0.016 m; $L_t$ = 0.08 m, $\Delta z$ = 2 m |
| 1-1-2 | $\Delta r$ = 0.001 m; $L_t$ = 0.01 m, $\Delta z$ = 2 m |
| 2-2-2 | $\Delta r$ = 0.002 m; $L_t$ = 0.02 m, $\Delta z$ = 2 m |
| 4-4-2 | $\Delta r$ = 0.004 m; $L_t$ = 0.04 m, $\Delta z$ = 2 m |
| 8-8-2 | $\Delta r$ = 0.008 m; $L_t$ = 0.08 m, $\Delta z$ = 2 m |
| 16-16-2 | $\Delta r$ = 0.016 m; $L_t$ = 0.16 m, $\Delta z$ = 2 m |
| 1-2-2 | $\Delta r$ = 0.001 m; $L_t$ = 0.02 m, $\Delta z$ = 2 m |
| 2-4-2 | $\Delta r$ = 0.002 m; $L_t$ = 0.04 m, $\Delta z$ = 2 m |
| 4-8-2 | $\Delta r$ = 0.004 m; $L_t$ = 0.08 m, $\Delta z$ = 2 m |
| 8-16-2 | $\Delta r$ = 0.008 m; $L_t$ = 0.16 m, $\Delta z$ = 2 m |
| 16-32-2 | $\Delta r$ = 0.016 m; $L_t$ = 0.32 m, $\Delta z$ = 2 m |
| 8-8-1 | $\Delta r$ = 0.008 m; $L_t$ = 0.08 m, $\Delta z$ = 1 m |

NOTES: $\Delta r$ is the repository cell length (also referred to as repository zone size), $L_t$ is the tensile failure characteristic length, and $\Delta z$ is the wellbore cell length (also referred to as wellbore zone size).

Because the characteristic length is the distance over which failure is evaluated and thus directly impacts spallings development, this length relative to the repository zone size is considered. A comparison of cavity radius histories for a range of repository zone sizes while maintaining a constant characteristic length to zone size ratio ($LR$, where $LR = L_t / \Delta r$) is shown in Figure 4-2 for the spherical geometry. The characteristic length ratio ($LR$) is held constant in each plot of Figure 4-2, with four plots shown to capture a range of $LR$ values. The drill bit penetrates the repository at about 35 s. Cavity growth due to spallings also starts at around 35 s, with drilling completed by 380 s.

Final cavity radius values and equivalent spall volumes are given in Table 4-3. An $LR$ value of 2.5 resulted in the lowest average final spallings volume of 0.520 $m^3$, while $LR$ values of 5, 10, and 20 resulted in average final spallings volumes of 0.604 $m^3$, 0.606 $m^3$, and 0.658 $m^3$, respectively. These results indicate that 2.5 zones per characteristic length (i.e., $LR$ = 2.5) are not sufficient to effectively evaluate failure. This study suggests using a minimum of 5 zones per characteristic length to optimize spallings development.

The effect of variations in repository zone size, $\Delta r$, is demonstrated in Figure 4-3, which compares cavity radius histories for a range of zone sizes ($\Delta r$ = 0.001 m, 0.002 m, 0.004 m, 0.008 m, and 0.016 m). The characteristic length ($L_t$) is held constant in each plot in Figure 4-3, with five plots shown to capture a range of $L_t$ values. Drilling occurs through the same time frame as in Figure 4-2. Depending on $L_t$ value, some differences in spallings development are

observed as zone size varies. $L_t$ values of 0.04 m and 0.08 m resulted in the highest average final spallings volumes of 0.679 $m^3$ and 0.667 $m^3$, respectively. Note that because 2.5 zones per characteristic length are not sufficient to effectively evaluate failure, test cases with $LR$ = 2.5 are excluded from the calculation of average values shown in Figure 4-3.

The effect of characteristic length on cavity radius is illustrated in Figure 4-4 for spherical geometry. The plots in this figure compare cavity radius histories for a range of characteristic length values ($L_t$ = 0.01 m, 0.02 m, 0.04 m, 0.08 m, and 0.16 m). The zone size ($\Delta r$) is held constant in each plot, with five plots shown to capture a range of $\Delta r$ values. Drilling occurs throughout the same time frame as in Figure 4-2. A $\Delta r$ value of 0.002 m resulted in the highest average final spallings volume of 0.676 $m^3$, while $\Delta r$ values of 0.004 m and 0.008 m resulted in similar values of 0.641 $m^3$ and 0.647 $m^3$, respectively.

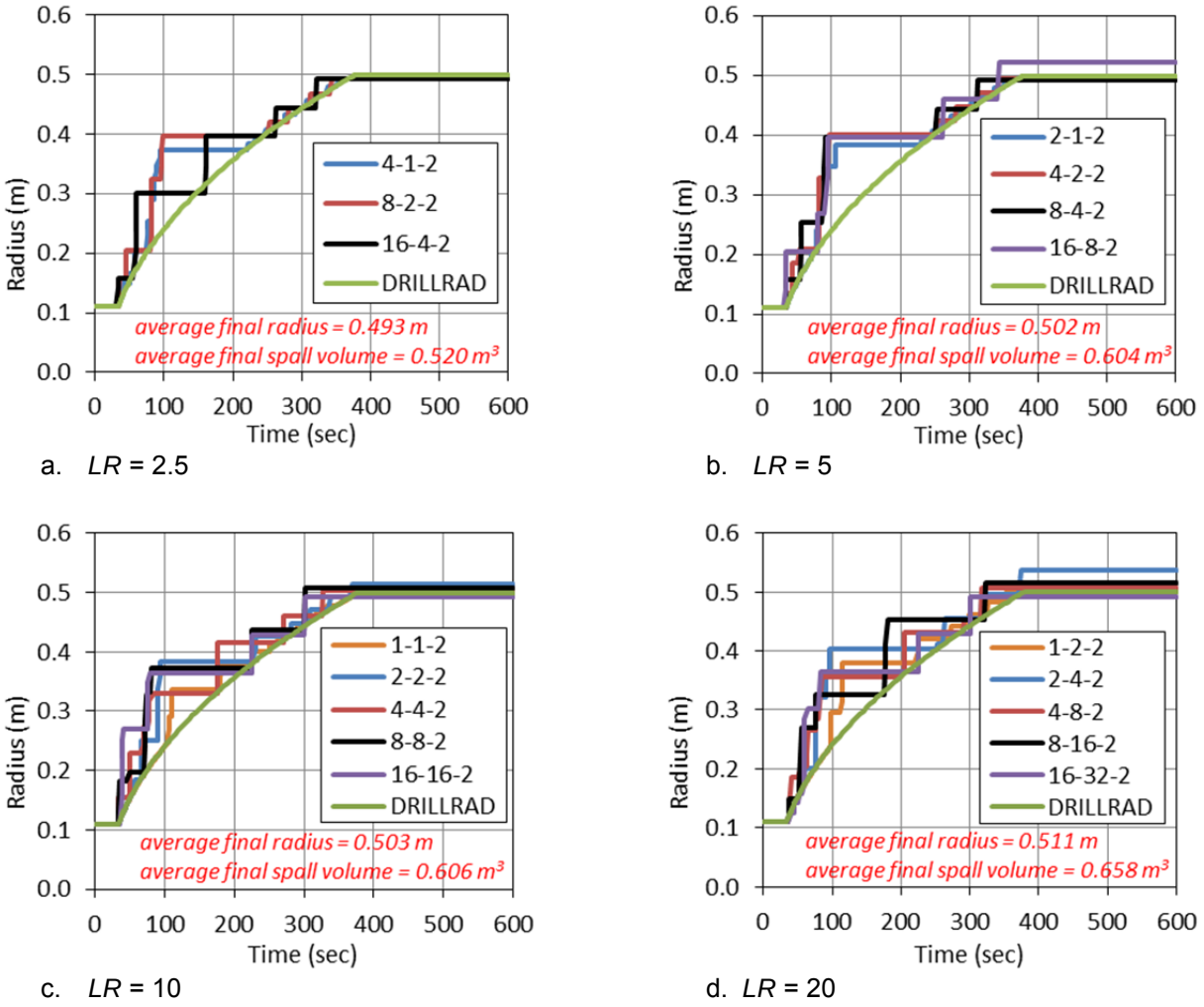


a. $LR$ = 2.5 b. $LR$ = 5

c. $LR$ = 10 d. $LR$ = 20

**Figure 4-2. Cavity Radius History as Repository Zone Size Varies for Four Characteristic Length Ratios ($LR$ = 2.5, 5, 10, and 20) in Spherical Geometry.**

## Table 4-3. Final Cavity Radius in Spherical Geometry.

| Case | Repository Zone Size, $\Delta r$ (m) | Characteristic Length, $L_t$ (m) | Wellbore Zone Size, $\Delta z$ (m) | Characteristic Length Ratio, $LR$ ($LR = L_t / \Delta r$) | Final Radius (m) | Final Spall Volume ($m^3$) |
|---|---|---|---|---|---|---|
| 1-1-2 | 0.001 | 0.01 | 2 | 10 | 0.499 | 0.484 |
| 2-1-2 | 0.002 | | | 5 | 0.498 | 0.554 |
| 4-1-2 | 0.004 | | | 2.5 | 0.496 | 0.515 |
| 1-2-2 | 0.001 | 0.02 | | 20 | 0.504 | 0.605 |
| 2-2-2 | 0.002 | | | 10 | 0.514 | 0.680 |
| 4-2-2 | 0.004 | | | 5 | 0.496 | 0.601 |
| 8-2-2 | 0.008 | | | 2.5 | 0.492 | 0.534 |
| 2-4-2 | 0.002 | 0.04 | | 20 | 0.538 | 0.794 |
| 4-4-2 | 0.004 | | | 10 | 0.504 | 0.655 |
| 8-4-2 | 0.008 | | | 5 | 0.492 | 0.589 |
| 16-4-2 | 0.016 | | | 2.5 | 0.492 | 0.512 |
| 4-8-2 | 0.004 | 0.08 | | 20 | 0.508 | 0.668 |
| 8-8-2 | 0.008 | | | 10 | 0.508 | 0.660 |
| 16-8-2 | 0.016 | | | 5 | 0.524 | 0.674 |
| 8-16-2 | 0.008 | 0.16 | | 20 | 0.516 | 0.692 |
| 16-16-2 | 0.016 | | | 10 | 0.492 | 0.550 |
| 16-32-2 | 0.016 | 0.32 | | 20 | 0.492 | 0.533 |
| 8-8-1 | 0.008 | 0.08 | 1 | 10 | 0.508 | 0.660 |
| DRILLRAD | — | — | — | — | 0.500 | 0.000 |

**Average Final Values**

| $LR$ | Average Final Radius (m) | Average Final Spall Volume ($m^3$) | $L_t$ (m) | Average Final Radius (m) | Average Final Spall Volume ($m^3$) | $\Delta r$ (m) | Average Final Radius (m) | Average Final Spall Volume ($m^3$) |
|---|---|---|---|---|---|---|---|---|
| 2.5 | 0.493 | 0.520 | 0.01 | 0.498 | 0.519 | 0.001 | 0.501 | 0.545 |
| 5 | 0.502 | 0.604 | 0.02 | 0.504 | 0.629 | 0.002 | 0.516 | 0.676 |
| 10 | 0.503 | 0.606 | 0.04 | 0.511 | 0.679 | 0.004 | 0.502 | 0.641 |
| 20 | 0.511 | 0.658 | 0.08 | 0.513 | 0.667 | 0.008 | 0.505 | 0.647 |
| | | | 0.16 | 0.504 | 0.621 | 0.016 | 0.502 | 0.585 |

NOTE: Because 2.5 zones per characteristic length are not sufficient to effectively evaluate failure, test cases with $LR = 2.5$ are excluded from the calculation of average values.

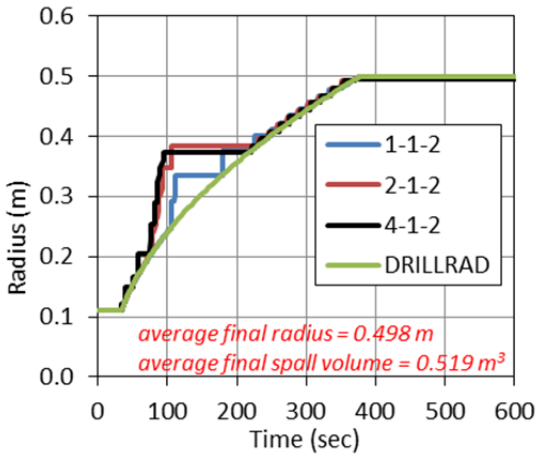


a. $L_t$ = 0.01 m

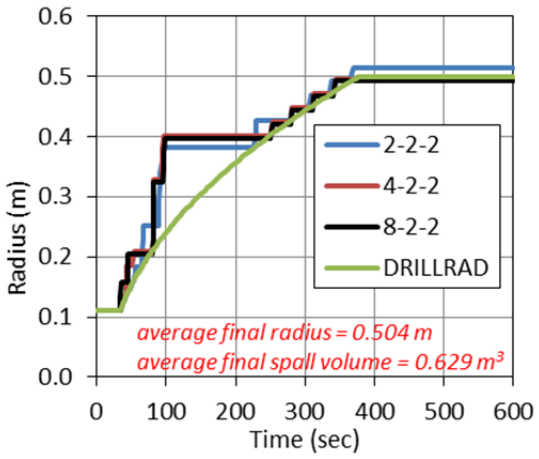


b. $L_t$ = 0.02 m

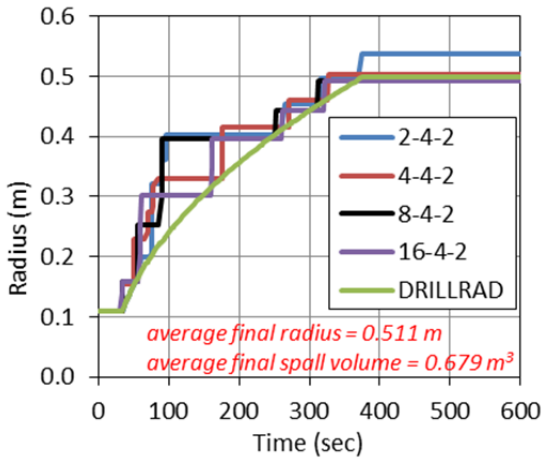


c. $L_t$ = 0.04 m

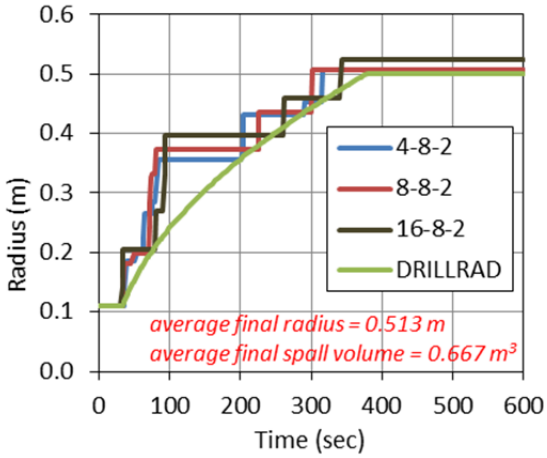


d. $L_t$ = 0.08 m

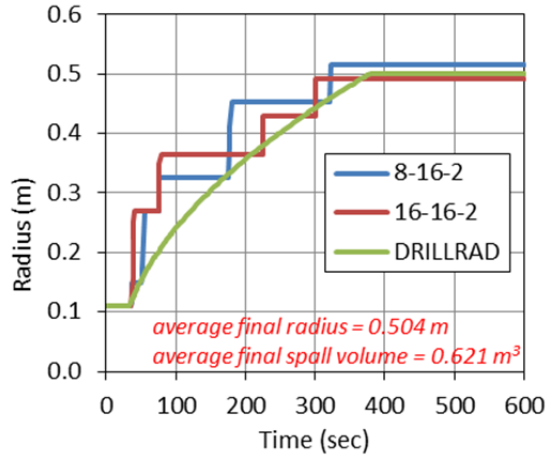


e. $L_t$ = 0.16 m

**Figure 4-3. Cavity Radius History as Repository Zone Size Varies for Five Failure Characteristic Lengths in Spherical Geometry.** Final radius and spall volumes are provided in Table 4-3. Note that because 2.5 zones per characteristic length are not sufficient to effectively evaluate failure, test cases with *LR* = 2.5 are excluded from the calculation of average values.

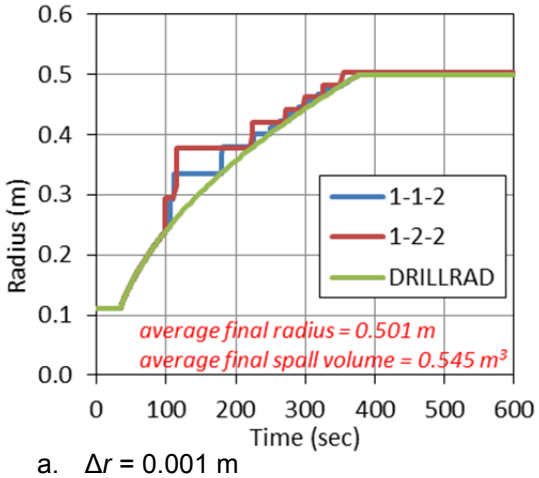


a. $\Delta r$ = 0.001 m

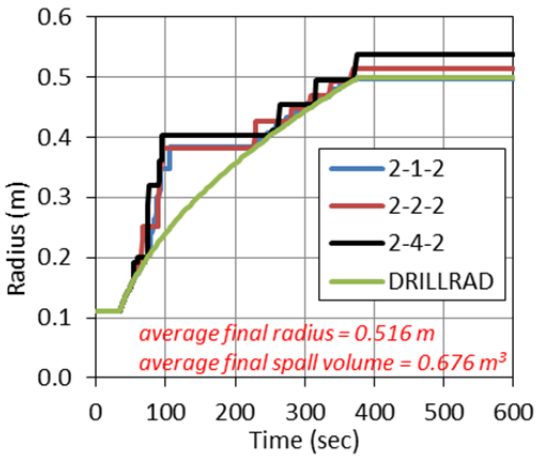


b. $\Delta r$ = 0.002 m

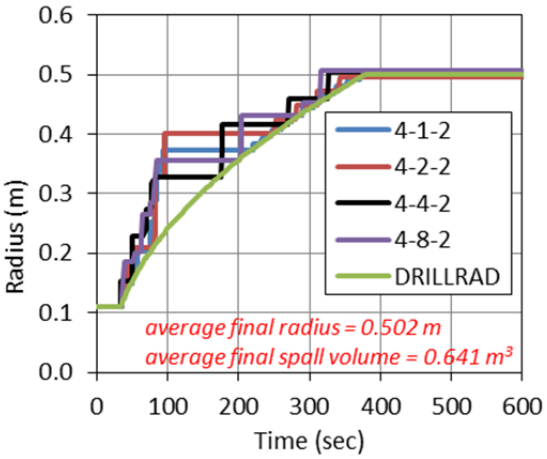


c. $\Delta r$ = 0.004 m

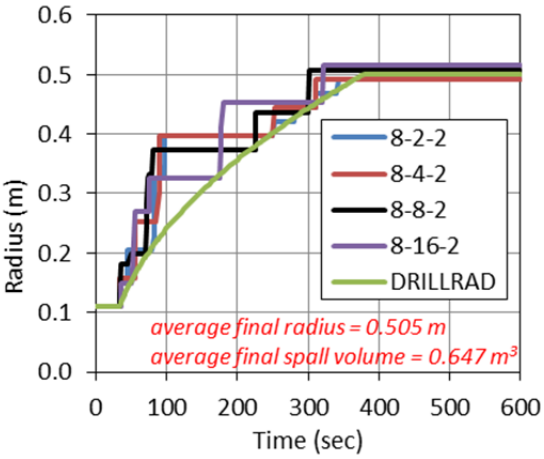


d. $\Delta r$ = 0.008 m

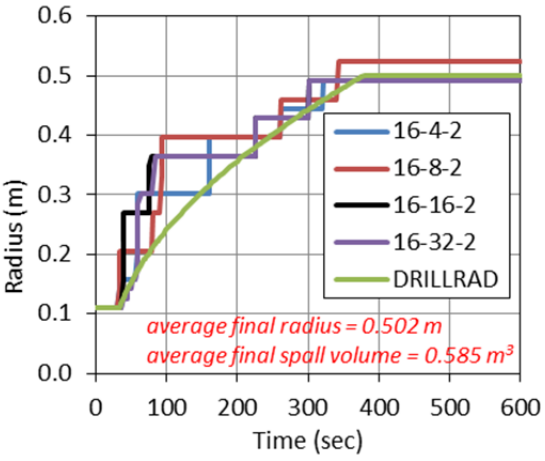


e. $\Delta r$ = 0.016 m

**Figure 4-4. Cavity Radius History as Characteristic Length Varies for Five Repository Zone Sizes in Spherical Geometry.** Final radius and spall volumes are provided in Table 4-3. Note that because 2.5 zones per characteristic length are not sufficient to effectively evaluate failure, test cases with *LR* = 2.5 are excluded from the calculation of average values.

Based on the cavity radius histories, a repository zone size ranging from 0.002 m to 0.008 m will maximize the spallings volume output and a characteristic length to zone size ratio ranging from 10 to 20 will maximize the spallings volume output.

### 4.4.2. Pore Pressure and Radial Stress Profiles with Failure Suppressed

Failure and fluidization, represented collectively by the cavity radius, are actually evaluated by post processing the solutions for porous flow and the mechanical stress state at each timestep. A more detailed measure of solution convergence with decreasing zone size is the comparison of radial profiles for the primary solution variables (pore pressure and the various radial stresses). However, profiles prior to failure do not show the fully developed tensile phases, and profiles are difficult to interpret once failure has started, because failure occurs over different shell sizes and with different cavity radii.

To facilitate comparison of the pore pressure and radial stress profiles, a new set of calculations were run using the same problem setup discussed above but with a large tensile strength to preclude tensile failure and spall. This approach allows comparisons of pore pressure and stress across all zone sizes with almost identical boundary conditions for the well bottomhole pressure and the cavity radius. These results, presented in Figure 4-5 for cases with a characteristic length of 0.04 m and with spherical geometry, show pore pressure and radial stress profiles in the repository at 120 s, soon after failure would have occurred. At this time the tensile region of the radial effective stress near the cavity interface is fairly well developed. These comparisons show similar results for all zone sizes. The bottom plot in Figure 4-5 has zoomed in on the tensile region. It shows similar profiles when the zone size is 0.004 m or less, implying convergence for the radial effective stress, which is a numerically sensitive parameter. The slight shift in the tensile pulse is due to the discrete mechanism used to remove cells from the repository domain as the drill bit penetrates the repository — a cell is removed when the equivalent 1-D drill radius exceeds a cell's far boundary radius. Smaller cells are therefore removed more rapidly.

While the data in Figure 4-5 show that the stress and pressure profiles are essentially the same for all zone sizes studied, this is only at one time, 120 s, in simulations that encompass several hundred seconds. To examine the evolution of the radial effective stress profiles, data for the four zone sizes ($\Delta r$ = 0.002 m, 0.004 m, 0.008 m, and 0.016 m) are plotted every 20 s from 40 to 500 s in Figure 4-6. Thus, proceeding from left to right along the "Radius" axis in each figure (Figures 4-6a through 4-6d), the first stress curve is taken at 40 s, while the next curve is taken at 60 s, etc., out to 500 s. The curves shift to the right along the radial axis because the cavity expands due to drilling. Note that after 380 s, the curves on the right end overlay because drilling stopped and cavity expansion stops at 0.5 m. Also displayed is the waste tensile strength of 0.144 MPa used to generate the cavity radius histories in Figures 4-2, 4-3, and 4-4. The profiles at 120 s for all cases exceed the tensile strength, with failure typically initiated soon after drilling begins. Examination of the cavity radius plots in Figures 4-2, 4-3, and 4-4 confirms this. After about 100 s, the evolution of cavity sizes in Figure 4-6 does not coincide with those given in Figures 4-2, 4-3, and 4-4 because failure is suppressed in Figure 4-6. What is clear, however, is that the stress profiles in Figure 4-6 have stabilized after about 400 s for all cases, that further failure is not expected, and that the profiles may be considered converged for the given zone sizes.

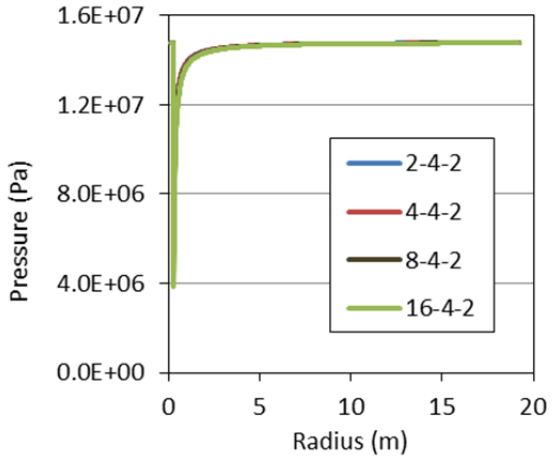


a. Pore pressure (POREPRS)

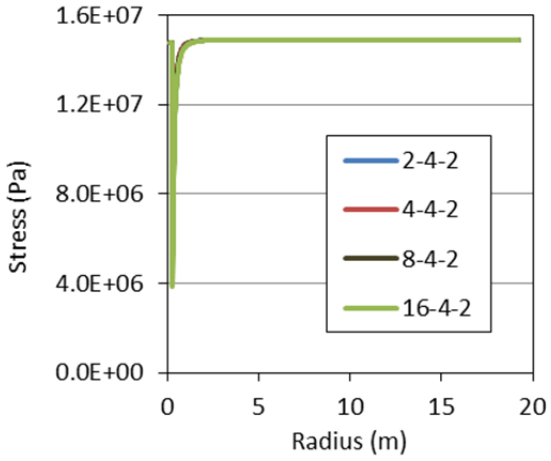


b. Radial elastic stress (RADELSTR)

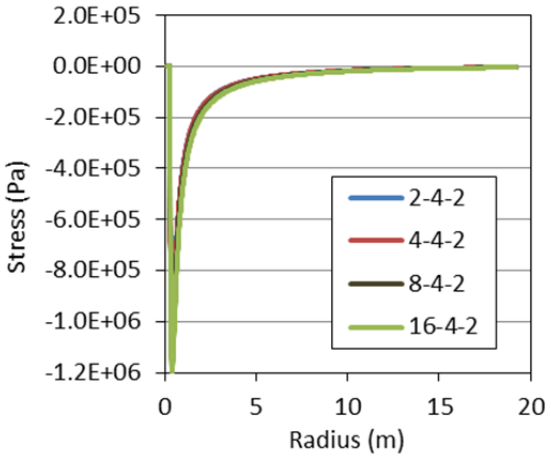


c. Radial seepage stress (RADSPSTR)

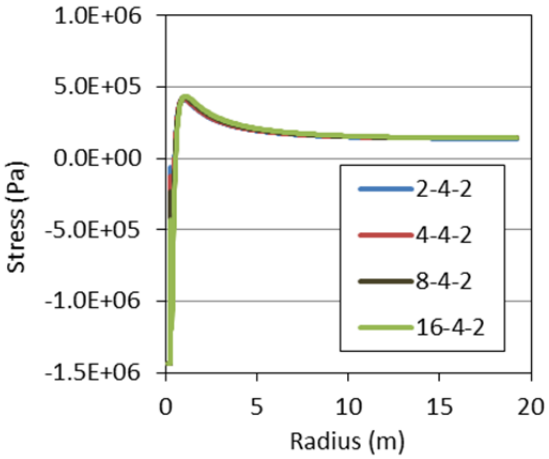


d. Radial effective stress (RADEFSTR)

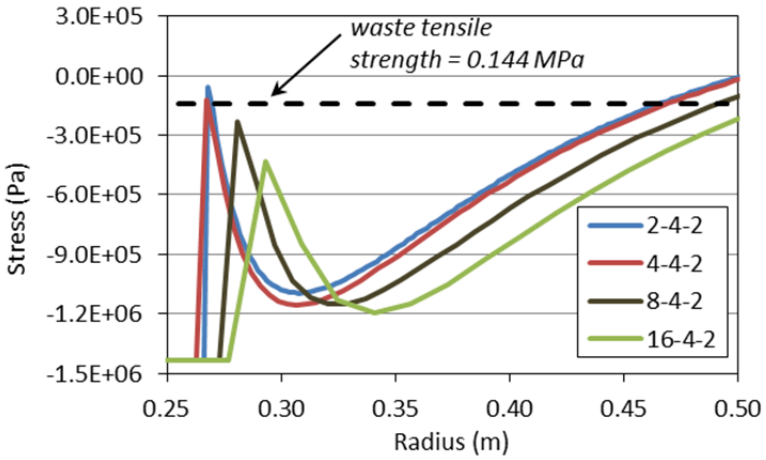


e. Radial effective stress (RADEFSTR) zoomed on tensile region

**Figure 4-5. Pore Pressure and Radial Stress Profiles at 120 s with No Failure, Spherical Geometry.**

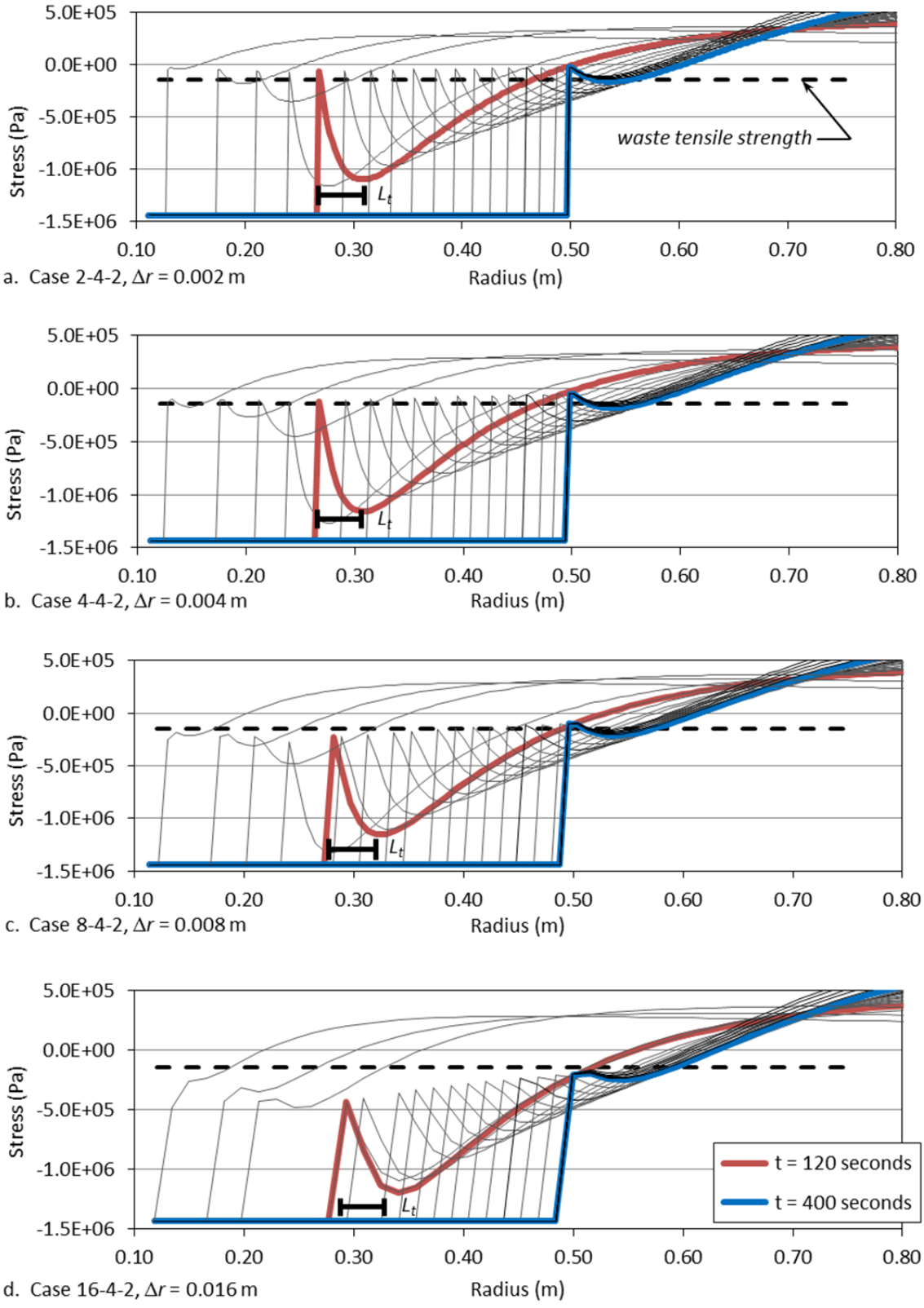


**Figure 4-6. Radial Effective Stress Profiles for Four Repository Zone Sizes as They Evolve Through Time Every 20 s from 40 to 500 s, Spherical Geometry.** Note that $L_t$ = 0.04 m in all test cases.

*Cylindrical Geometry*. The calculations that precluded failure were repeated in cylindrical geometry using the same four zone sizes ($\Delta r$ = 0.002 m, 0.004 m, 0.008 m, and 0.016 m). The radial effective stress profile at 120 s is shown in Figure 4-7. The stress profiles are similar for each zone size, converging to a consistent distribution as zone size decreases. The results are summarized in Figure 4-8 as radial effective stress profiles evolve through time from 80 to 500 s using 60-s increments. The results in Figure 4-8 are zoomed for more detail near the cavity wall. Except for the initial stress, a tensile region never develops at any time in the cylindrical geometry, so that failure and spalling never occur.

### 4.4.3. Final Spallings Volume with Latin Hypercube Sampling

The sensitivity of spallings volume (SPLVOL2) to zone size is evaluated using a sampling approach to account for uncertainty in four parameters: repository permeability, repository porosity, particle diameter of failed waste, and tensile strength of waste (Table 4-4). The uncertainty represented by these parameters pertains to the future state of the waste, which is modeled in performance assessment as a homogeneous material with uncertain properties. To ensure that sampled values were independent and that the extremes of each parameter's range were represented in the results, the sensitivity study used Latin hypercube sampling (LHS) to generate a sample of 100 parameter sets, or vectors, for the DRSPALL calculations. Spall volumes were computed for each of the 100 model runs. All other parameter values are listed in Table 4-1 and were held constant in each of the 100 vectors.

The cumulative frequency of occurrence of spallings volumes for the modified DRSPALL (Version 1.22) is shown in Figure 4-9 for a range of zone sizes ($\Delta r$ = 0.002 m, 0.004 m, 0.008 m, and 0.016 m). These results are compared to the distribution of spallings volumes from both DRSPALL Version 1.10, which was initially developed for the CRA-2004 PABC (Vugrin 2005, Figure 20) and DRSPALL Version 1.21, which was developed as part of the migration of PA codes to a Solaris platform (Kirchner, Gilkey, and Long 2013; CVS repository at */nfs/data/ CVSLIB / WIPP_ARCHIVES / PABC09 / DRSPALL / Output /mspall_drs_PABC09_r1.out*). The modified DRSPALL (Version 1.22) test cases (2-4-2, 4-4-2, 8-4-2, and 16-4-2) use a constant zone size ($\Delta r$) in each case with $L_t$ = 0.04 m and $\Delta z$ = 2 m. In comparison, both DRSPALL Versions 1.10 and 1.21 use a variable zone size with $\Delta r \geq 0.004$ m, $L_t$ = 0.02 m, and $\Delta z$ = 2.0 m.

Figure 4-9 shows that the cumulative distributions of modified spallings volumes (for $L_t$ = 0.04 m) are relatively similar. The range of spallings volumes are listed in Table 4-5, which shows the probability of occurrence based on the cumulative distribution. As $\Delta r$ increases, failure becomes less likely as shown by an increased number of simulations with no spallings. Generally, the modified DRSPALL results are more likely to produce higher spallings volumes compared to DRSPALL Versions 1.10 and 1.21. The change in spallings volumes between the modified DRSPALL code and DRSPALL Versions 1.10 and 1.21 is the result of changes to DRSPALL summarized in Section 3.2.

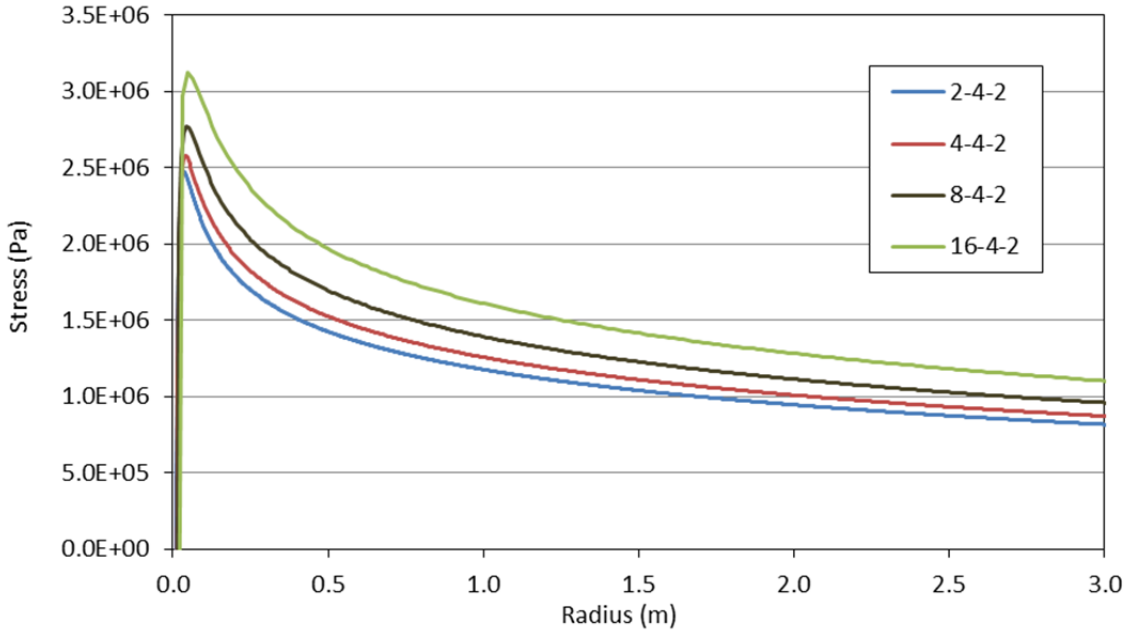


**Figure 4-7. Radial Effective Stress Profiles for Four Repository Zone Sizes at 120 s, Cylindrical Geometry.**

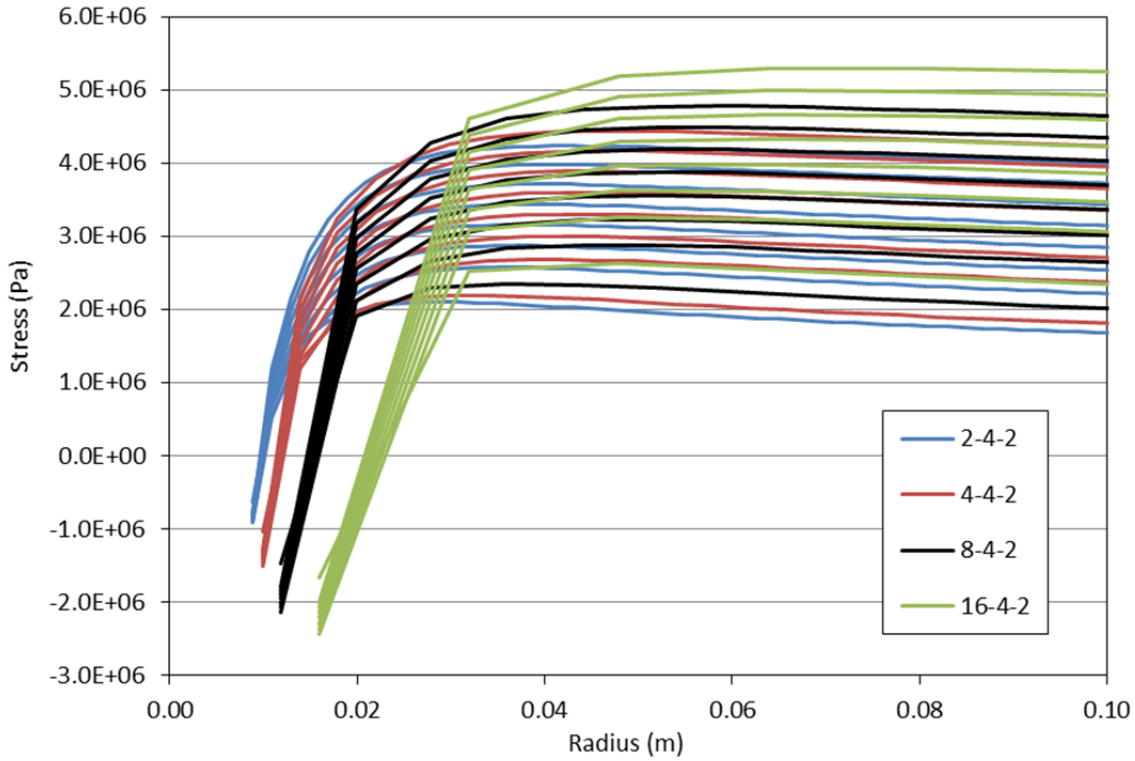


**Figure 4-8. Radial Effective Stress Profiles for Four Repository Zone Sizes as They Evolve Through Time Every 60 s from 80 to 500 s, Cylindrical Geometry.** Plot is zoomed in for more detail near the cavity wall.

**Table 4-4. Uncertain Parameters in DRSPALL Calculations (Kicker and Herrick 2013, Table 4).**

| Parameter | Variable | Implementation |
|---|---|---|
| Repository Permeability | REPIPERM | Waste permeability to gas local to intrusion borehole, implemented by parameter SPALLMOD/ REPIPERM.<br>Distribution: Loguniform<br>Maximum: 2.40E-12 $m^2$<br>Mean: 5.16E-13 $m^2$<br>Median: 2.40E-13 $m^2$<br>Minimum: 2.40E-14 $m^2$<br>Standard Deviation: 6.00E-13 $m^2$ |
| Repository Porosity | REPIPOR | Waste porosity at time of drilling intrusion, implemented by parameter SPALLMOD/REPIPOR.<br>Distribution: Uniform<br>Maximum: 6.60E-01<br>Mean: 5.05E-01<br>Median: 5.05E-01<br>Minimum: 3.50E-01<br>Standard Deviation: 8.95E-02 |
| Particle Diameter | PARTDIAM | Particle diameter of disaggregated waste, implemented by parameter SPALLMOD/ PARTDIAM.<br>Distribution: Loguniform<br>Maximum: 1.00E-01 m<br>Mean: 2.15E-02 m<br>Median: 1.00E-02 m<br>Minimum: 1.00E-03 m<br>Standard Deviation: 2.50E-02 m |
| Tensile Strength | TENSLSTR | Tensile strength of waste, implemented by parameter SPALLMOD/ TENSLSTR.<br>Distribution: Uniform<br>Maximum: 1.70E+05 Pa<br>Mean: 1.45E+05 Pa<br>Median: 1.45E+05 Pa<br>Minimum: 1.20E+05 Pa<br>Standard Deviation: 1.44E+04 Pa |

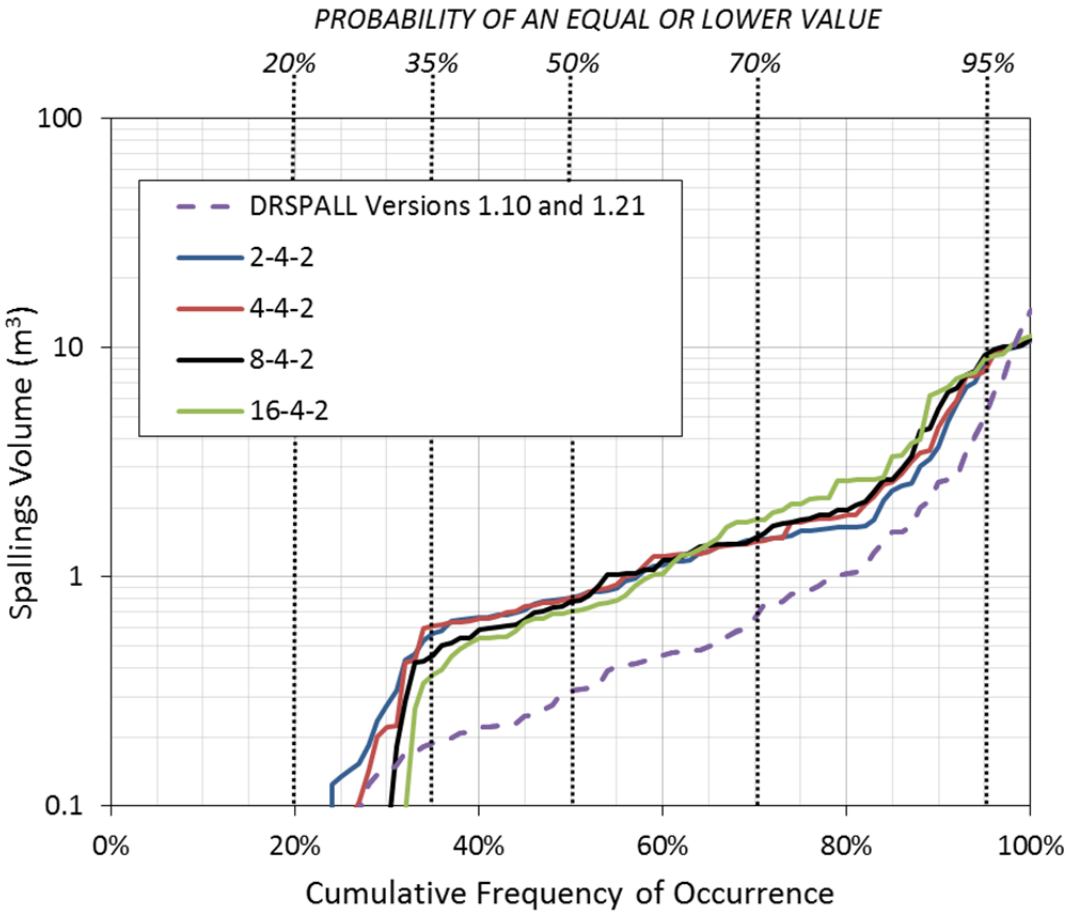


**Figure 4-9. The Distribution of Spallings Volumes for a 100-Vector Simulation (Replicate 1, Scenario 4) for a Range of Repository Zone Sizes.** Spallings volume data for test cases 2-4-2, 4-4-2, 8-4-2, and 16-4-2 are located in the Output module of the following CVS repositories:

- */nfs/data/CVSLIB/ WIPP_SPECIAL_ANALYSES/ DRSPALL_V122_ZONE_SIZE_ SENSITIVITY/ test1_02_04_02/DRSPALL*
- */nfs/data/CVSLIB/ WIPP_SPECIAL_ANALYSES/ DRSPALL_V122_ZONE_SIZE_ SENSITIVITY/ test2_04_04_02/DRSPALL*
- */nfs/data/CVSLIB/ WIPP_SPECIAL_ANALYSES/DRSPALL_V122_ZONE_SIZE_ SENSITIVITY/ test3_08_04_02/DRSPALL*
- */nfs/data/CVSLIB/ WIPP_SPECIAL_ANALYSES/DRSPALL_V122_ZONE_SIZE_ SENSITIVITY/ test4_16_04_02/DRSPALL*.

Spallings volume values at the selected probability levels are listed in Table 4-5. The DRSPALL Version 1.10 data shown were used in PA calculations beginning with the CRA-2004 PABC through the CRA-2014. The DRSPALL Version 1.21 spallings volume data (file *mspall_drs_PABC09_r1.out*) are located in the Output module of CVS repository, */nfs/data/CVSLIB/WIPP_ARCHIVES/PABC09/DRSPALL*.

**Table 4-5. Spallings Volume Cumulative Probability of Occurrence with Selected Levels of Probability for a 100-Vector Simulation (Replicate 1, Scenario 4).**

| Case | Percentage of Simulations with No Spallings | Spallings Volume ($m^3$) | | | | | | | |
|---|---|---|---|---|---|---|---|---|---|
| | | Range | | | Probability of Equal or Lower Value | | | | |
| | | Avg. | Min. | Max. | 20% | 35% | 50% | 70% | 95% |
| DRSPALL Versions 1.10 and 1.21 | 21% | 1.08 | 0.00 | 14.54 | 0.00 | 0.19 | 0.32 | 0.66 | 4.92 |
| 2-4-2 | 23% | 1.60 | 0.00 | 10.70 | 0.00 | 0.57 | 0.81 | 1.46 | 8.57 |
| 4-4-2 | 25% | 1.67 | 0.00 | 10.81 | 0.00 | 0.61 | 0.81 | 1.42 | 7.88 |
| 8-4-2 | 26% | 1.74 | 0.00 | 10.97 | 0.00 | 0.46 | 0.78 | 1.47 | 9.25 |
| 16-4-2 | 30% | 1.82 | 0.00 | 11.26 | 0.00 | 0.37 | 0.70 | 1.76 | 8.93 |

## 4.5. Wellbore Zone Size

The bottomhole pressure (BOTPRS), which results from the distribution of mud, waste and gas over the full length of the wellbore, provides a boundary condition for repository gas flow and waste solid stress calculations. The pressure difference between the repository and the wellbore drives gas flow in the pore space of the repository waste and can lead to waste failure and spall through the development of tensile effective stress. Therefore, sensitivity of BOTPRS to wellbore zone size ($\Delta z$) could have a significant impact on the overall sensitivity of DRSPALL. The effect of wellbore zone size is shown in Figure 4-10 where BOTPRS is compared for zone sizes of 1 and 2 m. BOTPRS shows excellent convergence for these zone sizes with only very slight timing differences throughout the pressure history.

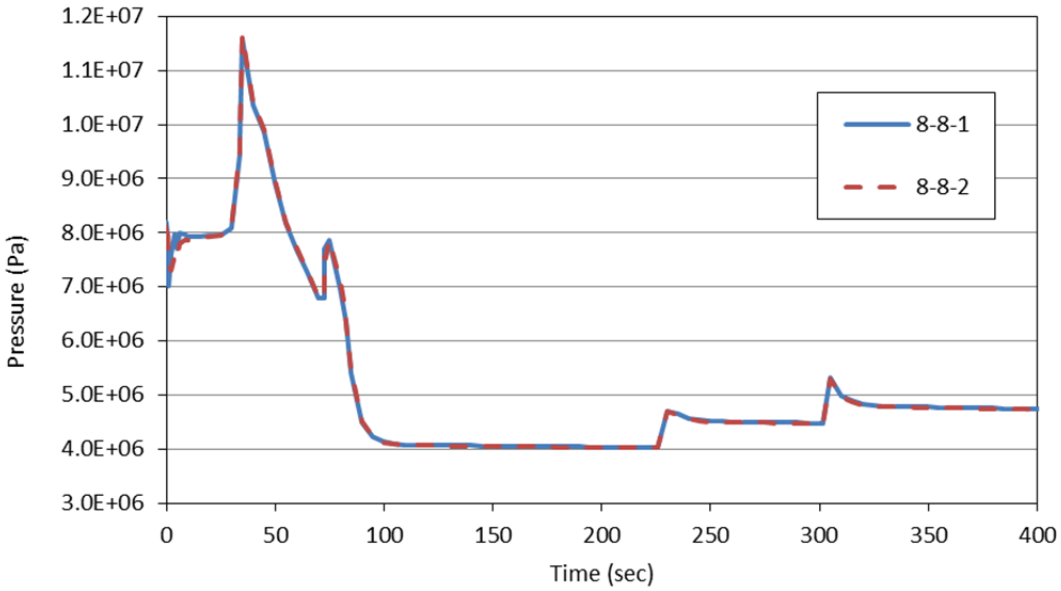


**Figure 4-10. Bottomhole Pressure (BOTPRS) History for Two Wellbore Zone Sizes.**

## 4.6. Recommendations for DRSPALL Zone Size Parameters

Zone size studies are used to ensure that the zone size being used for calculations is sufficient to consistently and accurately produce a solution. Recall that tensile failure is evaluated using the average tensile stress over the characteristic length. As the characteristic length increases and approaches the width of tensile region in the radial effective stress, failure becomes less likely because the average stress becomes less tensile. Decreasing the characteristic length could also reduce the likelihood of tensile failure as it approaches the zone size of the cell nearest the boundary (radial effective stress is zero at the wellbore interface).

This study used a range of 2.5 to 20 zones per characteristic length and showed that 2.5 zones per characteristic length (i.e., $LR$ = 2.5) are not sufficient for effectively evaluating failure. Evaluation of cavity radius histories indicates that a repository zone size ranging from 0.002 m to 0.008 m will maximize the spallings volume output and a characteristic length to zone size ratio ranging from 10 to 20 will maximize the spallings volume output.

The cavity radii in DRSPALL showed excellent convergence with zone size refinement over the range investigated, while the solution variables of pore pressure, solid stress, and spallings volume also showed convergence as zone size is reduced over the same range (Figures 4-5 and 4-9). Figure 4-5e shows similar radial effective stress profiles when the zone size is 0.004 m or less, suggesting the repository zone size should not exceed 0.004 m. Based on the data presented in the zone size study, the following ranges are likely to give consistent and reproducible results:

- Repository zone size $\Delta r$ = 0.002 – 0.004 m
- Characteristic length $L_t$ = 0.04 m with 10 to 20 zones per characteristic length
- Wellbore zone size, $\Delta z$ = 1 – 2 m.

The zone size parameters for case 4-4-2 ($\Delta r$ = 0.004 m, $L_t$ = 0.04 m, and $\Delta z$ = 2.0 m) have been selected as the standard configuration for DRSPALL calculations. These values show a significant gain in efficiency over the smaller zone sizes tested (i.e., $\Delta r$ = 0.001 m and 0.002 m) without sacrificing accuracy.

*This page is intentionally left blank.*

# 5. CODE VERIFICATION AND VALIDATION

This section describes the verification and validation testing of the DRSPALL code. The test methodology is governed by Nuclear Waste Management Program Procedure NP 19-1 *Software Requirements* (Long 2014), implemented for all WIPP PA codes used in compliance calculations. The NP 19-1 procedure was developed by Sandia National Laboratories to implement the regulatory software quality assurance requirements contained in 40 CFR 194.22 (EPA 1996).

The requirements for DRSPALL are listed in the *Requirements Document for DRSPALL Version 1.00* (WIPP PA 2003a). Those requirements are repeated below for convenience:

- Functional Requirements — In general DRSPALL shall calculate the volume of WIPP waste subject to material failure and transport to the surface as a result of an inadvertent drilling intrusion into the repository. More specifically DRSPALL will calculate the following:

  - **R.1**: Compressible, viscous, isothermal, multiphase mixture flow (mud, salt, waste, repository gas) in the wellbore using one-dimensional linear geometry and assuming a Newtonian fluid. Either laminar or turbulent flow shall be modeled depending on wellbore and fluid properties.

    Wellbore flow output variables will be evaluated against results from a commercial computational flow model configured to run the same test problem.

  - **R.2**: Repository gas flow as single-phase Darcy porous flow using either one dimensional cylindrical or spherical geometry

    Repository pressure distributions will be compared to independent solutions (numerical, analytic, or semi-analytic) of the governing equations obtained from published scientific literature.

  - **R.3**: Coupling of the wellbore and the repository flow models prior to and after penetration

    This requirement will be tested by reporting intermediate variables (pore velocity, gas density, cavity area) describing the mass flow between the repository and wellbore as a function of time in order to confirm mass balance.

  - **R.4**: Spalling (tensile) failure of the homogeneous waste material using an effective stress law with seepage forces

    The time-histories of the output variables pressure distribution, effective stress and tensile-failed volume will be examined for conceptually consistent behavior.

  - **R.5**: Fluidized bed transport of failed (disaggregated) waste material.

This requirement will be evaluated by comparing the DRSPALL fluidization velocity to that obtained from independent spreadsheet calculations.

- **R.6**: Mixture expulsion at the surface

  This requirement will be evaluated by reporting the time-history of waste expelled and computing a solids mass balance to assure that waste removed from the repository is accounted for at the surface.

- External Interface Requirements

  - **R.7**: DRSPALL shall read an input control file, which may be pre-generated using a text processor. It will contain numerical control parameters and, optionally, material properties and problem geometry.

  - **R.8**: Properties and non-numerical control parameters will, optionally, be read from a CDB.

  - **R.9**: Grid, properties, parameters and spatial and time dependent results will be written to an output CDB.

The verification and validation testing is described in greater detail in the *Verification and Validation Plan / Validation Document for DRSPALL Version 1.22* (WIPP PA 2015c), which contains listings of most input and output files.

All DRSPALL test cases were re-run with the modified code (DRSPALL Version 1.22). Three test cases were used to verify selected DRSPALL functionality, and one test case was designed to validate DRSPALL against observations from a field analog. The four test cases are summarized below and are presented in detail in following subsections:

- Porous flow – the transient, porous flow of gas through the repository waste material is verified, uncoupled from the wellbore flow model, with comparisons to a semi-analytical model developed by Djordjevic and Adams (2003).

- Coalbed methane validation – This test case examines the suitability of DRSPALL to simulate coalbed cavitation, an analog to the WIPP spallings scenario. DRSPALL is run with input parameters derived from a field-scale coalbed cavitation experiment by Khodaverdian et al. (1996), and measured results are compared to the DRSPALL output.

- Internal Logic checks – the following submodels are verified by spreadsheet calculations and visual examination of special detailed output files created during execution of this test case:
  - Coupling of wellbore and repository flow
  - Tensile failure
  - Fluidized bed transport of disaggregated waste
  - Expulsion of disaggregated waste at the ground surface

- Wellbore flow –the flow of a multicomponent fluid in the wellbore is verified, uncoupled from the repository model, with comparisons against an independent computational fluid dynamics model, FLUENT (2003). Results from six calculations with different combinations of fluid constituents (mud, gas, solid) are compared.

## 5.1. Test Case #1 – Porous Flow Verification

### 5.1.1. Test Objective

The purpose of this test case is to determine whether DRSPALL can accurately calculate transient gas pressures in the repository during the first few seconds after a borehole intrusion. The porous flow test problem is implemented by comparing the one-dimensional cylindrical and spherical pressure profiles generated by DRSPALL to those calculated using the utility code developed by Djordjevic and Adams (2003) for an identical problem.

Correctly performing this test case validates the satisfactory implementation of Functional Requirement R.2.

### 5.1.2. Problem Description

This test case involves solving the equations of transient, radial, isothermal, compressible gas flow through a porous medium. In this test case, no failure of the medium or transport of solids is allowed. Furthermore, the coupling of mass flow between the wellbore and repository is simplified to a zero pressure boundary condition. As such, the wellbore calculations in DRSPALL are ignored. The problem is solved in both cylindrical and spherical geometry.

#### 5.1.2.1. Cylindrical Geometry Equations

The cylindrical domain comprises a porous solid with a given porosity $\varphi$ and permeability $k$, shown in Figure 5-1. There is a cylindrical cavity of radius $r_o$ aligned with the axis that represents a borehole that depressurizes the simulated repository. The domain begins filled with an ideal gas at an initial pressure of $P_1$ with viscosity $\eta$. At $t > 0$, the gas pressure $p$ inside the borehole is set to zero, thus creating a pressure step that diffuses radially outward through the domain.

Starting with the governing equation for flow of gas through a porous material in a radially symmetric system gives:

$$\frac{\partial p}{\partial t} = \frac{k}{2\varphi\eta}\nabla^2 p^2, \quad p = p(r,t), \quad r \geq r_{0,} \quad t \geq 0 \tag{5.1-1}$$

where $p$ is the gas pressure in the porous medium at radius $r$ and time $t$. The boundary and initial conditions are expressed as:

$$p(r_0,t) = f(t), \quad \lim_{r\to\infty} p(r,t) = p_{ff}, \quad p(r,0) = p_{ff} \tag{5.1-2}$$

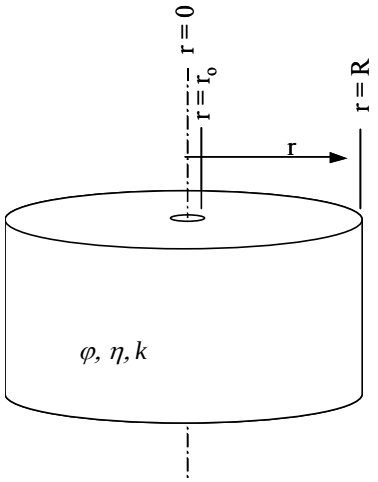


**Figure 5-1. Schematic of Cylindrical Domain for Porous Flow Test Problem.**

where $p_{ff}$ is the far-field pressure at large $r$. For this problem, the pressure at the inner boundary $r_o$ representing the wellbore wall is held constant at zero. As such, $f(t) = 0$ for $t > 0$.

A pseudopressure approach is introduced after Chan et al. (1993) utilizing the following change of variables:

$$\psi(p) = \frac{p^2}{\eta} \tag{5.1-3}$$

which leads to

$$\frac{\partial \psi}{\partial t} = \frac{k}{\varphi \sqrt{\eta}} \sqrt{\psi} \nabla^2 \psi, \quad \psi = \psi(r,t), \quad r \geq r_{0,} \quad t \geq 0 \tag{5.1-4}$$

and

$$\psi(r_0,t) = \frac{f^2}{\eta}, \quad \lim_{r \to \infty} \psi(r,t) = \frac{p_{ff}^2}{\eta}, \quad \psi(r,0) = \frac{p_{ff}^2}{\eta} \tag{5.1-5}$$

Nondimensional parameters may be defined as follows:

$$\psi = \frac{p_{ff}^2}{\eta} \Psi \quad t = t_0 \tau, \quad t_0 = \frac{\varphi \eta r_0^2}{k p_{ff}} \tag{5.1-6}$$

and for cylindrical coordinates:

$$z = \ln(\frac{r}{r_0}) \tag{5.1-7}$$

which upon substitution into Equation 5.1-4 yields the transformed equation:

$$\frac{\partial \Psi}{\partial \tau} = e^{-2z}\Psi^{1/2}\frac{\partial^2 \Psi}{\partial z^2} \tag{5.1-8}$$

Equation 5.1-8 is integrated numerically with the boundary and initial conditions

$$\Psi(0,\tau) = \frac{f^2}{p_{ff}^2}, \quad \lim_{z\to\infty}\Psi \to 1, \quad \Psi(z,0) = 1 \tag{5.1-9}$$

### 5.1.2.2. Spherical Geometry Equations

For the spherical problem, the cavity is hemispherical in shape with radius $r_o$ as shown in Figure 5-2.

Equations 5.1-4 to 5.1-6 apply to the spherical geometry, but in order to proceed, z must be re-defined as:

$$z = \frac{r_o}{r} \tag{5.1-10}$$

The resulting transformed governing equation is then

$$\frac{\partial \Psi}{\partial \tau} = z^4\Psi^{1/2}\frac{\partial^2 \Psi}{\partial z^2} \tag{5.1-11}$$

Equation 5.1-11 is integrated numerically with the boundary conditions

$$\Psi(1,\tau) = \frac{f^2}{p_{ff}^2}, \quad \Psi(0,\tau) = 1, \quad \Psi(z,0) = 1 \tag{5.1-12}$$

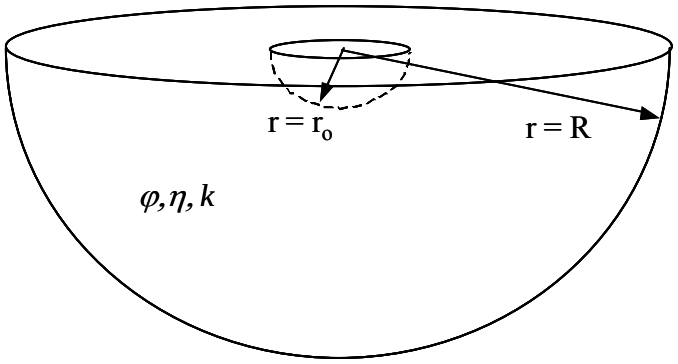


**Figure 5-2. Schematic of Spherical Domain in Porous Flow Test Problem.**

### 5.1.2.3. Boundary Conditions

The Djordjevic and Adams (2003) solution, modeled after Chan et al. (1993), requires that (1) the gas pressure at $r = r_o$, the face of the borehole, is set to zero at all times, and (2) pressure in the far field, where $r >> r_o$, remains at the initial pressure, $P_1$. During normal execution of DRSPALL, the pressure at the inner boundary $r_o$ is calculated by coupling mass flows from the repository and wellbore. However, for purposes of this test case, the cavity pressure variable is assigned a value of zero during each computational loop. This will cause the cavity mass to artificially increase, but will not cause inaccuracy in the validation procedure, since the cavity mass is irrelevant in this test case.

At the outer boundary ($r = R$), DRSPALL uses a no-flow condition. Djordjevic and Adams (2003) and Chan et al. (1993), however, use a constant pressure in the far-field, $p_{ff}$.. This difference will not be recognized by the models for the short execution times used in this test case because the pressure impulse travels at a finite speed away from the borehole, and will not reach the outer boundary in the time specified for this test. This can be confirmed by computing the approximate depth of penetration of a "dividing surface" defined as the point inside which $P(r) < P_1$, and outside which $P(r) = P_1$.

Chan et al. (1993) gives an approximate location of the dividing surface, $R(t)$, for small values of $t$ in the cylindrical domain as follows:

$$\frac{R(t)}{a} = 1 + \sqrt{\frac{t}{t_o}} \tag{5.1-13}$$

The default outer radius in DRSPALL is 19.2 m. Recognizing that $t/t_o = \tau$, the expression above evaluates to $R = 0.649$ m when $\tau = 10$ and $a = 0.156$ m. $\tau = 10$ represents the longest scaled time evaluated in this test problem. The dividing surface is therefore clearly interior to the outer boundary for this and shorter times.

Chan gives another expression for the approximate location of the dividing surface at large $t$:

$$\frac{R(t)}{a} \cong \frac{(t/t_o)^{0.5}}{[\log(t/t_o)]^{0.5}} \tag{5.1-14}$$

If the DRSPALL outer boundary of 19.2 m is substituted into Equation 5.1-14 for $R$, and $t_o$ is evaluated with the input values given in Table 5-1, the resulting time $t$ that satisfies the expression is $t \approx 2600$ s. Thus, for the short times ($t < 4$ s) examined in this test case, the pressure impulse will not reach the boundary of the domain and the specific boundary conditions are irrelevant.

### 5.1.2.4. Input Parameters

Relevant input parameters for this test case are given in Table 5-1. To avoid tensile failure of the repository material, tensile strength ($T_s$) is set to a high value of 0.690E+06 Pa (100 psi). The Forchheimer Beta input parameter was set to zero for Test Case #1, resulting in a constant

permeability by removing the velocity-dependence. The DRSPALL input files *drs_v122_tc11.drs* and *drs_v122_tc12.drs* are stored in CVS directory /nfs/data/CVSLIB/ WIPP_CODES/PA_CODES/DRSPALL/Test/Input. Note that the zone size growth rates were changed to 1.0 for the DRSPALL 1.22 validation (WIPP PA 2015c, Section 4.0).

**Table 5-1. Input Parameters for Test Case #1.**

| Symbol | Definition | Units | Value |
|---|---|---|---|
| $P_1$ | Initial gas pressure | Pa | 0.145E+08 |
| $\varphi$ | Porosity | – | 0.575 |
| $\eta$ | Gas viscosity | Pa·s | 0.8934E-05 |
| $k$ | Permeability | $m^2$ | 2.400E-13 |
| $T_s$ | Tensile strength | Pa | 0.690E+06 |

#### 5.1.2.5. Repository Zoning

The zoning scheme in the repository domain in DRSPALL is set to a constant zone size of 0.002 m.

### 5.1.3. Analysis Methods

Chan et al. (1993) present numerical results as the dimensionless pseudopressure, $\Psi$, versus the dimensionless plotting parameter, $\zeta$, for selected values of scaled time, $\tau$. The dimensionless plotting parameter, comparable to a dimensionless radius, is defined as:

$$\zeta = \frac{\left(e^{z} - 1\right)}{\tau^{1/2}} \tag{5.1-15}$$

This analysis entails comparing DRSPALL and Djordjevic and Adams (2003) pseudopressure profiles at designated scaled times. DRSPALL output in the form *P(r, t)* are thus converted to $\Psi(\zeta,\tau)$ at the four scaled times 0.01, 0.1, 1.0, 10. Output from DRSPALL and Djordjevic and Adams (2003) are displayed both graphically and in tabular form.

To provide a quantitative means for comparing DRSPALL and the independent solutions, the difference in $\Psi(\zeta)$ is computed for corresponding scaled times as follows:

$$DIFF(\zeta) = \left|\Psi(\zeta)_{DR\_SPALL} - \Psi(\zeta)_{Chan}\right| \tag{5.1-16}$$

For each array of DIFF values, a maximum value is calculated.

### 5.1.3.1. Cylindrical Case Output from Djordjevic and Adams (2003)

The cylindrical case solutions were obtained using the independent utility code developed by Djordjevic and Adams (2003). Dimensionless pseudopressure profiles were produced at four dimensionless times, $\tau = 0.01, 0.1, 1.0, 10$. The solutions are illustrated graphically in Figure 5-3. Tabular results are given in Appendix B.2 of the *Verification and Validation Plan and Validation Document for DRSPALL Version 1.00* (WIPP PA 2003b).

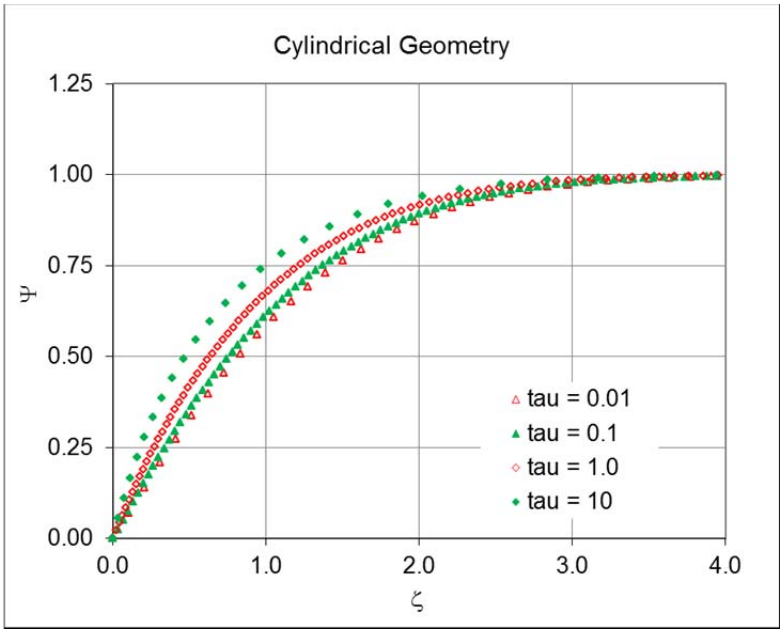


**Figure 5-3. Numerical Solutions to the Dimensionless Pseudopressure Profiles for Cylindrical Geometry.**

Since the numerical grid used in DRSPALL may be different from that used in the comparison solutions shown in Figure 5-3, a curve was fit to the comparison data to facilitate computation of the difference defined in Equation 5.1-16. The general form of the function fit to the comparison data was:

$$\Psi(\zeta) = 1\text{-}\exp\{-(C_1\zeta+C_2\zeta^2+C_3\zeta^3)\} \quad \text{for } 0 \geq \zeta \geq 1 \tag{5.1-17}$$

where $C_1$, $C_2$, and $C_3$ are constants determined by minimizing the sum of squares:

$$SUM = \sum_i \left[\Psi(\zeta)_a - \Psi(\zeta)_b\right]^2 \tag{5.1-18}$$

where the subscript *a* denotes the solution calculated by Djordjevic and Adams (2003), the subscript *b* denotes the value of the functional fit, and the sum is taken over all the reported grid indices *i*. The constants calculated for the four dimensionless times in the cylindrical geometry are given in Table 5-2. Details of the fitting procedure are provided in Appendix B.6 of the *Verification and Validation Plan and Validation Document for DRSPALL Version 1.00* (WIPP PA 2003b).

**Table 5-2. Constants for Functional Fit to Djordjevic and Adams (2003) Solution in Cylindrical Geometry.**

| $\tau$ | $C_1$ | $C_2$ | $C_3$ |
|---|---|---|---|
| 0.01 | 0.715 | 0.167 | 0.000 |
| 0.1 | 0.803 | 0.157 | 0.000 |
| 1 | 1.032 | 0.101 | 0.000 |
| 10 | 1.505 | -0.071 | 0.000 |

### 5.1.3.2. Spherical Case Output from Djordjevic and Adams (2003)

The spherical case solutions were obtained using an independent utility code developed by Djordjevic and Adams (2003). Dimensionless pseudopressure profiles were produced at the same four dimensionless times ($\tau$ = 0.01, 0.1, 1.0, 10) as for the cylindrical case. The solutions are illustrated graphically in Figure 5-4. Tabular results are given in Appendix B.2 of the *Verification and Validation Plan and Validation Document for DRSPALL Version 1.00* (WIPP PA 2003b). Functions in the form of Equation 5.1-17 were fit to the data using a least squares method with associated constants reported in Table 5-3, and details of the fitting procedure shown in Appendix B.6 of the *Verification and Validation Plan and Validation Document for DRSPALL Version 1.00* (WIPP PA 2003b).

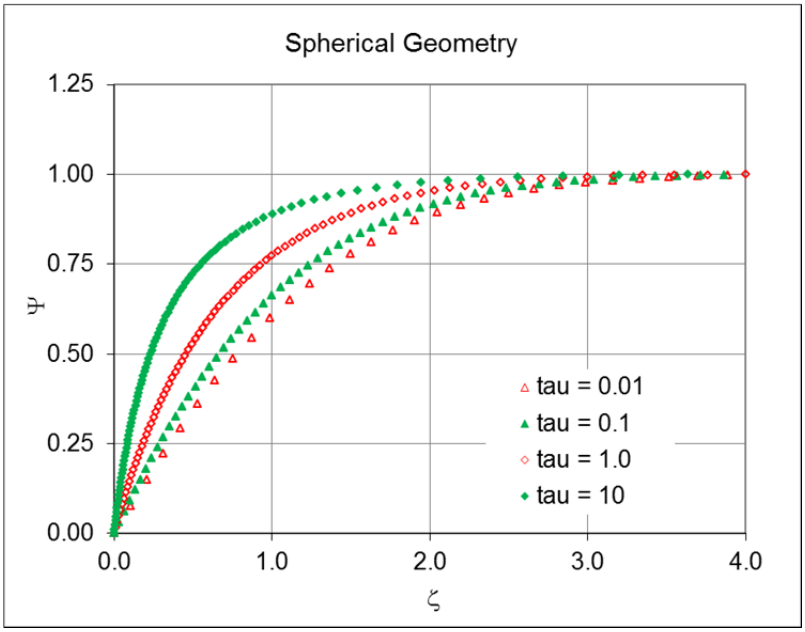


**Figure 5-4. Numerical Solutions to the Dimensionless Pseudopressure Profiles for Spherical Geometry.**

**Table 5-3. Constants for Functional Fit to Djordjevic and Adams (2003) Solution in Spherical Geometry.**

| $\tau$ | $C_1$ | $C_2$ | $C_3$ |
|---|---|---|---|
| 0.01 | 1.331 | -0.073 | 0.000 |
| 0.1 | 1.000 | 0.126 | 0.000 |
| 1 | 1.537 | -0.033 | 0.000 |
| 10 | 3.500 | -2.229 | 0.858 |

### 5.1.4. Test Procedure

DRSPALL is executed twice: once in cylindrical geometry and once in spherical geometry. Case 1.1 (tc11) refers to cylindrical geometry; Case 1.2 (tc12) refers to spherical geometry.

DRSPALL generates a "chan" validation file (e.g., *drs_122_tc11_chan.dat*) for each case. The validation files are imported to Excel file *drs_v122_tc1.xlsx* for post-processing and plotting. The output CAMDAT files are not examined.

The following command lines run both cases:

```
./drspall ./Input/drs_v122_tc11.drs DRSPALL/Test/Output/Solaris_122/drs_122_tc11.dbg
        CANCEL DRSPALL/Test/Output/Solaris_122/drs_122_tc11.cdb
        > DRSPALL/Test/Output/Solaris_122/drs_122_tc11.crt
./drspall ./Input/drs_v122_tc12.drs DRSPALL/Test/Output/Solaris_122/drs_122_tc12.dbg
        CANCEL DRSPALL/Test/Output/Solaris_122/drs_122_tc12.cdb
        > DRSPALL/Test/Output/Solaris_122/drs_122_tc12.crt
```

### 5.1.5. Acceptance Criteria

Test Case #1 will pass if the following statements are true for both the cylindrical case and the spherical case:

- **Acceptance Criterion 1-1** — Visual inspection of the pressure profiles generated by DRSPALL indicates a close approximation to the solutions by Djordjevic and Adams (2003) for corresponding dimensionless times.

- **Acceptance Criterion 1-2** — Maximum difference for $\Psi$ (dimensionless) between DRSPALL and Djordjevic and Adams (2003) for corresponding times does not exceed 0.1.

### 5.1.6. Results

The dimensionless pseudopressure ($\Psi$) is plotted versus the dimensionless plotting parameter ($\zeta$) at four selected values of dimensionless time ($\tau$). The comparison curves on each plot were generated from the parameters in Table 5-2 for the cylindrical geometry and Table 5-3 for the spherical geometry. Conceptually, the curves represent the evolution of the pore pressure profile.

The initial condition is set to $\Psi = 1$ throughout the domain. For $\tau > 0$, $\Psi$ at the inner boundary of the domain, $\zeta = 0$, is set to zero representing zero pressure in the wellbore. The outer boundary $\Psi$ is held at unity representing a constant far-field pressure. The tendency of the curves at different $\tau$ to nearly overlay one another is related, in part, to the presence of the $t^{-0.5}$ in the plotting parameter function (Equation 5.1-15).

Figure 5-5 shows the results of Case 1.1 in the cylindrical geometry, and Figure 5-6 shows the results of Case 1.2 in the spherical geometry. Visual inspection indicates that in both cases the DRSPALL results overlay the Djordjevic and Adams (2003) solutions quite closely, so **Acceptance Criterion 1-1** (Section 5.1.5) is met. The magnitude and shape of the curves match well over the entire range of interest.

The simple statistical analysis that reports the maximum value of DIFF also indicates close overlay, with values below 0.05 for all $\tau$ examined. The DIFF values for all times examined for both cylindrical and spherical geometry are summarized in Table 5-4. DIFF values for the cylindrical case ranged from 0.007 to 0.045, representing a favorable match between DRSPALL and the comparison solution. For the spherical case, the maximum differences fall at 0.016 or below, indicating close agreement between solutions. All maximum differences are less than 0.1, so **Acceptance Criterion 1-2** (Section 5.1.5) is met.

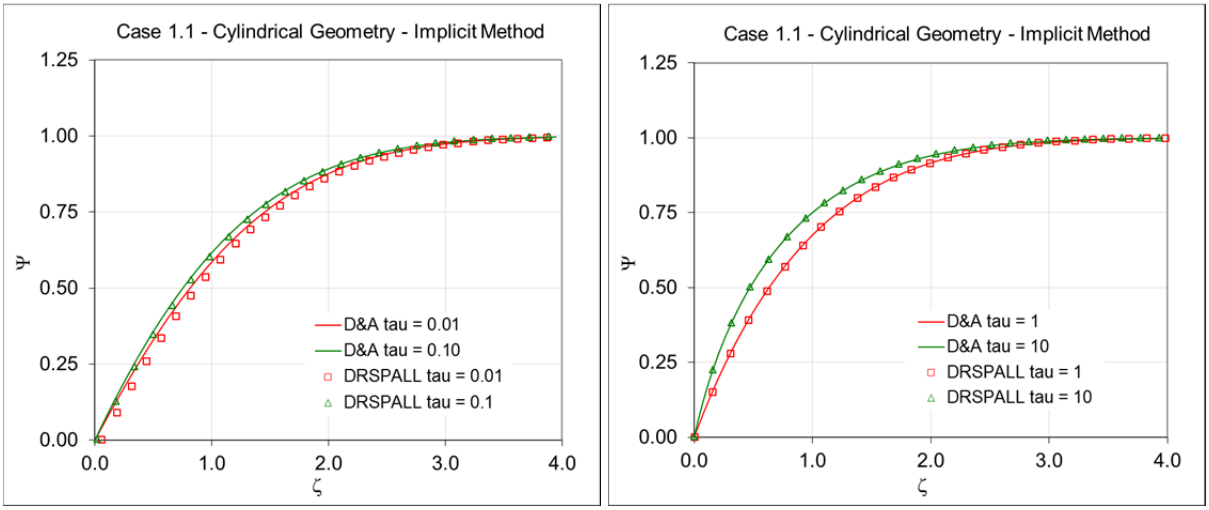


**Figure 5-5. Overlay of DRSPALL with Djordjevic and Adams Solutions for the Cylindrical Geometry with $\tau$ = 0.01, 0.1, 1, 10.**

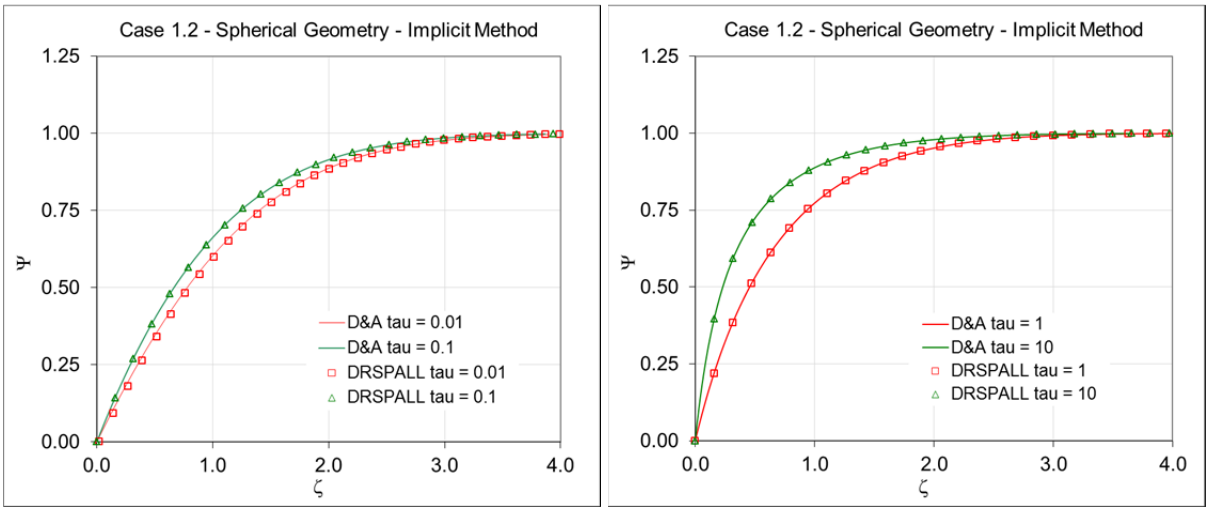


**Figure 5-6. Overlay of DRSPALL with Djordjevic and Adams Solutions for the Spherical Geometry with $\tau$ = 0.01, 0.1, 1, 10.**

**Table 5-4. Maximum Difference Values for Implicit Solution in Cylindrical and Spherical Geometry.**

| $\tau$ | Case 1.1 Cylindrical Maximum Difference | Case 1.2 Spherical Maximum Difference |
|---|---|---|
| 0.01 | 0.045 | 0.016 |
| 0.1 | 0.016 | 0.006 |
| 1 | 0.007 | 0.007 |
| 10 | 0.014 | 0.013 |

### 5.1.7. Conclusions

The discussion in Section 5.1.6 verifies that all acceptance criteria (Section 5.1.5) for this test case are met for both the cylindrical and spherical geometry. Thus, this test case passes.

The successful completion of this test case demonstrates that the DRSPALL solutions to transient, compressible, ideal gas flow compare favorably to those generated by an independent utility code developed by Djordjevic and Adams (2003). Both codes utilize an implicit solution algorithm to solve an initial boundary value problem that represents the evolution of pore pressure and resulting blowdown in a simplified gas repository following intrusion by an underbalanced (low-pressure) borehole.

## 5.2. Test Case #2 – Coalbed Methane Validation

### 5.2.1. Test Objective

The purpose of this test case is to demonstrate that DRSPALL can simulate the results of a field-scale coalbed cavitation completion experiment. Since this process of completing a coalbed methane well involves injecting high-pressure air and allowing a controlled blowout to occur which fails the coal and transports coal particles to the surface, it would appear to be an acceptable analog of the repository drilling intrusion spall phenomenon. The coalbed data chosen for comparison are reported by Khodaverdian et al. (1996).

Test Case #2 demonstrates the applicability of DRSPALL to simulating a drilling intrusion into the WIPP repository by modeling a field scale experiment that has similar characteristics. Test Cases #1, #4, and #5 are used to verify that DRSPALL correctly implements all requirements. Test Case #2 exercises all requirements except R.8 (input from CAMDAT file), but does not explicitly address any requirements directly. Some requirements are only partially exercised, i.e. there is no mud flow.

### 5.2.2. Problem Description

#### 5.2.2.1. Coalbed Cavitation

Coal is a naturally fractured organic material. The fractures, usually orthogonal and closely-spaced, are called “cleats.” In-situ, the cleats are normally saturated with water and methane. Cleat porosity is usually a few percent. Coal, however, is different than most other geologic materials in that its matrix can hold abundant methane in an adsorbed state. When a coal reservoir is de-watered, this adsorbed methane can flow to the cleats and then to a well. As a result, the amount of methane producible from some coal reservoirs is as if porosity was several tens of percent, rather than just a few percent. Because of this, these coal reservoirs are often drilled and produced as a methane source.

Wells in parts of certain coal reservoirs are most successfully completed using the “cavitation” process. To do this, the well is first drilled and cased to the top of the coal seam. Drilling then continues through the coal seam, which is left as an open hole. The completion process then takes several days to more than a week. The well is cyclically open to atmosphere and allowed to blow down, and then shut in and allowed to build up. When this is done (rarely) without any surface pumping, it is called “natural” cavitation. More often, air is introduced by high-pressure pumping at the surface to downhole pressures somewhere between reservoir pressure and lithostatic. This is “induced” cavitation. Anywhere from a few to many tens of cycles may be used, with possible bit runs between cycles to clean out the hole. When a cavitated well is blowing, a strongly flowing mixture of air, coal fines, methane, and some water comes to the surface. This is, in effect, an induced but controlled blowout. If successful, the cavitation process produces a cavity of a few meters in diameter in the coal and leads to greatly enhanced water and ultimately, methane production.

#### 5.2.2.2. An Acceptable Analog

Coalbed cavity completions would appear to be analogs to the WIPP drilling intrusion. This is because cavitated coal seams may be:

- in the same depth regime
- in the same thickness regime
- in the same mechanical property regime
- gas-pressurized during cavitation to the same pressure regime
- blown down in the same time regime as possible drilling intrusion occurrences.

Possible shortcomings of coalbed cavitation as an analog are that peak coal cavitation pressures are somewhat lower than peak possible WIPP pressures and the strength of coal may be outside the WIPP tensile strength range, with particulate properties that may be different than degraded WIPP waste.

### 5.2.3. Analysis Method

#### 5.2.3.1. Selected Field Test for Comparison

The cavitation experiments on the GRI COAL Site Well I#2 (Khodaverdian et al. 1996) have been selected for numerical simulation using DRSPALL. This selection was made based on the availability and quality of data. The well is in the Fruitland coals located in the San Juan Basin of New Mexico, and shown in Figure 5-7. The well was cavitated in July of 1991.

The key parameters, as reported by Khodaverdian et al. (1996), of the selected coal well are given in Table 5-5. After all cavitation procedures were finished, the final cavity diameter was determined by sonar logging, and is shown in Figure 5-8.

#### 5.2.3.2. Approach

The authors (Khodaverdian et al. 1996) used observed surface injection pressures to estimate bottomhole pressures over time for the various cavitation cycles, as shown for the first day of cavitation activities, in Figure 5-9.

The first day saw 6 cavitation cycles. Khodaverdian et al. felt most cavity growth was completed in that time, and have assumed so for their analysis. As can be seen from Figure 5-9, they assumed an instantaneous drawdown to 80 psi downhole upon the start of each cavitation blowdown. In actuality, the drawdown rate would depend on pipe flow to surface and take some time (a minute or so) to develop. DRSPALL simulates the drawdown time and rates, since it includes viscous pipe flow. The relevant values in the figure are thus the peak injection pressures and the cavitation time intervals. These pressures and times are simulated in DRSPALL. The duration of the last blowdown interval is not reported, but is assumed by us to be the same as #5.

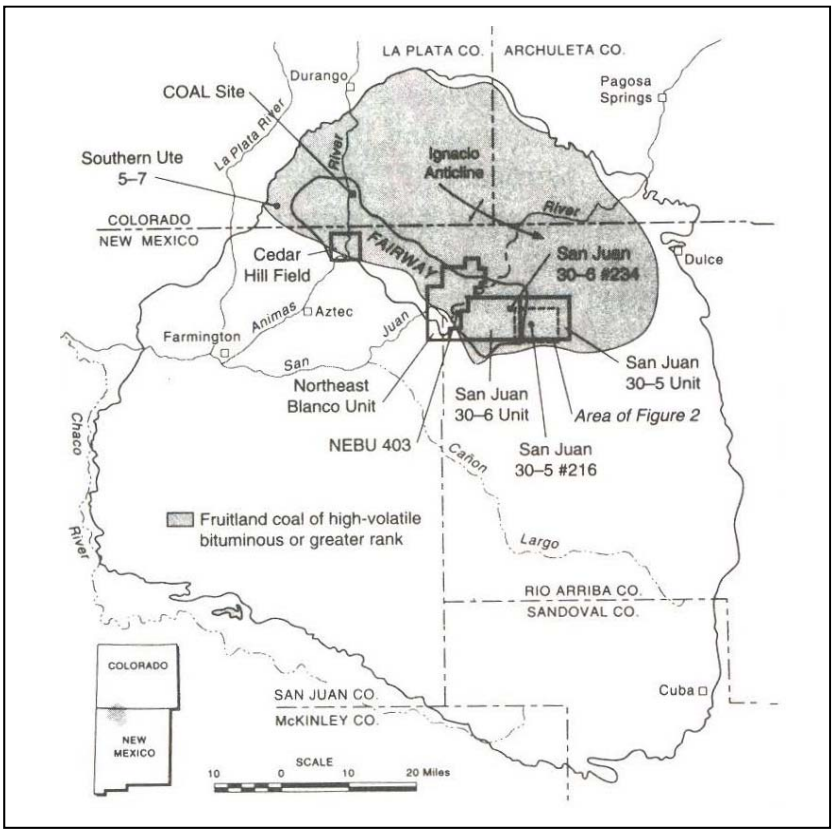


**Figure 5-7. Location of Cavitated Coalbed Well (Khodaverdian et al. 1996).**

**Table 5-5. Key Coal Well Parameters.**

| Parameter | Value (US) | Value (SI) |
|---|---|---|
| Depth | 3150 ft | 960 m |
| Thickness | 45 ft | 13.7 m |
| Bit Radius | 0.5 ft | 0.15 m |
| Post-Drilling (washout) Radius | 1.0 ft | 0.3 m |
| Horizontal Stress | 2220 psi | 15.3 MPa |
| Pore Pressure | 1020 psi | 7.0 MPa |
| Permeability | 25 md | $2.5 \times 10^{-14}$ $m^2$ |

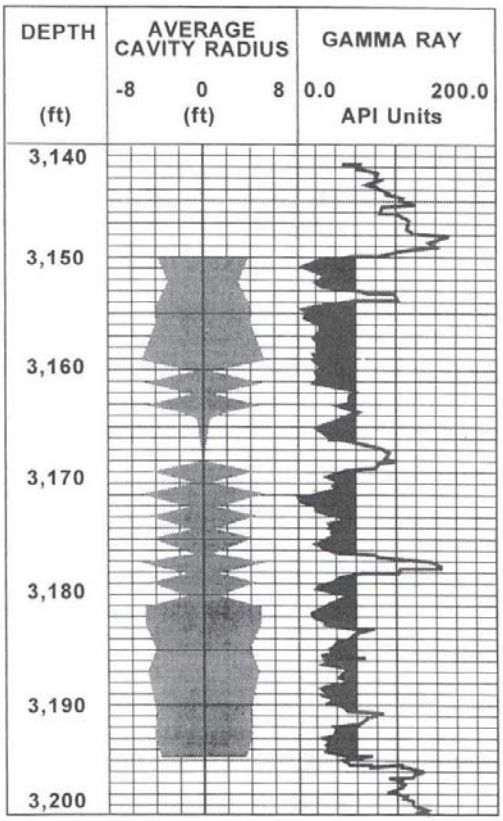


**Figure 5-8. Cavity Radius (Khodaverdian et al. 1996).**

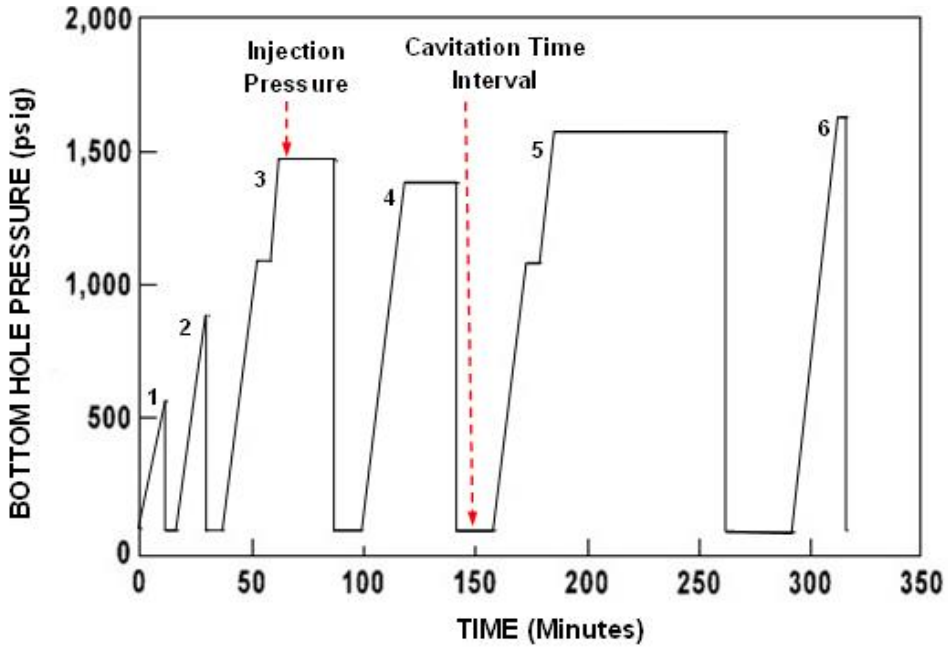


**Figure 5-9. Cavitation Times and Inferred Bottomhole Pressures (Khodaverdian et al. 1996).** Red arrows added for this report.

Khodaverdian et al. used a numerical model (without accounting for wellbore flow) to reproduce their interpretation of the final cavity diameter (after 6 cycles) from Figure 5-8. Their model used the tensile failure radius as the cavity radius. Their calculations for earlier cycles thus were used to infer the cavity diameters vs. time. They used a number of permeability values (2.5, 25, and 250 md) in an attempt to match the measured results, and found that a 25-md permeability gave the best match. This was accepted for their primary interpretation, supported also by rough laboratory measurements and other observations. Considerable uncertainty is added by having to interpret an average cavity size from the irregular data shown in Figure 5-8. Their final matching interpretations are shown in Figure 5-10. The input pressures and times, and results to compare with DRSPALL, as we obtain from the author's figures, are shown in Table 5-6.

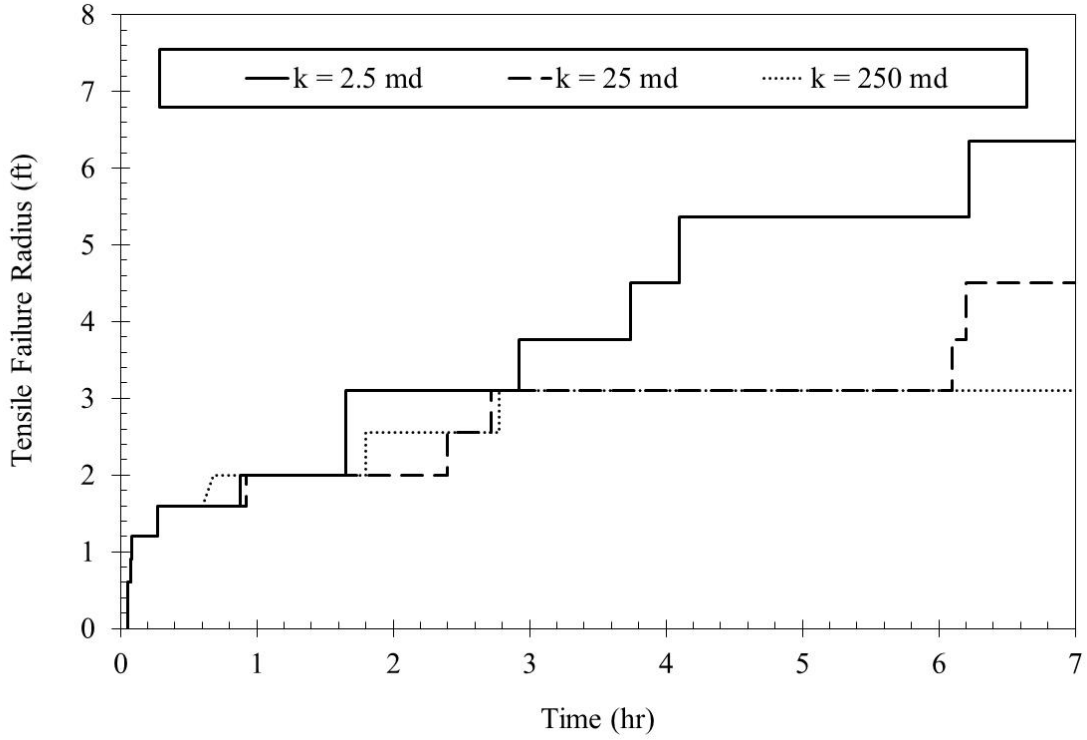


**Figure 5-10. Interpreted Cavity Radii (Based on Tensile Failure Radii) from Khodaverdian et al. (1996).**

**Table 5-6. Input Values and Experimental Results to be Used and Compared with DRSPALL Results.**

| Cycle | Pressure, MPa | Duration, s | Cavity Radius, m Best Estimate | Cavity Radius, m Range |
|---|---|---|---|---|
| 1 | 3.8 | 300 | 0.31 | .31 – .31 |
| 2 | 6.2 | 360 | 0.49 | .49 – .61 |
| 3 | 10.1 | 660 | 0.61 | .61 – .91 |
| 4 | 9.6 | 900 | 0.73 | .61 – .91 |
| 5 | 11.0 | 1680 | 0.91 | .91 – 1.65 |
| 6 | 11.4 | 1680 | 1.37 | .91 – 1.8 |

#### 5.2.3.3. Input Parameters

DRSPALL is set up for these runs to only model the wellbore from the cavity to the surface, with flow allowed in the annulus. Also, only gas (air) and coal particles are allowed to flow. The code is run in cylindrical symmetry to best match the observed cavity geometry. For each of the six runs required, an initial formation (repository) gas pressure is set to match the value in Table 5-6 and an initial cavity size is set to match the previous run results. The first cavity size is 0.31 m. Each run continues for the reported time. Recall that the duration of the last cavitation cycle is unknown, which adds additional uncertainty to the results for the last cavitation cycle.

DRSPALL results will depend on the tensile strength and permeability assumed in DRSPALL. It is unclear as to the exact tensile strength Khodaverdian et al. assumed. They discuss cohesion in detail as it pertains to shear failure, but not tensile strength explicitly. The DRSPALL input files *drs_v122_tc21.drs* through *drs_v122_tc26.drs* are stored in CVS directory /nfs/data/ CVSLIB/WIPP_CODES/PA_CODES/DRSPALL/Test/Input. All runs are the same, except for initial pressure, initial cavity size, and run time. Note that the zone size growth rates were changed to 1.0 for DRSPALL 1.22, as explained in the DRSPALL validation documentation (WIPP PA 2015c, Section 4.0). The following parameters that were assumed for the DRSPALL 1.21 validation have remained unchanged in the 1.22 validation: tensile strength is 0.25 MPa, permeability is 3.0 md (3.0E-15 $m^2$), and the minimum characteristic velocity is 0.5 m/s.

### 5.2.4. Test Procedure

DRSPALL is executed six times, once for each run. Each of the six DRSPALL runs is a subcase (Cases 2.1 through 2.6, labeled as tc21 through tc26).

For this validation, the cavity radius is extracted from the output CAMDAT files with a single SUMMARIZE (WIPP PA 2005 and 2012b) execution; for the DRSPALL 1.00 validation the same data was manually extracted from each diagnostics file. The SUMMARIZE input file is shown in Figure 5-11. The SUMMARIZE output is imported to Excel file *drs_v122_tc2.xlsx* for plotting.

The following command lines show the DRSPALL execution for Case 2.1 (Cases 2.2 through 2.6 are similar), and the single SUMMARIZE execution:

```
./drspall ./Input/drs_v122_tc21.drs DRSPALL/Test/Output/Solaris_122/drs_122_tc21.dbg
        CANCEL DRSPALL/Test/Output/Solaris_122/drs_122_tc21.cdb
        > DRSPALL/Test/Output/Solaris_122/drs_122_tc21.crt
… similarly for tc22, tc23, tc24, tc25, tc26
./summarize ./Input/drs_tc2_summarize.inp
        DRSPALL/Test/Output/Solaris_122/drs_122_tc2^.cdb
        DRSPALL/Test/Output/Solaris_122/drs_122_tc2_summarize.tbl
        drs_122_tc2_summarize.log NO   > x.x
```

```
! For DRSPALL Test Case 2, all 6 subcases
! Derived from GROPECDB file of HVAR CAVRAD at TIME 10000
!
! Note that final cdb times range from 300 to 1680.  Requesting a large time
! will read the item from the last time step.  The time on the output file
! will always be 9999 and should be ignored.
*times
      read=   years
      input=  years
      output= years
        time=   9999

*vectors
        vector= 1 to 6
        id=     ^
*items
      type=   history
        name=   CAVRAD

*output
      driver= text
      write=  vector vs item

*end
```

**Figure 5-11. SUMMARIZE Input Control File *drs_tc2_summarize.inp*.**

### 5.2.5. Acceptance Criteria

This test case is used as validation to show that DRSPALL can adequately simulate a drilling intrusion into the WIPP repository. The validation will be acceptable if DRSPALL reasonably predicts cavity growth over six cavitation cycles. Graphical comparisons of cavity radius as a function of time will be evaluated for consistent shape and scale.

### 5.2.6. Results

Table 5-7 and Figure 5-12 show the results of the DRSPALL runs and the comparison with field results. The DRSPALL results are for tensile failed and fluidized radii.

**Table 5-7. Field Inferred and DRSPALL Results Comparison.**

| Cycle | Field Inferred Cavity Radius, m | DRSPALL V1.22 CAVRAD |
|---|---|---|
| 1 | 0.31 | 0.30000 |
| 2 | 0.49 | 0.30000 |
| 3 | 0.61 | 0.64104 |
| 4 | 0.73 | 0.88227 |
| 5 | 0.91 | 1.10815 |
| 6 | 1.37 | 1.30824 |

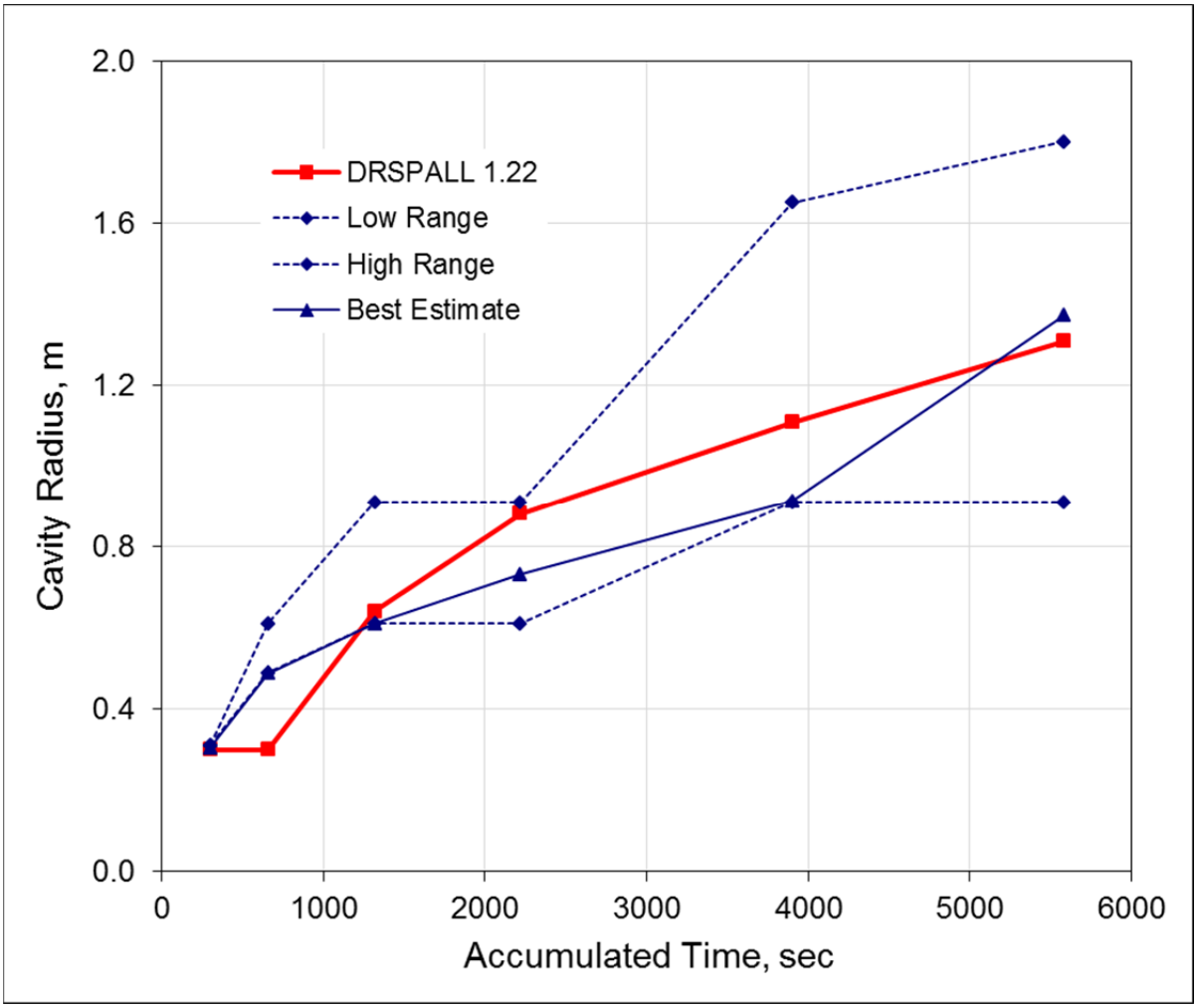


**Figure 5-12. Reported Field Results and DRSPALL Results Compared.**

### 5.2.7. Conclusions

The shape and scale of the cavity radius as a function of cavitation time show reasonable agreement as demonstrated in Figure 5-12 and, therefore, meets the acceptance criteria established in Section 5.2.5 for this test case. Thus, this test case passes.

As discussed in Section 5.2.2.2, the coalbed methane cavitation process is an acceptable analog to the WIPP drilling intrusion-created spall process. The analog is good because of the similarities between the DRSPALL conceptual model and the coalbed cavitation process, both in behavior and scale.

## 5.3. No Test Case #3 is Defined

In the original validation for DRSPALL Version 1.00, no Test Case #3 was defined. For consistency, there is no Test Case #3.

## 5.4. Test Case #4 – Internal Logic Checks

### 5.4.1. Test Objective

This test case demonstrates that DRSPALL accurately calculates:

1. Coupling of flows in the wellbore and the repository
2. Tensile failure of homogenous waste material using effective stress and seepage laws
3. Fluidized bed transport of disaggregated waste material
4. Expulsion of disaggregated waste material at the land surface.

Correctly performing this test case validates the satisfactory implementation of Functional Requirements R.3, R.4, R.5, and R.6 and External Interface Requirements R.7, R.8, and R.9.

### 5.4.2. Problem Description

The evolution of the WIPP underground over the 10,000-year regulatory period could result in a gas-filled repository at near-lithostatic pressure. DRSPALL is designed to estimate the mass of WIPP waste subject to tensile failure (spalling) and transport to the surface, if a drilling intrusion penetrates such a high-pressure repository. The problem domain here is a WIPP repository at a high, initial repository pressure in which a drilling intrusion results in a significant well blowout at the land surface. The repository domain is cast in hemispherical geometry.

This test case differs from the other DRSPALL test cases in that DRSPALL output are not compared against an independent model or experimental data. Rather, the selected intermediate and standard output variables are reported in tabular and graphical format to facilitate tests of (1) the program logic, and (2) verification or proper implementation of the mathematics outlined in the *Design Document for DRSPALL Version 1.22* (WIPP PA 2015a).

#### 5.4.2.1. Boundary Conditions

The boundary conditions are set by the default conditions in DRSPALL. This includes a constant mud pump rate into the drill pipe at the inlet to the wellbore, a constant pressure (1 atm) boundary condition at the outlet from the wellbore, and a no-flow gas boundary at the outer edge of the repository domain.

#### 5.4.2.2. Input Parameters

The DRSPALL input file *drs_v122_tc41.drs* is stored in CVS directory /nfs/data/CVSLIB/ WIPP_CODES/PA_CODES/DRSPALL/Test/Input. In order to assure a spalling event, the repository initial pressure will be near lithostatic pressure at 14.8 MPa, and the tensile strength will be set to a low value in its range, 1.2E+05 Pa (17.4 psi). Note that the zone size growth rates were changed to 1.0 for the DRSPALL 1.22 validation (WIPP PA 2015c, Section 4.0). Also note that the fluidized particle shape factor was changed to 0.25 for the DRSPALL 1.22 validation.

### 5.4.3. Analysis Methods

#### 5.4.3.1. Coupling of the Wellbore and the Repository Flow Models

The coupling of the wellbore and repository flow models in DRSPALL is handled differently before and after bit penetration into the repository. Before penetration, a cylinder of altered-permeability salt material (called the drilling-damaged zone, or DDZ) with diameter equal to the drill bit moves ahead of the drill bit and is assumed to carry limited porous gas flow from the repository to the wellbore. Gas flow is driven by the difference between the gas pressure at the face of the waste and the gas pressure in the bottom of the approaching wellbore. Once the repository is penetrated, these two pressures equalize and gas flow from the repository is added directly to the wellbore. In order to avoid forcing gas to flow to a point in the 1-D, radially symmetric repository domain prior to bit penetration, a preliminary cavity, referred to throughout the DRSPALL documentation as the "pseudocavity," is formed where the repository meets the DDZ. The volume of this cavity is small, with a surface area equal to that of a circle with a diameter equal to the bit diameter. The purpose of this pseudocavity is to avoid forcing gas flow to converge to a single point (spherical geometry) or line (cylindrical geometry) at the origin of the radial coordinate system.

Coupling of the wellbore and repository flow models will be tested by reporting intermediate variables near the time of bit penetration. The variables include:

- Run time (s)
- Bit above repository (m) – Distance between bit and top of repository
- Repository penetrated (true/false)
- Cavity pressure (Pa) – Gas pressure in the preliminary cavity created at the point where the repository domain meets the DDZ
- Wellbore bottomhole pressure (Pa)
- Total gas in well (kg) – Spatial integral of gas mass over entire wellbore domain
- Total gas injected (kg) – Time integral of gas mass injected at bottom of well
- Gas mass in repository (kg) – Spatial integral over entire pore space in repository
- Gas mass from repository (kg) – Difference between starting gas mass in repository and current gas mass in repository
- Gas in storage[2] (kg) – Gas removed from repository by removal of repository zones is added to "storage" before it is released to the cavity

[2] Both gas and solids removed from the repository by drilling are moved into "storage" before being released to the wellbore domain. Mass in storage is then released to the wellbore over a mixing time = (radius/superficial gas velocity) where the radius is the center of the cell that forms the cavity wall, the first intact repository zone. This is done because instantaneously adding the entire contents of one computational zone to the cavity causes numerical noise, and the controlled release from store dampens the numerical shock.

- Mass balance error (-) – Error in the mass of gas in the entire repository and wellbore system relative to time 0.

While distance of the bit above the repository is greater than zero, the logical variable, repository penetrated, should be false. In addition, the cavity pressure at the face of the repository and wellbore bottomhole pressure should converge as gas bleeds from the repository to the wellbore through the drilling-damaged zone. Once the height of the bit above the repository reaches zero, repository penetrated should be true. The cavity pressure and well bottomhole pressure should then be the same. Also, the spatial integral of total gas in well should be equivalent to the time integral of gas injected into the bottom of the well until gas is ejected at the annulus outlet at the land surface. The 'gas mass from repository' should be similar to but not necessarily the same as the 'total gas injected.' Recall that pressure is the dependent variable in the repository model and gas density and flux are found by post processing using the equation-of-state and Darcy's law, respectively. 'Gas mass from repository' includes all mass sources and sinks in the repository model including the wellbore boundary, far-field boundary and local mass balance errors due to errors in the pressure solution. The wellbore boundary should dominate the term and therefore be similar in value to total gas injected. The 'total gas injected' is calculated using Darcy's law applied at the interior boundary of repository domain and requires an approximation of the pressure gradient at the boundary which is discontinuous.

#### 5.4.3.2. Tensile Failure of Waste Material

In DRSPALL, the radial effective stress at any radius $r$ is calculated as the sum of the radial seepage and elastic stress, minus the pore pressure:

$$\sigma_r'(r) = \sigma_{sr}(r) + \sigma_{er}(r) - \beta\, p(r) \tag{5.4-1}$$

where the radial seepage stress is evaluated with the following integral:

$$\sigma_{sr}(r) = (m-1)\beta\left(\frac{1-2\upsilon}{1-\upsilon}\right)\frac{1}{r^m}\int_{r_c}^{r}(p(r) - p_{ff})r^{m-1}dr \tag{5.4-2}$$

and the radial elastic stress is evaluated as:

$$\sigma_{er}(r) = \left\{\sigma_{ff}\left[1-\left(\frac{r_c}{r}\right)^m\right] + p_c\left(\frac{r_c}{r}\right)^m\right\} \tag{5.4-3}$$

and the pore pressure, *p(r)*, is obtained from the transient solution to porous flow. The terms for Equations 5.4-1 to 5.4-3 are defined in Table 5-8.

**Table 5-8. Nomenclature for Stress Calculations.**

| Symbol | Definition | Units |
|---|---|---|
| $m$ | Geometry exponent ($m$=2 for cylindrical, $m$=3 for spherical) | – |
| $p(r)$ | Gas pressure at a distance $r$ from wellbore axis | Pa |
| $p_c$ | Pressure at cavity face | Pa |
| $p_{ff}$ | Pressure in far-field (constant) | Pa |
| $r$ | Radius | m |
| $r_c$ | Radius at cavity face | m |
| $T_s$ | Tensile strength | Pa |
| $\beta$ | Biot's constant | – |
| $\sigma_{ff}$ | Stress in far-field (constant) | Pa |
| $\sigma_{sr}(r)$ | Radial seepage stress | Pa |
| $\sigma_{er}(r)$ | Radial elastic stress | Pa |
| $\sigma_r'(r)$ | Radial effective stresses | Pa |
| $\upsilon$ | Poisson's ratio | – |
| $L_t$ | Characteristic length for testing tensile failure | m |
| $I$ | Zone index in discretized repository domain | – |

Tensile failure of the solid waste material is determined by comparing the radial effective stress ($\sigma_r'(r)$) at every point in the repository domain to the tensile strength $T_s$ of the solid, shown graphically in drawing in Figure 5-13. DRSPALL uses the convention that a positive stress denotes compression, while a negative stress denotes tension. The maximum effective radial stress in tension (where $\sigma_r'(r) < 0$) will typically appear near the cavity wall and transition to compression ($\sigma_r'(r) > 0$) as $r$ increases to the far-field. As such, tensile failure in the solid starts near the cavity wall and moves outward.

In the DRSPALL discretized repository domain, the failure criterion is tested according to the following expression:

$$\text{if } \frac{\sum_{i=1}^{n} \sigma'_{r,i}}{n} < T_s \text{, then failure is initiated over } L_t \qquad (5.4\text{-}4)$$

where the sum is evaluated over $n$ repository zones in a characteristic length $L_t$. Note that since $T_s$ is represented by negative constant in the current calculations, a tensile stress exceeding $T_s$ would actually evaluate to less than $T_s$, hence the "less than" symbol in Equation 5.4-4. Failure in DRSPALL thus occurs only when the mean radial effective stress (in tension) over a characteristic length, $L_t$, exceeds the tensile strength. $L_t$ in this analysis was 2 cm. The characteristic length concept is introduced because without it, the stress formulations in Equations 5.4-1 to 5.4-3 preclude tensile failure in zones near the wall at small zone size. Close examination of Equations 5.4-1 to 5.4-3 will reveal that the radial effective stress is exactly zero

at the cavity wall. This is also illustrated in Figure 5-13. A zone size can always be found in which the very first zone representing the cavity wall has an effective stress insufficient to fail the solids. Also, numerical noise at the cavity boundary can cause spurious failure of the first zone, independent of the physical conditions in the simulation. For these reasons, a characteristic length is introduced that averages the stress over the first several repository zones to capture the expected physical behavior rather than allow failure, or lack thereof, from numerical artifacts.

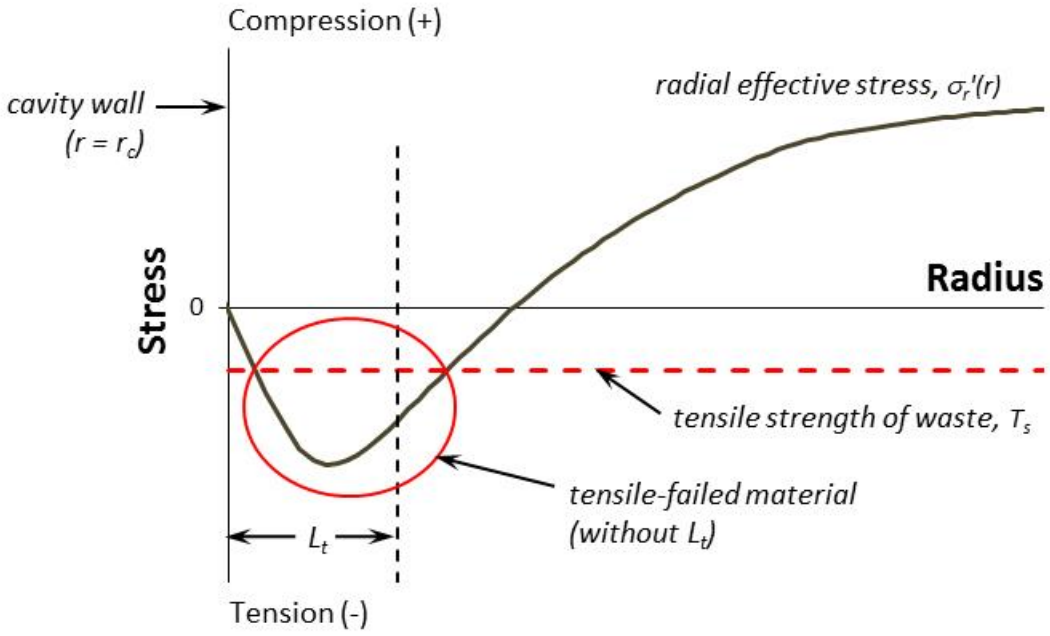


**Figure 5-13. Drawing of a Theoretical Radial Effective Stress Curve.** Material is subject to tensile failure where $\sigma_r'(r) < T_s$.

Tensile failure of waste material will be tested by reporting the following output variables for selected times:

- Run time (s)
- Cavity pressure (Pa)
- Cavity radius (m)
- Drilled radius (m)
- Cavity volume ($m^3$).

For computational cells in the repository in the vicinity of the wellbore, the following will be reported as a function of selected times:

- Repository cell index (-)
- Radius of cell center (m)
- Pore pressure in cell (Pa)
- Radial elastic stress in cell (Pa)
- Radial seepage stress in cell (Pa)
- Radial effective stress in cell (Pa)

- Tensile failure started (true/false)
- Fraction of cell fluidized (-).

In addition, elastic stress, seepage stress and effective stress will be calculated from Equations 5.4-1 to 5.4-3 in an independent spreadsheet analysis using a pore pressure profile, *p(r)*, generated by DRSPALL at one selected time. The spreadsheet values will be compared to those outputs from DRSPALL to verify that the stress calculations in DRSPALL are implemented correctly.

#### 5.4.3.3. Fluidized Bed Transport of Disaggregated Waste Material

Once tensile failure occurs, material is moved from the repository to the wellbore by fluidized bed transport. In DRSPALL, the Ergun (1952) equation:

$$\frac{1.75}{a\phi^3}\left(\frac{d_p U_f \rho}{\eta}\right)^2 + 150\left(\frac{1-\phi}{a^2\phi^3}\right)\left(\frac{d_p U_f \rho}{\eta}\right) = \frac{{d_p}^3 \rho(\rho_w - \rho)g}{\eta^2} \tag{5.4-5}$$

is solved for fluidization velocity, and compared with the superficial gas velocity perpendicular to the cavity wall. The superficial gas velocity is defined as the volume flow rate divided by the area perpendicular to flow direction. If the superficial gas velocity exceeds the fluidization velocity, the failed solids are assumed fluidized and added to the wellbore. The terms for Equation 5.4-5 are defined in Table 5-9.

**Table 5-9. Nomenclature for Fluidization Calculations.**

| Symbol | Definition | Units |
|---|---|---|
| $a$ | Particle shape factor | – |
| $d_p$ | Diameter of particles (mean) | m |
| $g$ | Acceleration of gravity | m/s$^2$ |
| $U_f$ | Fluidization velocity | m/s |
| $\eta$ | Viscosity of gas | kg /m s |
| $\rho$ | Density of gas | kg/m$^3$ |
| $\rho_w$ | Density of waste solids | kg/m$^3$ |
| $\phi$ | Porosity | – |
| $U_s$ | Superficial fluid velocity | m/s |
| $r_{c1}$ | Radius to center of first intact cell | m |
| $t_f$ | Fluidization time | s |

In DRSPALL, the fluidization velocity is nearly constant for a given set of input parameters, though it does change slightly as pressure near the cavity decreases and gas density decreases as a result.

Fluidization of a given zone requires a finite period of time, defined by the fluidization time $t_f$:

$$t_f = \frac{r_{c1}}{U_s} \tag{5.4-6}$$

Fluidized bed transport will be tested by reporting the following output variables as a function of time:

- Runtime (s)
- Cavity pressure (Pa)
- Cavity radius (m)
- Fluidization velocity (m/s)
- Superficial gas velocity at the cell center (m/s)
- Total waste in well (kg).

For computational cells in the repository in the vicinity of the wellbore, the following will be reported as a function of time:

- Cell index (-)
- Radius of cell center (m)
- Tensile failure completed (true/false)
- Fluidization started (true/false)
- Fluidization completed (true/false)
- Fraction fluidized (-).

Also, the fluidization velocity and fluidization time will be calculated given specific input variables using Equation 5.4-5, independent of DRSPALL. These values will be compared to output from DRSPALL to verify that DRSPALL computed the values correctly.

Finally, the volume and mass of material removed from the repository due to drilling (cuttings) and/or failure and fluidization will be verified by spreadsheet calculations based on the repository computational grid and zone removal tracking variables stored on the CAMDAT output file. The CAMDAT variables to be verified are:

- CUTMASS – mass of material removed by drilling (kg)
- TOTMASS – total mass of material remove due to either drilling or spall (kg)
- SPLMASS – difference between TOTMASS and CUTMASS (kg
- SPLMAS2 – incrementally summed mass of material removed due to failure and fluidization (spall) (kg)
- CUTVOLEQ – equivalent uncompacted volume of material removed by drilling ($m^3$)
- TOTVOLEQ – equivalent uncompacted total volume of material remove due to either drilling or spall ($m^3$)

- SPLVOLEQ – difference between TOTVOLEQ and CUTVOLEQ ($m^3$)
- SPLVOL2 – incrementally summed equivalent uncompacted volume of material removed due to spall ($m^3$).

#### 5.4.3.4. Expulsion of Disaggregated Waste Material

Upon transport of the waste material from the cavity at the bottom of the wellbore to the land surface, DRSPALL expels the waste from the problem domain and calculates the total mass of waste expelled as a function of time.

Expulsion of disaggregated waste material at the land surface will be tested by displaying the following output variables at selected times:

- Run time (s)
- Repository penetrated (true/false)
- Zones removed from repository domain (-) – Actual number of computational cells removed from the inner wall of the repository domain due to cutting action of the drill bit or spalling
- Mass of waste removed (kg) – Mass of waste solids removed from repository domain
- Waste in store (kg) – Mass of waste in "store" after fluidization of a zone has completed but before it is released to the cavity
- Total waste in well (kg) – Spatial integral of waste mass in wellbore domain
- Waste mass ejected (kg) – Time integral of waste mass ejected at annulus outlet to land surface
- Waste position in well (m) – Position of waste front in well, where approximately -655 m is the well bottom, and 0 m is the land surface
- Mass balance error (-) – Relative difference between mass removed from repository domain and mass ejected to the surface.

Once the bit penetrates the repository, waste cuttings and potentially spallings will be transported up the wellbore to the surface. Monitoring the position of the waste front in the well will indicate how close it is to the land surface. Once the front reaches the surface, the quantity ejected will increase from zero. The mass of waste removed from the repository should balance with the sum of the waste in the well and the waste ejected.

### 5.4.4. Test Procedure

DRSPALL is executed once to 450 s (Case 4.1) to verify DRSPALL processing (Functional Requirements R.3 through R.6). DRSPALL is executed again (Case 4.2) for a short period of time to verify the External Interface Requirements R.7 through R.9 only.

DRSPALL generates four validation files for Case 4.1 (tc41), as follows.

- *drs_122_tc41_coupling.dat* coupling data at selected times.
- *drs_122_tc41_stress.dat* pore pressure and stress profiles.
- *drs_122_tc41_fluidization.dat* fluidization data at selected times.
- *drs_122_tc41_expulsion.dat* solids transport data.

For Case 4.1, the output CAMDAT file is post-processed with GROPECDB (WIPP PA 1996 and 2012a), using the input control file shown in Figure 5-14. The diagnostics file is also examined. The validation files, GROPECDB output, and diagnostics file for Case 4.1 are imported to Excel file *drs_v122_tc4.xlsx* for post-processing and plotting.

```
DIGITS 8  !apg V1.22 use 8 digits for all
!
!apg For history plots in VD (were done by BLOTCDB)
SELECT ALLTIMES
SELECT HVAR CAVPRS BOTPRS
PRINT HVAR
SELECT HVAR DRILLRAD TENSRAD CAVRAD  !apg may not be used
PRINT HVAR
!
!v1.22 fluidization time comes from separate file
!!!SELECT HVAR FLUIDTIM
!
!apg For drilling and spall volume and masses table in VD
!apg DIGITS 8
SELECT PROP CAVRAD0
PRINT PROP
SELECT TIME 450
SELECT HVAR CUTMASS TOTMASS SPLMASS SPLMAS2 &
            CUTVOLEQ TOTVOLEQ SPLVOLEQ SPLVOL2
PRINT HVAR
!
!For Excel SPLVOL CHECK
SELECT TIME 450
SELECT BLOCK 2  !FLUDSTOP defined in REPOS only
SELECT EVARS COORD FLUDSTOP
PRINT EVARS
!
EXIT
```

**Figure 5-14. GROPECDB Input Command File *drs_tc41_grope.inp*.**

The following command lines run DRSPALL and GROPECDB for Case 4.1:

```
./drspall ./Input/drs_v122_tc41.drs DRSPALL/Test/Output/Solaris_122/drs_122_tc41.dbg
        CANCEL DRSPALL/Test/Output/Solaris_122/drs_122_tc41.cdb
        > DRSPALL/Test/Output/Solaris_122/drs_122_tc41.crt

./gropecdb DRSPALL/Test/Output/Solaris_122/drs_122_tc41.cdb
        ./Input/drs_tc41_grope.inp
        DRSPALL/Test/Output/Solaris_122/drs_122_tc41.gr  > x.x
```

Case 4.2 is the only test case that inputs a CAMDAT file. For Case 4.2, the diagnostics file is examined to verify that DRSPALL is setting the input parameters as instructed by the DRSPALL input file using the properties in the input CAMDAT file. The output CAMDAT file is not examined. The four validation files mentioned above are generated, but are not examined.

The following command line runs DRSPALL for Case 4.2 (tc42). Note that this is the only case that reads an input CAMDAT file (*drs_tc42_ms.cdb*):

```
./drspall ./Input/drs_v122_tc42.drs DRSPALL/Test/Output/Solaris_122/drs_122_tc42.dbg
        ./Input/drs_tc42_ms.cdb DRSPALL/Test/Output/Solaris_122/drs_122_tc42.cdb
        > DRSPALL/Test/Output/Solaris_122/drs_122_tc42.crt
```

### 5.4.5. Acceptance Criteria

Note that **Acceptance Criteria 4-1 through 4-15** (Sections 5.4.5.1 through 5.4.5.4) and **Acceptance Criterion 4-17** (Section 5.4.5.5) are addressed by Case 4.1. **Acceptance Criterion 4-16** (Section 5.4.5.5) is verified for Case 4.2 only.

#### 5.4.5.1. Coupling of the Wellbore and the Repository Flow Models

As the bit approaches the repository [Bit Above Repository > 0], the following should be observed:

- **Acceptance Criterion 4-1** — Cavity pressure decreases and well bottomhole pressure increases with time (after they stabilize).

- **Acceptance Criterion 4-2** — Repository has not yet been penetrated, indicated by the logical variable Repository Penetrated = "F" (false).

- **Acceptance Criterion 4-3** — The total mass of gas in the bottom of the well is updated by adding gas from the waste. The total mass balance error should be less than 0.10.

When the bit intersects the repository [Bit Above Repository <= 0], the following should be observed:

- **Acceptance Criterion 4-4** — Cavity pressure and well bottomhole pressure are equal.

- **Acceptance Criterion 4-5** — Repository has been penetrated, indicated by the logical variable Repository Penetrated = "T" (true).

- **Acceptance Criterion 4-6** — The total mass of gas in the well is updated by adding gas from the waste. The total mass balance error should be less than 0.10.

#### 5.4.5.2. Tensile Failure of Waste Material

This test will pass if, for a selected output time, the following is observed:

- **Acceptance Criterion 4-7** — The radial effective stress is equal to the sum of the component stresses per Equation 5.4-1.

- **Acceptance Criterion 4-8** — If the average radial effective stress over characteristic length $L_t$ = 2 cm exceeds the material tensile strength, then tensile failure is started, otherwise, tensile failure has not started.

- **Acceptance Criterion 4-9** — Independent spreadsheet calculations of the radial effective stress, radial seepage stress, and radial elastic stress based on Equations 5.4-1 to 5.4-3 and the given DRSPALL pore pressure profile demonstrate agreement within a relative difference of 1E-4.

#### 5.4.5.3. Fluidized Bed Transport of Disaggregated Waste Material

This test will pass if, for a selected output time, the following is observed:

- **Acceptance Criterion 4-10** — If the superficial gas velocity for any cell within the characteristic length exceeds the critical fluidization velocity, the fluidization of the disaggregated waste should be started.

- **Acceptance Criterion 4-11** — The fluidization velocity calculated independently using the Ergun equation (Equation 5.4-5) is consistent with the value reported by DRSPALL to within a relative difference of 1E-4.

- **Acceptance Criterion 4-12** — The volume and mass of waste material removed by drilling and spall agree with independent calculations to within a relative difference of 1E-4.

#### 5.4.5.4. Expulsion of Disaggregated Waste Material

Once waste has been transported up the borehole, it must be ejected at the land surface. This test will pass if the following is observed:

- **Acceptance Criterion 4-13** — The position of the waste front in the well must move from the bottom (-653 m) to the top (0 m) as time progresses after repository penetration.

- **Acceptance Criterion 4-14** — The cumulative mass of waste ejected must be small (< 1.0 kg) before the waste position in the well reaches z = 0, after which the cumulative mass of waste ejected will be a monotonically increasing positive number.

- **Acceptance Criterion 4-15** — The mass of waste removed from the repository must correspond with the mass of waste present in the cavity, wellbore, and ejected to the land surface. The relative mass balance error must not exceed 0.01.

#### 5.4.5.5. External Interfaces

The proper use of external interfaces will be verified if:

- **Acceptance Criterion 4-16** — The program successfully reads the DRSPALL parameters from the input control file and the input CAMDAT file, as confirmed by the parameter values listed on the diagnostics file.

- **Acceptance Criterion 4-17** — An output CAMDAT file is generated by DRSPALL. The file must be readable by the BLOTCDB utility or the GROPECDB utility to confirm that it is a valid CAMDAT file.

Test Case #4 will pass if all criteria listed in Sections 5.4.5.1 – 5.4.5.5 are satisfied.

### 5.4.6. Results

The presentation of results starts with a general description of the run behavior, and then breaks out into discussions of specific functionality.

Key history variables for this run are shown in Figure 5-15 and Figure 5-16. Note that the code was executed for 450 s DRSPALL time. This was sufficient time to allow for the cavity pressure to stabilize (Figure 5-15), drilling to complete and failure of repository material to stop and cavity radius to stabilize (Figure 5-16). Output variable names shown in the figures represent the CAMDAT variable names, described in the DRSPALL user's manual (WIPP PA 2004b, 2013c, and 2015b). The plot data was extracted from the output CAMDAT file with GROPECDB, and plotted with Excel.

Understanding DRSPALL output typically begins with studying the pressure and cavity radius history plots. The pressure history plot in Figure 5-15 shows the fluid pressure at the bottom of the well (BOTPRS) and the repository pressure at the point of impending intrusion (CAVPRS). At the start of the simulation, BOTPRS is near hydrostatic (approximately 8 MPa), and CAVPRS is at the initial repository pressure, 14.8 MPa. The well pressure is a little noisy at startup because the initial pressure distribution is chosen arbitrarily, and stable, dynamic flowing solution must be found, which takes a few seconds of DRSPALL time. The important issue here is for the wellbore pressure to settle down before bit penetration of the repository, which it does in all DRSPALL runs. As the bit nears the repository, gas bleed between the repository and wellbore cause BOTPRS and CAVPRS to converge and reach a common value near 9.5 MPa at the time of intrusion. After intrusion, direct coupling between the high-pressure repository and wellbore causes the drilling mud column to blow out, resulting in a drop in BOTPRS to near 3.0 MPa where it stays for the remainder of the run. The pressure spikes observed between 130

and 200 s are caused by tensile failure of repository solids and subsequent entrainment into the wellbore flow stream.

Also instructive is the radius history plot, shown here in Figure 5-16. Recall that the repository geometry is hemispherical in this study. Note that the initial cavity radius (CAVRAD) is small but not zero, representing the radius of the pseudocavity (Section 5.4.3.1) created prior to bit penetration. The cavity then grows upon penetration of the repository, starting at 34 s. Until about 107 s, all radial variables grow due to drilling. After 107 s, tensile failure occurs, and tensile radius (TENSRAD) and cavity radius (CAVRAD) grow accordingly. Drilled radius (DRILLRAD) continues along its path independent of the growing cavity in front of it, and stops only when the drill bit would have hit the bottom of the repository in the real system. In this case, the effective (spherical) drilled radius is 0.48 m. The cavity radius and tensile-failed radius settle to constant values of 0.71 m and 0.73 m, respectively. The tensile-failed radius (TENSRAD) identifies solid material that has failed due to the stress state, but has not mobilized into the flow stream. The tensile-failed radius is equal to or greater than the cavity radius. The difference between these radii represents the material considered to be "spalled" in this conceptual model.

Relative difference is used several times in this section. It is calculated as:

$$\text{ABS}\ (\textit{DRSPALL\_value} - \textit{Excel\_value}) \,/\, \textit{DRSPALL\_value} \qquad (5.4\text{-}7)$$

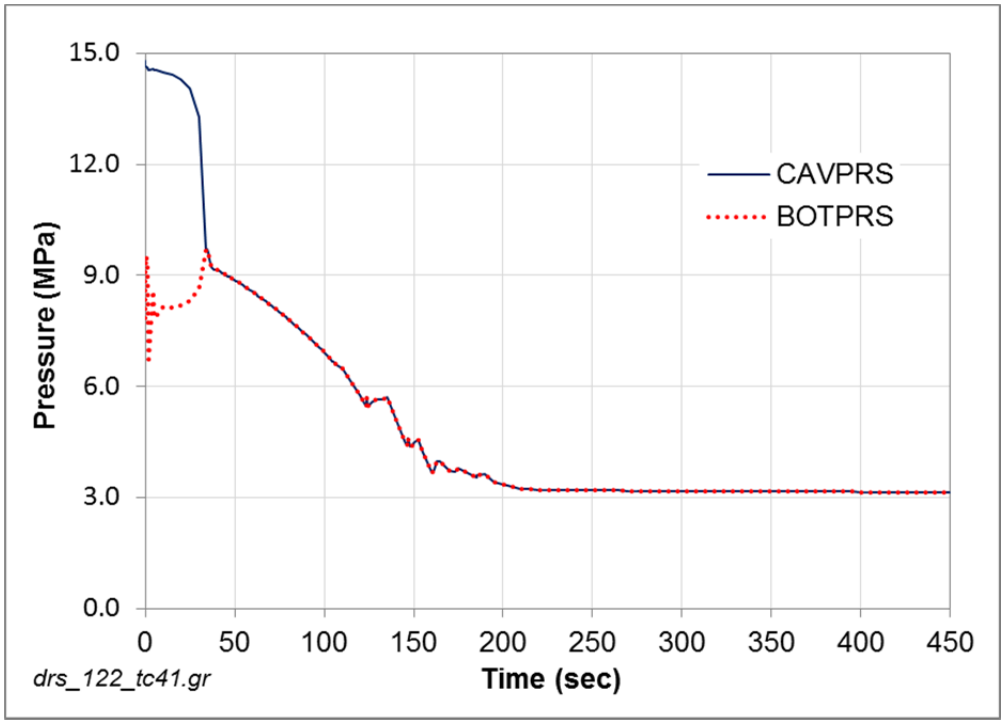


**Figure 5-15. Pressure History Plot.**

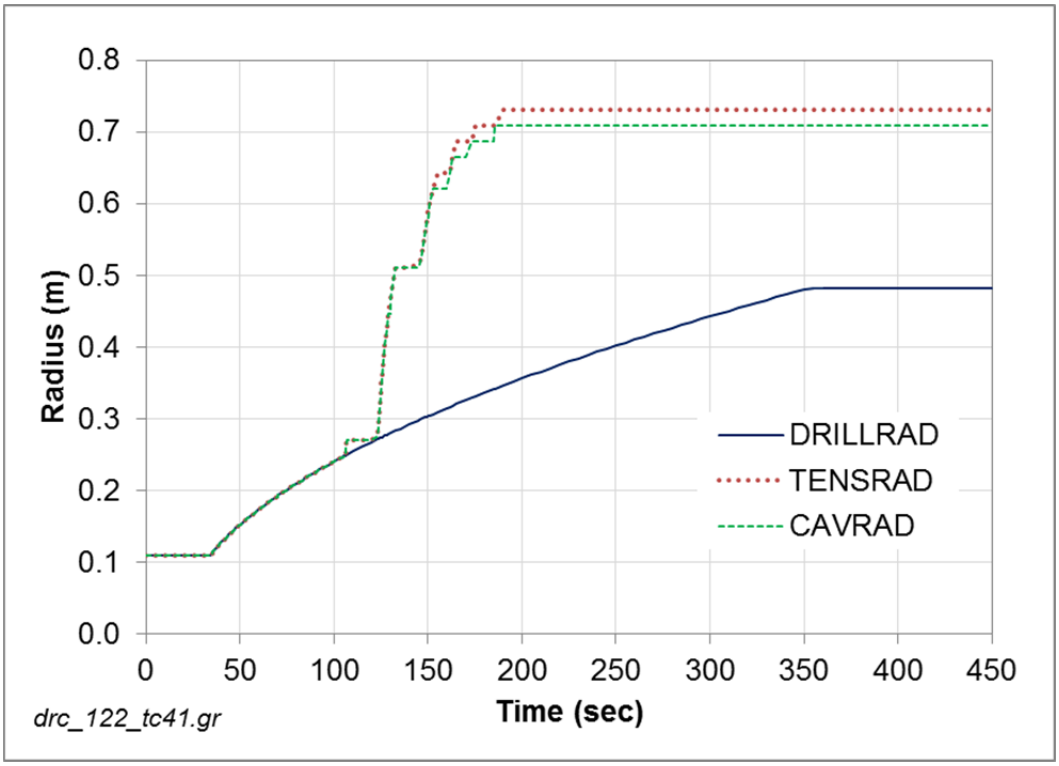


**Figure 5-16. Radius History Plot.**

### 5.4.6.1. Coupling of the Wellbore and Repository Flow Models

An excerpt from the coupling file (as formatted by Excel) is shown in Table 5-10. The information shown in this table relates to gas transport from the repository domain to the wellbore domain. The table columns are defined in Section 5.4.3.1. Figure 5-17 shows a pressure versus time plot.

Reporting in Table 5-10 starts at a run time of approximately 28.28 s. The bit is 0.02428 m above the top of the repository at this point, and the Repository Penetrated logical is "F" (false). Gas pressure in the repository (Cavity Pressure = 13.67 MPa) is greater than Well Bottom Pressure at 8.48 MPa. This causes some gas to bleed from the repository to the well bottom through the drilling damaged zone (DDZ), resulting in a nonzero and growing Total Gas in Well = 1.90 kg. As the bit proceeds downward with time, Cavity Pressure and Well Bottom Pressure converge to a common value of 9.69 MPa at approximately 33.77 s when the repository is penetrated. A horizontal line is drawn in the table at the time of penetration. The pressure behavior is also illustrated graphically in Figure 5-17, where data from Figure 5-15 is plotted on a time scale from 0 to 50 s to zoom in on events around the time of intrusion. The plot data was extracted from the output CAMDAT file with GROPECDB, and plotted with Excel.

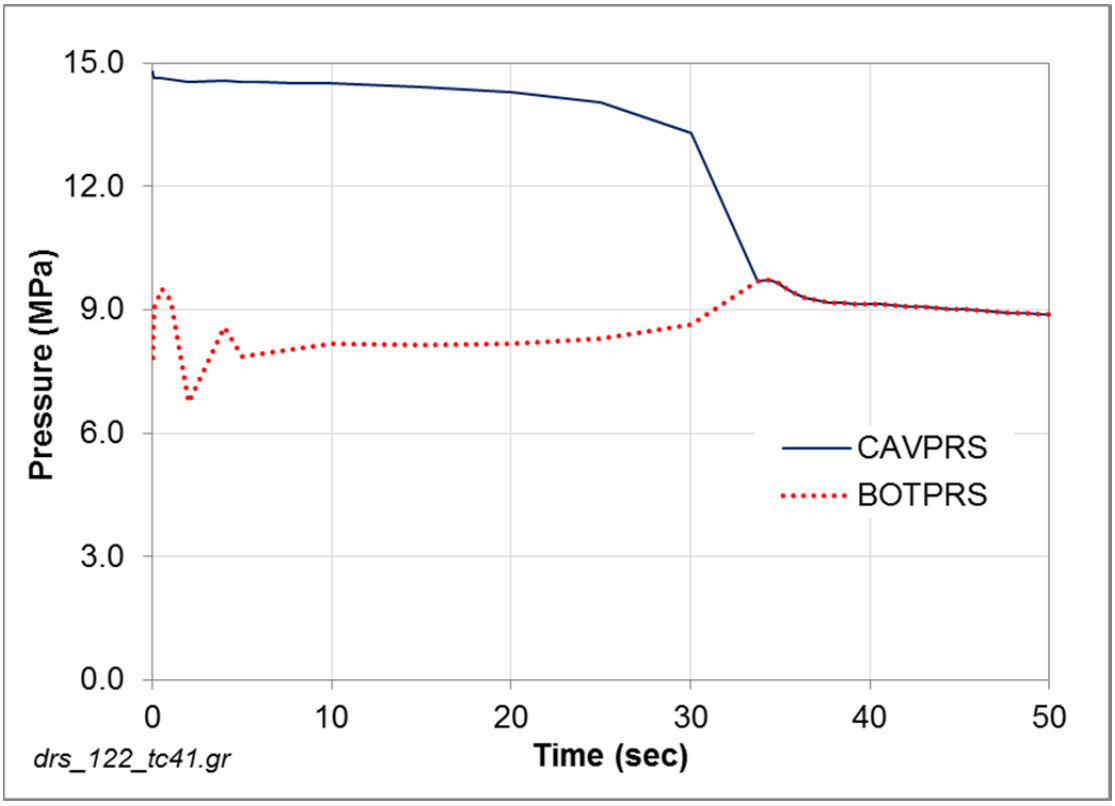


**Figure 5-17. Pressure History Plot for Time = 0 to 50 s.**

An examination of Table 5-10 and *drs_122_tc41_coupling.dat* confirms that **Acceptance Criteria 4-2 and 4-5** (Section 5.4.5.1) are met: the Repository Penetrated is always "F" (false) when Bit Above Repository is greater than zero, and always "T" (true) when Bit Above Repository is less than or equal to zero. An examination of Table 5-10 and Figure 5-17 confirms that **Acceptance Criterion 4-1** (Section 5.4.5.1) is met: Cavity Pressure (CAVPRS) decreases and Well Bottom Pressure (BOTPRS) increases (after CAVPRS stabilizes) as the bit approaches the repository. Further examination confirms that **Acceptance Criterion 4-4** (Section 5.4.5.1) is met: Cavity Pressure (CAVPRS) and Well Bottom Pressure (BOTPRS) are equal when the bit intersects the repository.

In Table 5-10, the spatial integral Total Gas In Well agrees closely with the time integral Total Gas Injected until gas transports all the way to the top of the wellbore at the land surface (run time approximately 107 s) at which point gas is ejected to the atmosphere and out of the problem domain. Mass of gas injected and gas mass from repository are similar as expected and explained in Section 5.4.3.1. The global mass balance error remains on the order of 1E-3 to 1E-7 for all reported times in Table 5-10 and in *drs_122_tc41_coupling.dat*, so **Acceptance Criteria 4-3 and 4-6** (Section 5.4.5.1) are met. The global mass balance error is defined as the absolute value of [Initial Gas in Repository – (Gas Mass In Repository + Gas Storage + Total Gas Injected)] / Initial Gas in Repository.

## Table 5-10. Excerpt from *drs_122_tc41_coupling.dat*.

Initial Repository Pressure (Pa): 1.480000000000000E+07
Initial Gas in Repository (kg): 1.021635964442423E+05

| Runtime (s) | Bit Above Repository (m) | Repository Penetrated (T/F) | Cavity Pressure (Pa) | Well Bottom Pressure (Pa) | Total Gas In Well (kg) | Total Gas Injected (kg) | Gas Mass In Repository (kg) | Gas Mass From Repository (kg) | Gas Storage (kg) | Mass Balance Error (-) |
|---|---|---|---|---|---|---|---|---|---|---|
| 28.28294 | 0.02428 | F | 13.66737E+06 | 8.47892E+06 | 1.90195 | 1.90195 | 102161.71000 | 1.88951 | 0.00E+00 | 1.22E-07 |
| 28.44442 | 0.02356 | F | 13.63988E+06 | 8.49156E+06 | 1.92857 | 1.92857 | 102161.68000 | 1.91522 | 0.00E+00 | 1.31E-07 |
| 28.60589 | 0.02285 | F | 13.61106E+06 | 8.50489E+06 | 1.95578 | 1.95578 | 102161.65000 | 1.94147 | 0.00E+00 | 1.40E-07 |
| 28.76736 | 0.02213 | F | 13.58077E+06 | 8.51871E+06 | 1.98359 | 1.98359 | 102161.63000 | 1.96829 | 0.00E+00 | 1.50E-07 |
| 28.92883 | 0.02141 | F | 13.54890E+06 | 8.53302E+06 | 2.01205 | 2.01205 | 102161.60000 | 1.99570 | 0.00E+00 | 1.60E-07 |
| 29.09030 | 0.02069 | F | 13.51535E+06 | 8.54812E+06 | 2.04118 | 2.04118 | 102161.57000 | 2.02372 | 0.00E+00 | 1.71E-07 |
| 29.25178 | 0.01998 | F | 13.48000E+06 | 8.56410E+06 | 2.07101 | 2.07101 | 102161.54000 | 2.05239 | 0.00E+00 | 1.82E-07 |
| 29.41325 | 0.01926 | F | 13.44268E+06 | 8.58076E+06 | 2.10157 | 2.10157 | 102161.51000 | 2.08173 | 0.00E+00 | 1.94E-07 |
| 29.57472 | 0.01854 | F | 13.40319E+06 | 8.59812E+06 | 2.13290 | 2.13290 | 102161.48000 | 2.11178 | 0.00E+00 | 2.07E-07 |
| 29.73619 | 0.01782 | F | 13.36138E+06 | 8.61638E+06 | 2.16504 | 2.16504 | 102161.45000 | 2.14257 | 0.00E+00 | 2.20E-07 |
| 29.89766 | 0.01710 | F | 13.31705E+06 | 8.63566E+06 | 2.19804 | 2.19804 | 102161.42000 | 2.17413 | 0.00E+00 | 2.34E-07 |
| 30.05914 | 0.01639 | F | 13.26995E+06 | 8.65596E+06 | 2.23193 | 2.23193 | 102161.39000 | 2.20652 | 0.00E+00 | 2.49E-07 |
| 30.22061 | 0.01567 | F | 13.21982E+06 | 8.67730E+06 | 2.26677 | 2.26677 | 102161.36000 | 2.23976 | 0.00E+00 | 2.64E-07 |
| 30.38208 | 0.01495 | F | 13.16635E+06 | 8.69971E+06 | 2.30260 | 2.30260 | 102161.32000 | 2.27392 | 0.00E+00 | 2.81E-07 |
| 30.54355 | 0.01423 | F | 13.10920E+06 | 8.72335E+06 | 2.33949 | 2.33949 | 102161.29000 | 2.30903 | 0.00E+00 | 2.98E-07 |
| 30.70503 | 0.01352 | F | 13.04803E+06 | 8.74839E+06 | 2.37749 | 2.37749 | 102161.25000 | 2.34515 | 0.00E+00 | 3.17E-07 |
| 30.86650 | 0.01280 | F | 12.98239E+06 | 8.77489E+06 | 2.41668 | 2.41668 | 102161.21000 | 2.38235 | 0.00E+00 | 3.36E-07 |
| 31.02797 | 0.01208 | F | 12.91177E+06 | 8.80287E+06 | 2.45713 | 2.45713 | 102161.18000 | 2.42068 | 0.00E+00 | 3.57E-07 |
| 31.18944 | 0.01136 | F | 12.83557E+06 | 8.83246E+06 | 2.49891 | 2.49891 | 102161.14000 | 2.46022 | 0.00E+00 | 3.79E-07 |
| 31.35091 | 0.01065 | F | 12.75318E+06 | 8.86390E+06 | 2.54212 | 2.54212 | 102161.10000 | 2.50104 | 0.00E+00 | 4.02E-07 |
| 31.51239 | 0.00993 | F | 12.66383E+06 | 8.89736E+06 | 2.58685 | 2.58685 | 102161.05000 | 2.54323 | 0.00E+00 | 4.27E-07 |
| 31.67386 | 0.00921 | F | 12.56662E+06 | 8.93294E+06 | 2.63320 | 2.63320 | 102161.01000 | 2.58688 | 0.00E+00 | 4.53E-07 |
| 31.83533 | 0.00849 | F | 12.46047E+06 | 8.97078E+06 | 2.68130 | 2.68130 | 102160.96000 | 2.63210 | 0.00E+00 | 4.82E-07 |
| 31.99680 | 0.00777 | F | 12.34416E+06 | 9.01112E+06 | 2.73127 | 2.73127 | 102160.92000 | 2.67898 | 0.00E+00 | 5.12E-07 |
| 32.15827 | 0.00706 | F | 12.21623E+06 | 9.05425E+06 | 2.78325 | 2.78325 | 102160.87000 | 2.72767 | 0.00E+00 | 5.44E-07 |
| 32.31975 | 0.00634 | F | 12.07493E+06 | 9.10041E+06 | 2.83741 | 2.83741 | 102160.82000 | 2.77829 | 0.00E+00 | 5.79E-07 |
| 32.48122 | 0.00562 | F | 11.91813E+06 | 9.14985E+06 | 2.89391 | 2.89391 | 102160.77000 | 2.83101 | 0.00E+00 | 6.16E-07 |
| 32.64269 | 0.00490 | F | 11.74323E+06 | 9.20285E+06 | 2.95296 | 2.95296 | 102160.71000 | 2.88598 | 0.00E+00 | 6.56E-07 |
| 32.80416 | 0.00419 | F | 11.54708E+06 | 9.25980E+06 | 3.01477 | 3.01477 | 102160.65000 | 2.94341 | 0.00E+00 | 6.98E-07 |
| 32.96563 | 0.00347 | F | 11.32579E+06 | 9.32110E+06 | 3.07960 | 3.07960 | 102160.59000 | 3.00351 | 0.00E+00 | 7.45E-07 |
| 33.12711 | 0.00275 | F | 11.07443E+06 | 9.38719E+06 | 3.14771 | 3.14771 | 102160.53000 | 3.06652 | 0.00E+00 | 7.95E-07 |
| 33.28858 | 0.00203 | F | 10.78673E+06 | 9.45848E+06 | 3.21943 | 3.21943 | 102160.46000 | 3.13271 | 0.00E+00 | 8.49E-07 |
| 33.45005 | 0.00131 | F | 10.45457E+06 | 9.53546E+06 | 3.29511 | 3.29511 | 102160.39000 | 3.20239 | 0.00E+00 | 9.08E-07 |
| 33.61152 | 0.00060 | F | 10.06728E+06 | 9.61869E+06 | 3.37513 | 3.37513 | 102160.32000 | 3.27591 | 0.00E+00 | 9.71E-07 |
| 33.77299 | -0.00012 | T | 9.69412E+06 | 9.69412E+06 | 3.45954 | 3.45954 | 102160.24000 | 3.35345 | 0.00E+00 | 1.04E-06 |
| 33.93447 | -0.00084 | T | 9.71260E+06 | 9.71260E+06 | 3.54407 | 3.54407 | 102160.16000 | 3.43145 | 0.00E+00 | 1.10E-06 |
| 34.09594 | -0.00156 | T | 9.72454E+06 | 9.72454E+06 | 3.62803 | 3.62803 | 102160.09000 | 3.50893 | 0.00E+00 | 1.17E-06 |
| 34.25741 | -0.00227 | T | 9.72844E+06 | 9.72844E+06 | 3.71168 | 3.71168 | 102160.01000 | 3.58615 | 0.00E+00 | 1.23E-06 |
| 34.41888 | -0.00299 | T | 9.74328E+06 | 9.74328E+06 | 3.79600 | 3.79600 | 102159.93000 | 3.66460 | 6.10E-04 | 1.29E-06 |
| 34.58035 | -0.00371 | T | 9.71818E+06 | 9.71818E+06 | 3.88187 | 3.88187 | 102159.85000 | 3.74358 | 3.32E-04 | 1.36E-06 |
| 34.74183 | -0.00443 | T | 9.68029E+06 | 9.68029E+06 | 3.96780 | 3.96780 | 102159.77000 | 3.82273 | 1.80E-04 | 1.42E-06 |
| 34.90330 | -0.00515 | T | 9.64311E+06 | 9.64311E+06 | 4.05394 | 4.05394 | 102159.69000 | 3.90215 | 9.69E-05 | 1.49E-06 |
| 35.06477 | -0.00586 | T | 9.62382E+06 | 9.62382E+06 | 4.14111 | 4.14111 | 102159.61000 | 3.98317 | 6.87E-04 | 1.55E-06 |
| 35.22624 | -0.00658 | T | 9.58827E+06 | 9.58827E+06 | 4.23014 | 4.23014 | 102159.53000 | 4.06500 | 3.74E-04 | 1.62E-06 |
| 35.38771 | -0.00730 | T | 9.53688E+06 | 9.53688E+06 | 4.31932 | 4.31932 | 102159.45000 | 4.14709 | 2.03E-04 | 1.69E-06 |
| *… lines deleted …* | | | | | | | | | | |
| 104.98405 | -0.31665 | T | 6.66468E+06 | 6.66468E+06 | 86.76156 | 86.76156 | 102083.60000 | 79.99610 | 1.38E-03 | 6.62E-05 |

## Table 5-10. Excerpt from *drs_122_tc41_coupling.dat*. (Continued)

| Runtime (s) | Bit Above Repository (m) | Repository Penetrated (T/F) | Cavity Pressure (Pa) | Well Bottom Pressure (Pa) | Total Gas In Well (kg) | Total Gas Injected (kg) | Gas Mass In Repository (kg) | Gas Mass From Repository (kg) | Gas Storage (kg) | Mass Balance Error (-) |
|---|---|---|---|---|---|---|---|---|---|---|
| 105.14554 | -0.31737 | T | 6.65570E+06 | 6.65570E+06 | 87.05083 | 87.05083 | 102083.33000 | 80.26217 | 1.04E-03 | 6.65E-05 |
| 105.30703 | -0.31809 | T | 6.64657E+06 | 6.64657E+06 | 87.34003 | 87.34003 | 102083.07000 | 80.52825 | 7.84E-04 | 6.67E-05 |
| 105.46852 | -0.31881 | T | 6.63731E+06 | 6.63731E+06 | 87.62923 | 87.62923 | 102082.80000 | 80.79439 | 5.91E-04 | 6.69E-05 |
| 105.63001 | -0.31953 | T | 6.62789E+06 | 6.62789E+06 | 87.91847 | 87.91847 | 102082.54000 | 81.06062 | 4.46E-04 | 6.71E-05 |
| 105.79150 | -0.32024 | T | 6.61837E+06 | 6.61837E+06 | 88.20778 | 88.20778 | 102082.27000 | 81.32694 | 3.36E-04 | 6.74E-05 |
| 105.95299 | -0.32096 | T | 6.60877E+06 | 6.60877E+06 | 88.49717 | 88.49717 | 102082.00000 | 81.59337 | 2.53E-04 | 6.76E-05 |
| 106.11448 | -0.32168 | T | 6.60276E+06 | 6.60276E+06 | 88.79001 | 88.79001 | 102081.73000 | 81.86931 | 2.31E-03 | 6.78E-05 |
| 106.27597 | -0.32240 | T | 6.56678E+06 | 6.56678E+06 | 89.06987 | 89.06987 | 102081.44000 | 82.15643 | 1.77E-03 | 6.77E-05 |
| 106.42141 | -0.32304 | T | 6.55711E+06 | 6.55711E+06 | 89.31080 | 89.31080 | 102081.18000 | 82.41516 | 1.40E-03 | 6.75E-05 |
| 106.54897 | -0.32361 | T | 6.60301E+06 | 6.60301E+06 | 89.54398 | 89.54398 | 102080.94000 | 82.65961 | 1.54E-02 | 6.75E-05 |
| 106.71046 | -0.32433 | T | 6.57967E+06 | 6.57967E+06 | 89.85990 | 89.85990 | 102080.63000 | 82.96303 | 1.19E-02 | 6.76E-05 |
| 106.85322 | -0.32496 | T | 6.56536E+06 | 6.56536E+06 | 90.12532 | 90.12532 | 102080.37000 | 83.23102 | 9.54E-03 | 6.76E-05 |
| 106.99329 | -0.32559 | T | 6.60298E+06 | 6.60298E+06 | 90.40881 | 90.40881 | 102080.09000 | 83.50995 | 1.96E-02 | 6.77E-05 |
| 107.15478 | -0.32630 | T | 6.59833E+06 | 6.59833E+06 | 90.74304 | 90.74304 | 102079.78000 | 83.81396 | 1.53E-02 | 6.80E-05 |
| 107.31627 | -0.32702 | T | 6.59661E+06 | 6.59661E+06 | 91.07486 | 91.07487 | 102079.48000 | 84.11666 | 1.20E-02 | 6.82E-05 |
| 107.47776 | -0.32774 | T | 6.59429E+06 | 6.59429E+06 | 91.40513 | 91.40514 | 102079.18000 | 84.41862 | 9.40E-03 | 6.85E-05 |
| 107.63925 | -0.32846 | T | 6.58948E+06 | 6.58948E+06 | 91.73435 | 91.73436 | 102078.88000 | 84.72017 | 7.37E-03 | 6.87E-05 |
| 107.80075 | -0.32917 | T | 6.58518E+06 | 6.58518E+06 | 92.06277 | 92.06279 | 102078.58000 | 85.02141 | 5.77E-03 | 6.90E-05 |
| 107.96224 | -0.32989 | T | 6.57868E+06 | 6.57868E+06 | 92.39061 | 92.39066 | 102078.27000 | 85.32246 | 4.52E-03 | 6.92E-05 |
| 108.12373 | -0.33061 | T | 6.57261E+06 | 6.57261E+06 | 92.71802 | 92.71810 | 102077.97000 | 85.62337 | 3.54E-03 | 6.95E-05 |
| 108.28523 | -0.33133 | T | 6.56647E+06 | 6.56647E+06 | 93.04506 | 93.04519 | 102077.67000 | 85.92417 | 2.78E-03 | 6.97E-05 |
| 108.44672 | -0.33205 | T | 6.55919E+06 | 6.55919E+06 | 93.37183 | 93.37205 | 102077.37000 | 86.22492 | 2.17E-03 | 7.00E-05 |
| 108.60821 | -0.33276 | T | 6.55179E+06 | 6.55179E+06 | 93.69837 | 93.69876 | 102077.07000 | 86.52565 | 1.70E-03 | 7.02E-05 |
| 108.76971 | -0.33348 | T | 6.54416E+06 | 6.54416E+06 | 94.02467 | 94.02534 | 102076.77000 | 86.82636 | 1.33E-03 | 7.05E-05 |
| 108.93120 | -0.33420 | T | 6.53579E+06 | 6.53579E+06 | 94.35072 | 94.35188 | 102076.47000 | 87.12711 | 1.04E-03 | 7.07E-05 |
| 109.09269 | -0.33492 | T | 6.52740E+06 | 6.52740E+06 | 94.67640 | 94.67838 | 102076.17000 | 87.42790 | 8.16E-04 | 7.10E-05 |
| 109.25419 | -0.33563 | T | 6.51884E+06 | 6.51884E+06 | 95.00156 | 95.00489 | 102075.87000 | 87.72874 | 6.38E-04 | 7.12E-05 |
| 109.41568 | -0.33635 | T | 6.51012E+06 | 6.51012E+06 | 95.32596 | 95.33142 | 102075.57000 | 88.02963 | 4.99E-04 | 7.15E-05 |
| 109.57718 | -0.33707 | T | 6.50126E+06 | 6.50126E+06 | 95.64932 | 95.65799 | 102075.27000 | 88.33060 | 3.90E-04 | 7.17E-05 |
| 109.73867 | -0.33779 | T | 6.49224E+06 | 6.49224E+06 | 95.97128 | 95.98462 | 102074.96000 | 88.63165 | 3.05E-04 | 7.20E-05 |
| 109.90016 | -0.33851 | T | 6.48311E+06 | 6.48311E+06 | 96.29149 | 96.31132 | 102074.66000 | 88.93279 | 2.38E-04 | 7.22E-05 |
| 110.06166 | -0.33922 | T | 6.47385E+06 | 6.47385E+06 | 96.60959 | 96.63810 | 102074.36000 | 89.23402 | 1.86E-04 | 7.25E-05 |
| 110.22315 | -0.33994 | T | 6.46448E+06 | 6.46448E+06 | 96.92522 | 96.96498 | 102074.06000 | 89.53535 | 1.45E-04 | 7.27E-05 |
| 110.38465 | -0.34066 | T | 6.45500E+06 | 6.45500E+06 | 97.23805 | 97.29196 | 102073.76000 | 89.83678 | 1.13E-04 | 7.30E-05 |
| 110.54614 | -0.34138 | T | 6.44541E+06 | 6.44541E+06 | 97.54777 | 97.61905 | 102073.46000 | 90.13833 | 8.80E-05 | 7.32E-05 |
| 110.70764 | -0.34210 | T | 6.43570E+06 | 6.43570E+06 | 97.85409 | 97.94625 | 102073.16000 | 90.44000 | 6.85E-05 | 7.35E-05 |
| 110.86913 | -0.34281 | T | 6.42590E+06 | 6.42590E+06 | 98.15675 | 98.27358 | 102072.85000 | 90.74178 | 5.34E-05 | 7.37E-05 |
| 111.03063 | -0.34353 | T | 6.41604E+06 | 6.41604E+06 | 98.45550 | 98.60104 | 102072.55000 | 91.04369 | 4.15E-05 | 7.40E-05 |
| 111.19212 | -0.34425 | T | 6.40613E+06 | 6.40613E+06 | 98.75014 | 98.92862 | 102072.25000 | 91.34572 | 3.23E-05 | 7.42E-05 |
| 111.35362 | -0.34497 | T | 6.39614E+06 | 6.39614E+06 | 99.04046 | 99.25634 | 102071.95000 | 91.64789 | 2.51E-05 | 7.45E-05 |
| 111.51512 | -0.34568 | T | 6.38610E+06 | 6.38610E+06 | 99.32628 | 99.58420 | 102071.65000 | 91.95018 | 1.95E-05 | 7.47E-05 |
| 111.67661 | -0.34640 | T | 6.37600E+06 | 6.37600E+06 | 99.60746 | 99.91220 | 102071.34000 | 92.25261 | 1.52E-05 | 7.50E-05 |
| 111.83811 | -0.34712 | T | 6.36583E+06 | 6.36583E+06 | 99.88383 | 100.24034 | 102071.04000 | 92.55518 | 1.18E-05 | 7.52E-05 |
| 111.99961 | -0.34784 | T | 6.35559E+06 | 6.35559E+06 | 100.15530 | 100.56863 | 102070.74000 | 92.85788 | 9.14E-06 | 7.55E-05 |
| *… lines deleted …* | | | | | | | | | | |
| 258.43264 | -0.99873 | T | 3.18546E+06 | 3.18546E+06 | 50.72704 | 801.32800 | 101220.54000 | 943.05560 | 1.35E-15 | 1.39E-03 |
| 258.59483 | -0.99945 | T | 3.18540E+06 | 3.18540E+06 | 50.72612 | 802.16028 | 101219.46000 | 944.13930 | 1.26E-15 | 1.39E-03 |

### 5.4.6.2. Tensile Failure of Waste Material

An excerpt from the stress output file (as formatted by Excel) is shown in Table 5-11. The header to this table gives information such as run time, cavity pressure, cavity radius, drilled radius, cavity volume, far-field pressure at the no-flow outer boundary (R = 19.2 m), and first intact zone. The first intact zone is defined as the repository computational cell corresponding to the intact cavity wall. Zones that are failed and fluidizing are considered intact until the fluidization process is complete. Below the header is a listing of repository cells in the vicinity of the cavity wall showing selected properties related to stress and material failure. Shown are the cell index, radius of the cell center relative to the origin of the repository domain, pore (gas) pressure, radial elastic stress, radial seepage stress, radial effective stress, logical flag for tensile failure, and fraction of the zone fluidized. Tensile strength for this test case is 0.12 MPa.

**Acceptance Criterion 4-7** (Section 5.4.5.2) states that the radial effective stress must equal the sum of the component stresses. This criterion is checked by Excel calculations of the radial effective stress for every zone, shown as "*Excel EffStre*" (in italics) in Table 5-11. In each case, the DRSPALL-calculated radial effective stress EffStre is equal to the Excel-calculated stress (*Excel EffStre* = SeepStr + ElastStr – PorePres) for all digits shown. Thus, **Acceptance Criterion 4-7** (Section 5.4.5.2) is met.

#### *5.4.6.2.1. Stress and failure logic*

Reviewing Table 5-11 allows for an examination of the logic that controls waste material failure due to stresses in the solid. Starting with the first intact zone 104, if radial effective stress is less than tensile strength ($T_s$ = -0.12 MPa), the material is subject to failure. Section 8.4.3.2 of the *Verification and Validation Plan and Validation Document for DRSPALL Version 1.00* (WIPP PA 2003b) explains that negative stress denotes tension. Recall that failure is allowed only if the mean radial effective stress in the cells that cover the specified characteristic length, $L_t$, exceeds the tensile strength. For this problem, $L_t$ = 2 cm or 11 zones for the region where zone size is constant at slightly less than 0.2 cm. Examination of the radial effective stress EffStre for zones 104-114 reveals that the mean stress = -4.2340E+05 Pa, which is less than $T_s$ = -0.12 MPa, and the logical variable Failed is thus True for zones within the characteristic length. Zones beyond the characteristic length are not allowed to fail until all the zones within the characteristic length have fluidized. The Failed variable value of "T" (true) for zones 104-114 (within the characteristic length), and "F" (false) for zones 115-124 (outside the characteristic length) confirms that **Acceptance Criterion 4-8** (Section 5.4.5.2) is met.

**Table 5-11. Excerpt from *drs_122_tc41_stress.dat*, Run Time = 124.080 s.**

Runtime(sec) = 1.24080283E+02
CavPres(Pa) = 5.47070376E+06
CavRadius(m) = 3.14827842E-01
DrilledRad(m) = 2.73076705E-01
CavityVol(m^3) = 1.01603354E-01
Pff(Pa) = 1.47965369E+07
FirstIntactZone = 104

| Zone Index | Radius (m) | PorePres (Pa) | ElastStr (Pa) | SeepStr (Pa) | EffStre (Pa) | *Excel EffStre (Pa)* | Failed (T/F) | Fluidized (-) |
|---|---|---|---|---|---|---|---|---|
| 94 | 0.295937 | 5.50255E+06 | 5.65951E+06 | 4.13257E+00 | 1.56962E+05 | *1.56962E+05* | T | 1.00 |
| 95 | 0.297925 | 5.53753E+06 | 5.84331E+06 | 8.81201E+00 | 3.05783E+05 | *3.05783E+05* | T | 1.00 |
| 96 | 0.299914 | 5.57201E+06 | 6.02226E+06 | 1.33505E+01 | 4.50269E+05 | *4.50269E+05* | T | 1.00 |
| 97 | 0.301902 | 5.60565E+06 | 6.19653E+06 | 1.77529E+01 | 5.90903E+05 | *5.90903E+05* | T | 1.00 |
| 98 | 0.303891 | 5.63846E+06 | 6.36627E+06 | 2.20241E+01 | 7.27838E+05 | *7.27838E+05* | T | 1.00 |
| 99 | 0.305879 | 5.67046E+06 | 6.53163E+06 | 2.61687E+01 | 8.61193E+05 | *8.61193E+05* | T | 1.00 |
| 100 | 0.307868 | 5.70170E+06 | 6.69274E+06 | 3.01913E+01 | 9.91075E+05 | *9.91075E+05* | T | 1.00 |
| 101 | 0.309856 | 5.73221E+06 | 6.84974E+06 | 3.40960E+01 | 1.11757E+06 | *1.11757E+06* | T | 1.00 |
| 102 | 0.311845 | 5.76226E+06 | 7.00276E+06 | 3.78869E+01 | 1.24054E+06 | *1.24054E+06* | T | 1.00 |
| 103 | 0.313834 | 5.79445E+06 | 7.15193E+06 | 4.15672E+01 | 1.35752E+06 | *1.35752E+06* | T | 1.00 |
| 104 | 0.315822 | 5.47070E+06 | 5.47070E+06 | -4.51746E+04 | -4.51746E+04 | *-4.51746E+04* | T | 0.00 |
| 105 | 0.317811 | 5.92116E+06 | 5.64660E+06 | -8.81347E+04 | -3.62702E+05 | *-3.62702E+05* | T | 0.00 |
| 106 | 0.319799 | 6.13043E+06 | 5.81814E+06 | -1.28458E+05 | -4.40751E+05 | *-4.40751E+05* | T | 0.00 |
| 107 | 0.321788 | 6.28300E+06 | 5.98547E+06 | -1.66932E+05 | -4.64463E+05 | *-4.64463E+05* | T | 0.00 |
| 108 | 0.323776 | 6.41925E+06 | 6.14872E+06 | -2.03784E+05 | -4.74321E+05 | *-4.74321E+05* | T | 0.00 |
| 109 | 0.325765 | 6.54813E+06 | 6.30800E+06 | -2.39119E+05 | -4.79246E+05 | *-4.79246E+05* | T | 0.00 |
| 110 | 0.327753 | 6.67183E+06 | 6.46344E+06 | -2.73013E+05 | -4.81400E+05 | *-4.81400E+05* | T | 0.00 |
| 111 | 0.329742 | 6.79108E+06 | 6.61515E+06 | -3.05530E+05 | -4.81453E+05 | *-4.81453E+05* | T | 0.00 |
| 112 | 0.331730 | 6.90624E+06 | 6.76325E+06 | -3.36731E+05 | -4.79723E+05 | *-4.79723E+05* | T | 0.00 |
| 113 | 0.333719 | 7.01760E+06 | 6.90784E+06 | -3.66674E+05 | -4.76430E+05 | *-4.76430E+05* | T | 0.00 |
| 114 | 0.335708 | 7.12537E+06 | 7.04902E+06 | -3.95412E+05 | -4.71754E+05 | *-4.71754E+05* | T | 0.00 |
| 115 | 0.337696 | 7.22976E+06 | 7.18690E+06 | -4.22997E+05 | -4.65853E+05 | *-4.65853E+05* | F | 0.00 |
| 116 | 0.339685 | 7.33096E+06 | 7.32157E+06 | -4.49476E+05 | -4.58867E+05 | *-4.58867E+05* | F | 0.00 |
| 117 | 0.341673 | 7.42914E+06 | 7.45312E+06 | -4.74896E+05 | -4.50919E+05 | *-4.50919E+05* | F | 0.00 |
| 118 | 0.343662 | 7.52446E+06 | 7.58164E+06 | -4.99300E+05 | -4.42120E+05 | *-4.42120E+05* | F | 0.00 |
| 119 | 0.345650 | 7.61707E+06 | 7.70723E+06 | -5.22729E+05 | -4.32571E+05 | *-4.32571E+05* | F | 0.00 |
| 120 | 0.347639 | 7.70709E+06 | 7.82995E+06 | -5.45224E+05 | -4.22359E+05 | *-4.22359E+05* | F | 0.00 |
| 121 | 0.349627 | 7.79465E+06 | 7.94990E+06 | -5.66821E+05 | -4.11567E+05 | *-4.11567E+05* | F | 0.00 |
| 122 | 0.351616 | 7.87986E+06 | 8.06716E+06 | -5.87556E+05 | -4.00265E+05 | *-4.00265E+05* | F | 0.00 |
| 123 | 0.353604 | 7.96284E+06 | 8.18178E+06 | -6.07463E+05 | -3.88521E+05 | *-3.88521E+05* | F | 0.00 |
| 124 | 0.355593 | 8.04368E+06 | 8.29386E+06 | -6.26575E+05 | -3.76392E+05 | *-3.76392E+05* | F | 0.00 |

### *5.4.6.2.2. Verification of stress calculations*

The data from Table 5-11 was used to verify the stress calculations with Excel (Table 5-12). The DRSPALL pore pressure profile shown in Table 5-11 was used to calculate a stress profile, which is compared back to the stress profile calculated by DRSPALL. Table 5-12 displays the new stress profile calculations.

The header in Table 5-12 contains global properties such as Far-Field Stress, Tensile Strength, Poisson's Ratio, Geometry Index (2 = cylindrical, 3 = spherical), Far-Field Pressure, Biot's Beta, and the prefactor which is a convenient coupling of terms to create an intermediate variable as follows:

$$prefactor = (m-1)\beta\left(\frac{1-2\upsilon}{1-\upsilon}\right) \tag{5.4-8}$$

The calculations start at the first intact zone 104 and are carried through to zone 124. The following notes apply:

- $r_c/r$ denotes the ratio cavity radius to zone center radius
- The Radial Elastic Stress is calculated per Equation 5.4-3
- The Integral Over *dr* represents the integral in Equation 5.4-2 over one zone
- The sum is the integral over all zones from First Intact Zone to the given zone
- The Radial Seepage Stress is calculated by Equation 5.4-2
- The Radial Effective Stress is calculated by Equation 5.4-1

The Excel-calculated stress values are compared to DRSPALL values and the results appear in Table 5-13. The maximum relative difference was 9.01E-14 for Radial Elastic Stress, 1.09E-12 for Radial Seepage Stress, and 1.11E-12 for Radial Effective Stress. The small differences for the three stresses confirm that **Acceptance Criterion 4-9** (Section 5.4.5.2) is met.

### Table 5-12. Independent Excel Calculations of Stress Profiles from Pore Pressure Data Obtained from Table 5-11.

| | | |
|---|---|---|
| Far-field stress | 1.4900E+07 | |
| Tensile strength | 1.2000E+05 | |
| Poisson's ratio | 3.8000E-01 | |
| Geometry index | 3 | |
| Far-field pressure | 1.4794E+07 | |
| Biot Beta | 1.0000E+00 | |
| Prefactor | 7.7419E-01 | |

| Zone Index | $r_c/r$ | Radial Elastic Stress | Integral over dr | Sum | Radial Seepage Stress | Radial Effective Stress |
|---|---|---|---|---|---|---|
| 104 | 1.0000000 | 5.470704E+06 | -1.838115E+03 | -1.838115E+03 | -4.517464E+04 | -4.517464E+04 |
| 105 | 0.9937430 | 5.646596E+06 | -1.816171E+03 | -3.654286E+03 | -8.813467E+04 | -3.627022E+05 |
| 106 | 0.9875638 | 5.818140E+06 | -1.772526E+03 | -5.426812E+03 | -1.284583E+05 | -4.407510E+05 |
| 107 | 0.9814610 | 5.985471E+06 | -1.757721E+03 | -7.184533E+03 | -1.669320E+05 | -4.644633E+05 |
| 108 | 0.9754331 | 6.148715E+06 | -1.749671E+03 | -8.934204E+03 | -2.037841E+05 | -4.743210E+05 |
| 109 | 0.9694789 | 6.307998E+06 | -1.743497E+03 | -1.067770E+04 | -2.391194E+05 | -4.792461E+05 |
| 110 | 0.9635969 | 6.463439E+06 | -1.738103E+03 | -1.241580E+04 | -2.730127E+05 | -4.814001E+05 |
| 111 | 0.9577858 | 6.615153E+06 | -1.733218E+03 | -1.414902E+04 | -3.055298E+05 | -4.814530E+05 |
| 112 | 0.9520444 | 6.763251E+06 | -1.728757E+03 | -1.587778E+04 | -3.367312E+05 | -4.797228E+05 |
| 113 | 0.9463714 | 6.907840E+06 | -1.724677E+03 | -1.760246E+04 | -3.666740E+05 | -4.764296E+05 |
| 114 | 0.9407657 | 7.049024E+06 | -1.720948E+03 | -1.932340E+04 | -3.954121E+05 | -4.717540E+05 |
| 115 | 0.9352259 | 7.186901E+06 | -1.717545E+03 | -2.104095E+04 | -4.229966E+05 | -4.658534E+05 |

**Table 5-12. Independent Excel Calculations of Stress Profiles from Pore Pressure Data Obtained from Table 5-11. (Continued)**

| Zone Index | $r_c/r$ | Radial Elastic Stress | Integral over dr | Sum | Radial Seepage Stress | Radial Effective Stress |
|---|---|---|---|---|---|---|
| 116 | 0.9297510 | 7.321569E+06 | -1.714446E+03 | -2.275540E+04 | -4.494758E+05 | -4.588670E+05 |
| 117 | 0.9243399 | 7.453120E+06 | -1.711630E+03 | -2.446703E+04 | -4.748957E+05 | -4.509190E+05 |
| 118 | 0.9189913 | 7.581644E+06 | -1.709081E+03 | -2.617611E+04 | -4.992996E+05 | -4.421203E+05 |
| 119 | 0.9137043 | 7.707227E+06 | -1.706781E+03 | -2.788289E+04 | -5.227292E+05 | -4.325706E+05 |
| 120 | 0.9084778 | 7.829953E+06 | -1.704716E+03 | -2.958760E+04 | -5.452237E+05 | -4.223593E+05 |
| 121 | 0.9033108 | 7.949903E+06 | -1.702872E+03 | -3.129047E+04 | -5.668207E+05 | -4.115667E+05 |
| 122 | 0.8982022 | 8.067155E+06 | -1.701236E+03 | -3.299171E+04 | -5.875557E+05 | -4.002654E+05 |
| 123 | 0.8931510 | 8.181784E+06 | -1.699797E+03 | -3.469151E+04 | -6.074629E+05 | -3.885207E+05 |
| 124 | 0.8881563 | 8.293864E+06 | -1.698544E+03 | -3.639005E+04 | -6.265747E+05 | -3.763916E+05 |

**Table 5-13. Summary of Differences Between DRSPALL and Excel Calculations for Stress Verification.**

| Zone Index | Radial Elastic Stress | | Radial Seepage Stress | | Radial Effective Stress | |
|---|---|---|---|---|---|---|
| | Absolute Diff | Relative Diff | Absolute Diff | Relative Diff | Absolute Diff | Relative Diff |
| 104 | 0.000E+00 | 0.00E+00 | 4.938E-08 | 1.09E-12 | 4.993E-08 | 1.11E-12 |
| 105 | 1.695E-07 | 3.00E-14 | 9.577E-08 | 1.09E-12 | 4.761E-08 | 1.31E-13 |
| 106 | 2.813E-07 | 4.83E-14 | 1.389E-07 | 1.08E-12 | 2.226E-07 | 5.05E-13 |
| 107 | 5.392E-07 | 9.01E-14 | 1.789E-07 | 1.07E-12 | 3.501E-07 | 7.54E-13 |
| 108 | 1.034E-07 | 1.68E-14 | 3.149E-08 | 1.55E-13 | 1.750E-07 | 3.69E-13 |
| 109 | 1.397E-08 | 2.21E-15 | 7.066E-08 | 2.96E-13 | 3.027E-09 | 6.32E-15 |
| 110 | 2.477E-07 | 3.83E-14 | 1.090E-07 | 3.99E-13 | 4.849E-08 | 1.01E-13 |
| 111 | 3.884E-07 | 5.87E-14 | 1.398E-07 | 4.58E-13 | 2.191E-07 | 4.55E-13 |
| 112 | 5.392E-07 | 7.97E-14 | 1.683E-07 | 5.00E-13 | 3.402E-07 | 7.09E-13 |
| 113 | 1.024E-07 | 1.48E-14 | 4.738E-08 | 1.29E-13 | 1.200E-07 | 2.52E-13 |
| 114 | 1.248E-07 | 1.77E-14 | 7.747E-08 | 1.96E-13 | 5.763E-08 | 1.22E-13 |
| 115 | 2.729E-07 | 3.80E-14 | 1.125E-07 | 2.66E-13 | 1.199E-07 | 2.57E-13 |
| 116 | 4.312E-07 | 5.89E-14 | 1.329E-07 | 2.96E-13 | 2.972E-07 | 6.48E-13 |
| 117 | 1.248E-07 | 1.67E-14 | 3.626E-08 | 7.64E-14 | 1.302E-07 | 2.89E-13 |
| 118 | 3.818E-08 | 5.04E-15 | 6.013E-08 | 1.20E-13 | 5.239E-08 | 1.18E-13 |
| 119 | 1.332E-07 | 1.73E-14 | 8.586E-08 | 1.64E-13 | 6.804E-08 | 1.57E-13 |
| 120 | 2.384E-07 | 3.04E-14 | 1.051E-07 | 1.93E-13 | 1.527E-07 | 3.61E-13 |
| 121 | 4.303E-07 | 5.41E-14 | 1.311E-07 | 2.31E-13 | 2.992E-07 | 7.27E-13 |
| 122 | 4.098E-08 | 5.08E-15 | 4.878E-08 | 8.30E-14 | 6.967E-08 | 1.74E-13 |
| 123 | 9.779E-08 | 1.20E-14 | 7.311E-08 | 1.20E-13 | 5.541E-08 | 1.43E-13 |
| 124 | 2.161E-07 | 2.61E-14 | 9.057E-08 | 1.45E-13 | 4.488E-08 | 1.19E-13 |
| Maximum | 5.392E-07 | 9.01E-14 | 1.789E-07 | 1.09E-12 | 3.501E-07 | 1.11E-12 |

### 5.4.6.3. Fluidized Bed Transport of Disaggregated Waste Material

An excerpt from the fluidization output file (formatted in Excel) is shown in Table 5-14. The header to this table gives information such as run time, cavity pressure, cavity radius, gas density in the cavity, minimum fluidization velocity, superficial gas velocity at the cavity wall, mass of waste in well, and the first intact zone. The first intact zone is defined as the repository computational cell corresponding to the intact cavity wall. Zones that are failed and fluidizing

are considered intact until the fluidization process is complete. Below the header is a listing of repository cells in the vicinity of the cavity wall showing selected properties related to fluidization: cell index, radius of the cell center relative to the origin of the repository domain, logical flags for failure of the cell completed, fluidization started, and fluidization completed, and the fraction of the cell fluidized. A value of -1.0 in the Fraction Fluidized column indicates that the cell was removed by drilling, while a 1.0 indicates that the zone was removed by tensile failure and fluidized bed transport.

**Table 5-14. Excerpt from *drs_122_tc41_fluidization.dat*, Run Time = 124.67269 s.**

Runtime (sec) = 1.2467268699803E+02
Cavity Pressure (Pa) = 5.5163168803599E+06
Cavity Radius (m) = 3.3670179085049E-01
Gas Density (kg/m^3) = 4.4672932317824E+00
Fluidization Velocity (m) = 2.7732542845385E-01
Superficial Gas Velocity (m)
(First Intact Zone) = 5.0686054509911E-01
Waste In Well (kg) = 5.5043059478159E+01
FirstIntactZone = 115

| Cell Index | Radius (m) | Failure Completed (T/F) | Fluidization Start (T/F) | Fluidization Complete (T/F) | Fraction Fluidized |
|---|---|---|---|---|---|
| 105 | 0.3178107 | T | T | T | 1 |
| 106 | 0.3197992 | T | T | T | 1 |
| 107 | 0.3217877 | T | T | T | 1 |
| 108 | 0.3237763 | T | T | T | 1 |
| 109 | 0.3257648 | T | T | T | 1 |
| 110 | 0.3277534 | T | T | T | 1 |
| 111 | 0.3297419 | T | T | T | 1 |
| 112 | 0.3317304 | T | T | T | 1 |
| 113 | 0.3337190 | T | T | T | 1 |
| 114 | 0.3357075 | T | T | T | 1 |
| 115 | 0.3376961 | T | T | F | 0.0001 |
| 116 | 0.3396846 | T | T | F | 0.0001 |
| 117 | 0.3416731 | T | T | F | 0.0001 |
| 118 | 0.3436617 | T | T | F | 0 |
| 119 | 0.3456502 | F | F | F | 0 |
| 120 | 0.3476388 | F | F | F | 0 |
| 121 | 0.3496273 | F | F | F | 0 |
| 122 | 0.3516158 | F | F | F | 0 |
| 123 | 0.3536044 | F | F | F | 0 |
| 124 | 0.3555929 | F | F | F | 0 |
| 125 | 0.3575815 | F | F | F | 0 |
| 126 | 0.3595700 | F | F | F | 0 |
| 127 | 0.3615586 | F | F | F | 0 |
| 128 | 0.3635471 | F | F | F | 0 |
| 129 | 0.3655356 | F | F | F | 0 |
| 130 | 0.3675242 | F | F | F | 0 |
| 131 | 0.3695127 | F | F | F | 0 |
| 132 | 0.3715013 | F | F | F | 0 |
| 133 | 0.3734898 | F | F | F | 0 |
| 134 | 0.3754783 | F | F | F | 0 |
| 135 | 0.3774669 | F | F | F | 0 |

#### 5.4.6.3.1. Fluidization logic

At the point in the code execution shown in Table 5-14, 114 computational cells in the repository have been removed and transported into the cavity and wellbore by a combination of drilling and tensile failure/fluidization. The first intact zone that forms the cavity wall is cell 115. Zones 105-114 were completely removed by tensile failure and fluidization (Fraction Fluidized = 1.0). Zones 115-118 have failed in tension (Failure Completed = T), and zones 115-117 are currently fluidizing (Fraction Fluidized > 0). In order for zones to fluidize, the superficial gas velocity at the cavity wall must exceed the minimum fluidization velocity. The header in Table 5-14 confirms that the Superficial Gas Velocity at the first intact zone (115) = 0.5069 m/s, while the Fluidization Velocity = 0.2773 m/s. As such, the failed zone 115 is subject to fluidization, and fluidization is currently in process. **Acceptance Criterion 4-10** (Section 5.4.5.3) is met because the Fluidization Start = "T" (true) in zone 115 confirms that fluidization has started in the first intact zone. Zones must complete fluidization in sequence such that zone 116 cannot completely fluidize until after zone 115 has completely fluidized. Also, zones require a finite time to fluidize. The progress of a particular zone through the fluidization process is given by the fraction fluidized, which varies from 0.0 (not fluidized) to 1.0 (fully fluidized). Notice that zones 115-117 are just starting to fluidize in Table 5-14 (run time 124.67269, line 4871 in *drs_122_tc41_fluidization.dat*). These zones are fully fluidized at run time 125.34018 s (line 5135 in *drs_122_tc41_fluidization.dat*).

#### 5.4.6.3.2. Verification of fluidization velocity

Data from Table 5-14 were imported into an EXCEL spreadsheet (Table 5-15) in order to verify proper calculation of Ergun's minimum fluidization velocity (Equation 5.4-5). The dependent variable in Ergun's formula is $U_f$, which can be solved for by the quadratic formula:

$$AU_f^{\,2} + BU_f + C = 0 \tag{5.4-9}$$

$$U_f = \frac{-B \pm \sqrt{B^2 - 4AC}}{2A} \tag{5.4-10}$$

Equation 5.4-5 was rearranged to form the constants A, B, and C, defined in Equation 5.4-9, which are evaluated in Table 5-15. The final lines in Table 5-15 compare the fluidization velocity calculated by Excel to that calculated by DRSPALL for the given input conditions. The relative difference evaluated to 1.30E-14. This small relative difference is less than 1E-4, so **Acceptance Criterion 4-11** (Section 5.4.5.3) is met.

#### 5.4.6.3.3. Verification of fluidization time

The Excel calculation of the fluidization time is shown in Table 5-16. For the given conditions, the fluidization time using parameters from run time = 124.67267 s was $t_f$ = 0.666 s. For comparison, the fluidization time, $t_f$, provided in output file *drs_122_tc41_fluidization_time.dat* for zone 115 is 0.665 s (Figure 5-18).

**Table 5-15. Excel Solution for Minimum Fluidization Velocity, $U_f$.**

| Parameter | Value | Units |
|---|---|---|
| run time | 1.2467269E+02 | s |
| gas density | 4.4672932E+00 | $kg/m^3$ |
| porosity | 5.7500000E-01 | - |
| waste density | 2.6500000E+03 | $kg/m^3$ |
| gas viscosity | 8.9339000E-06 | Pa·s |
| particle diameter | 1.0000000E-03 | m |
| shape factor | 2.5000000E-01 | - |
| gravity | 9.8067000E+00 | $m/s^2$ |
| a | 9.2066419E+06 | |
| b | 2.6828724E+06 | |
| c | -1.4521060E+06 | |
| $b^2$-4ac | 6.0673883E+13 | |
| **Excel fluidization velocity** | **0.27732543** | **m/s** |
| **DRSPALL fluidization velocity** | **0.27732543** | **m/s** |
| **Relative difference** | **1.30E-14** | |

Confirmation of proper implementation of $t_f$ in DRSPALL is possible by examining the amount of time required to completely fluidize zone 115 that started to fluidize near run time = 124.67267 s. The reporting frequency in *drs_122_tc41_fluidization.dat* is not sufficient to capture both the beginning and ending of fluidization for zone 115, but the report of fraction fluidized at two times may be used to extrapolate an approximate fluidization time. This strategy is shown in the lower half of Table 5-16, with runtime #1 and runtime #2 representing the two selected run time reports from which the fluidization time is extrapolated. The projected fluidization time from this coarse method is 0.646 s. This compares favorably with the values calculated by Excel ($t_f$ = 0.666 s) and extracted from output file *drs_122_tc41_fluidization_time.dat* (Figure 5-18, zone 115, $t_f$ = 0.665).

**Table 5-16. Excel Solution for Fluidization Time, $t_f$.**

| Parameter | Value | Units |
|---|---|---|
| run time | 124.67267 | s |
| radius to center of first intact cell | 0.3376961 | m |
| superficial gas velocity | 0.5071014 | m/s |
| **fluidization time** | **0.6659340** | **s** |
| *From drs_122_tc41_fluidization.dat* | | |
| runtime #1 | 124.67267 | s |
| fraction fluidized #1 | 0.00010 | - |
| runtime #2 | 124.67274 | s |
| fraction fluidized #2 | 0.00020 | - |
| **projected fluidization time** | **0.646** | **s** |

DRSPALL/Test/Output/Solaris_122/drs_122_tc41_fluidization_time.dat
Program DR_SPALL - WIPP PA 2003
ASCII Output file for Test Case #4

| Zone | Fluidization Time |
|---|---|
| 71 | 4.65E-01 |
| 72 | 2.93E-01 |
| *…lines deleted…* | |
| 114 | 5.25E-01 |
| 115 | 6.65E-01 |
| 116 | 4.00E-01 |
| *…lines deleted…* | |
| 311 | 1.26E+00 |
| 312 | 1.30E+00 |

**Figure 5-18. Fluidization Time Values from *drs_122_tc41_fluidization_time.dat*.**

#### *5.4.6.3.4. Verification of drilling and spall volumes and masses*

The Excel calculations of waste volumes and masses removed from the repository due to drilling and spall (failure and fluidization) are shown in Table 5-17. The table also gives the values that were extracted from the diagnostics file and the output CAMDAT file. The difference in CAVRAD0 between the diagnostics and CAMDAT files is due the precision in the displayed number not the actual value. The maximum relative difference evaluated to 4.31E-06 for SPLMASS. This small relative difference is less than 1E-4, so **Acceptance Criterion 4-12** (Section 5.4.5.3) is met.

**Table 5-17. Drilling and Spall Volumes and Masses from Output CAMDAT File.**

| CAMDAT Variable | Description | Diagnostics File | Output CAMDAT File | Excel Calculation | Relative Difference |
|---|---|---|---|---|---|
| CAVRAD0 | Initial pseudo-cavity radius | 1.100E-01 | 1.10008E-01 | 1.10008E-01 | 2.29E-08 |
| CUTMASS | Cuttings mass | 2.60780E+02 | 2.60779E+02 | 2.60779E+02 | 2.36E-06 |
| TOTMASS | Total mass | 8.35980E+02 | 8.35976E+02 | 8.35978E+02 | 2.23E-06 |
| SPLMASS | Spall mass | 5.75200E+02 | 5.75197E+02 | 5.75200E+02 | 4.31E-06 |
| SPL2MASS | Incremental spall mass | 8.02610E+02 | 8.02610E+02 | 8.02608E+02 | 2.36E-06 |
| CUTVOLEQ | Equivalent uncompacted cuttings volume | 6.56050E-01 | 6.56048E-01 | 6.56047E-01 | 2.34E-06 |
| TOTVOLEQ | Equivalent uncompacted total volume | 2.10310E+00 | 2.10309E+00 | 2.10309E+00 | 2.21E-06 |
| SPLVOLEQ | Equivalent uncompacted spall volume | 1.44700E+00 | 1.44704E+00 | 1.44704E+00 | 4.28E-06 |
| SPLVOL2EQ | Equivalent uncompacted incremental spall volume | 2.01910E+00 | 2.01915E+00 | 2.01914E+00 | 2.38E-06 |

### 5.4.6.4. Expulsion of Disaggregated Waste Material

Excerpts from the expulsion output file (as formatted by Excel) show data at various run times as follows:

a) Table 5-18 shows data near the time of penetration (run time = 33.2 to 34.8 s).

b) Table 5-19 shows data exhibiting early waste expulsion (run time = 113.5 to 115.3 s).

c) Table 5-20 shows late time waste expulsion data approaching steady conditions (run time = 404.0 to 405.7 s).

#### *5.4.6.4.1. Near bit penetration*

Table 5-18 shows the expulsion data at several times near bit penetration at 33.9 s. Prior to bit penetration, the logical variable Repository Penetrated = "F" (false), and no zones have been removed from the repository. Also, all of the waste mass accounting variables (i.e., total waste in well) are zero, and the waste position in the well is -653 m, representing the well bottom. After bit penetration, the number of zones removed increases monotonically due to drilling. The drill bit must completely penetrate a zone before that zone is removed from the repository, so there is a time lag between bit penetration (33.9 s) and the removal of the first zone (34.5 s). Mass Waste Removed is the sum of Waste in Store + Total Waste In Well + Waste Mass Ejected. Waste Mass Ejected is still zero since it has not had time to transport 653 m to the land surface, and Waste Position In Well shows that the location of the waste front moves upward with time.

**Table 5-18. Excerpt from *drs_122_tc41_expulsion.dat* Near the Time of Bit Penetration.**

| Runtime (s) | Repository Penetrated (T/F) | Zones Removed (-) | Mass Waste Removed (kg) | Waste In Store (kg) | Total Waste In Well (kg) | Waste Mass Ejected (kg) | Waste Position In Well (m) | Mass Balance Error (-) |
|---|---|---|---|---|---|---|---|---|
| 33.20878 | F | 0 | 0.00000 | 0.00000 | 0.00000 | 0.00000 | -653.0 | 0.00E+00 |
| 33.37025 | F | 0 | 0.00000 | 0.00000 | 0.00000 | 0.00000 | -653.0 | 0.00E+00 |
| 33.53172 | F | 0 | 0.00000 | 0.00000 | 0.00000 | 0.00000 | -653.0 | 0.00E+00 |
| 33.69319 | F | 0 | 0.00000 | 0.00000 | 0.00000 | 0.00000 | -653.0 | 0.00E+00 |
| 33.85467 | T | 0 | 0.00000 | 0.00000 | 0.00000 | 0.00000 | -653.0 | 0.00E+00 |
| 34.01614 | T | 0 | 0.00000 | 0.00000 | 0.00000 | 0.00000 | -653.0 | 0.00E+00 |
| 34.17761 | T | 0 | 0.00000 | 0.00000 | 0.00000 | 0.00000 | -653.0 | 0.00E+00 |
| 34.33908 | T | 0 | 0.00000 | 0.00000 | 0.00000 | 0.00000 | -653.0 | 0.00E+00 |
| 34.50055 | T | 1 | 0.17339 | 0.11157 | 0.06182 | 0.00000 | -651.0 | 7.20E-16 |
| 34.66203 | T | 1 | 0.17339 | 0.06056 | 0.11284 | 0.00000 | -649.0 | 6.80E-16 |
| 34.82350 | T | 1 | 0.17339 | 0.03273 | 0.14066 | 0.00000 | -648.0 | 8.36E-15 |

#### *5.4.6.4.2. Early waste expulsion at surface*

Table 5-19 shows the expulsion data near the time of the first arrival of waste solids at the land surface. Note that the position of the waste front in the well approaches z = 0 with time, and waste is first expelled at the surface at about 114.7 s. The Waste Mass Ejected variable reflects a time integral at the wellbore outlet, and the leading "tail" of the waste causes this variable to compute small but nonzero releases prior to the arrival of the "front" defined by Waste Position

in Well. The mass balance error in this table is defined as [Mass Waste Removed – (Waste In Store + Total Waste In Well + Waste Mass Ejected)] / Mass Waste Removed.

**Table 5-19. Excerpt from *drs_122_tc41_expulsion.dat* Near the Time of Early Waste Expulsion at Land Surface.**

| Runtime (s) | Repository Penetrated (T/F) | Zones Removed (-) | Mass Waste Removed (kg) | Waste In Store (kg) | Total Waste In Well (kg) | Waste Mass Ejected (kg) | Waste Position In Well (m) | Mass Balance Error (-) |
|---|---|---|---|---|---|---|---|---|
| 113.53477 | T | 81 | 43.84768 | 0.00029 | 43.83104 | 0.01635 | -29.1 | 6.49E-13 |
| 113.69626 | T | 81 | 43.84768 | 0.00022 | 43.82632 | 0.02114 | -25.1 | 6.43E-13 |
| 113.85776 | T | 81 | 43.84768 | 0.00017 | 43.82042 | 0.02709 | -21.0 | 6.40E-13 |
| 114.01926 | T | 81 | 43.84768 | 0.00013 | 43.81313 | 0.03441 | -17.0 | 6.48E-13 |
| 114.18076 | T | 81 | 43.84768 | 0.00010 | 43.80423 | 0.04335 | -12.0 | 6.61E-13 |
| 114.34226 | T | 81 | 43.84768 | 0.00008 | 43.79345 | 0.05415 | -6.0 | 6.56E-13 |
| 114.50376 | T | 81 | 43.84768 | 0.00006 | 43.78052 | 0.06709 | -2.0 | 6.50E-13 |
| 114.66526 | T | 81 | 43.84768 | 0.00005 | 43.76516 | 0.08247 | 0.0 | 6.56E-13 |
| 114.82676 | T | 81 | 43.84768 | 0.00004 | 43.74706 | 0.10058 | 0.0 | 6.48E-13 |
| 114.98825 | T | 81 | 43.84768 | 0.00003 | 43.72592 | 0.12173 | 0.0 | 6.56E-13 |
| 115.14975 | T | 81 | 43.84768 | 0.00002 | 43.70142 | 0.14623 | 0.0 | 6.48E-13 |
| 115.31125 | T | 81 | 43.84768 | 0.00002 | 43.67327 | 0.17439 | 0.0 | 6.44E-13 |

#### *5.4.6.4.3. Late time waste expulsion*

Table 5-20 shows expulsion data at late time (run time > 404 s) showing steady state behavior with a total of 301 zones removed, corresponding to 836.0 kg of waste removed from the repository and an identical 836.0 kg of waste expelled to the surface. The mass balance error is reported as 6.69E-12.

**Table 5-20. Excerpt from *drs_122_tc41_expulsion.dat* at Late Time Nearing Steady Conditions.**

| Runtime (s) | Repository Penetrated (T/F) | Zones Removed (-) | Mass Waste Removed (kg) | Waste In Store (kg) | Total Waste In Well (kg) | Waste Mass Ejected (kg) | Waste Position In Well (m) | Mass Balance Error (-) |
|---|---|---|---|---|---|---|---|---|
| 404.01292 | T | 301 | 835.97639 | 9.80E-41 | -1.22E-11 | 835.97639 | -653.0 | 6.69E-12 |
| 404.17662 | T | 301 | 835.97639 | 9.12E-41 | -1.22E-11 | 835.97639 | -653.0 | 6.69E-12 |
| 404.34033 | T | 301 | 835.97639 | 8.49E-41 | -1.22E-11 | 835.97639 | -653.0 | 6.69E-12 |
| 404.50403 | T | 301 | 835.97639 | 7.90E-41 | -1.22E-11 | 835.97639 | -653.0 | 6.69E-12 |
| 404.66774 | T | 301 | 835.97639 | 7.35E-41 | -1.22E-11 | 835.97639 | -653.0 | 6.69E-12 |
| 404.83145 | T | 301 | 835.97639 | 6.84E-41 | -1.22E-11 | 835.97639 | -653.0 | 6.69E-12 |
| 404.99516 | T | 301 | 835.97639 | 6.36E-41 | -1.22E-11 | 835.97639 | -653.0 | 6.69E-12 |
| 405.15887 | T | 301 | 835.97639 | 5.92E-41 | -1.22E-11 | 835.97639 | -653.0 | 6.69E-12 |
| 405.32258 | T | 301 | 835.97639 | 5.51E-41 | -1.22E-11 | 835.97639 | -653.0 | 6.69E-12 |
| 405.48630 | T | 301 | 835.97639 | 5.12E-41 | -1.22E-11 | 835.97639 | -653.0 | 6.69E-12 |
| 405.65001 | T | 301 | 835.97639 | 4.77E-41 | -1.22E-11 | 835.97639 | -653.0 | 6.69E-12 |

#### *5.4.6.4.4. Summary*

The acceptance criteria for the expulsion of disaggregated waste material will be confirmed by examining *drs_122_tc41_expulsion.dat* (excerpts of which are shown in Tables 5-18, 5-19, and 5-20). Waste Position In Well decreases from -653 to 0, so **Acceptance Criterion 4-13** (Section 5.4.5.4) is met. Waste Mass Ejected is very small (< 0.08 kg) before z = 0 (when Waste Position

in Well reaches 0), then it monotonically increases, confirming the **Acceptance Criterion 4-14** (Section 5.4.5.4) is met. The Mass Balance Error is small (≤ 6.69E-12) for all times, so **Acceptance Criterion 4-15** (Section 5.4.5.4) is met.

#### 5.4.6.5. External Interfaces

The output CAMDAT file from Case 4.1 was successfully examined with GROPECDB in the analysis presented above (Sections 5.4.6.1 and 0), confirming that the output file is in the proper CAMDAT file format, so **Acceptance Criterion 4-17** (Section 5.4.5.5) is met.

Case 4.2 is the only test case that reads data from an input CAMDAT file. The GROPECDB excerpt of all properties of the input CAMDAT file for Case 4.2 is shown in Figure 5-19. The input control file for Case 4.2 is shown in Figure 5-20. Many of the inputs are from properties on the input CAMDAT file; some values are explicitly specified; and some are set to DEFAULT. The excerpt of the diagnostics file for Case 4.2 is shown in Figure 5-21. An examination of this file confirms that the DRSPALL parameters are being read correctly from the input control file and the input CAMDAT file.

The diagnostics file echoes the input file (not shown in Figure 5-21), then echoes the input file with numeric values replacing all CAMDAT properties and DEFAULT values, then lists the parameters used in the run. Note that under "Parameters used in this run", the parameters are listed in order within category in the input control file, as explained in the DRSPALL user's manual (WIPP PA 2004b, 2013c, and 2015b). The parameter identifier in the input control file is just a comment and may not match the identifier in the diagnostics file.

When a CAMDAT property is referenced in the input control file, its value matches the value listed in the diagnostics file with one exception: Exit Pipe Diameter under "Parameters used in this run". When a value is explicitly specified in the input control file, the value matches the value listed in the diagnostics file with two exceptions: Total Thickness and First Wellbore Zone under "Parameters used in this run". Note that the "Input Echo (with numeric values)" always lists the input values. The calculations below apply to "Parameters used in this run" only.

Exit Pipe Diameter is read from CAMDAT property DRSPALL:EXITPDIA (0.2032), but there is no exit pipe, i.e., the Exit Pipe Length (DRSPALL:EXITPLEN) is zero. The Exit Pipe Diameter is overwritten with the annulus diameter. The annulus diameter is calculated with the Bit Diameter (DRSPALL:BITDIAM) = 0.31115 and Pipe Diameter (DRSPALL:PIPEDIAM) = 0.11430. Thus, the Exit Pipe Diameter is calculated as follows:

$$ExitPipeDiameter = 2\sqrt{\frac{\pi(BitDiameter/2)^2 - \pi(PipeDiameter/2)^2}{\pi}} = 0.2894 \quad (5.4\text{-}11)$$

Total Thickness is specified as 0.0 by the user, so it is calculated internally from the initial repository height (H = constant 3.96), the uncompacted waste porosity ($\varphi_u$ = constant 0.85) and the input initial waste porosity ($\varphi_i$ = 0.575 = DRSPALL:REPIPOS) as follows:

$$T_{rep} = H\left(\frac{1-\varphi_u}{1-\varphi_i}\right) = 3.96\left(\frac{1-0.85}{1-0.575}\right) = 1.3976 \tag{5.4-12}$$

First Wellbore Zone is a flag indicating whether downward flow inside of the pipe is modeled. If the input value is greater than zero (only the flow up the annulus is modeled), First Wellbore Zone is set to the index of the computational cell at the bottom of wellbore, or 651 for this problem.

Tensile Velocity, Bit Nozzle Number, Bit Nozzle Diameter, and Choke Efficiency request DEFAULT values in the input control file. The default values as specified in the DRSPALL user's manual (WIPP PA 2004b, 2013c, and 2015b) are: 1000.0, 3.0, 0.011112, and 0.9, respectively.

```
CAMDAT File:  /home/run_mast/Test_Run/DRSPALL/DRSPALL/Input/drs_tc42_ms.cdb

PROPERTIES

Element Block 1)    "GLOBAL  "     1=ID     1 elements (1..1)

Element Block 2)    "DRSPALL "     2=ID     0 elements
  SURFELEV    REPOSTOP    REPOSTCK    DRZTCK      DRZPERM     REPOTRAD
 1.0373E+03  3.8531E+02  1.4200E+00  8.5000E-01  1.0000E-15  1.9200E+01
  REPIPRES    FFPORPRS    FFSTRESS    REPIPOR     REPIPERM    BIOTBETA
 1.4800E+07  1.4800E+07  1.4900E+07  5.7500E-01  1.7000E-13  1.0000E+00
  POISRAT     COHESION    FRICTANG    TENSLSTR    PARTDIAM    GASBSDEN
 3.8000E-01  1.3000E+05  4.5800E+01  1.2000E+05  1.0000E-03  8.2000E-02
  GASVISCO    INITMDEN    MUDVISCO    ANNUROUG    MUDSOLMX    MUDSOLVE
 8.9339E-06  1.2100E+03  1.1000E-02  3.9400E-04  6.1500E-01 -1.5000E+00
  BITDIAM     PIPEDIAM    COLRDIAM    PIPEID      COLRLNGT    DRILRATE
 3.1115E-01  1.1430E-01  2.0320E-01  9.7180E-02  1.8290E+02  4.4450E-03
  INITBAR     MUDPRATE    DDZTHICK    DDZPERM     STPDVOLR    STPPVOLR
 1.5000E-01  2.0181E-02  1.6000E-01  1.0000E-14  1.0000E+03  1.0000E+03
  STPDTIME    SHAPEFAC    FRCHBETA    CHARLEN     PIPEROUG    EXITPLEN
 1.0000E+03  5.5000E-01  1.1500E-06  2.0000E-02  5.0000E-05  0.0000E+00
  EXITPDIA    MAXPPRES
 2.0320E-01  2.7500E+07

Element Block 3)    "REFCON  "     3=ID     0 elements
  PI          GRAVACC
 3.1416E+00  9.8067E+00

Element Block 4)    "BLOWOUT "     4=ID     0 elements
  RGAS        TREPO       RHOS
 4.1160E+03  3.0000E+02  2.6500E+03

Element Block 5)    "BRINESAL"     5=ID     0 elements
  COMPRES
 3.1000E-10
```

**Figure 5-19. Properties from Input CAMDAT File *drs_tc42_ms.cdb* for Case 4.2.**

```
REPOSITORY
Land Elevation                  (m):  DRSPALL SURFELEV
Repository top                  (m):  DRSPALL REPOSTOP
Total Thickness                 (m):  0.0
DRZ Thickness                   (m):  DRSPALL DRZTCK
DRZ Permeability              (m^2):  DRSPALL DRZPERM
Outer Radius                    (m):  1.9200E+01
Initial Gas Pressure            (m):  DRSPALL REPIPRES
Far-Field In-Situ Stress        (m):  DRSPALL FFSTRESS

WASTE
Porosity                        (-):  DRSPALL REPIPOR
Permeability                  (m^2):  DRSPALL REPIPERM
Forchheimer Beta                (-):  DRSPALL FRCHBETA
Biot Beta                       (-):  DRSPALL BIOTBETA
Poisson's Ratio                 (-):  DRSPALL POISRAT
Cohesion                       (Pa):  DRSPALL COHESION
Friction Angle                (deg):  DRSPALL FRICTANG
Tensile Strength               (Pa):  DRSPALL TENSLSTR
Lt                              (m):  0.02
Particle Diameter               (m):  DRSPALL PARTDIAM
Gas Viscosity                (Pa-s):  DRSPALL GASVISCO

MUD
Density                    (kg/m^3):  DRSPALL INITMDEN
Viscosity                    (Pa-s):  DRSPALL MUDVISCO
Wall Roughness Pipe             (m):  DRSPALL PIPEROUG
Wall Roughness Annulus          (m):  DRSPALL ANNUROUG
Max Solids Vol. Frac.        (Pa-s):  DRSPALL MUDSOLMX
Solids Viscosity Exp.        (Pa-s):  DRSPALL MUDSOLVE

WELLBORE/DRILLING
Bit Diameter                    (m):  DRSPALL BITDIAM
Pipe Diameter                   (m):  DRSPALL PIPEDIAM
Collar Diameter                 (m):  DRSPALL COLRDIAM
Pipe Inside Diameter            (m):  DRSPALL PIPEID
Collar Length                   (m):  DRSPALL COLRLNGT
Exit pipe Length                (m):  DRSPALL EXITPLEN
Exit Pipe Diameter              (m):  DRSPALL EXITPDIA
Drilling Rate                 (m/s):  DRSPALL DRILRATE
Bit Above Respository(init.)    (m):  DRSPALL INITBAR
Mud Pump Rate               (m^3/s):  DRSPALL MUDPRATE
Max Pump Pressure              (Pa):  27.5d6
DDZ Thickness                   (m):  DRSPALL DDZTHICK
DDZ Permeability              (m^2):  DRSPALL DDZPERM
Stop Drill Exit Vol Rate    (m^3/s):  DRSPALL STPDVOLR
Stop Pump Exit Vol Rate     (m^3/s):  DRSPALL STPPVOLR
Stop Drilling Time              (s):  DRSPALL STPDTIME
```

**Figure 5-20. Input Control File *drs_v122_tc42.drs* for Case 4.2.**

```
COMPUTATIONAL
Spherical/Cylindrical        (S/C): S
Allow Fluidization           (Y/N): Y
Max Run Time                   (s): 1.0
Respository Cell Length        (m): 0.002
radius, Growth rate          (m,-): 0.5, 1.0 !V1.22 growth always 1, was 1.01
Wellbore Cell Length           (m): 1.0
wellbore Zone Growth Rate      (-): 1.0  !V1.22 growth always 1, was 1.01
First wellbore Zone            (-): 10
Well Stability factor          (-): 0.02
Repository Stability factor    (-): 5.0
Mass Diffusion factor          (-): 0.002
Momentum Diffusion factor      (-): 0.002

VALIDATION
Validation Test Case           (-): 4.2

PARAMETERS
Pi                             (-): REFCON   PI
Atmospheric Pressure          (Pa): 1.0170E+05
gravity                    (m/s^2): REFCON   GRAVACC
Gas Constant              (J/kg K): BLOWOUT  RGAS
Repository Temperature         (K): BLOWOUT  TREPO
Water Compressibility       (1/Pa): 12.4e-10
Waste Density             (kg/m^3): BLOWOUT  RHOS
Salt Density              (kg/m^3): 2.1800E+3
Shape Factor                   (-): DRSPALL SHAPEFAC
Tensile Velocity             (m/s): DEFAULT
Bit Nozzle Number              (-): DEFAULT
Bit Nozzle Diameter            (m): DEFAULT
Choke Efficiency               (-): DEFAULT
```

**Figure 5-20. Input Control File *drs_v122_tc42.drs for Case 4.2*. (Continued)**

```
Input Echo (with numeric values)
 -------------------------------
REPOSITORY
  surfaceElevation              :  1.037300E+03   !!DRSPALL SURFELEV
  repositoryTop                 :  3.853100E+02   !!DRSPALL REPOSTOP
  repositoryThickness           : 0.0
  dRZThickness                  :  8.500000E-01   !!DRSPALL DRZTCK
  dRZPerm                       :  1.000000E-15   !!DRSPALL DRZPERM
  repositoryOuterRadius         : 1.9200E+01
  repositoryInitialPressure     :  1.480000E+07   !!DRSPALL REPIPRES
  farFieldStress                :  1.490000E+07   !!DRSPALL FFSTRESS
WASTE
  repositoryInitialPorosity     :  5.750000E-01   !!DRSPALL REPIPOR
  repositoryInitialPerm         :  1.700000E-13   !!DRSPALL REPIPERM
  forchBeta                     :  1.150000E-06   !!DRSPALL FRCHBETA
  biotBeta                      :  1.000000E+00   !!DRSPALL BIOTBETA
  poissonsRatio                 :  3.800000E-01   !!DRSPALL POISRAT
  cohesion                      :  1.300000E+05   !!DRSPALL COHESION
  frictionAngle                 :  4.580000E+01   !!DRSPALL FRICTANG
  tensileStrength               :  1.200000E+05   !!DRSPALL TENSLSTR
  Lt                            : 0.02
  particleDiameter              :  1.000000E-03   !!DRSPALL PARTDIAM
  gasViscosity                  :  8.933900E-06   !!DRSPALL GASVISCO
MUD
  initialMudDensity             :  1.210000E+03   !!DRSPALL INITMDEN
  mudViscosity                  :  1.100000E-02   !!DRSPALL MUDVISCO
  wallRoughness(1)              :  5.000000E-05   !!DRSPALL PIPEROUG
  wallRoughness(2)              :  3.940000E-04   !!DRSPALL ANNUROUG
  mudSolidsMax                  :  6.150000E-01   !!DRSPALL MUDSOLMX
  mudSolidsViscosityExponent    : -1.500000E+00   !!DRSPALL MUDSOLVE
WELL
  bitDiameter                   :  3.111500E-01   !!DRSPALL BITDIAM
  pipeDiameter                  :  1.143000E-01   !!DRSPALL PIPEDIAM
  collarDiameter                :  2.032000E-01   !!DRSPALL COLRDIAM
  pipeInsideDiameter            :  9.718000E-02   !!DRSPALL PIPEID
  collarLength                  :  1.829000E+02   !!DRSPALL COLRLNGT
  exitPipeLength                :  0.000000E+00   !!DRSPALL EXITPLEN
  exitPipeDiameter              :  2.032000E-01   !!DRSPALL EXITPDIA
  drillingRate                  :  4.445000E-03   !!DRSPALL DRILRATE
  initialBitAboveRepository     :  1.500000E-01   !!DRSPALL INITBAR
  mudPumpRate                   :  2.018100E-02   !!DRSPALL MUDPRATE
  maxPumpPressure               : 27.5D6
  dDZThickness                  :  1.600000E-01   !!DRSPALL DDZTHICK
  dDZPerm                       :  1.000000E-14   !!DRSPALL DDZPERM
  stopDrillingExitVolRate       :  1.000000E+03   !!DRSPALL STPDVOLR
  stopPumpingExitVolRate        :  1.000000E+03   !!DRSPALL STPPVOLR
  stopDrillingTime              :  1.000000E+03   !!DRSPALL STPDTIME
COMPUTATIONAL
  geometry                      : S
  allowFluidization             : Y
  maxTime                       : 1.0
  initialReposZoneSize          : 0.002
  radius,growthRate             : 0.5, 1.0 !V1.22 GROW
  initialWellZoneSize           : 1.0
```

**Figure 5-21. Excerpts from *drs_122_tc42.dbg*, Diagnostics File for Case 4.2.**

```
  wellGRowthRate                : 1.0
  firstWellZone                 : 10
  wellStabilityFactor           : 0.02
  reposStabilityFactor          : 5.0
  massDiffusionFactor           : 0.002
  momentumDiffusionFactor       : 0.002
VALIDATION
  ValidationTestCase            : 4.2
PARAMETER
  Pi                            :  3.141593E+00   !!REFCON PI
  AtmosphericPressure           : 1.0170E+05
  gravity                       :  9.806650E+00   !!REFCON GRAVACC
  GasConstant                   :  4.116000E+03   !!BLOWOUT RGAS
  ReposTemp                     :  3.000000E+02   !!BLOWOUT TREPO
  WaterCompressibility          : 12.4E-10
  WasteDensity                  :  2.650000E+03   !!BLOWOUT RHOS
  SaltDensity                   : 2.1800E+3
  ShapeFactor                   :  5.500000E-01   !!DRSPALL SHAPEFAC
  TensileVelocity               :  1.000000E+03   !!DEFAULT
  BitNozzleNumber               :  3.000000E+00   !!DEFAULT
  BitNozzleDiameter             :  1.111250E-02   !!DEFAULT
  ChokeEfficiency               :  9.000000E-01   !!DEFAULT

  VALIDATION TEST CASE:  4  SUBCASE:  2

*******************************************************************************
PARAMETERS USED IN THIS RUN
*******************************************************************************

REPOSITORY
Land Elevation                    (m):  1.0373E+03
Repository top                    (m):  3.8531E+02
Total Thickness                   (m):  1.3976E+00
DRZ Thickness                     (m):  8.5000E-01
DRZ Permeability                (m^2):  1.0000E-15
Outer Radius                      (m):  1.9200E+01
Initial Gas Pressure              (m):  1.4800E+07
Far-Field In-Situ Stress          (m):  1.4900E+07

WASTE
Porosity                          (-):  5.7500E-01
Permeability                    (m^2):  1.7000E-13
Forchheimer Beta                  (-):  1.1500E-06
Biot Beta                         (-):  1.0000E+00
Poissons   Ratio                  (-):  3.8000E-01
Cohesion                         (Pa):  1.3000E+05
Friction Angle                  (deg):  4.5800E+01
Tensile Strength                 (Pa):  1.2000E+05
Failure Characteristic Length     (m):  2.0000E-02
Particle Diameter                 (m):  1.0000E-03
Gas Viscosity                  (Pa-s):  8.9339E-06
```

**Figure 5-21. Excerpts from *drs_122_tc42.dbg*, Diagnostics File for Case 4.2. (Continued)**

```
MUD
Density                      (kg/m^3):  1.2100E+03
Viscosity                      (Pa-s):  1.1000E-02
Wall Roughness Pipe               (m):  5.0000E-05
Wall Roughness Annulus            (m):  3.9400E-04
Max Solids Vol. Frac.          (Pa-s):  6.1500E-01
Solids Viscosity Exp.          (Pa-s): -1.5000E+00

WELLBORE/DRILLING
Bit Diameter                      (m):  3.1115E-01
Pipe Diameter                     (m):  1.1430E-01
Collar Diameter                   (m):  2.0320E-01
Pipe Inside Diameter              (m):  9.7180E-02
Collar Length                     (m):  1.8290E+02
Exit Pipe Length                  (m):  0.0000E+00
Exit Pipe Diameter                (m):  2.8940E-01
Drilling Rate                   (m/s):  4.4450E-03
Bit Above Respository             (m):  1.5000E-01
Mud Pump Rate                 (m^3/s):  2.0181E-02
Max Pump Pressure                (Pa):  2.7500E+07
DDZ Thickness                     (m):  1.6000E-01
DDZ Permeability                (m^2):  1.0000E-14
Stop Drill Exit Vol Rate      (m^3/s):  1.0000E+03
Stop Pump Exit Vol Rate       (m^3/s):  1.0000E+03
Stop Drilling Time                (s):  1.0000E+03

COMPUTATIONAL
Spherical/Cylindrical           (S/C): S
Allow Fluidization            (Y/N/A): Y
Max Run Time                      (s):  1.0000E+00
Respository Cell Length           (m):  2.0000E-03
Radius, Growth Rate             (m,-):  0.500  1.000
Wellbore Cell Length              (m):  1.0000E+00
Wellbore Cell Growth Rate         (-):  1.0000E+00
First Wellbore Zone               (-): 651
Well Stability factor             (-):  2.0000E-02
Repository Stability factor       (-):  5.0000E+00
Mass Diffusion factor             (-):  2.0000E-03
Momentum Diffusion factor         (-):  2.0000E-03

VALIDATION
Validation Test Case              (-): 4.2
Initial Cavity Radius             (-):  0.0000E+00
Minimum Characteristic Vel        (-):  1.0000E-06
Minimum Number Zones/Lt           (-):   5

PARAMETERS
Pi                                (-):  3.1416E+00
Atmospheric Pressure             (Pa):  1.0170E+05
```

**Figure 5-21. Excerpts from *drs_122_tc42.dbg*, Diagnostics File for Case 4.2. (Continued)**

```
gravity                    (m/s^2):  9.8067E+00
Gas Constant              (J/kg K):  4.1160E+03
Repository Temperature         (K):  3.0000E+02
Reference gas Density     (kg/m^3):  8.2362E-02
Water Compressibility       (1/Pa):  1.2400E-09
Waste Density             (kg/m^3):  2.6500E+03
Salt Density              (kg/m^3):  2.1800E+03
Shape Factor                   (-):  5.5000E-01
Tensile Velocity             (m/s):  1.0000E+03
Bit Nozzle Number              (-):  3.0000E+00
Bit Nozzle Diameter            (m):  1.1112E-02
Choke Efficiency               (-):  9.0000E-01
```

**Figure 5-21. Excerpts from *drs_122_tc42.dbg*, Diagnostics File for Case 4.2. (Continued)**

Initial Cavity Radius, Min Characteristic Velocity and Min Number Zones/Lt are listed in the diagnostics file under "Parameters used in this run", but not in the input control file. These are optional input parameters that were not specified in the input control file and were set to default values.

Comparisons of the input CAMDAT file, and input control file with the excerpt from the diagnostics file indicated that all parameters were properly set to CAMDAT property values, set explicitly, or set to default values as directed by the input control file. This confirms that **Acceptance Criterion 4-16** (Section 5.4.5.5) is met.

### 5.4.7. Conclusions

The discussion in Section 5.4.6 verifies that all acceptance criteria (Section 5.4.5) for this test case are met. Thus, this test case passes.

The successful completion of this test case verifies that DRSPALL demonstrates the correct, expected behavior for the functionality examined. Coupling data shows that the gas transported from the repository is successfully accounted for in the wellbore and ejected at the land surface. An analysis of the stress data indicates proper implementation of the stress equations and failure logic. A similar analysis of the fluidization data reveals proper calculation of the fluidization velocity and mobilization of solids by fluidized bed theory. The waste expulsion analysis demonstrates proper accounting for waste solids drilled or spalled from the repository, transported up the wellbore, and ejected at the land surface. Finally, (1) examination of the diagnostic file indicating correct specification of input parameters and (2) proper execution of the GROPECDB utility verifies the external interfaces to CAMDAT files.

## 5.5. Test Case #5 – Wellbore Flow Verification

### 5.5.1. Test Objective

The objective of this test case is to verify the wellbore flow model against an independent computational fluid dynamics model FLUENT (2003). Details of the FLUENT runs are provided

in Section 8.5.3.7 of the *Verification and Validation Plan and Validation Document for DRSPALL Version 1.00* (WIPP PA 2003b).

Correctly performing this test case validates the satisfactory implementation of Functional Requirement R.1.

### 5.5.2. Problem Description

This test case will focus on the wellbore model, and thus decouple its behavior from the repository. Known boundary conditions will be imposed to observe the model's response to steady flow of:

1. mud
2. mud and gas
3. mud, gas, and solids.

Independent calculations will be run in parallel with the commercial computational fluid dynamics code FLUENT (2003).

The problem domain is the wellbore annulus in a typical WIPP intrusion. The geometric description of the wellbore is given in the *Parameter Justification Report for DRSPALL* (Hansen et al. 2003), and default values are used for most DRSPALL parameters. A schematic of the domain is shown in Figure 5-22.

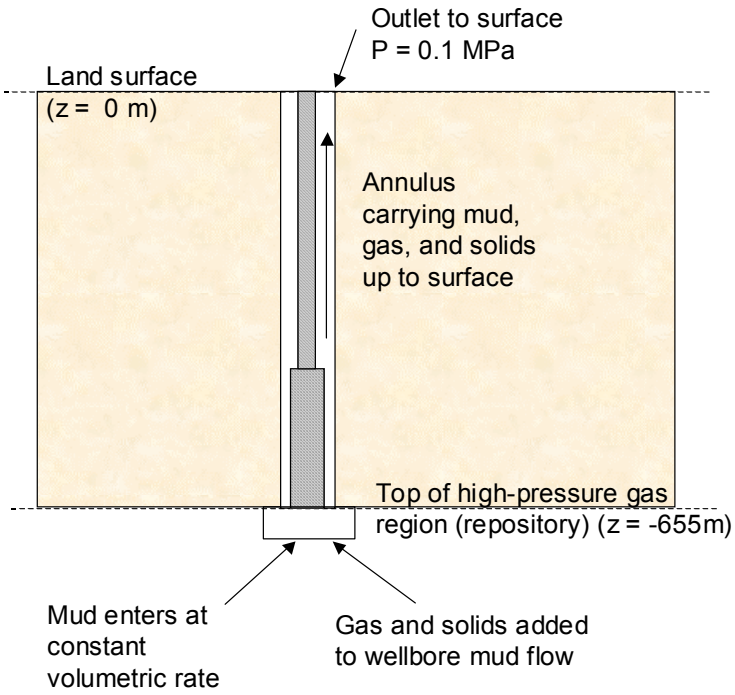


**Figure 5-22. Schematic of Wellbore Flow Test Problem Domain.**

#### 5.5.2.1. Boundary Conditions

Boundary conditions are set to simulate a WIPP intrusion scenario, however the bottom of the wellbore is decoupled from the repository and controlled directly to facilitate comparison between DRSPALL and the FLUENT code. The inlet boundary to the wellbore annulus is a constant volumetric flow rate. The outlet boundary from the wellbore annulus is constant at atmospheric pressure, 0.1 MPa. Gas and solids are added at pre-determined mass flow rates at the lower boundary to the annulus.

#### 5.5.2.2. Input Parameters

Input parameters for the wellbore domain represent a typical WIPP intrusion. Repository flow parameters are irrelevant since the domains are decoupled in this test case. There are several run-specific parameters such as mud density, mud pump rate, and gas/solids loading rate that vary among runs and are discussed below. The DRSPALL input files *drs_v122_tc51.drs* through *drs_v122_tc57.drs* are stored in CVS directory /nfs/data/CVSLIB/WIPP_CODES/PA_CODES/DRSPALL/Test/Input. Note that the zone size growth rates were changed to 1.0 for the DRSPALL 1.22 validation (WIPP PA 2015c, Section 4.0).

### 5.5.3. Analysis Method

Six runs will be executed under this test case. The run matrix is shown in Table 5-21. More detailed descriptions are given in the text that follows.

**Table 5-21. Run Conditions for FLUENT Comparison.**

| Case | Mud Density, $kg/m^3$ | Mud Flow Rate, $m^3/s$ | Gas Flow Rate, kg/s | Solid Flow Rate, kg/s | Description |
|---|---|---|---|---|---|
| 5.1 | 1210 | 0 | 0 | 0 | Static mud in wellbore |
| 5.2 | 1210 | 0.02081 | 0 | 0 | Mud-only, steady flow, nominal mud density |
| 5.3 | 1380 | 0.02081 | 0 | 0 | Mud-only, steady flow, high-end mud density |
| *5.4* | – | – | – | – | *Not used* |
| 5.5 | 1210 | 0.02081 | 0.25 | 0 | Steady mud flow, gas added to flow at low, constant rate |
| 5.6 | 1210 | 0.02081 | 2.5 | 0 | Steady mud flow, gas added to flow at medium, constant rate |
| 5.7 | 1210 | 0.02081 | 2.5 | 2.5 | Steady mud flow, gas added to flow at medium, constant rate; solids added at low constant rate |

Steady-state runs. Steady state runs will be examined to establish that the steady pressure profiles in the wellbore are matched reasonably between DRSPALL and FLUENT. Three basic types of runs will be required:

1. Mud only
2. Mud and gas
3. Mud, gas, and solids.

For mud only, two mud densities will be examined. In addition, a static case will be run with no mud pumping to assure that the mud column settles to an equilibrium hydrostatic distribution. For the mud and gas case, gas input rate will be controlled as the independent variable. For the three-phase run (Case 5.7), gas and solid loading rates representative of near-steady conditions in a WIPP spallings intrusion will be tested.

Specific test run information is given below.

#### 5.5.3.1. Case 5.1 – Static Mud in Wellbore

The mud pump will be turned off and the pressure distribution will be monitored to assure that it settles to a hydrostatic distribution. The boundaries at the pump inlet and annulus outlet will both be set to atmospheric pressure. No gas or solids will be added to the wellbore domain. Mud density will be set to the DRSPALL default value 1210 kg/m$^3$. DRSPALL is a transient code, and the initial pressure distribution in the wellbore is arbitrary. The objective of this seemingly simple test is to see whether DRSPALL will eventually arrive at a stable solution demonstrating the hydrostatic pressure distribution.

#### 5.5.3.2. Case 5.2 – Mud-only, Steady Flow, Nominal Mud Density

Volumetric mud flow rate at the pump inlet and mud density will be set to the DRSPALL default values of 0.02081 m$^3$/s and 1210 kg/m$^3$, respectively. No gas or solids will be added.

#### 5.5.3.3. Case 5.3 – Mud-only, Steady Flow, High-end Mud Density

This test run is the same as Case 5.2, Section 5.5.3.2 above, except that the mud density is increased to $\rho$ = 1380 kg/m$^3$, the highest value in its sampling range recommended in the *Parameter Justification Report for DRSPALL* (Hansen et al. 2003). The slightly higher density should lead to a proportionally higher pressure at the bottom of the well due to the weight of the mud column.

#### 5.5.3.4. Case 5.5 – Gas Added to Flow at Low, Constant Rate

This test run will add hydrogen gas to the flow stream at the bottom of the well. Mudflow rate and physical properties are set to defaults as in Case 5.2. The hydrogen mass flow rate is fixed at 0.25 kg/s, a value representative of the gas flow rate into the wellbore through the DDZ just prior to bit penetration of the repository.

#### 5.5.3.5. Case 5.6 – Gas Added to Flow at Medium, Constant Rate

This test run will add hydrogen gas to the flow stream at the bottom of the well. Mud flow and physical properties are set to defaults as in Case 5.2. The hydrogen mass flow rate = 2.5 kg/s, a value representative of the gas flow rate into the wellbore during a blowout while the mud column is accelerating.

#### 5.5.3.6. Case 5.7 – Gas Added to Flow at Medium, Constant Rate; Solids Added at Low, Constant Rate

This test run is the same as Case 5.6, Section 5.5.3.5, with gas flowing into the well bottom, except solids are also added. A solids loading rate of 2.5 kg/s is selected to represent a slow, steady material failure case. In normal model executions where a spalling event occurs, this mass loading rate tends to spike early and diminish to zero. The constant rate was selected here for simplicity in implementation and comparison between models.

### 5.5.4. Test Procedure

DRSPALL is executed once for each of the six cases: Cases 5.1, 5.2, 5.3, 5.5, 5.6, and 5.7 (there is no Case 5.4).

DRSPALL generates a "wellbore" validation file for each case, but these files are not examined. Each output CAMDAT file is post-processed with GROPECDB (WIPP PA 1996 and 2012a) to extract the pressure, fluid velocities and volume fraction profiles in the wellbore. The GROPECDB data are imported into Excel file *drs_v122_tc5.xlsx* for comparison with the corresponding data generated from FLUENT. The GROPECDB input command file is shown in Figure 5-23.

The following command lines run DRSPALL and GROPECDB for Case 5.1 (tc51). The other cases are similar:

*./drspall ./Input/drs_v122_tc51.drs DRSPALL/Test/Output/Solaris_122/drs_122_tc51.dbg*
*CANCEL DRSPALL/Test/Output/Solaris_122/drs_122_tc51.cdb*
*> DRSPALL/Test/Output/Solaris_122/drs_122_tc51.crt*
*./gropecdb DRSPALL/Test/Output/Solaris_122/drs_122_tc51.cdb*
*./Input/drs_tc5_grope.inp*
*DRSPALL/Test/Output/Solaris_122/drs_122_tc51.gr > x.x*

select block 1

```
select property INITMDEN GASBSDEN WASTDENS MUDPRATE
print property

!apg WELLGSVF is only needed for TC55-TC57
!apg WELLWSVF is only needed for TC57
select time 450.  !apg select final time step, may be <450
select block  4
select evar COORD WELLPRS WELLVEL WELLGSVF WELLWSVF
print evar

exit
```

**Figure 5-23. GROPECDB Input Command File *drs_tc5_grope.inp*.**

### 5.5.5. Acceptance Criteria

This test will pass if the following are observed when comparing DRSPALL and FLUENT output:

- **Acceptance Criterion 5-1** — The fluid pressure agrees within 20%.
- **Acceptance Criterion 5-2** — The volume fraction of gas in two- and three-phase runs (Cases 5.5, 5.6, 5.7) agrees within 0.02.
- **Acceptance Criterion 5-3** — The volume fraction of waste in the three-phase run (Case 5.7) agrees within 20%.
- **Acceptance Criterion 5-4** — The velocity of the mixture agrees within 25%. Analytical velocities will be used as the basis of comparison for Case 5.2 and 5.3. Case 5.1 is static, therefore, velocities should be near zero (< 1E-4).

Verification will be evaluated by visual comparison of graphical results that contain error bounds consistent with the acceptance criteria.

### 5.5.6. Results

Results for each case are presented individually in the following subsections. Results consist of graphical comparisons of pressure, fluid velocity and volume fractions as a function of wellbore position. The DRSPALL values are extracted from output CAMDAT file element variables WELLPRS (pressure), WELLVEL (fluid velocity), WELLGSVF (gas volume fraction), WELLWSVF (waste volume fraction), and COORD (wellbore position) for all elements in element block UP_WB (the wellbore annulus). The bottom of the wellbore is located at 0.0 and the land surface is located at 653 m. FLUENT actually solves the steady state problem. DRSPALL solves the transient problem for constant boundary conditions. DRSPALL cases were run until pressure and velocity maintained a relatively constant value, therefore run time varied for each subcase.

This validation uses the same FLUENT curve data as the *Verification and Validation Plan and Validation Document for DRSPALL Version 1.00* (WIPP PA 2003b), so the FLUENT calculations are not repeated.

#### 5.5.6.1. Case 5.1 – Static with Nominal Mud Density

Results for Case 5.1 are summarized by the pressure and velocity profile comparisons shown in Figure 5-24. DRSPALL results are at 90 s because it takes some time for the code to settle to a steady pressure profile after the arbitrary starting profile. The results visually overlay, and are within the 20% error bounds, so **Acceptance Criterion 5-1** (Section 5.5.5) is met for this case. A simple hydrostatic model gives the expected bottomhole pressure as $\rho gh$ = 7.75 MPa, where $\rho$ = 1210 kg/m$^3$ is the mud density, $g$ = 9.81 m/s$^2$, and $h$ = 653 m is the wellbore height. In the code results, the pressure decreases linearly to 0.1 MPa at the land surface. FLUENT calculated a bottomhole pressure value of 7.74 MPa. DRSPALL calculated a value of 7.77 MPa. The velocities for this test case should be zero. But, because DRSPALL uses a transient algorithm, a

small residual velocity can be expected. The velocities shown in Figure 5-24 are well below 1E-4, so **Acceptance Criterion 5-4** (Section 5.5.5) is met for this case. (**Acceptance Criteria 5-2 and 5-3** do not apply to this case.) While this test problem may seem trivial, stable behavior of a transient code under steady-state conditions is not guaranteed. Correct and stable solution of this problem lends confidence that the differencing scheme and mass balance are working as designed.

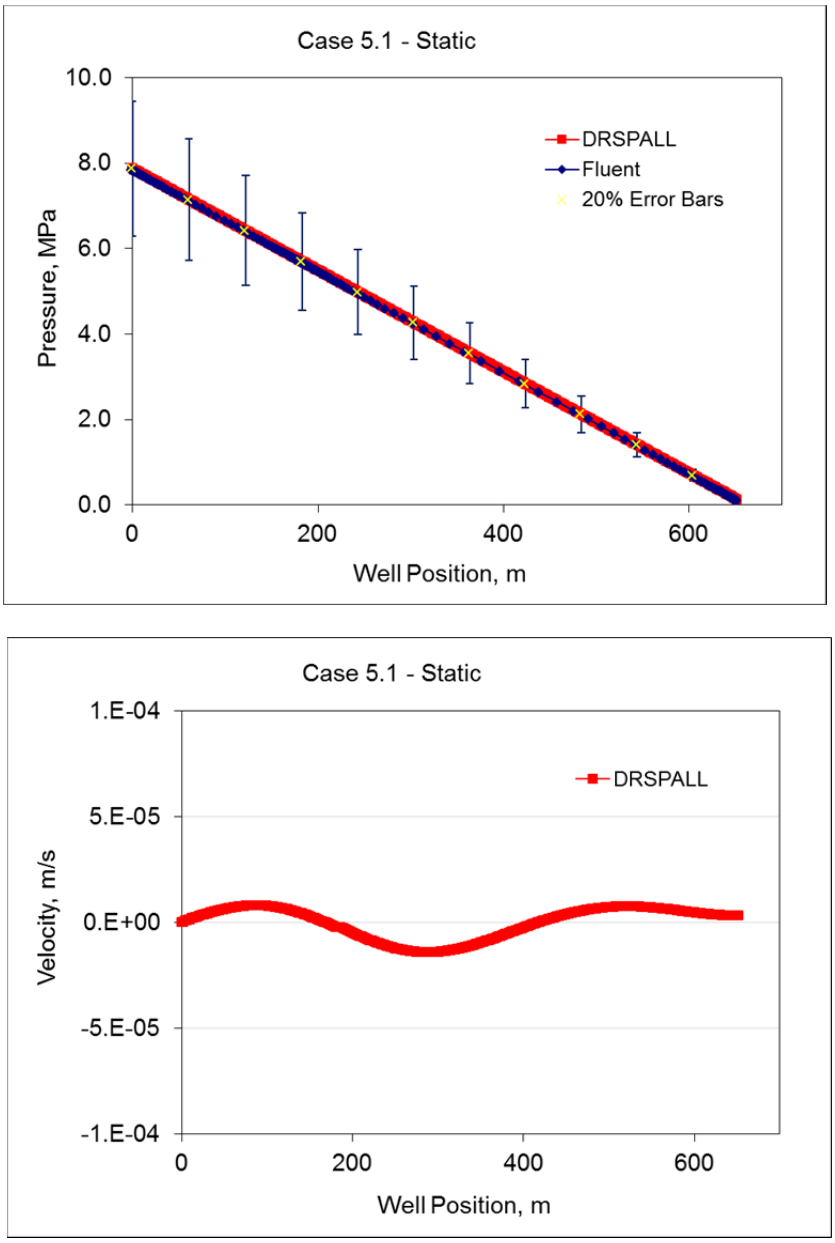


**Figure 5-24. Pressure and Velocity Profiles for Static Wellbore, Case 5.1.**

### 5.5.6.2. Case 5.2 – Steady Flow, Nominal Mud Density

The results for Case 5.2 (mud pumping rate = 0.02018 $m^3/s$ and nominal mud density = 1210 $kg/m^3$) are summarized by the pressure and fluid velocity profiles at 90 s shown in Figure 5-25 are similar to Case 5.1 with only very minor differences due to dynamic effects. Pressures are within the 20% error bars, so **Acceptance Criterion 5-1** (Section 5.5.5) is met for this case. The velocity profiles show the effects of the two annulus areas – one for the collar region just above the well bottom and another for the drill pipe extending to the land surface. Velocities are within the 25% error bars, so **Acceptance Criterion 5-4** (Section 5.5.5) is met for this case. Fluid velocities, $u_{i,}$ can be determined analytically from the pumping rates, $R$ = 0.02018, and the annulus cross sectional areas, $A_1$ = 0.044, $A_2$ = 0.066, as follows: $u_i = R/A_i$, where, $i$=1 is the collar region and 2 is the drill pipe region. This gives analytic values for the fluid velocities of 0.46 m/s and 0.31 m/s for the collar and drill pipe regions, respectively. (**Acceptance Criteria 5-2 and 5-3** do not apply to this case.)

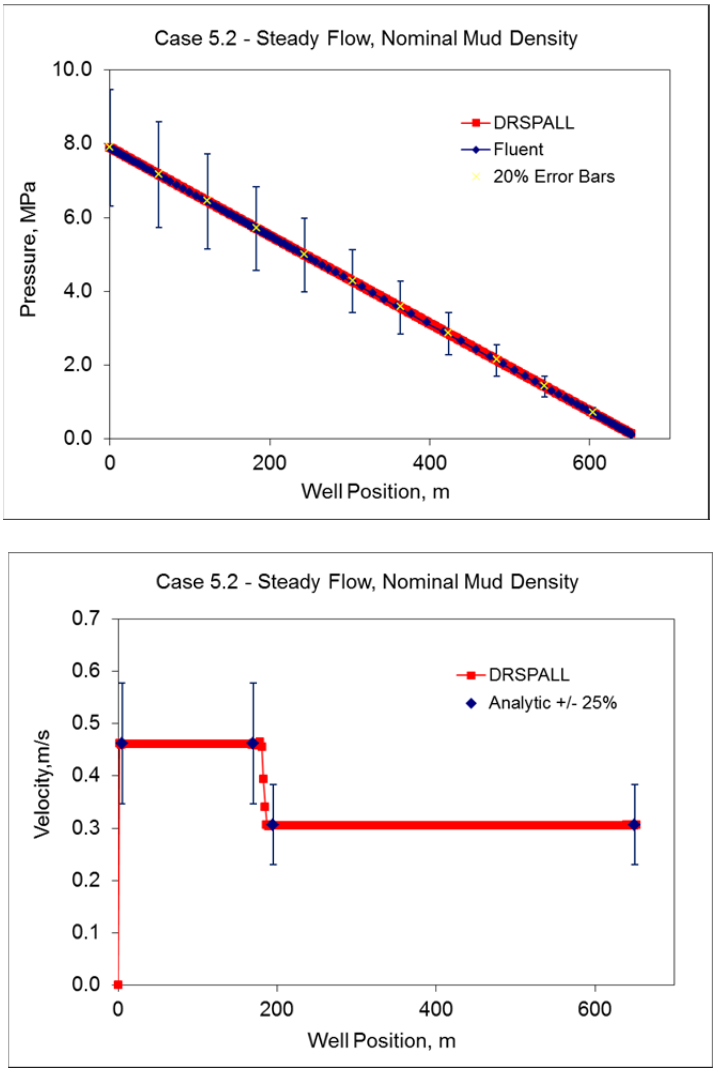


**Figure 5-25. Pressure and Velocity Profiles for Steady State and Nominal Mud Density, Case 5.2.**

### 5.5.6.3. Case 5.3 – Steady Flow, High Mud Density

The results for Case 5.3 (constant mud pumping rate = 0.02018 $m^3/s$ and a high mud density = 1380 $kg/m^3$) are summarized by the pressure and fluid velocity profiles at 90 s shown in Figure 5-26. The results from FLUENT and DRSPALL visually overlay. The pressure profiles are similar to Case 5.2 except for an increase in bottomhole pressure due the increase in mud density. Pressures are within the 20% error bars, so **Acceptance Criterion 5-1** (Section 5.5.5) is met for this case. The estimated value of bottomhole pressure is $\rho gh$ = 8.84 MPa, where $\rho$ = 1380 $kg/m^3$ is the mud density, $g$ = 9.81 $m/s^2$, and $h$ = 653 m is the wellbore height. The calculated values for bottomhole pressure were 8.85 MPa and 8.89 MPa for FLUENT and DRSPALL, respectively. The velocity profiles show the effects of the two annulus areas – one for the collar region just above the well bottom and another for the drill pipe extending to the land surface. Velocities are within the 25% error bars, so **Acceptance Criterion 5-4** (Section 5.5.5) is met for this case. The expected values of fluid velocities are the same as in Case 5.2. (**Acceptance Criteria 5-2 and 5-3** do not apply to this case.)

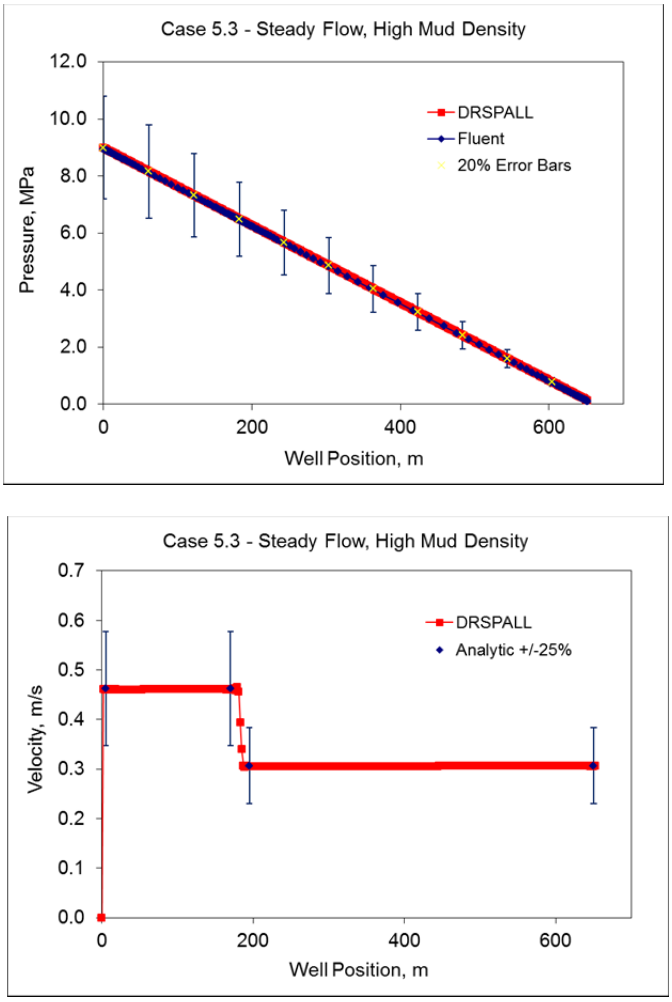


**Figure 5-26. Pressure and Velocity Profiles for Steady State and High Mud Density, Case 5.3.**

#### 5.5.6.4. There is no Case 5.4

In the original validation for DRSPALL Version 1.00, Case 5.4 was not defined. For consistency, there is no Case 5.4.

#### 5.5.6.5. Case 5.5 – Low Gas Injection Rate

The results for Case 5.5 (constant mud pumping rate = 0.02018 $m^3/s$, nominal mud density = 1210 $kg/m^3$, and a low gas injection rate = 0.25 kg/s) are summarized by the pressure, fluid velocity, and gas volume fraction profiles at 450 s shown in Figure 5-27. The pressure profile results from FLUENT and DRSPALL visually overlay. Pressures are within the 20% error bars, so **Acceptance Criterion 5-1** (Section 5.5.5) is met for this case. Note that the bottomhole pressures have dropped from 9 MPa to 0.5 MPa because of the large amount of gas in the wellbore. Gas volume fractions are around 98% with differences between FLUENT and DRSPALL less than 0.2. Gas volume fractions are within the 0.01 error bars and the acceptance criterion of 0.02, so **Acceptance Criterion 5-2** (Section 5.5.5) is met for this case. The fluid velocity profiles show increasing fluid acceleration with height because of the decrease in gas density and pressure. The drop in velocity at about 180 m is at the collar drill pipe interface and indicates the increase in annulus area. Velocities are within the 25% error bounds, so **Acceptance Criterion 5-4** (Section 5.5.5) is met for this case. (**Acceptance Criterion 5-3** does not apply to this case.)

#### 5.5.6.6. Case 5.6 – Medium Gas Injection

The results for Case 5.6 (constant mud pumping rate = 0.02018 $m^3/s$; nominal mud density = 1210 $kg/m^3$; and a medium gas injection rate = 2.5 kg/s) are summarized by the pressure, fluid velocity, and gas volume fraction profiles at 120 s shown in Figure 5-28. The gas injection rate was ten times larger than in Case 5.5. The bottomhole pressure, gas volume fraction, and fluid velocity have increased relative to Case 5.5 because of the increased gas injection rate. Pressure profiles compare very well. Pressures are within the 20% error bars, so **Acceptance Criterion 5-1** (Section 5.5.5) is met for this case. Gas volume fractions are above 99% for both DRSPALL and FLUENT. Gas volume fractions are within the 0.01 error bars and the acceptance criterion of 0.02, so **Acceptance Criterion 5-2** (Section 5.5.5) is met for this case. DRSPALL fluid velocities are slightly low relative to FLUENT because of the slightly lower gas volume fraction. Velocities are within the 25% error bars, so **Acceptance Criterion 5-4** (Section 5.5.5) is met for this case. (**Acceptance Criterion 5-3** does not apply to this case.)

#### 5.5.6.7. Case 5.7 – Medium Gas and Low Solid Injection

The results for Case 5.7 (constant mud pumping rate = 0.02018 $m^3/s$; nominal mud density = 1210 $kg/m^3$; medium gas injection rate = 2.5 kg/s; and low solid injection rate = 2.5 kg/s) are summarized by the pressure, fluid velocity and gas and solid volume fraction profiles at 100 s shown in Figure 5-29. The gas injection rate was the same as in Case 5.6. The pressure profiles essentially overlay with an increase in bottomhole pressure relative to Case 5.6 due to the presence of solids in the wellbore. Pressures are within the 20% error bars, so **Acceptance Criterion 5-1** (Section 5.5.5) is met for this case. Gas volume fractions are near 99% but are lower than Case 5.6 because of the solids. Gas volume fractions are within the 0.01 error bars

and the acceptance criterion of 0.02, so **Acceptance Criterion 5-2** (Section 5.5.5) is met for this case. Solid volume fractions are very small, near 5E-4. Solid volume fractions are within the 20% error bars, so **Acceptance Criterion 5-3** (Section 5.5.5) is met for this case. The fluid velocity profiles are very similar to Case 5.6 because of the dominance of the gas. Velocities are within the 25% error bars, so **Acceptance Criterion 5-4** (Section 5.5.5) is met for this case.

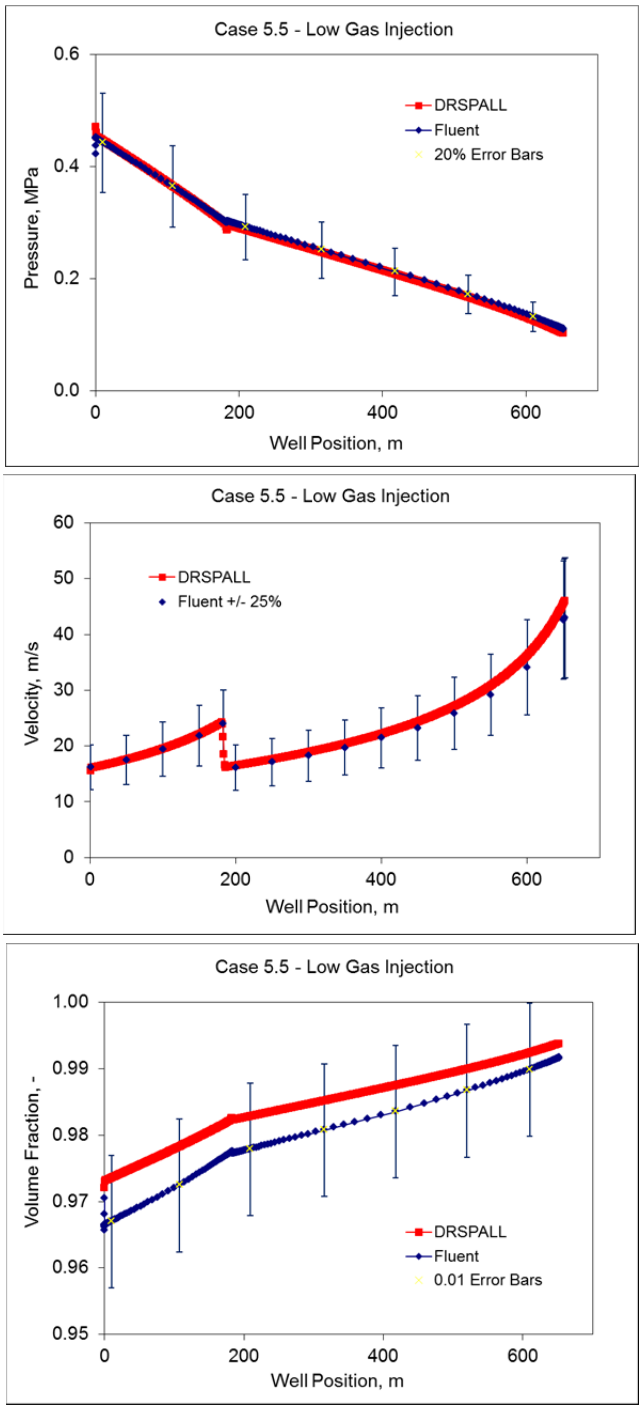


**Figure 5-27. Pressure, Velocity, and Gas Volume Fraction Profiles for Steady State, Nominal Mud Density, and Low Gas Injection Rate, Case 5.5.**

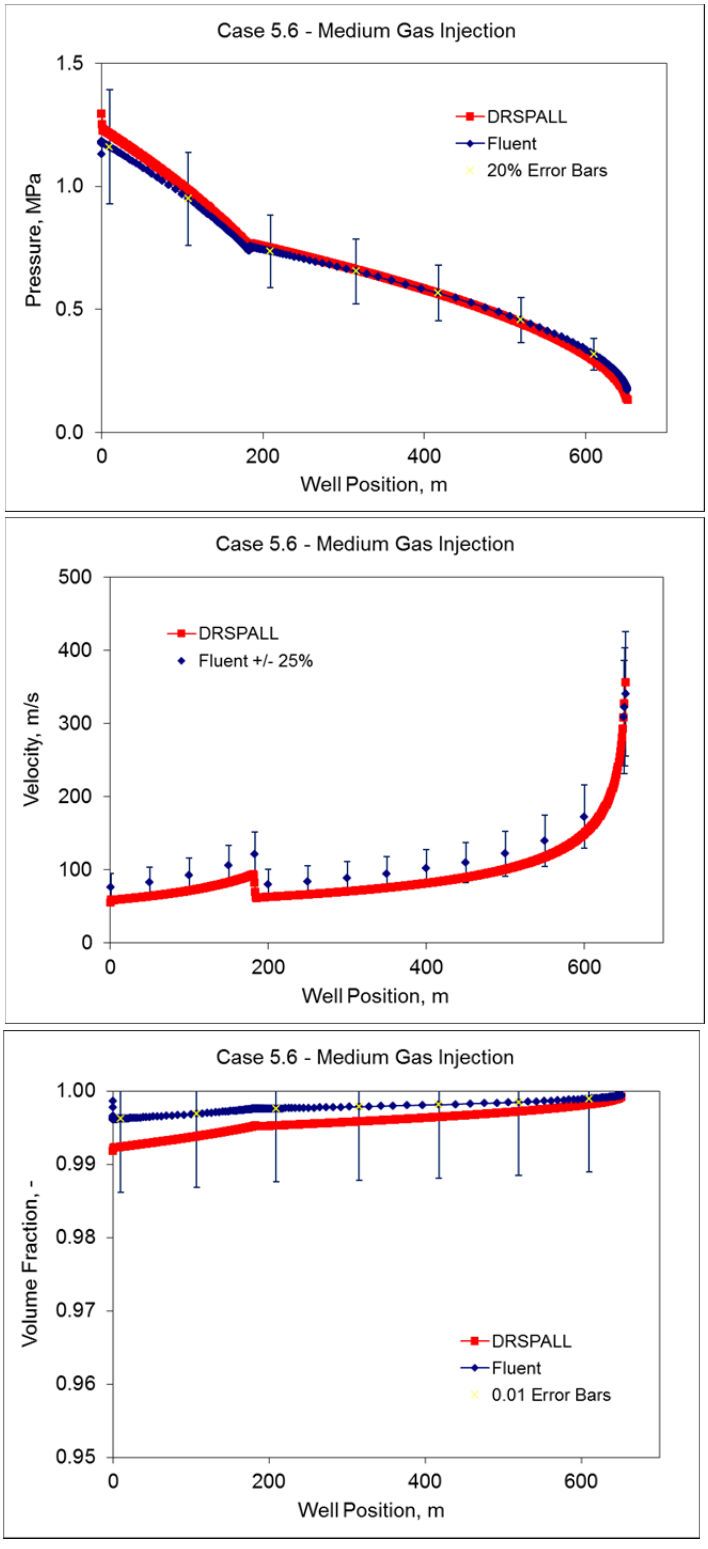


**Figure 5-28. Pressure, Velocity, and Gas Volume Fraction Profiles for Steady State, Nominal Mud Density, and Medium Gas Injection Rate, Case 5.6.**

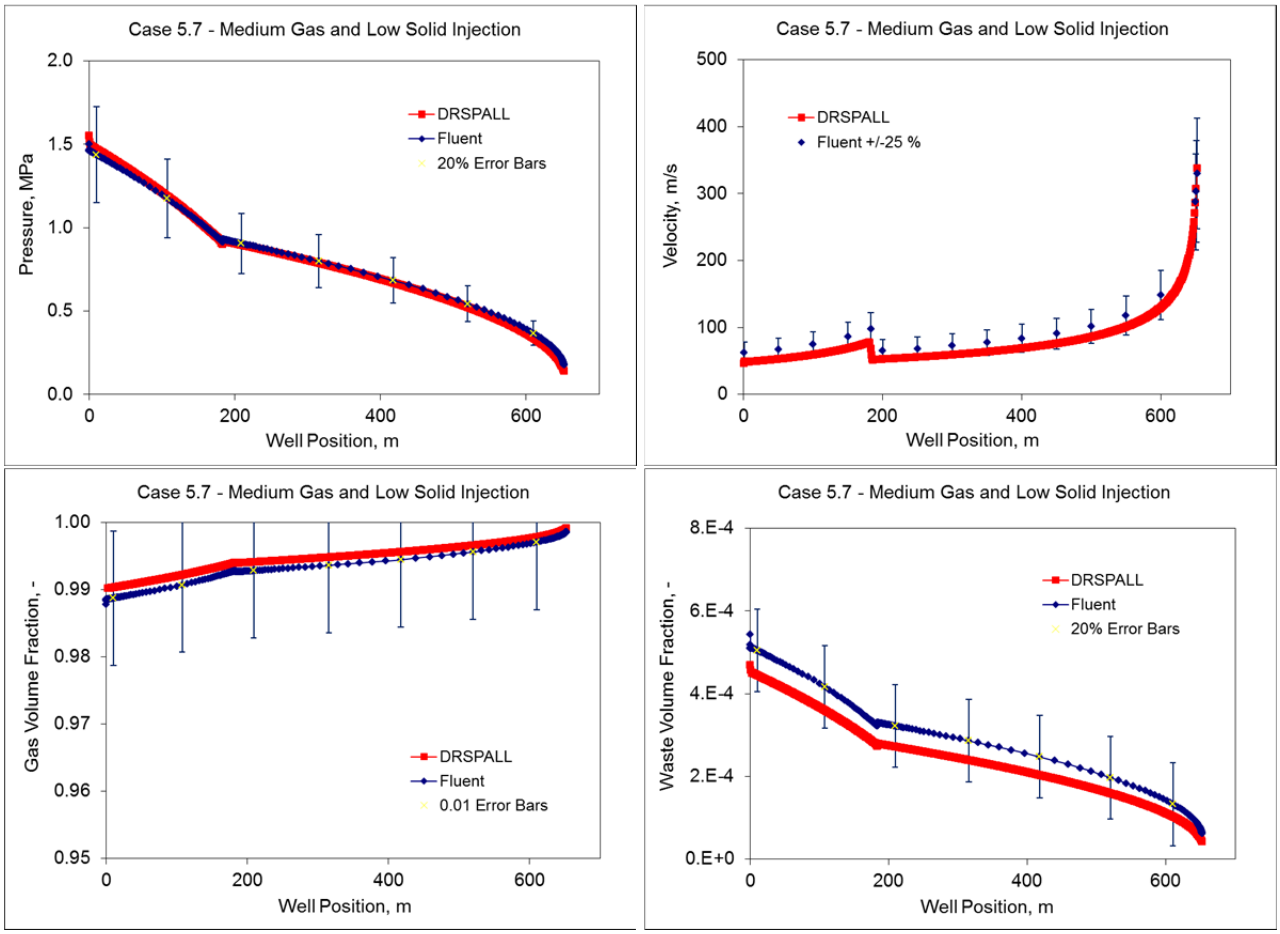


**Figure 5-29. Pressure, Velocity, and Gas Volume Fraction Profiles for Steady State, Nominal Mud Density, Medium Gas and Low Solid Injection Rate, Case 5.7.**

### 5.5.7. Conclusions

The discussion in Section 5.5.6 verifies that all acceptance criteria (Section 5.5.5) for this test case are met. Thus, this test case passes.

Comparisons of the FLUENT and DRSPALL results for both the static (Case 5.1) and steady state, mud-only (Cases 5.2, 5.3) calculations show very close agreement. All steady state cases with mud and gas injection (Cases 5.5, 5.6) or mud, gas and solid injection (Case 5.7) are also in good agreement. Much of the differences are probably due to the way friction loss is handled in the two models. DRSPALL uses an empirical friction factor that is a function of wall roughness and Reynolds number. FLUENT calculates shear forces in its two-dimensional cylindrical flow domain and assumed smooth walls for this analysis.

The successful completion of this test case confirms that DRSPALL is properly calculating the multi-component mixture flow in the wellbore.

## 5.6. Summary of Verification/Validation Tests

Testing for DRSPALL Version 1.22 has been completed and all test cases meet the acceptance criteria. The testing verifies that DRSPALL satisfies all the requirements listed in the *Requirements Document for DRSPALL Version 1.00* (WIPP PA 2003a), thus providing assurance that the model is operating within design requirements so that it may be considered qualified for use in WIPP compliance calculations.

# 6. IMPACT TO WIPP PERFORMANCE ASSESSMENT CALCULATIONS

A DRSPALL impact assessment was developed to assess the impact of modified spallings data on four PA calculations, including the VMS PABC-2009, the migrated PABC-2009 (Revision 0), the VMS CRA-2014, and the migrated CRA-2014 (Revision 0) (Kicker, Herrick, and Zeitler 2015). The structure of calculations performed is the same as that used in corresponding PAs. The first step for this impact assessment was to run DRSPALL Version 1.22 to produce a modified set of spallings volumes. Next, only those PA codes impacted by the change in spallings volume were rerun, including CUTTINGS_S, BRAGFLO_DBR, and CCDFGF. The output from the remaining PA codes (EPAUNI, LHS, BRAGFLO, NUTS, PANEL, and SECOTP2D) was unchanged, so their Revision 0 results were used in the impact assessment (Kirchner, Gilkey, and Long 2015). The updated PAs (Revision 1) use the same waste inventory information, drilling rate and plugging pattern parameters, and radionuclide solubility parameters as were used in the corresponding VMS and migrated PAs.

## 6.1. Spallings

Two procedures are used to calculate the volume of solid waste material released to the surface from a single drilling intrusion into the repository due to spallings. First, the code DRSPALL calculates the spallings volumes at four values of repository pressure (10, 12, 14, and 14.8 MPa). Then the code CUTTINGS_S interpolates between DRSPALL volumes based on calculated (by the code BRAGFLO) repository pressures for a set of discrete times and locations.

### 6.1.1. Calculation of Spall Volumes by DRSPALL

Four initial repository pressures are considered for DRSPALL calculations. These pressures correspond to what are referred to as DRSPALL pressure scenarios (DPSs). DPS 1 has an initial repository pressure of 10.0 MPa, DPS 2 has an initial repository pressure of 12.0 MPa, DPS 3 has an initial repository pressure of 14.0 MPa, and DPS 4 has an initial repository pressure of 14.8 MPa. DRSPALL was executed once for each vector and scenario combination, resulting in 1,200 separate runs. Based on a zone size sensitivity study (Section 4), the following zone size parameters have been selected as the standard configuration for DRSPALL calculations:

- Repository zone size, $\Delta r = 0.004$ m
- Characteristic length, $L_t = 0.04$ m
- Wellbore zone size, $\Delta z = 2.0$ m.

#### 6.1.1.1. Output Variables

A complete list of DRSPALL variables and their definitions is given in WIPP PA (2015a, 2004b, 2013c, 2015b). The discussion of the following variables is required for comprehension of this document:

- Drilled radius (DRILLRAD) – This variable represents the contribution of the cavity radius in the repository that is due to drill cuttings. This variable is a function of time and is bounded by the variable CUTRAD, the maximum equivalent cuttings radius.

- Maximum equivalent cuttings radius (CUTRAD) – This variable represents the length of the radius of the hemisphere (or cylinder, depending on choice of geometric model) with the same amount of surface area as the lateral surface area of a cylinder with height equal to the repository height and diameter equal to the drill-bit diameter. This variable is constant with respect to time.

- Cavity radius (CAVRAD) – This variable represents the length of the radius of the cavity and includes contributions from drill cuttings and spallings. This variable changes with time.

- Repository thickness (REPOSTCK) – This variable represents the thickness of the repository. This variable is constant with respect to time.

- SPLVOL2 – This variable represents the accumulated uncompacted spall volumes. This variable changes with time and is the major variable of interest.

#### 6.1.1.2. Exception Runs — Increased Run Time

The DRSPALL input control file allows the user to specify the length of time of the drilling intrusion (WIPP PA 2004b, 2013c, 2015b). All DRSPALL calculations were run for a 600-s drilling intrusion time, which is generally long enough to capture all drilling and spalling activity.

CAVRAD is a non-decreasing quantity, and two processes can occur that result in an increase of CAVRAD. The first process that causes CAVRAD to increase is the passage of the drill bit through the repository, and as drilling occurs, the radius of the equivalent cavity increases. Secondly, if spalling is occurring, the cavity radius will increase, and the quantity CAVRAD increases. When the drill bit reaches the bottom of the repository and spallings have ceased, CAVRAD does not increase.

CAVRAD is used as an indicator to determine when the system has stabilized and the spallings process has ceased. If CAVRAD has increased at a time close to the end of the simulation, the spallings process may not have finished, and the run time for the simulation needs to be increased to ensure that all of the spallings volume has been calculated. All runs that had an increase in CAVRAD after 500 s indicate that cavity growth was occurring in the final 100 s of the DRSPALL simulation, and thus were rerun with an increased "maximum run time" and "stop drilling time" of 1500 s.

#### 6.1.1.3. Repository — Spherical and Cylindrical Geometries

The spallings model domain is divided into two regions that are coupled. The first is the wellbore domain, and this document does not discuss the details associated with flow in the wellbore. For a thorough discussion of the wellbore domain, see Sandia Report SAND2004-0730 (Lord et al. 2006) and the DRSPALL design document (WIPP PA 2015a). This section briefly discusses the geometries associated with the repository domain.

DRSPALL has the capability to model the repository using either the cylindrical model or the spherical model as discussed in Section 4.2. When the user specifies the cylindrical model, the repository and cavity are modeled as a cylinder of constant height equal to the constant REPOSTCK. The calculation of REPOSTCK is discussed in Section 6.1.1.4. All spallings executions were begun using the spherical model. Certain exception runs required restarting the code with the cylindrical model. These exception runs are discussed in further detail in the following section.

#### 6.1.1.4. Exception Runs

The repository thickness at the time of intrusion, represented by the variable REPOSTCK, is determined from the repository porosity $\phi$ (the sampled parameter SPALLMOD:REPIPOR), the height of the repository at burial time, $H_o$, and porosity $\phi_o$ of a waste-filled room prior to closure:

$$REPOSTCK = \frac{(1-\phi_o)H_o}{1-\phi}. \tag{6-1}$$

WIPP PA assigns the values of $H_o$ = 3.96 m (BLOWOUT:HREPO) and $\phi_o$ = 0.85 (BLOWOUT:INPORO). By the end of some DRSPALL simulations, the cavity radius exceeded the height of the repository. In an actual intrusion, this would correspond to spalling occurring into the disturbed rock zone (DRZ) below the repository. Lord et al. (2003) state that "the unsteady porous flow and stress equations that describe the repository in hemispherical geometry do not address the presence of the lower DRZ." When the cavity radius reaches the height of the repository, the cavity no longer expands vertically and cavity growth can only result from lateral expansion, thus the DRSPALL calculation proceeds in the cylindrical mode from that point forward. For the DRSPALL cylindrical exception runs, the height of the cylinder remains equal to the height of the repository while the radius of cylinder increases as spalling occurs. An initial radius for the cylindrical cavity was specified to be the height of the repository. This initial radius was specified to account for the cavity calculated when DRSPALL was executed in spherical mode. The initial radius is set equal to the repository thickness so that the initial cylindrical cavity has a lateral surface area equivalent to the surface area of the hemispherical cavity at the time when the hemispherical cavity reaches the base of the repository. The volume of spalled material (SPLVOL2) from the cylindrical run was added to the volume of spalled material (SPLVOL2) at the time step when CAVRAD first exceeded the repository height during the spherical run, and this total volume is used by CUTTINGS_S.

The procedure for implementing each exception run was as follows:

1) DRSPALL was run for all vectors and DPSs with a maximum run time of 600 s.

2) All DRSPALL runs were examined to determine in which runs CAVRAD exceeded REPOSTCK.

3) For each run in which CAVRAD exceeded REPOSTCK, a new DRSPALL input control file was created. This control file differed from the control file that was used for the initial run in the following ways (Figure 6-1):

```
.....
Stop Pump Exit Vol Rate     (m^3/s) :  SPALLMOD STPPVOLR
Stop Drilling Time              (s) :  33.78

COMPUTATIONAL
Spherical/Cylindrical           (S/C) :  C
Allow Fluidization              (Y/N) :  Y
Max Run Time                      (s) :  600.
Respository Cell Length           (m) :  0.004
radius, Growth rate             (m,-) :  1.5, 1.00
Wellbore Cell Length              (m) :  2.0
wellbore Zone Growth Rate         (-) :  1.0
First wellbore Zone               (-) :  10
Well Stability factor             (-) :  0.05
Repository Stability factor       (-) :  5.0
Mass Diffusion factor             (-) :  0.0001
Momentum Diffusion factor         (-) :  0.01

INITIAL CAVITY RADIUS           (m) :  0.939427
```

**Figure 6-1. Excerpt of Modified DRSPALL Control File for Cylindrical Runs.** Lines in bold differ from control files for spherical runs.

a. The flag indicating use of the spherical model was changed from "S" to "C" to indicate that the cylindrical model is used.

b. "INITIAL CAVITY RADIUS" is specified to a length equal to the height of the repository.

c. To assist in establishing "true" initial conditions from the inputted approximate initial conditions for restarting the run in cylindrical mode, the drill bit is started 0.15 m above the repository with a velocity of 0.00444 m/s. At 33.78 s, the drill bit is at the top of the repository. "STOP DRILLING TIME" was changed from "1.0000E+03" to "33.78." At this point, sufficient initial conditions have been re-established and the code proceeds with the normal coupled wellbore/repository calculations without drilling. Since the drilled volume was already determined in the spherical run, the drill bit is stopped before penetration, and spalling proceeds as determined by the model.

d. "RADIUS, GROWTH RATE" was changed from "0.5, 1.00" to "1.5, 1.00." "RADIUS" separates the region in the repository where zone size is constant from the region where zone size grows at "GROWTH RATE." Note that in DRSPALL Version 1.22, the zone size growth rate is always 1.00, which means the zone size remains constant. The value specified for "RADIUS" in the cylindrical runs results in about 0.5 m (1.5 - 1) outside the initial cavity radius where zone size remains constant. This assumes a repository height of approximately 1.0 m.

4) DRSPALL was run using the new input control file.

5) SPLVOL2 at time 600 s from the cylindrical run was added to the spherical SPLVOL2 value at the first time when CAVRAD exceeded REPOSTCK. This procedure is discussed in greater detail in Section 6.1.1.5. Note that for all cylindrical DRSPALL runs, CAVRAD attained a steady state value within 500 s, and thus it was not necessary to increase the run time as described in Section 6.1.1.2.

The code does not have the capability to start with an arbitrary pressure profile within the repository or fluid/solid distribution in the wellbore, and, therefore, a uniform pressure distribution and mud-filled column are used for the initial conditions at the beginning of the cylindrical run (end of the run in spherical geometry). Thus, the cylindrical calculations start with a similar initial pressure difference between the wellbore and repository as the spherical calculations.

#### 6.1.1.5. Creation of the Spallings Data File for CUTTINGS_S

The code CUTTINGS_S calculates spall volumes for the PA drilling intrusion scenarios from the DRSPALL calculated spall volumes. A spall volume is calculated for each PA vector and at each of a set of discrete times and locations (unique pressure) within the repository for each drilling intrusion scenario.

CUTTINGS_S requires an input file that contains the spallings volumes calculated by DRSPALL for each vector and DPS for one replicate (WIPP PA 2004c). This section details how this spallings data file was created for a PA calculation.

The first step involved a series of SUMMARIZE runs. The code SUMMARIZE was run using the DRSPALL data from the spherical runs, once per DPS and replicate combination. As an example, the SUMMARIZE input file for replicate 1, DPS 1 is provided by Vugrin (2005, Appendix B, Figure 21) for the CRA-2004 PABC and has not changed for the PABC-2009 and subsequent PAs. A fragment of the corresponding output table from the migrated PABC-2009 is shown in Figure 6-2. The entire file, *sum_drs_PABC09_sphere_r1_p1.tbl*, is stored in the CVS repository at /nfs/data/CVSLIB/WIPP_ARCHIVES/PABC09/SUMMARIZE/Output.

The output file (Figure 6-2) contains data for the variables REPOSTCK, CAVRAD, and SPLVOL2 at a set of discrete set of times for each vector of a DPS. The output contains two header lines followed by a blank line. The first header line lists the CAMDAT variable names of the data contained in the file: vector, time, REPOSTCK, CAVRAD, and SPLVOL2. The second header line contains information pertaining to the type of CAMDAT variable listed in line 1. The data following the header lines are grouped in sections containing 100 lines and five columns. The first column contains the vector number of the DRSPALL run, the second column contains a time (multiples of 2 s), the third column contains the repository height for each vector (constant for all times), the fourth column contains the value of CAVRAD calculated by DRSPALL at the time in the second column for the vector in the first column, and the fifth column contains the value of SPLVOL2 calculated by DRSPALL for the same time and vector. Each group of 100 lines has the same time value. The structure of the output file for spherical runs has not changed for the PABC-2009 and subsequent PAs.

A second set of SUMMARIZE runs was performed using the output from the DRSPALL cylindrical exception runs. SUMMARIZE was run once per DPS and replicate combination that produced spallings in the spherical runs. The output from these runs contained the accumulated spall volume, SPLVOL2, calculated at 600 s for the cylindrical exception DRSPALL runs. As an example, Figure 6-3 shows the output for Replicate 1, DPS 3 for the migrated PABC-2009. The structure of the output file for cylindrical runs has not changed for the PABC-2009 and subsequent PAs.

```
vector,time REPOSTCK CAVRAD   SPLVOL2
 ,[P:9],[H],[H]
     .
     .
     .
  95  0.000000E+00  1.143436E+00  0.000000E+00  0.000000E+00
  96  0.000000E+00  1.326540E+00  0.000000E+00  0.000000E+00
  97  0.000000E+00  1.035864E+00  0.000000E+00  0.000000E+00
  98  0.000000E+00  1.232377E+00  0.000000E+00  0.000000E+00
  99  0.000000E+00  1.728078E+00  0.000000E+00  0.000000E+00
 100  0.000000E+00  1.010622E+00  0.000000E+00  0.000000E+00

   1  2.000000E+00  1.520442E+00  1.100081E-01  0.000000E+00
   2  2.000000E+00  1.071487E+00  1.100081E-01  0.000000E+00
   3  2.000000E+00  1.092032E+00  1.100081E-01  0.000000E+00
   4  2.000000E+00  9.150674E-01  1.100081E-01  0.000000E+00
   5  2.000000E+00  1.242655E+00  1.100081E-01  0.000000E+00
     .
     .
     .
```

**Figure 6-2. Fragment of SUMMARIZE Output File for Spherical DRSPALL Run – Migrated PABC-2009 (Revision 0) Replicate 1, DPS 1.**

```
vector,time SPLVOL2
 ,[H]

  32  6.000000E+02  1.915924E+00
  36  6.000000E+02  6.617699E-01
  42  6.000000E+02  0.000000E+00
```

**Figure 6-3. SUMMARIZE Output file for DRSPALL Cylindrical Run – Migrated PABC-2009 (Revision 0) Replicate 1, DPS 3.**

The final step in the creation of the spallings data files (one for each DPS) was execution of the utility MERGESPALL to combine the "summarized" results from the spherical and cylindrical runs. This utility was developed for the CRA-2004 PABC (Vugrin 2005, Appendix C). MERGESPALL works in the following manner:

1) MERGESPALL reads a SUMMARIZE output file containing the DRSPALL data from the spherical calculations for a single DPS. For each vector, MERGESPALL reads through all the times and finds the first time where CAVRAD exceeds REPOSTCK and

writes the value of SPLVOL2 at that time to an intermediate text file. If CAVRAD does not exceed REPOSTCK, MERGESPALL records the value of SPLVOL2 at the final time. For all vectors, MERGESPALL also writes the final time listed in the SUMMARIZE output file.

2) MERGESPALL reads the SUMMARIZE output file containing SPLVOL2 quantities from the cylindrical exception runs for the same DPS (if the file exists). For all of the vectors whose CAVRAD value exceeded its REPOSTCK value, MERGESPALL adds the SPLVOL2 quantity from the cylindrical run to the corresponding spherical SPLVOL2 quantity. If MERGESPALL does not find a SPLVOL2 value for a vector that requires one, an error message is logged in the log output file.

3) MERGESPALL checks the output directory to see if a file already exists with the user specified output file name. If one does exist, it appends the data to the end of that file. MERGESPALL writes 3 columns: the vector number, a time, and the spall volume for the vector. Otherwise, MERGESPALL creates a new text output file with a three line header. The first line contains the number of vectors, the second line contains the number of DPSs, and the third line contains the initial repository pressures used for each DPS. MERGESPALL assumes four pressure scenarios with initial pressures of 10, 12, 14, and 14.8 MPa. After writing the header, MERGESPALL writes the spall data to the new output text file.

For the CRA-2004 PABC, MERGESPALL was executed four times per replicate (data for the 4 DPSs are merged) for a total of three separate spallings data files (one for each replicate). The CRA-2004 PABC MERGESPALL files were developed using DRSPALL Version 1.10. Note that DRSPALL Version 1.10 used a variable zone size with a zone size growth rate of 1.01. DRSPALL Version 1.22 uses a constant zone size (i.e., a growth rate of 1.0) as described in Section 3.

### 6.1.2. DRSPALL Results

The VMS DRSPALL results (i.e., the MERGESPALL spallings data files developed using DRSPALL Version 1.10) were produced as part of the CRA-2004 PABC, and provided input for all subsequent PAs including the CRA-2014. With the migration of PA codes to a new operating platform (see Section 2.3), a new set of DRSPALL results were developed on Solaris for PABC-2009 using DRSPALL Version 1.21. Both the VMS DRSPALL (Version 1.10) and the migrated DRSPALL (Version 1.21) used zone size parameters $\Delta r$ = 0.004 m, $L_t$ = 0.02 m, and $\Delta z$ = 2.0 m as recommended by Lord et al. (2006, Section 5.7) with a variable zone size.

Using the calculation procedure described in Section 6.1.1, the final spallings volumes calculated for PABC-2009 using DRSPALL Version 1.22 (using a constant zone size with zone size parameters $\Delta r$ = 0.004 m, $L_t$ = 0.04 m, and $\Delta z$ = 2.0 m as recommended by Kicker 2015) are listed in Appendix C (Tables C-1, C-2, and C-3). The tables correspond to the spallings data files mspall_drs_PABC09_r1.out, *mspall_drs_PABC09_r2.out*, and *mspall_drs_PABC09_r3.out*, respectively, and are located in the CVS repository at /nfs/data/CVSLIB/WIPP_ANALYSES/ PABC09/DRSPALL/Output. These volumes were calculated by the procedures outlined in Sections 6.1.1.4 and 6.1.1.5. All spallings volumes statistics presented in the following sections

were calculated using these volumes, which represent the volumes after processing by MERGESPALL and not the volumes listed in the DRSPALL output files.

#### 6.1.2.1. DPS 1 Results

For DPS 1, the initial repository pressure was set to 10 MPa. All DPS 1 DRSPALL calculations resulted in no spalling. These modified results (DRSPALL Version 1.22) are identical to what was observed in both the VMS DRSPALL (Version 1.10) and migrated DRSPALL (Version 1.21). Lord et al. (2003) explain this phenomenon by noting that the initial pressure difference between the repository and the wellbore (hydrostatic pressure of approximately 7.8 MPa) is not large enough to cause tensile failure of the waste material. As a result, no spalling occurs.

#### 6.1.2.2. DPS 2 Results

For DPS 2 the initial repository pressure was set to 12 MPa. Table 6-1 lists the DRSPALL volume statistics from the modified DRSPALL (Version 1.22), the migrated DRSPALL (Version 1.21), and the VMS DRSPALL (Version 1.10). They are separated by replicate, and the pooled statistics (combined replicates 1, 2, and 3) are presented, as well. Of the modified DRSPALL replicates, replicate 1 has the largest individual spall volume (9.68 $m^3$) and the largest mean volume (0.360 $m^3$). All three replicates yield similar percentages of nonzero spall volume vectors (66% to 68%), and the percentages of large spall volume vectors are also similar, ranging from 3% to 5%.

The modified DRSPALL mean spall volume exceeds the VMS DRSPALL mean spall volume by approximately 86% (0.15 $m^3$). The largest DPS 2 spall volume from the VMS DRSPALL is 7.71 $m^3$, and the largest DPS 2 spall volume from the modified DRSPALL is 9.68 $m^3$. The modified DRSPALL have a much higher percentage of nonzero spall vectors (67% versus 21%), while both the modified and VMS DRSPALL vectors yield a similar percentage of spall volumes greater than 1 $m^3$ (4%). Note that while the migrated DRSPALL (Version 1.21) maximum and mean spall volumes are lower than the VMS DRSPALL (Version 1.10), their cumulative distributions are essentially identical as shown in Figure 6-4.

##### *6.1.2.2.1. Exception Runs – Increased Run Times*

As discussed in Section 6.1.1.2, the cavity radius (CAVRAD) is the key indicator for determining when the spallings process has ceased. Table 6-2 lists the vectors that have CAVRAD values that increased after 500 s of the DRSPALL simulation, and Figures 6-5, 6-6, and 6-7 plot the DPS 2 cavity radii for all vectors versus time for the modified DRSPALL (Version 1.22). As shown in these figures, all vectors are no longer increasing after 600 s.

##### *6.1.2.2.2. Exception Runs – Cylindrical Model Restarts*

Table 6-3 lists the vectors that were restarted using the cylindrical model and the values of REPOSTCK and CAVRAD after 600 s using the spherical model for the modified DRSPALL (Version 1.22). Additionally, the final spall volume calculated for each vector is broken down into the contributions from the spherical model run and the cylindrical model restart.

## Table 6-1. Statistics for DRSPALL Volumes: DPS 2.

| Replicate | Maximum ($m^3$) | Mean ($m^3$) | Median ($m^3$) | % of Vectors with Volumes > 0 $m^3$ | % of Vectors with Volumes > 1 $m^3$ |
|---|---|---|---|---|---|
| Modified DRSPALL[1], Version 1.22 (replicates 1, 2, and 3 combined) | 9.68 | 0.320 | 0.138 | 67 | 4 |
| Modified DRSPALL – replicate 1 | 9.68 | 0.360 | 0.145 | 68 | 5 |
| Modified DRSPALL – replicate 2 | 7.07 | 0.262 | 0.128 | 68 | 3 |
| Modified DRSPALL – replicate 3 | 7.96 | 0.338 | 0.108 | 66 | 5 |
| Migrated DRSPALL[2], Version 1.21 (replicates 1, 2, and 3 combined) | 5.99 | 0.156 | 0.000 | 21 | 4 |
| Migrated DRSPALL – replicate 1 | 5.99 | 0.179 | 0.000 | 21 | 4 |
| Migrated DRSPALL – replicate 2 | 5.83 | 0.140 | 0.000 | 21 | 3 |
| Migrated DRSPALL – replicate 3 | 5.97 | 0.148 | 0.000 | 20 | 4 |
| VMS DRSPALL[3], Version 1.10 (replicates 1, 2, and 3 combined) | 7.71 | 0.172 | 0.000 | 21 | 4 |
| VMS DRSPALL – replicate 1 | 7.71 | 0.196 | 0.000 | 21 | 4 |
| VMS DRSPALL – replicate 2 | 6.27 | 0.163 | 0.000 | 21 | 3 |
| VMS DRSPALL – replicate 3 | 6.86 | 0.157 | 0.000 | 20 | 4 |

NOTES: [1]Modified DRSPALL (Version 1.22) spallings volumes are listed in Appendix C and correspond to data files *mspall_drs_PABC09_r1.out*, *mspall_drs_PABC09_r2.out*, and *mspall_drs_PABC09_r3.out*, which are stored in the CVS repository at /nfs/data/CVSLIB/WIPP_ANALYSES/PABC09/DRSPALL/Output.

[2]Migrated DRSPALL (Version 1.21) spallings volumes are described by Kirchner, Gilkey, and Long (2013). Spallings data (files *mspall_drs_PABC09_r1.out*, *mspall_drs_PABC09_ r2.out*, and *mspall_ drs_PABC09_r3.out*) are stored in the CVS repository at /nfs/data/CVSLIB/WIPP_ARCHIVES/PABC09/DRSPALL/Output (Revision 0).

[3]VMS DRSPALL (Version 1.10) spallings volumes are from Vugrin (2005, Appendix D) and correspond to the spallings data files *MERGESPALL_DRS_CRA1BC_R1.OUT*, *MERGESPALL_ DRS_CRA1BC_R2.OUT*, and *MERGESPALL_DRS_CRA1BC_R3.OUT*, which are stored in the SCMS library PACMS2:[CMS_CRA1BC.CRA1BC_DRS] in the class CRA1BC-0.

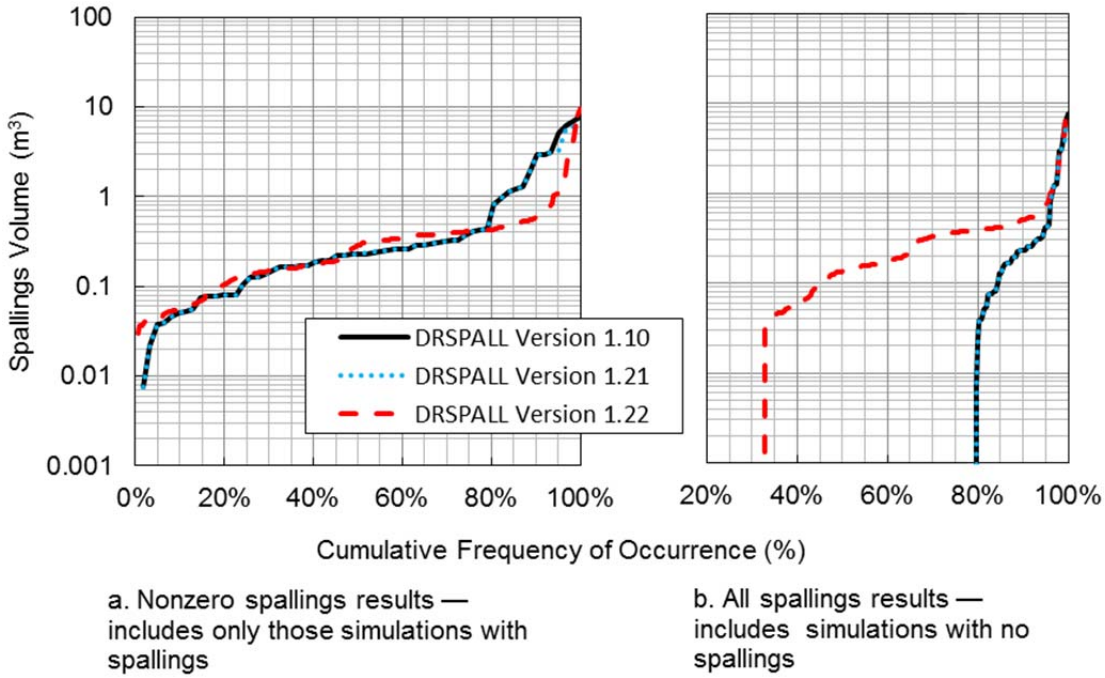


**Figure 6-4. The Cumulative Distributions of DRSPALL Spallings Volumes for Replicates 1, 2, and 3 at a Repository Pressure of 12 MPa (DPS 2).**

**Table 6-2. Vectors with Increasing CAVRAD Values after 500 s: DPS 2.**

| Replicate 1 Vectors | Replicate 2 Vectors | Replicate 3 Vectors |
|---|---|---|
| V032 | V041 | V025 |

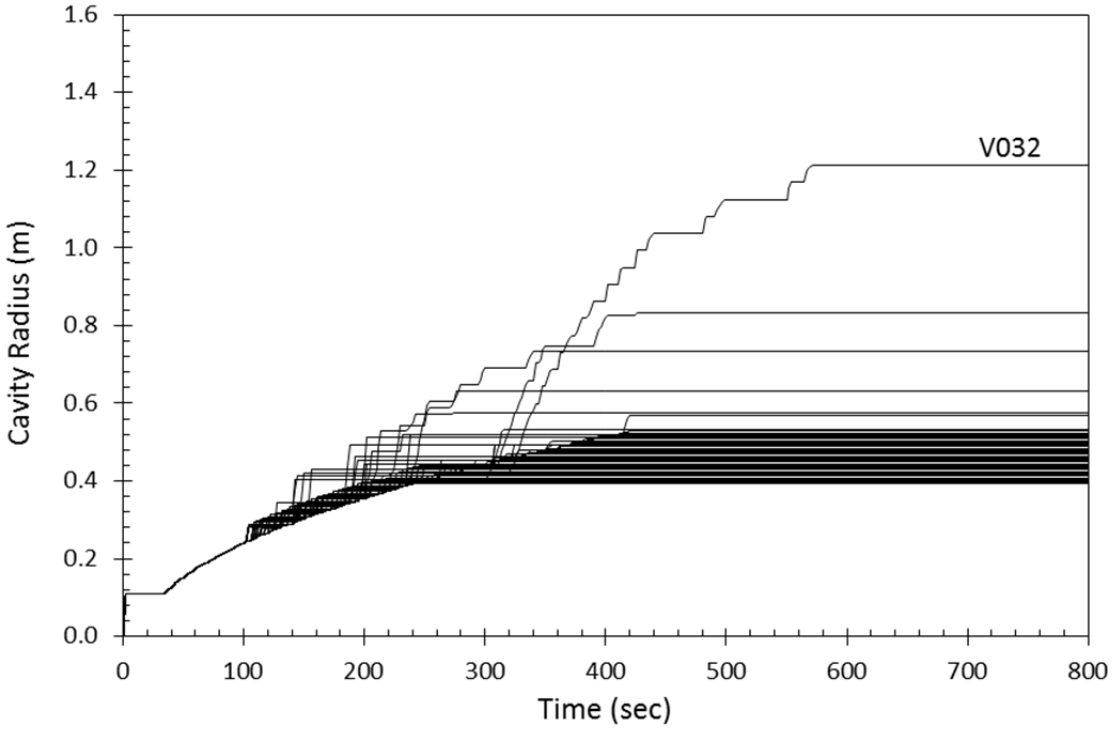


**Figure 6-5. Cavity Radius Versus Time: Replicate 1, DPS 2.**

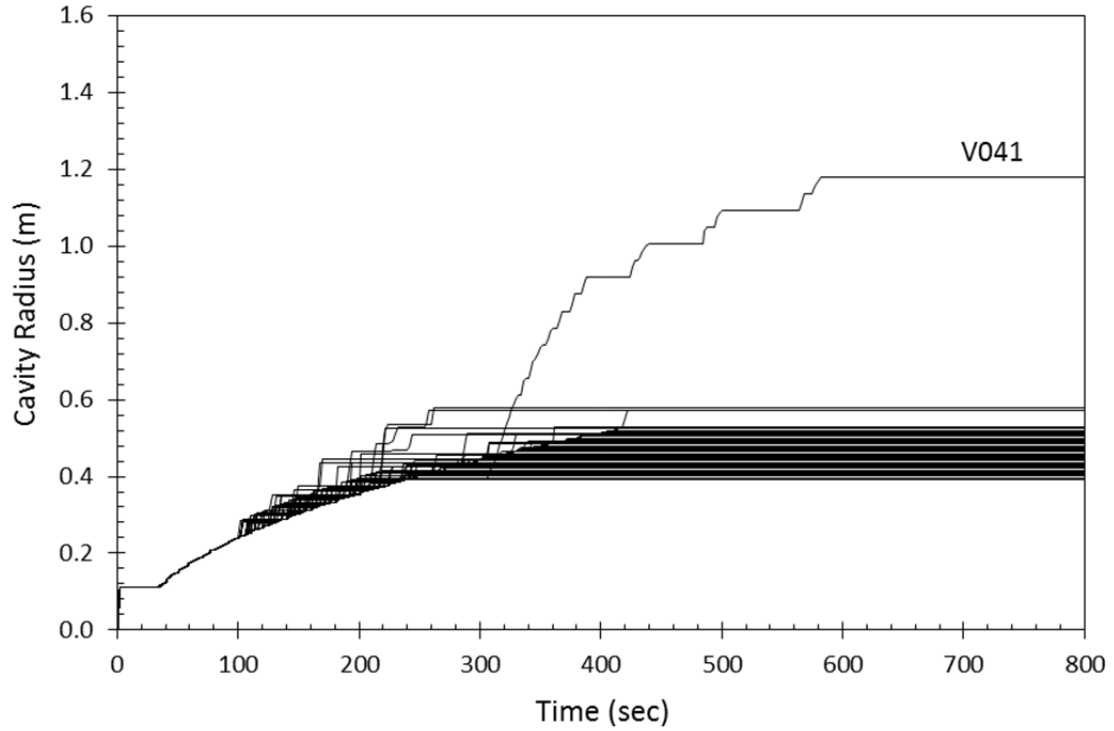


**Figure 6-6. Cavity Radius Versus Time: Replicate 2, DPS 2.**

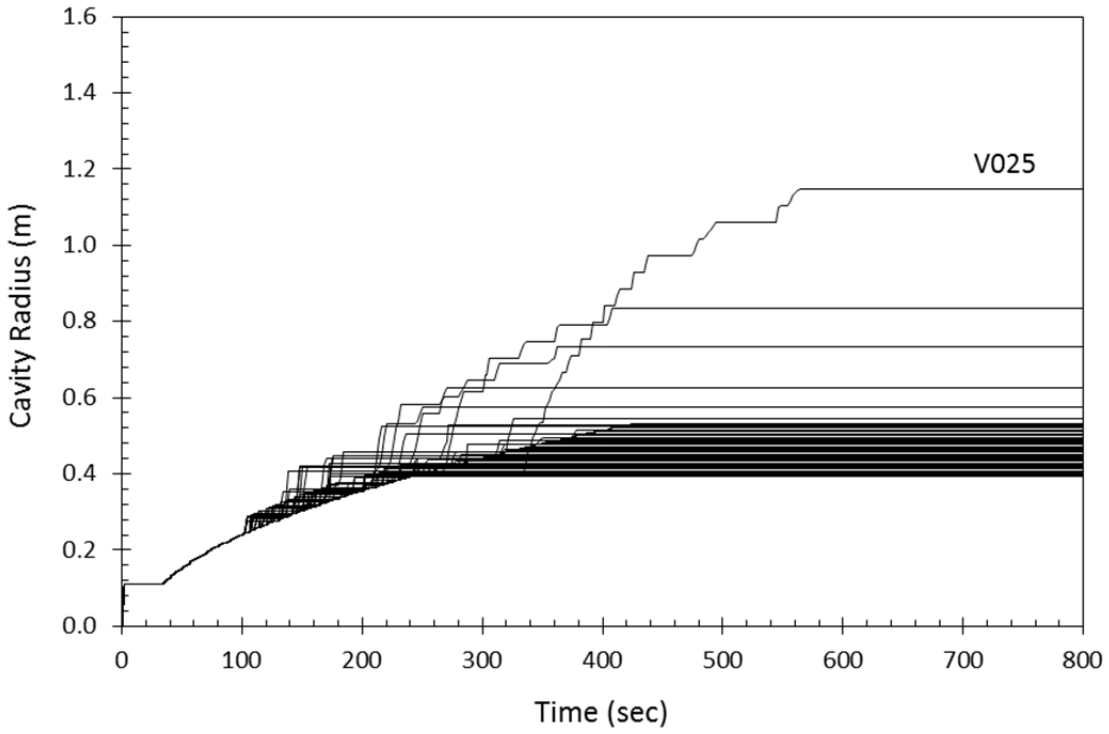


**Figure 6-7. Cavity Radius Versus Time: Replicate 3, DPS 2.**

**Table 6-3. DPS 2 Cylindrical Model Restarts.**

| Replicate - Vector | REPOSTCK (m) | Final CAVRAD (m) | Spherical Volume ($m^3$) | Cylindrical Volume ($m^3$) | Total Volume ($m^3$) |
|---|---|---|---|---|---|
| R1-V032 | 1.10 | 1.21 | 9.676 | 0.000 | 9.676 |
| R2-V041 | 0.92 | 1.18 | 7.070 | 0.000 | 7.070 |
| R3-V025 | 0.99 | 1.15 | 7.958 | 0.000 | 7.958 |

### 6.1.2.3. DPS 3 Results

For DPS 3 the initial repository pressure was set to 14 MPa. Table 6-4 lists the DRSPALL volume statistics from the modified DRSPALL (Version 1.22), the migrated DRSPALL (Version 1.21), and the VMS DRSPALL (Version 1.10). They are separated by replicate, and the pooled statistics (combined replicates 1, 2, and 3) are presented, as well. Of the modified DRSPALL replicates, replicate 3 has the largest individual spall volume (10.18 $m^3$), while replicate 1 has the largest mean volume (1.243 $m^3$). All three replicates yield similar percentages of nonzero spall volume vectors (approximately 74%), and the percentages of large spall volume vectors are also similar, ranging from 23% to 28%.

The modified DRSPALL mean spall volume exceeds the VMS DRSPALL mean spall volume by approximately 64% (0.42 $m^3$). The largest DPS 3 spall volume from both the VMS and migrated DRSPALL is 11.83 $m^3$, and the largest DPS 3 spall volume from the modified DRSPALL is 10.18 $m^3$. Both the VMS and migrated DRSPALL have a slightly higher percentage of nonzero spall vectors compared to the modified DRSPALL (76% versus 74%), and 13% of the VMS and migrated DRSPALL vectors yield spall volumes greater than 1 $m^3$, whereas 26% of the modified DRSPALL vectors result in spall volumes exceeding 1 $m^3$.

The cumulative distributions of DRSPALL spallings volumes for DPS 3 (repository pressure of 14 MPa) are shown in Figure 6-8.

**Table 6-4. Statistics for DRSPALL Volumes: DPS 3.**

| Replicate | Maximum ($m^3$) | Mean ($m^3$) | Median ($m^3$) | % of Vectors with Volumes > 0 $m^3$ | % of Vectors with Volumes > 1 $m^3$ |
|---|---|---|---|---|---|
| Modified DRSPALL[1], Version 1.22 (replicates 1, 2, and 3 combined) | 10.18 | 1.089 | 0.599 | 74 | 26 |
| Modified DRSPALL – replicate 1 | 10.00 | 1.243 | 0.643 | 74 | 28 |
| Modified DRSPALL – replicate 2 | 9.43 | 0.928 | 0.592 | 74 | 23 |
| Modified DRSPALL – replicate 3 | 10.18 | 1.097 | 0.548 | 74 | 28 |
| Migrated DRSPALL[2], Version 1.21 (replicates 1, 2, and 3 combined) | 11.83 | 0.657 | 0.160 | 76 | 13 |
| Migrated DRSPALL – replicate 1 | 11.83 | 0.745 | 0.162 | 76 | 13 |
| Migrated DRSPALL – replicate 2 | 7.11 | 0.507 | 0.156 | 77 | 11 |
| Migrated DRSPALL – replicate 3 | 8.86 | 0.718 | 0.166 | 76 | 16 |
| VMS DRSPALL[3], Version 1.10 (replicates 1, 2, and 3 combined) | 11.83 | 0.665 | 0.160 | 76 | 13 |
| VMS DRSPALL – replicate 1 | 11.83 | 0.745 | 0.162 | 76 | 13 |
| VMS DRSPALL – replicate 2 | 7.72 | 0.530 | 0.156 | 77 | 11 |
| VMS DRSPALL – replicate 3 | 8.86 | 0.721 | 0.166 | 76 | 16 |

NOTES: [1]Modified DRSPALL (Version 1.22) spallings volumes are listed in Appendix C and correspond to data files *mspall_drs_PABC09_r1.out*, *mspall_drs_PABC09_r2.out*, and *mspall_drs_PABC09_r3.out*, which are stored in the CVS repository at /nfs/data/CVSLIB/WIPP_ANALYSES/PABC09/DRSPALL/Output.

[2]Migrated DRSPALL (Version 1.21) spallings volumes are described by Kirchner, Gilkey, and Long (2013). Spallings data (files *mspall_drs_PABC09_r1.out*, *mspall_drs_PABC09_ r2.out*, and *mspall_drs_PABC09_r3.out*) are stored in the CVS repository at /nfs/data/CVSLIB/WIPP_ARCHIVES/PABC09/DRSPALL/Output (Revision 0).

[3]VMS DRSPALL (Version 1.10) spallings volumes are from Vugrin (2005, Appendix D) and correspond to the spallings data files *MERGESPALL_DRS_CRA1BC_R1.OUT*, *MERGESPALL_DRS_CRA1BC_R2.OUT*, and *MERGESPALL_DRS_CRA1BC_R3.OUT*, which are stored in the SCMS library PACMS2:[CMS_CRA1BC.CRA1BC_DRS] in the class CRA1BC-0.

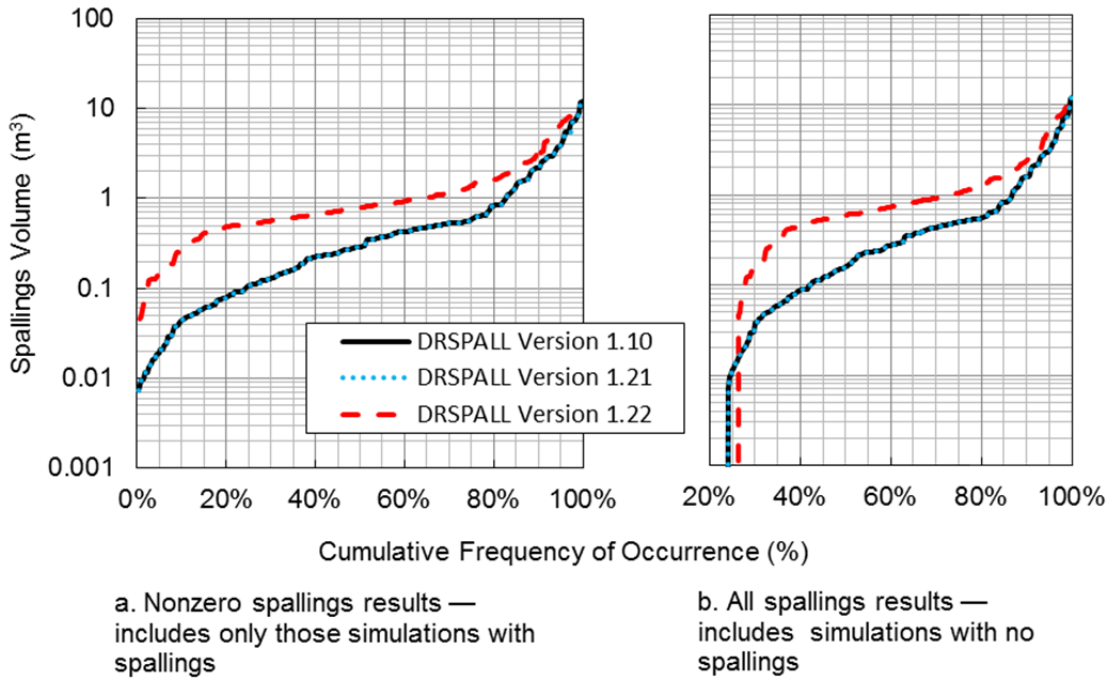


**Figure 6-8. The Cumulative Distributions of DRSPALL Spallings Volumes for Replicates 1, 2, and 3 at a Repository Pressure of 14 MPa (DPS 3).**

#### *6.1.2.3.1. Exception Runs – Increased Run Times*

As discussed in Section 6.1.1.2, the cavity radius (CAVRAD) is the key indicator for determining when the spallings process has ceased. Table 6-5 lists the vectors that have CAVRAD values that increased after 500 s of the DRSPALL simulation, and Figures 6-9, 6-10, and 6-11 plot the DPS 3 cavity radii for all vectors versus time for the modified DRSPALL (Version 1.22). As shown in these figures, all vectors were no longer increasing after 600 s.

**Table 6-5. Vectors with Increasing CAVRAD Values after 500 s: DPS 3.**

| Replicate 1 Vectors | Replicate 2 Vectors | Replicate 3 Vectors |
|---|---|---|
| V032 | V041 | V025 |

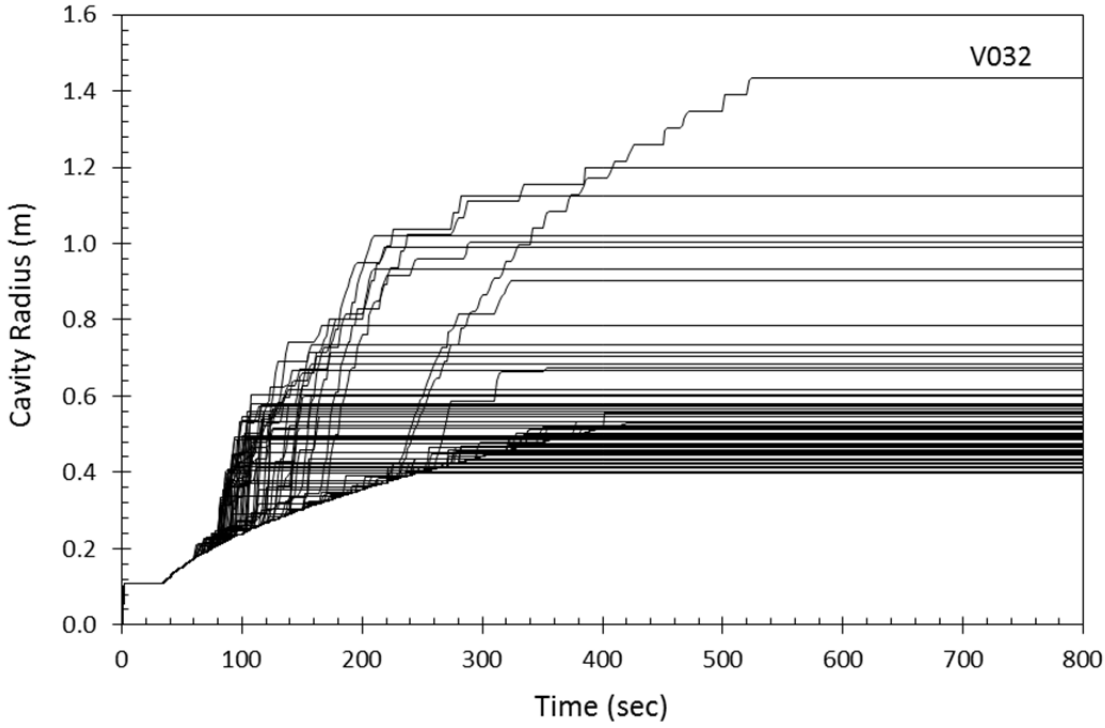


**Figure 6-9. Cavity Radius Versus Time: Replicate 1, DPS 3.**

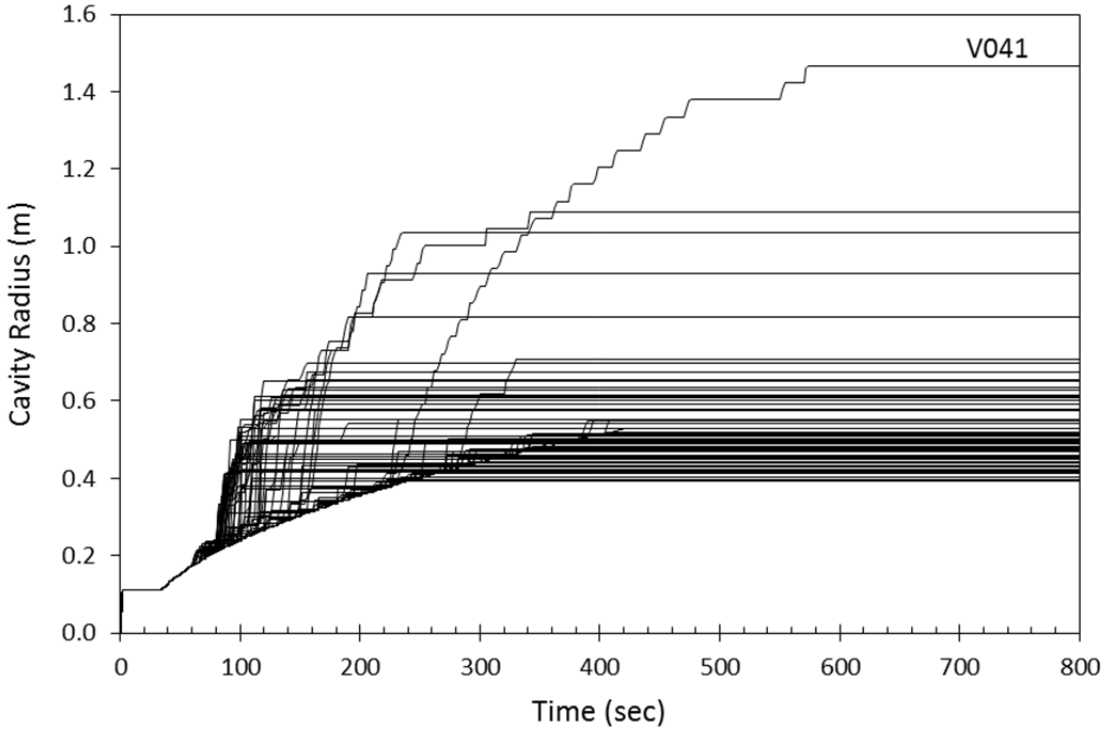


**Figure 6-10. Cavity Radius Versus Time: Replicate 2, DPS 3.**

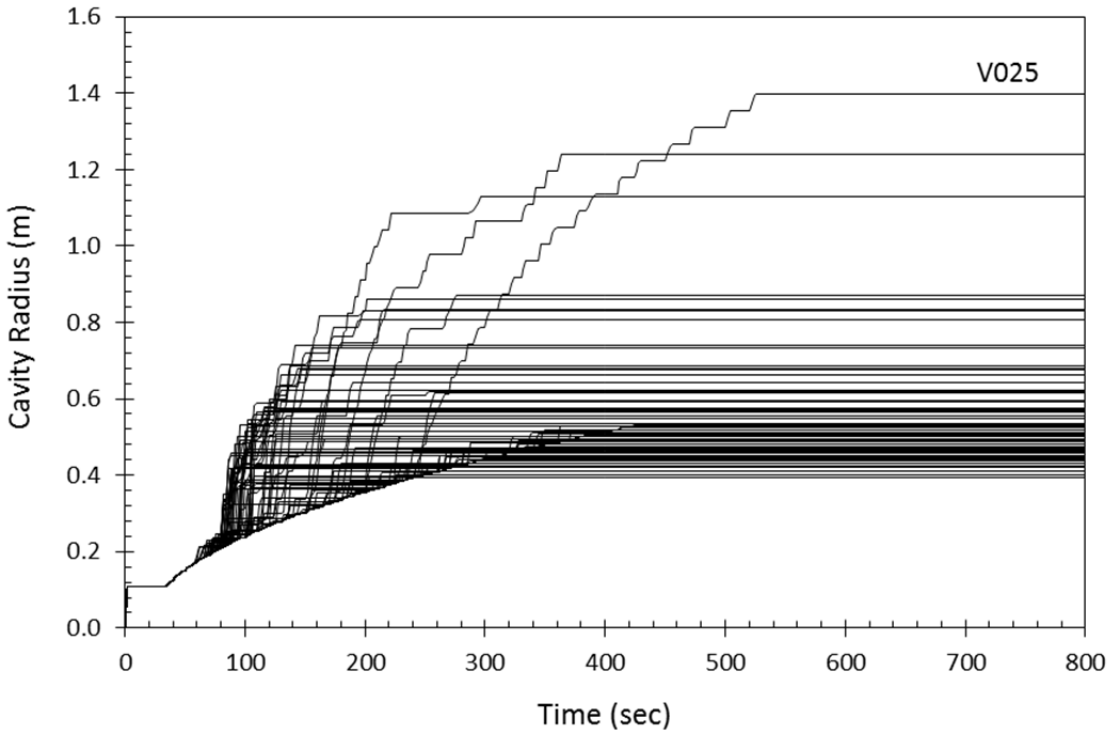


**Figure 6-11. Cavity Radius Versus Time: Replicate 3, DPS 3.**

#### *6.1.2.3.2. Exception Runs – Cylindrical Model Restarts*

Table 6-6 lists the vectors that were restarted using the cylindrical model and the values of REPOSTCK and CAVRAD after 600 s using the spherical model for the modified DRSPALL (Version 1.22). Additionally, the final spall volume calculated for each vector is broken down into the contributions from the spherical model run and the cylindrical model restart.

**Table 6-6. DPS 3 Cylindrical Model Restarts.**

| Replicate - Vector | REPOSTCK (m) | Final CAVRAD (m) | Spherical Volume ($m^3$) | Cylindrical Volume ($m^3$) | Total Volume ($m^3$) |
|---|---|---|---|---|---|
| R1-V032 | 1.10 | 1.43 | 9.996 | 0.000 | 9.996 |
| R1-V059 | 1.06 | 1.20 | 9.262 | 0.000 | 9.262 |
| R2-V041 | 0.92 | 1.47 | 6.749 | 0.000 | 6.749 |
| R2-V071 | 0.92 | 0.93 | 7.027 | 0.000 | 7.027 |
| R2-V086 | 0.95 | 1.04 | 7.663 | 0.000 | 7.663 |
| R3-V001 | 0.94 | 1.24 | 7.486 | 0.996 | 8.482 |
| R3-V025 | 0.99 | 1.40 | 8.018 | 0.000 | 8.018 |

#### 6.1.2.4. DPS 4 Results

For DPS 4 the initial repository pressure was set to 14.8 MPa. Table 6-7 lists the DRSPALL volume statistics from the modified DRSPALL (Version 1.22). For comparison, the statistics from the VMS DRSPALL (Version 1.10) and migrated DRSPALL (Version 1.21) are also included. Of the modified DRSPALL replicates, replicate 2 has the largest individual spall volume (15.82 $m^3$), and replicate 1 has the largest mean volume (1.672 $m^3$). All three replicates yield similar percentages of nonzero spall volume vectors (approximately 75%), and the percentages of large spall volume vectors range from 35% to 45%.

The modified DRSPALL mean spall volume exceeds both the VMS and migrated DRSPALL mean spall volumes by approximately 50% (0.49 $m^3$). The largest DPS 4 spall volume from both the VMS and migrated DRSPALL is 14.54 $m^3$, and the largest DPS 4 spall volume from the modified DRSPALL is 15.82 $m^3$. Both the VMS and migrated DRSPALL have a slightly higher percentage of nonzero spall vectors compared to the modified DRSPALL (79% versus 75%), and 20% of the VMS and migrated DRSPALL vectors yield spall volumes greater than 1 $m^3$, whereas 40% of the modified DRSPALL vectors result in spall volumes exceeding 1 $m^3$.

The cumulative distributions of DRSPALL spallings volumes for DPS 4 (repository pressure of 14.8 MPa) are shown in Figure 6-12.

##### *6.1.2.4.1. Exception Runs – Increased Run Times*

Table 6-8 lists the vectors that have CAVRAD values that continued to increase after 500 s of the DRSPALL simulation, and Figures 6-13, 6-14, and 6-15 plot the DPS 4 cavity radii for all vectors versus time for the modified DRSPALL (Version 1.22). As shown in these figures, all vectors are no longer increasing after 600 s. For each of the vectors listed in Table 6-8, their respective CAVRAD values exceed their respective repository height (REPOSTCK) values within the first 600 s of the simulation. These vectors were restarted with the cylindrical model and are addressed in Section 6.1.2.4.2.

##### *6.1.2.4.2. Exception Runs – Cylindrical Model Restarts*

Table 6-9 lists the DPS 4 vectors that were restarted using the cylindrical model and the values of REPOSTCK and CAVRAD after 600 s using the spherical model for the modified DRSPALL (Version 1.22). Additionally, the spall volume for each vector is broken down into the contributions from the spherical model run and the cylindrical model restart.

## Table 6-7. Statistics for DRSPALL Volumes: DPS 4.

| Replicate | Maximum ($m^3$) | Mean ($m^3$) | Median ($m^3$) | % of Vectors with Volumes > 0 $m^3$ | % of Vectors with Volumes > 1 $m^3$ |
|---|---|---|---|---|---|
| Modified DRSPALL[1], Version 1.22 (replicates 1, 2, and 3 combined) | 15.82 | 1.471 | 0.772 | 75 | 40 |
| Modified DRSPALL – replicate 1 | 10.81 | 1.672 | 0.811 | 75 | 45 |
| Modified DRSPALL – replicate 2 | 15.82 | 1.321 | 0.744 | 75 | 40 |
| Modified DRSPALL – replicate 3 | 13.33 | 1.420 | 0.753 | 74 | 35 |
| Migrated DRSPALL[2], Version 1.21 (replicates 1, 2, and 3 combined) | 14.54 | 0.968 | 0.318 | 79 | 20 |
| Migrated DRSPALL – replicate 1 | 14.54 | 1.076 | 0.320 | 79 | 22 |
| Migrated DRSPALL – replicate 2 | 9.89 | 0.764 | 0.327 | 79 | 16 |
| Migrated DRSPALL – replicate 3 | 11.90 | 1.065 | 0.312 | 78 | 23 |
| VMS DRSPALL[3], Version 1.10 (replicates 1, 2, and 3 combined) | 14.54 | 0.978 | 0.318 | 79 | 20 |
| VMS DRSPALL – replicate 1 | 14.54 | 1.077 | 0.320 | 79 | 22 |
| VMS DRSPALL – replicate 2 | 9.89 | 0.789 | 0.327 | 79 | 16 |
| VMS DRSPALL – replicate 3 | 11.90 | 1.068 | 0.312 | 78 | 23 |

NOTES: [1]Modified DRSPALL (Version 1.22) spallings volumes are listed in Appendix C and correspond to data files *mspall_drs_PABC09_r1.out*, *mspall_drs_PABC09_r2.out*, and *mspall_drs_PABC09_r3.out*, which are stored in the CVS repository at /nfs/data/CVSLIB/WIPP_ANALYSES/PABC09/DRSPALL/Output.

[2]Migrated DRSPALL (Version 1.21) spallings volumes are described by Kirchner, Gilkey, and Long (2013). Spallings data (files *mspall_drs_PABC09_r1.out*, *mspall_drs_PABC09_r2.out*, and *mspall_drs_PABC09_r3.out*) are stored in the CVS repository at /nfs/data/CVSLIB/WIPP_ARCHIVES/PABC09/DRSPALL/Output (Revision 0).

[3]VMS DRSPALL (Version 1.10) spallings volumes are from Vugrin (2005, Appendix D) and correspond to the spallings data files *MERGESPALL_DRS_CRA1BC_R1.OUT*, *MERGESPALL_DRS_CRA1BC_R2.OUT*, and *MERGESPALL_DRS_CRA1BC_R3.OUT*, which are stored in the SCMS library PACMS2:[CMS_CRA1BC.CRA1BC_DRS] in the class CRA1BC-0.

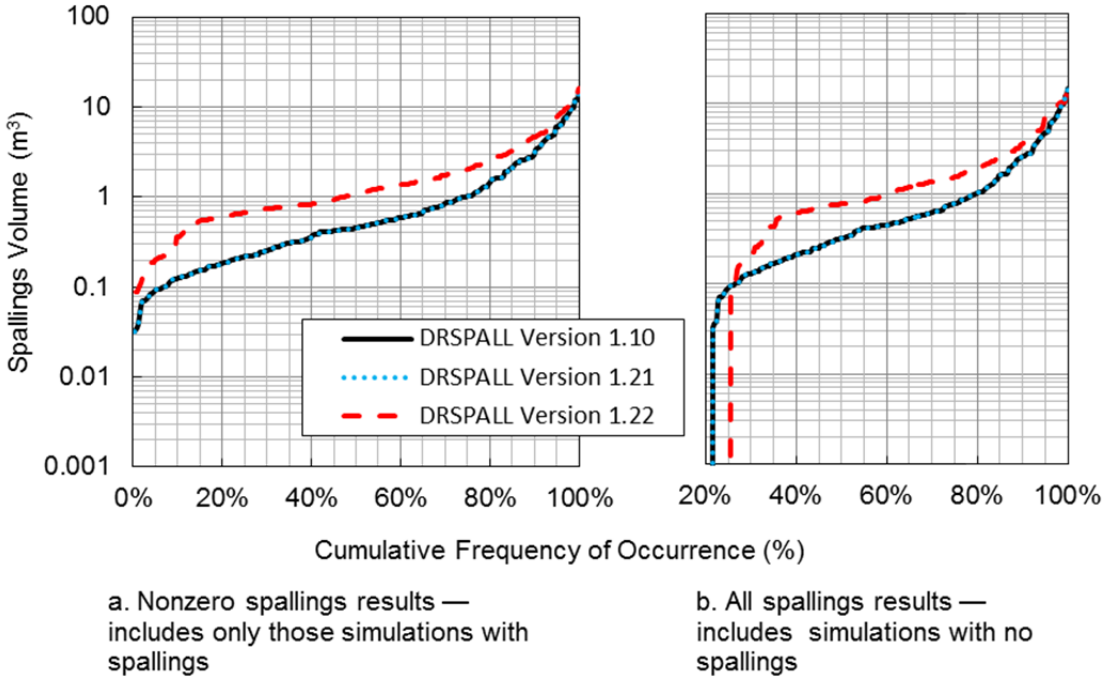


**Figure 6-12. The Cumulative Distributions of DRSPALL Spallings Volumes for Replicates 1, 2, and 3 at a Repository Pressure of 14.8 MPa (DPS 4).**

**Table 6-8. Vectors with Increasing CAVRAD Values after 500 s: DPS 4.**

| Replicate 1 Vectors | Replicate 2 Vectors | Replicate 3 Vectors |
|---|---|---|
| V032 | V041 | V025 |

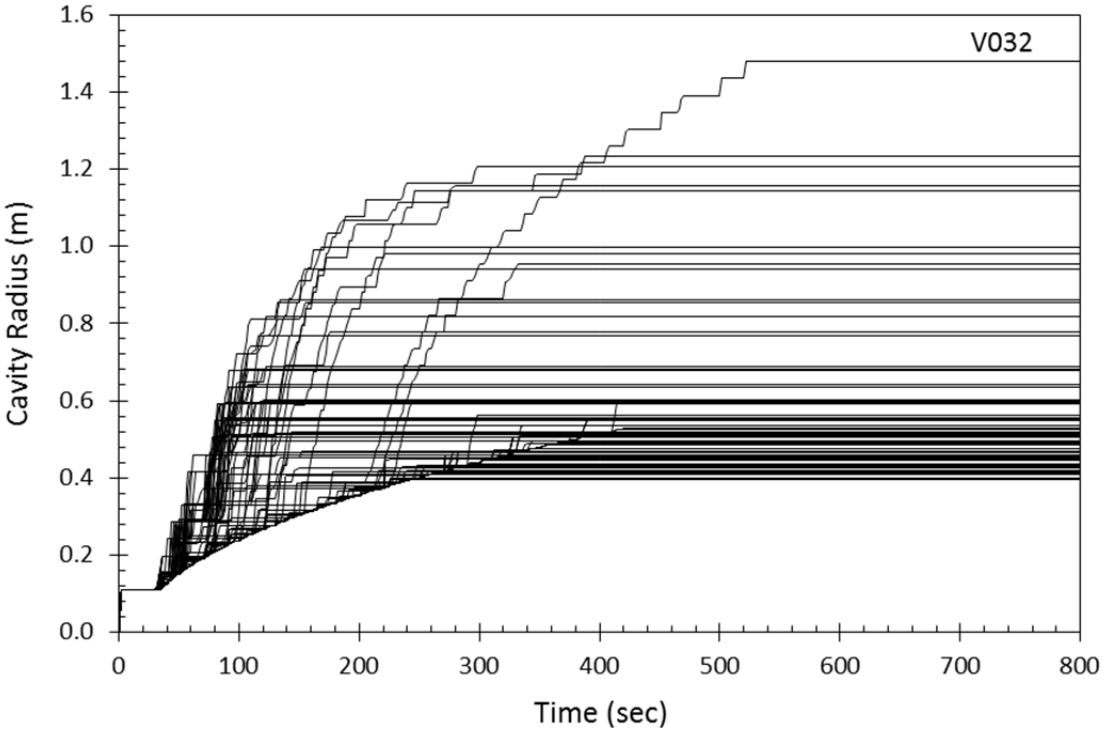


**Figure 6-13. Cavity Radius Versus Time: Replicate 1, DPS 4.**

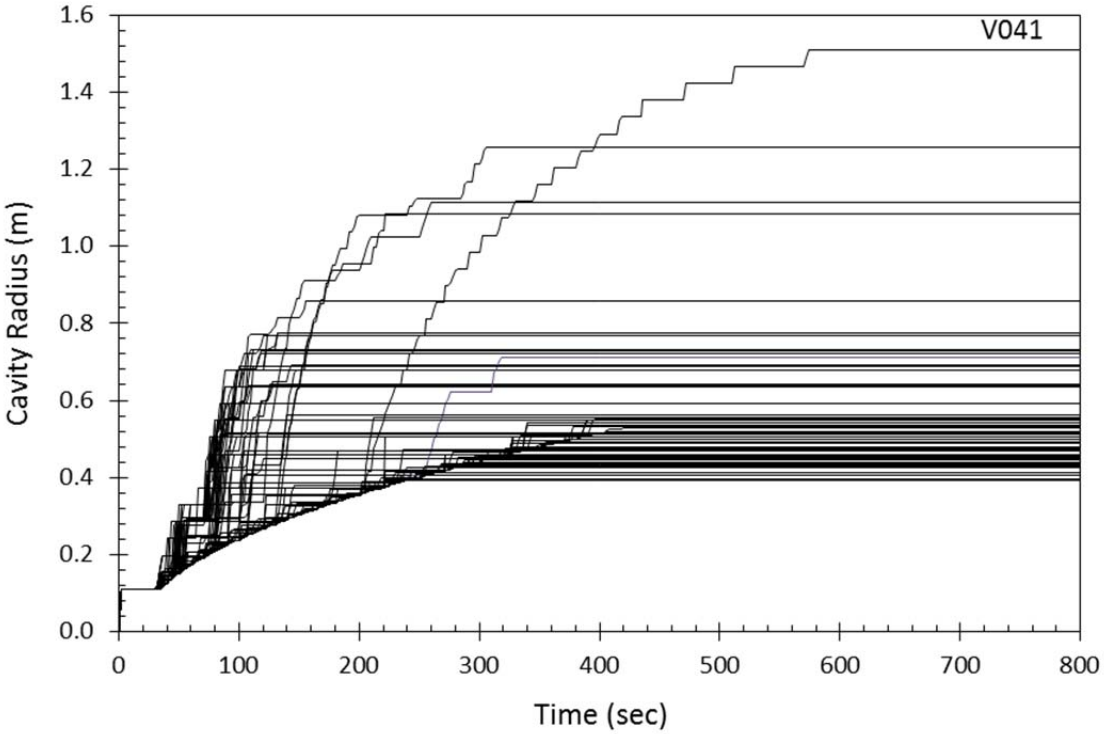


**Figure 6-14. Cavity Radius Versus Time: Replicate 2, DPS 4.**

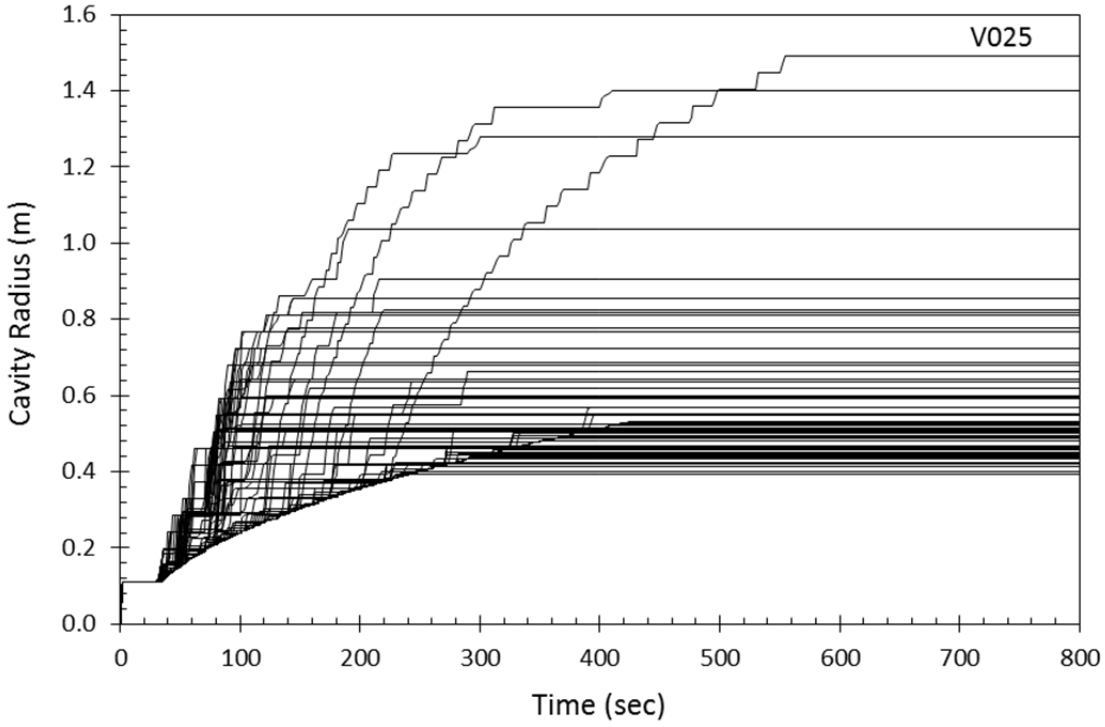


**Figure 6-15. Cavity Radius Versus Time: Replicate 3, DPS 4.**

**Table 6-9. DPS 4 Cylindrical Model Restarts.**

| Replicate - Vector | REPOSTCK (m) | Final CAVRAD (m) | Spherical Volume ($m^3$) | Cylindrical Volume ($m^3$) | Total Volume ($m^3$) |
|---|---|---|---|---|---|
| R1-V002 | 1.07 | 1.16 | 9.682 | 1.129 | 10.811 |
| R1-V028 | 0.92 | 0.94 | 7.473 | 0.000 | 7.473 |
| R1-V032 | 1.10 | 1.48 | 10.229 | 0.000 | 10.229 |
| R1-V059 | 1.06 | 1.23 | 9.426 | 0.000 | 9.426 |
| R2-V025 | 1.11 | 1.11 | 10.183 | 0.000 | 10.183 |
| R2-V041 | 0.92 | 1.51 | 6.748 | 9.069 | 15.817 |
| R2-V071 | 0.92 | 1.08 | 7.051 | 0.000 | 7.051 |
| R2-V086 | 0.95 | 1.26 | 8.045 | 1.010 | 9.055 |
| R3-V001 | 0.94 | 1.40 | 7.698 | 0.996 | 8.694 |
| R3-V025 | 0.99 | 1.49 | 8.036 | 0.000 | 8.036 |
| R3-V067 | 1.15 | 1.28 | 12.123 | 1.204 | 13.326 |
| R3-V068 | 0.92 | 1.04 | 7.668 | 0.000 | 7.668 |

It should be noted that vector 32 of replicate 1, vector 41 of replicate 2, and vector 25 of replicate 3 were restarted with the cylindrical model for DPSs 2, 3, and 4. If DRSPALL recorded SPLVOL2 values at the precise time the CAVRAD equaled REPOSTCK, the spherical volumes in Tables 6-3, 6-6, and 6-9 for the corresponding vectors should be equal because the hemispherical cavities that contribute to the spalling calculations would have the same radii (REPOSTCK) for DPS2, DPS3, and DPS4. However, SPLVOL2 was recorded only at discrete times, so spherical volumes are not precisely equal. This analysis handles this limitation is a conservative manner. When determining the volume contribution from the spherical run, MERGESPALL selected the SPLVOL2 value at the first time when CAVRAD *exceeded* REPOSTCK and then added the volume contribution from the cylindrical run. Thus, the SPLVOL2 volumes reported are actually slightly larger than the volume of the cavity when CAVRAD equals REPOSTCK.

#### 6.1.2.5. Scenario 4 Scatter Plots

This section presents scatter plots of DPS 4 spall volumes calculated by the modified DRSPALL (Version 1.22) versus the uncertain sampled parameters waste porosity, waste permeability, waste particle diameter, and waste tensile strength. The sampled values of the uncertain parameters used in the modified DRSPALL calculations have not changed from the sampled values used in the VMS DRSPALL and are provided in Table 4-4. The final SPLVOL2 values have been pooled and are plotted against each input variable on a vector by vector basis. The final SPLVOL2 numbers correspond to numbers given in Appendix C (Tables C-1, C-2, and C-3) and the sampled parameters match the values provided by Vugrin (2005, Appendix A, Tables 11, 12, and 13). Scatter plots can give a rough visual indication of how these parameters affect the resulting spall volumes. DPS 4 plots are shown because the high pressure results in more vectors that contain spallings compared to the lower pressures. Scatter plots for DPS 3 yield similar conclusions.

Figure 6-16 indicates that the largest spall volumes occur when waste permeability is less than 1.00E-13 $m^2$, but larger permeability values result in a higher frequency of nonzero spall volumes. This observation can be explained as follows: the higher permeability values that were sampled result in less tensile stresses and less tensile failure but promote fluidization. Lower permeability leads to greater tensile stresses and tensile failure, but failed material may not be able to fluidize at this low permeability. Smaller particle diameter values (see Figure 6-17) tend to result in larger spall volumes and higher frequency of nonzero spall volumes. This can be explained by the particle diameter's impact on fluidization velocities: smaller particle diameters lead to lower minimum fluidization velocities (Lord et al. 2006). No obvious correlations could be established between waste tensile strength and spall volume over the small sampled range of tensile strengths (Figure 6-18); Lord et al. (2003) reached this same conclusion. Lord et al. (2003) concluded that lower waste porosity values tended to correlate with larger spallings volumes for the 2004 Compliance Recertification Application (CRA-2004). For the modified DRSPALL results, a similar correlation is observed (Figure 6-19). The conclusions in this section using spallings volumes from the modified DRSPALL (Volume 1.22) are consistent with those made in Lord et al. (2003).

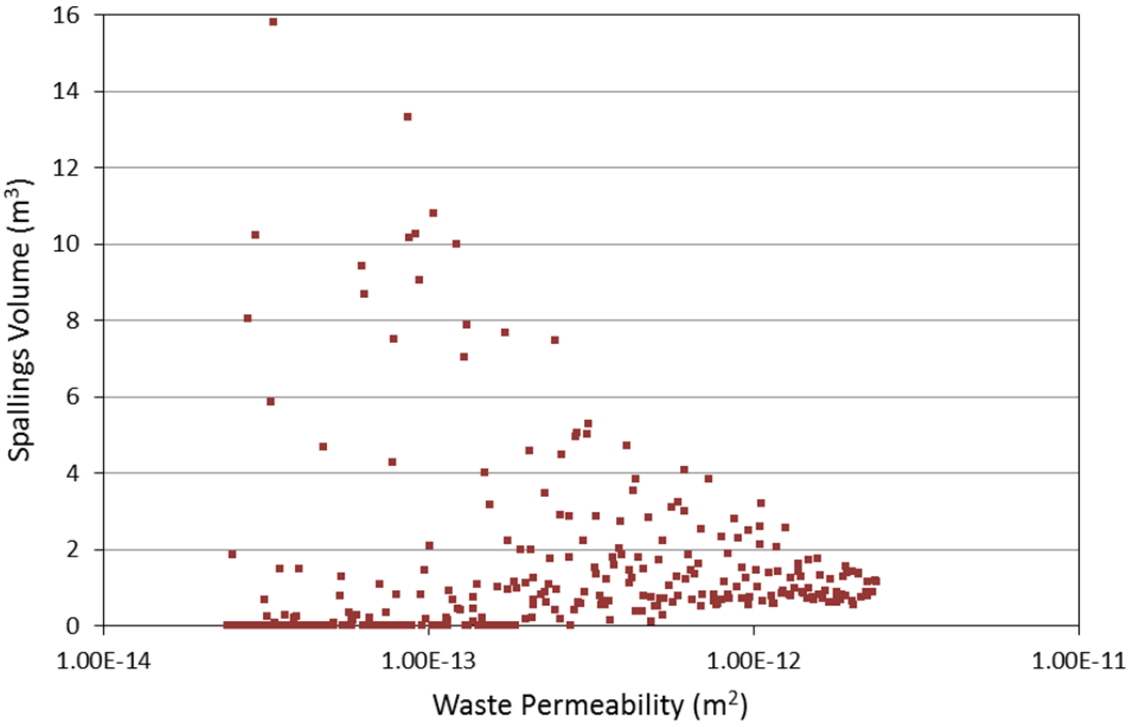


**Figure 6-16. Scatter Plot of Pooled Vectors: Waste Permeability vs SPLVOL2.**

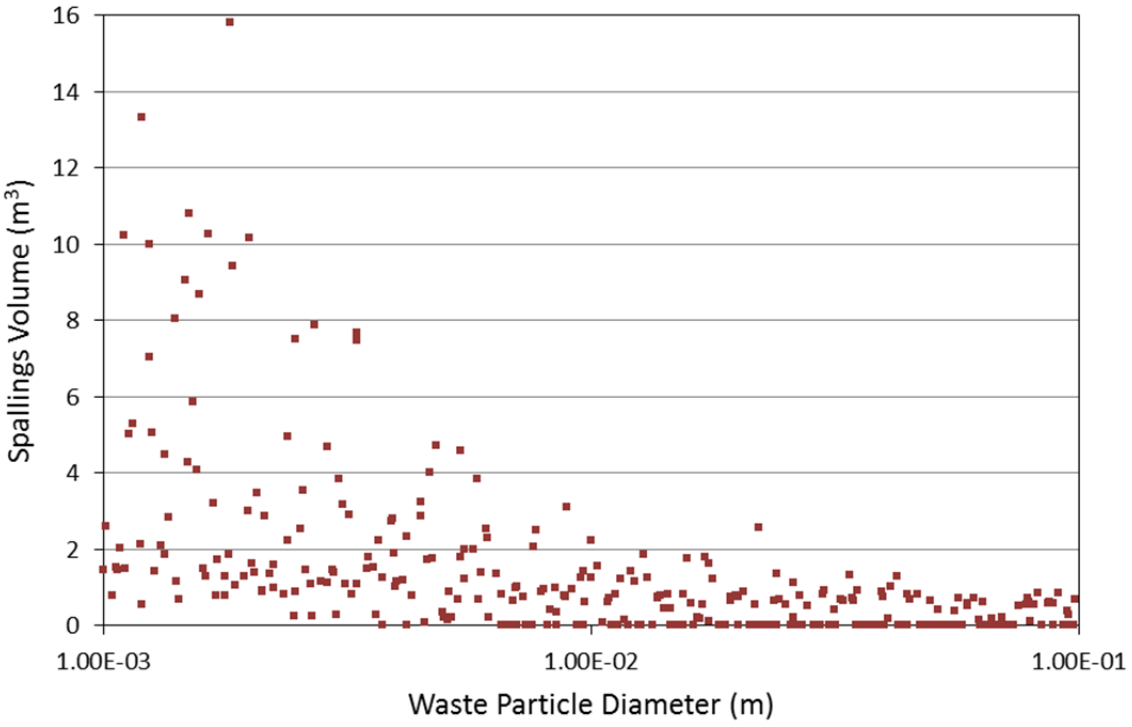


**Figure 6-17. Scatter Plot of Pooled Vectors: Waste Particle Diameter vs SPLVOL2.**

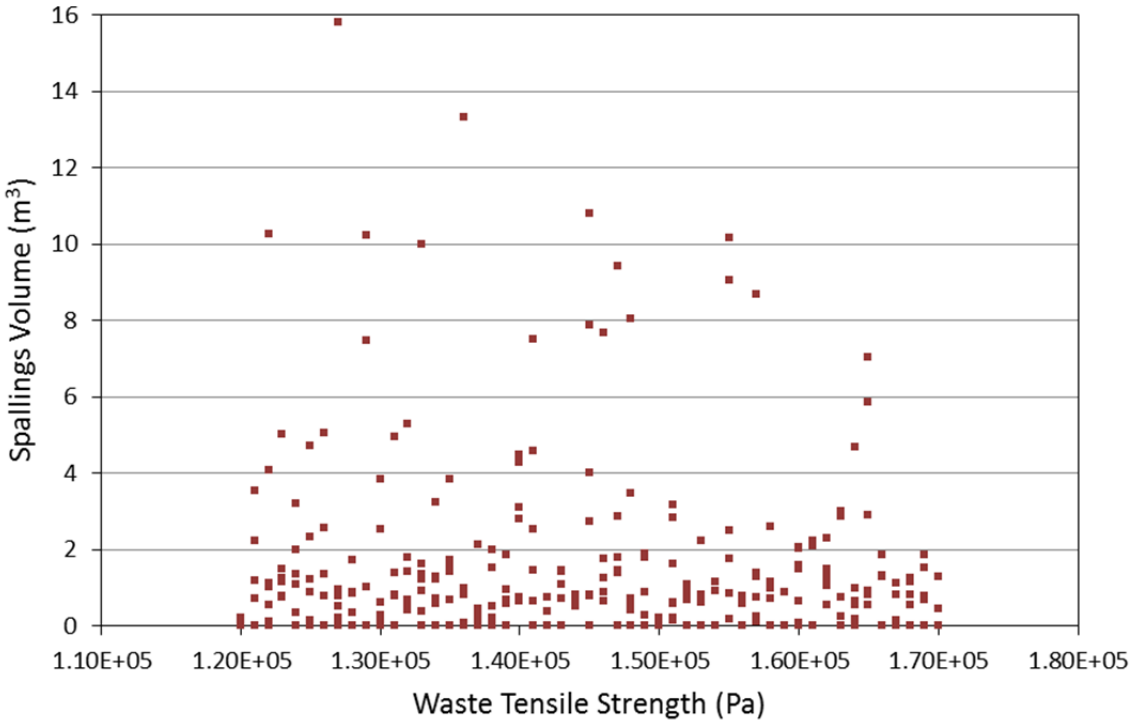


**Figure 6-18. Scatter Plot of Pooled Vectors: Waste Tensile Strength vs SPLVOL2.**

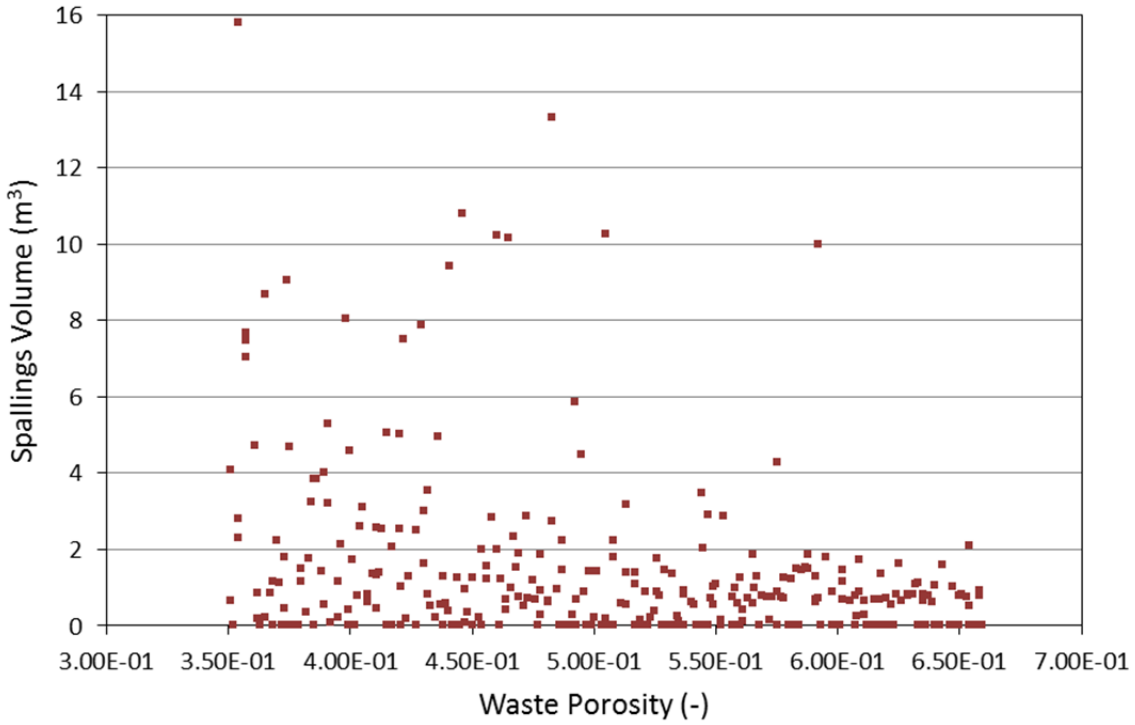


**Figure 6-19. Scatter Plot of Pooled Vectors: Waste Porosity vs SPLVOL2.**

### 6.1.3. Calculation of Repository Spall Volumes in CUTTINGS_S

The spallings volume for a given vector is determined in CUTTINGS_S by linearly interpolating between volumes calculated by DRSPALL based on the pressure calculated by BRAGFLO in each realization. DRSPALL volumes used in the VMS PABC-2009, the migrated PABC-2009, the VMS CRA-2014, and the migrated CRA-2014 have been updated based on the modified DRSPALL code (Version 1.22) as described in Section 6.1.2 and listed in Appendix C.

PA code CUTTINGS_S is also used as a transfer program between the BRAGFLO Salado flow calculation and the BRAGFLO direct brine release (DBR) calculation. Results obtained by BRAGFLO for each realization in scenarios S1-BF to S5-BF (Camphouse 2013b) are used to initialize the flow field properties necessary for the calculation of DBRs. This requires that results obtained on the BRAGFLO grid be mapped appropriately to the DBR grid. Code CUTTINGS_S is used to transfer the appropriate scenario results obtained with BRAGFLO to the DBR calculation. These transferred flow results are used as initial conditions in the calculation of DBRs. As a result, intrusion scenarios and times used in the calculation of spallings volumes correspond to those used in the calculation of DBRs. Five intrusion scenarios are considered in the DBR calculations, and are listed in Table 6-10.

**Table 6-10. PA Intrusion Scenarios Used in Calculating Direct Solids Releases.**

| Scenario | Conditioning (or 1st) Intrusion Time (year) and Type | Intrusion Times – Subsequent (year) |
|---|---|---|
| S1-DBR | None | 100, 350, 1000, 3000, 5000, 10000 |
| S2-DBR | 350, E1 | 550, 750, 2000, 4000, 10000 |
| S3-DBR | 1000, E1 | 1200, 1400, 3000, 5000, 10000 |
| S4-DBR | 350, E2 | 550, 750, 2000, 4000, 10000 |
| S5-DBR | 1000, E2 | 1200, 1400, 3000, 5000, 10000 |

While CUTTINGS_S uses these standard DBR scenarios as a basis for its calculations, it does so to provide flow field results (generated with BRAGFLO) as initial conditions to the DBR calculation at each subsequent intrusion time. CUTTINGS_S does not model the intrusion scenario itself. Scenario S1-DBR corresponds to an initial intrusion into the repository, with repository flow conditions at the time of intrusion transferred from BRAGFLO scenario S1-BF results. Scenarios S2-DBR through S5-DBR are used to model an intrusion into a repository that has already been penetrated. The times at which intrusions are assumed to occur for each scenario are outlined in the last column of Table 6-10; six intrusion times are modeled for scenario S1-DBR, while five times are modeled for each of scenarios S2-DBR through S5-DBR.

#### 6.1.3.1. PABC-2009 Spallings Volumes

Using the spallings volumes calculated by DRSPALL and the repository pressures calculated by BRAGFLO, the impact of DRSPALL Version 1.22 output on repository spallings volumes for PABC-2009 can be determined. Summary statistics of spallings volumes for the intrusion scenarios considered by CUTTINGS_S are shown in Table 6-11 for the PABC-2009

**Table 6-11. Summary of PABC-2009 Spallings Volumes by Scenario.**

| | | Scenarios | | | | | Total |
|---|---|---|---|---|---|---|---|
| | | S1-DBR | S2-DBR | S3-DBR | S4-DBR | S5-DBR | |
| **Updated PABC-2009 (Revision 1) Using DRSPALL Version 1.22** | | | | | | | |
| **R1** | **Maximum [$m^3$]** | 7.47 | 9.73 | 9.70 | 7.47 | 7.47 | 9.73 |
| | **Average nonzero volume [$m^3$]** | 0.84 | 0.73 | 0.80 | 0.77 | 0.78 | 0.79 |
| | **Number of nonzero volumes** | 244 | 225 | 232 | 107 | 166 | 974 |
| | **Percent of nonzero volumes** | 13.6% | 15.0% | 15.5% | 7.1% | 11.1% | 12.5% |
| **R2** | **Maximum [$m^3$]** | 2.53 | 2.24 | 2.23 | 2.03 | 2.07 | 2.53 |
| | **Average nonzero volume [$m^3$]** | 0.38 | 0.29 | 0.28 | 0.34 | 0.32 | 0.32 |
| | **Number of nonzero volumes** | 257 | 225 | 228 | 106 | 150 | 966 |
| | **Percent of nonzero volumes** | 14.3% | 15.0% | 15.2% | 7.1% | 10.0% | 12.4% |
| **R3** | **Maximum [$m^3$]** | 4.68 | 5.23 | 4.52 | 3.55 | 4.52 | 5.23 |
| | **Average nonzero volume [$m^3$]** | 0.61 | 0.41 | 0.34 | 0.38 | 0.41 | 0.44 |
| | **Number of nonzero volumes** | 222 | 214 | 228 | 103 | 150 | 917 |
| | **Percent of nonzero volumes** | 12.3% | 14.3% | 15.2% | 6.9% | 10.0% | 11.8% |
| **R1, R2, R3 Pooled** | **Maximum [$m^3$]** | 7.47 | 9.73 | 9.70 | 7.47 | 7.47 | 9.73 |
| | **Average nonzero volume [$m^3$]** | 0.61 | 0.48 | 0.48 | 0.50 | 0.51 | 0.52 |
| | **Number of nonzero volumes** | 723 | 664 | 688 | 316 | 466 | 2857 |
| | **Percent of nonzero volumes** | 13.4% | 14.8% | 15.3% | 7.0% | 10.4% | 12.2% |
| **Migrated PABC-2009 (Revision 0) Using DRSPALL Version 1.21** | | | | | | | |
| **R1** | **Maximum [$m^3$]** | 2.24 | 6.84 | 6.38 | 1.67 | 1.67 | 6.84 |
| | **Average nonzero volume [$m^3$]** | 0.37 | 0.51 | 0.46 | 0.30 | 0.37 | 0.42 |
| | **Number of nonzero volumes** | 142 | 118 | 111 | 59 | 76 | 506 |
| | **Percent of nonzero volumes** | 7.9% | 7.9% | 7.4% | 3.9% | 5.1% | 6.5% |
| **R2** | **Maximum [$m^3$]** | 2.36 | 2.76 | 1.86 | 2.29 | 1.96 | 2.76 |
| | **Average nonzero volume [$m^3$]** | 0.32 | 0.38 | 0.36 | 0.49 | 0.47 | 0.38 |
| | **Number of nonzero volumes** | 168 | 120 | 123 | 59 | 84 | 554 |
| | **Percent of nonzero volumes** | 9.3% | 8.0% | 8.2% | 3.9% | 5.6% | 7.1% |
| **R3** | **Maximum [$m^3$]** | 4.90 | 6.19 | 2.62 | 1.47 | 1.49 | 6.19 |
| | **Average nonzero volume [$m^3$]** | 0.53 | 0.39 | 0.28 | 0.30 | 0.28 | 0.38 |
| | **Number of nonzero volumes** | 156 | 114 | 119 | 45 | 71 | 505 |
| | **Percent of nonzero volumes** | 8.7% | 7.6% | 7.9% | 3.0% | 4.7% | 6.5% |
| **R1, R2, R3 Pooled** | **Maximum [$m^3$]** | 4.90 | 6.84 | 6.38 | 2.29 | 1.96 | 6.84 |
| | **Average nonzero volume [$m^3$]** | 0.40 | 0.42 | 0.37 | 0.37 | 0.38 | 0.39 |
| | **Number of nonzero volumes** | 466 | 352 | 353 | 163 | 231 | 1565 |
| | **Percent of nonzero volumes** | 8.6% | 7.8% | 7.8% | 3.6% | 5.1% | 6.7% |

**Table 6-11. Summary of PABC-2009 Spallings Volumes by Scenario. (Continued)**

| | | Scenarios | | | | | Total |
|---|---|---|---|---|---|---|---|
| | | S1-DBR | S2-DBR | S3-DBR | S4-DBR | S5-DBR | |
| VMS PABC-2009 Using DRSPALL Version 1.10 | | | | | | | |
| R1 | Maximum [$m^3$] | 2.24 | 8.29 | 7.97 | 1.67 | 1.67 | 8.29 |
| | Average nonzero volume [$m^3$] | 0.37 | 0.54 | 0.50 | 0.30 | 0.37 | 0.43 |
| | Number of nonzero volumes | 142 | 117 | 111 | 59 | 77 | 506 |
| | Percent of nonzero volumes | 7.9% | 7.8% | 7.4% | 3.9% | 5.1% | 6.5% |
| R2 | Maximum [$m^3$] | 2.36 | 2.76 | 1.86 | 2.26 | 1.93 | 2.76 |
| | Average nonzero volume [$m^3$] | 0.32 | 0.39 | 0.37 | 0.50 | 0.47 | 0.39 |
| | Number of nonzero volumes | 168 | 122 | 122 | 57 | 84 | 553 |
| | Percent of nonzero volumes | 9.3% | 8.1% | 8.1% | 3.8% | 5.6% | 7.1% |
| R3 | Maximum [$m^3$] | 4.91 | 6.23 | 2.62 | 1.47 | 1.49 | 6.23 |
| | Average nonzero volume [$m^3$] | 0.53 | 0.39 | 0.28 | 0.30 | 0.28 | 0.38 |
| | Number of nonzero volumes | 156 | 113 | 118 | 45 | 72 | 504 |
| | Percent of nonzero volumes | 8.7% | 7.5% | 7.9% | 3.0% | 4.8% | 6.5% |
| R1, R2, R3 Pooled | Maximum [$m^3$] | 4.91 | 8.29 | 7.97 | 2.26 | 1.93 | 8.29 |
| | Average nonzero volume [$m^3$] | 0.40 | 0.44 | 0.38 | 0.37 | 0.38 | 0.40 |
| | Number of nonzero volumes | 466 | 352 | 351 | 161 | 233 | 1563 |
| | Percent of nonzero volumes | 8.6% | 7.8% | 7.8% | 3.6% | 5.2% | 6.7% |

NOTES: The notation Rr stands for Replicate *r*. Summary results for the updated PABC-2009 (Revision 1) and the migrated PABC-2009 (Revision 0) are provided in file *CUTTINGS_PABC09.xlsx*, which is stored in the CVS repository at /nfs/data/CVSLIB/WIPP_ANALYSES/PABC09/CUTTINGS_S/Auxiliary. The VMS PABC-2009 results using DRSPALL Version 1.10 are provided by Ismail (2010).

using spallings output from DRSPALL Version 1.22, DRSPALL Version 1.21, and DRSPALL Version 1.10. The VMS PABC-2009 results (using DRSPALL Version 1.10 output) reported in Table 6-11 are provided by Ismail (2010). As seen in Table 6-11, values obtained using the DRSPALL Version 1.22 output are similar for many of the scenarios when compared to those obtained using DRSPALL Version 1.10. In replicate 1, the updated PABC-2009 using DRSPALL Version 1.22 output result in higher maximum spallings volumes, average spallings volumes, and number of nonzero spallings for all five scenarios. In replicate 2, the updated PABC-2009 produces slightly higher maximum for scenarios S1-DBR, S3-DBR, and S5-DBR, while average spallings volumes generally are slightly lower than the VMS PABC-2009 data. In replicate 3, the updated PABC-2009 produces higher maximum spallings volumes for scenarios S3-DBR, S4-DBR, and S5-DBR, with slightly higher average spallings volumes across all five scenarios compared to the VMS PABC-2009 data. For the updated PABC-2009 (using DRSPALL Version 1.22), there is a higher percentage of vectors resulting in nonzero spallings volumes for all replicates and scenarios compared to both the VMS PABC 2009 (using DRSPALL Version 1.10) and the migrated PABC-2009 (using DRSPALL Version 1.21).

The cumulative frequency of occurrence of spallings volumes (for replicates 1, 2, and 3 combined) for PABC-2009 is shown in Figure 6-20. This figure provides a summary of spallings data from all scenarios, repository regions, and times. Figure 6-20 shows that the cumulative distributions of spallings volumes are essentially identical for the VMS PABC-2009 (using DRSPALL Version 1.10) and the migrated PABC-2009 (run on Solaris using DRSPALL Version 1.21). Figure 6-20a considers only those simulations in which spallings occur. The cumulative distribution of spallings volumes from the updated PABC-2009 (run on Solaris using DRSPALL Version 1.22) is similar to the VMS and migrated PABC-2009. Figure 6-20b is the same plot except that all spallings results are used, including those simulations where no spallings occur. In this case the cumulative distribution of spallings volumes from the updated results is quite different than those from the VMS and migrated PABC-2009 results. The shift in the cumulative frequency of occurrence curve for the updated PABC-2009 spallings volumes (Figure 6-20b) is the result of more simulations with nonzero spallings.

### 6.1.3.2. CRA-2014 Spallings Volumes

Using the spallings volumes calculated by DRSPALL for the updated PABC-2009 and the repository pressures calculated by BRAGFLO, the impact of DRSPALL Version 1.22 output on repository spallings volumes for CRA-2014 can be determined. Summary statistics of spallings volumes for the intrusion scenarios considered by CUTTINGS_S are shown in Table 6-12 for the CRA-2014 using spallings output from DRSPALL Version 1.22, DRSPALL Version 1.21, and DRSPALL Version 1.10.

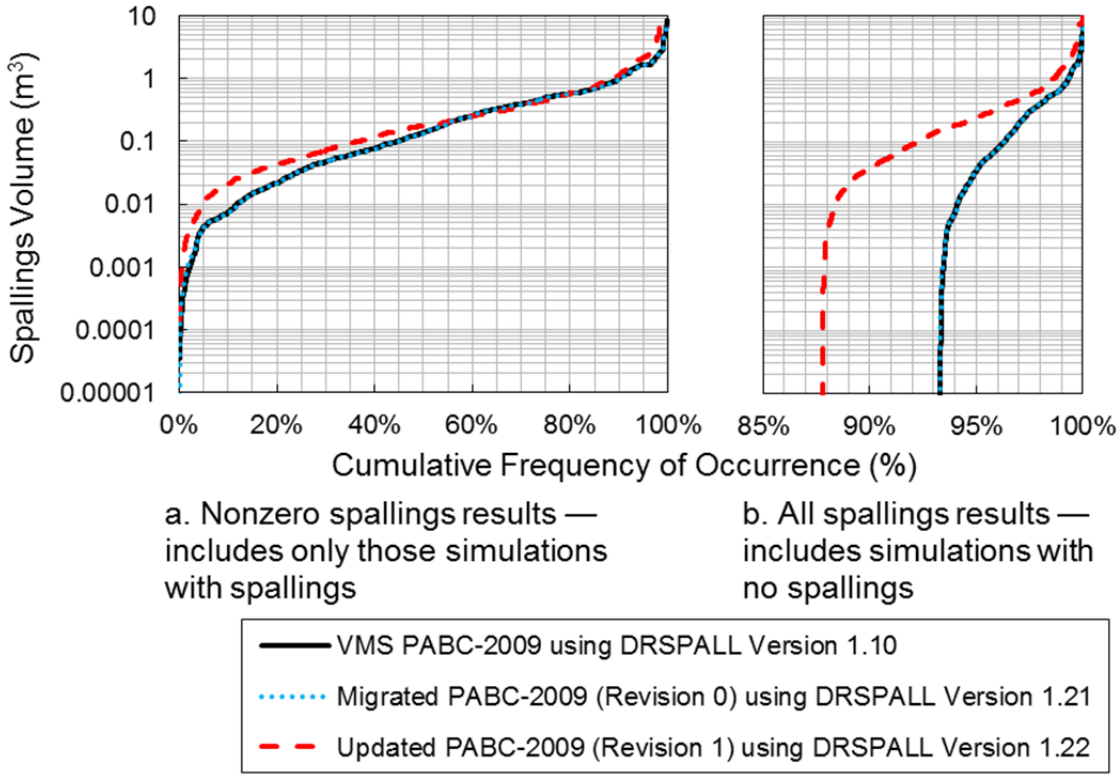


**Figure 6-20. Cumulative Distributions of Spallings Volumes in the PABC-2009 for Pooled Vectors (Replicates 1, 2, and 3 Combined).**

**Table 6-12. Summary of CRA-2014 Spallings Volumes by Scenario.**

| | | Scenarios | | | | | Total |
|---|---|---|---|---|---|---|---|
| | | S1-DBR | S2-DBR | S3-DBR | S4-DBR | S5-DBR | |
| **Updated CRA-2014 (Revision 1) Using Modified DRSPALL Version 1.22** | | | | | | | |
| **R1** | **Maximum [$m^3$]** | 7.47 | 9.84 | 9.80 | 7.47 | 7.47 | 9.84 |
| | **Average nonzero volume [$m^3$]** | 1.05 | 0.78 | 0.90 | 0.98 | 1.09 | 0.90 |
| | **Number of nonzero volumes** | 69 | 161 | 114 | 31 | 38 | 413 |
| | **Percent of nonzero volumes** | 3.8% | 10.7% | 7.6% | 2.1% | 2.5% | 5.3% |
| **R2** | **Maximum [$m^3$]** | 2.02 | 4.18 | 1.90 | 1.79 | 1.79 | 4.18 |
| | **Average nonzero volume [$m^3$]** | 0.28 | 0.32 | 0.28 | 0.32 | 0.31 | 0.30 |
| | **Number of nonzero volumes** | 77 | 168 | 116 | 34 | 43 | 438 |
| | **Percent of nonzero volumes** | 4.3% | 11.2% | 7.7% | 2.3% | 2.9% | 5.6% |
| **R3** | **Maximum [$m^3$]** | 4.73 | 5.26 | 5.04 | 2.93 | 2.71 | 5.26 |
| | **Average nonzero volume [$m^3$]** | 0.59 | 0.53 | 0.43 | 0.57 | 0.44 | 0.50 |
| | **Number of nonzero volumes** | 54 | 144 | 99 | 21 | 28 | 346 |
| | **Percent of nonzero volumes** | 3.0% | 9.6% | 6.6% | 1.4% | 1.9% | 4.4% |
| **R1, R2, R3 Pooled** | **Maximum [$m^3$]** | 7.47 | 9.84 | 9.80 | 7.47 | 7.47 | 9.84 |
| | **Average nonzero volume [$m^3$]** | 0.63 | 0.54 | 0.54 | 0.62 | 0.61 | 0.57 |
| | **Number of nonzero volumes** | 200 | 473 | 329 | 86 | 109 | 1197 |
| | **Percent of nonzero volumes** | 3.7% | 10.5% | 7.3% | 1.9% | 2.4% | 5.1% |
| **Migrated CRA-2014 (Revision 0) Using DRSPALL Version 1.21** | | | | | | | |
| **R1** | **Maximum [$m^3$]** | 1.67 | 8.89 | 8.08 | 1.67 | 1.67 | 8.89 |
| | **Average nonzero volume [$m^3$]** | 0.41 | 0.54 | 0.65 | 0.42 | 0.41 | 0.52 |
| | **Number of nonzero volumes** | 41 | 95 | 60 | 16 | 23 | 235 |
| | **Percent of nonzero volumes** | 2.3% | 6.3% | 4.0% | 1.1% | 1.5% | 3.0% |
| **R2** | **Maximum [$m^3$]** | 1.24 | 2.76 | 1.97 | 0.64 | 0.65 | 2.76 |
| | **Average nonzero volume [$m^3$]** | 0.28 | 0.30 | 0.23 | 0.22 | 0.25 | 0.27 |
| | **Number of nonzero volumes** | 41 | 100 | 64 | 23 | 26 | 254 |
| | **Percent of nonzero volumes** | 2.3% | 6.7% | 4.3% | 1.5% | 1.7% | 3.3% |
| **R3** | **Maximum [$m^3$]** | 0.96 | 6.13 | 4.87 | 0.49 | 0.43 | 6.13 |
| | **Average nonzero volume [$m^3$]** | 0.25 | 0.41 | 0.44 | 0.17 | 0.16 | 0.35 |
| | **Number of nonzero volumes** | 30 | 86 | 46 | 16 | 17 | 195 |
| | **Percent of nonzero volumes** | 1.7% | 5.7% | 3.1% | 1.1% | 1.1% | 2.5% |
| **R1, R2, R3 Pooled** | **Maximum [$m^3$]** | 1.67 | 8.89 | 8.08 | 1.67 | 1.67 | 8.89 |
| | **Average nonzero volume [$m^3$]** | 0.32 | 0.41 | 0.44 | 0.26 | 0.28 | 0.38 |
| | **Number of nonzero volumes** | 112 | 281 | 170 | 55 | 66 | 684 |
| | **Percent of nonzero volumes** | 2.1% | 6.2% | 3.8% | 1.2% | 1.5% | 2.9% |

**Table 6-12. Summary of CRA-2014 Spallings Volumes by Scenario. (Continued)**

| | | Scenarios | | | | | Total |
|---|---|---|---|---|---|---|---|
| | | S1-DBR | S2-DBR | S3-DBR | S4-DBR | S5-DBR | |
| VMS CRA-2014 Using DRSPALL Version 1.10 | | | | | | | |
| R1 | Maximum [$m^3$] | 1.67 | 9.69 | 9.13 | 1.67 | 1.67 | 9.69 |
| | Average nonzero volume [$m^3$] | 0.41 | 0.58 | 0.70 | 0.42 | 0.41 | 0.55 |
| | Number of nonzero volumes | 41 | 95 | 60 | 16 | 23 | 235 |
| | Percent of nonzero volumes | 2.3% | 6.3% | 4.0% | 1.1% | 1.5% | 3.0% |
| R2 | Maximum [$m^3$] | 1.23 | 2.76 | 1.96 | 0.64 | 0.64 | 2.76 |
| | Average nonzero volume [$m^3$] | 0.28 | 0.31 | 0.23 | 0.22 | 0.25 | 0.27 |
| | Number of nonzero volumes | 41 | 98 | 64 | 23 | 26 | 252 |
| | Percent of nonzero volumes | 2.3% | 6.5% | 4.3% | 1.5% | 1.7% | 3.2% |
| R3 | Maximum [$m^3$] | 0.96 | 6.14 | 4.91 | 0.48 | 0.43 | 6.14 |
| | Average nonzero volume [$m^3$] | 0.25 | 0.41 | 0.44 | 0.17 | 0.16 | 0.35 |
| | Number of nonzero volumes | 30 | 85 | 46 | 16 | 17 | 194 |
| | Percent of nonzero volumes | 1.7% | 5.7% | 3.1% | 1.1% | 1.1% | 2.5% |
| R1, R2, R3 Pooled | Maximum [$m^3$] | 1.67 | 9.69 | 9.13 | 1.67 | 1.67 | 9.69 |
| | Average nonzero volume [$m^3$] | 0.32 | 0.43 | 0.45 | 0.26 | 0.28 | 0.39 |
| | Number of nonzero volumes | 112 | 278 | 170 | 55 | 66 | 681 |
| | Percent of nonzero volumes | 2.1% | 6.2% | 3.8% | 1.2% | 1.5% | 2.9% |

NOTES: The notation Rr stands for Replicate *r*. Summary results for the updated CRA-2014 (Revision 1) and the migrated CRA-2014 (Revision 0) are provided in file *CUTTINGS_CRA14.xlsx*, which is stored in the CVS repository at /nfs/data/CVSLIB/WIPP_ANALYSES/CRA14/CUTTINGS_S/Auxiliary. The VMS CRA-2014 results using DRSPALL Version 1.10 are provided by Kicker (2013).

There are four cases for CRA-2014, which are denoted CRA14BL, CRA14BV, CRA14TP, and CRA14-0 (Camphouse 2013a). Case CRA14-0 includes all changes from cases CRA14BL, CRA14BV, and CRA14TP, as well as refinements to the steel corrosion rate and a water balance that includes MgO hydration. Case CRA14-0 represents the new baseline for CRA-2014 and is the only case evaluated in this impact assessment.

The VMS CRA-2014 results (using DRSPALL Version 1.10 output) reported in Table 6-12 are provided by Kicker (2013). As seen in Table 6-12, values obtained using DRSPALL Version 1.22 output are similar for many of the scenarios when compared to those obtained using DRSPALL Version 1.10. In replicates 1 and 3, the updated CRA-2014 using DRSPALL Version 1.22 output results in higher maximum spallings volumes, average spallings volumes, and number of nonzero spallings for all five scenarios. In replicate 2, the updated CRA-2014 generally produces higher maximum spallings volumes for all scenarios, while average spallings volumes are similar. For the updated CRA 2014 (using DRSPALL Version 1.22), there is a higher percentage of vectors resulting in nonzero spallings volumes for all replicates and scenarios compared to both the VMS CRA-2014 (using DRSPALL Version 1.10) and the migrated CRA-2014 (using DRSPALL Version 1.21).

The cumulative frequency of spallings volumes for CRA-2014 (replicates 1, 2, and 3), is shown in Figure 6-21. This figure provides a summary of spallings data from all scenarios, repository regions, and times. Figure 6-21a considers only those simulations in which spallings occur. The cumulative distribution of spallings volumes from the updated CRA-2014 (run on Solaris using DRSPALL Version 1.22) is similar to the VMS and migrated CRA-2014. Figure 6-21b is the same plot except that all spallings results are used, including those simulations where no spallings occur. Again, as was the case for the PABC-2009 spallings volumes, the cumulative distribution of spallings volumes from the updated results is quite different than those from the VMS and migrated CRA-2014 results. The shift in the cumulative frequency of occurrence curve for the updated CRA-2014 spallings volumes (Figure 6-21b) is the result of more simulations with nonzero spallings.

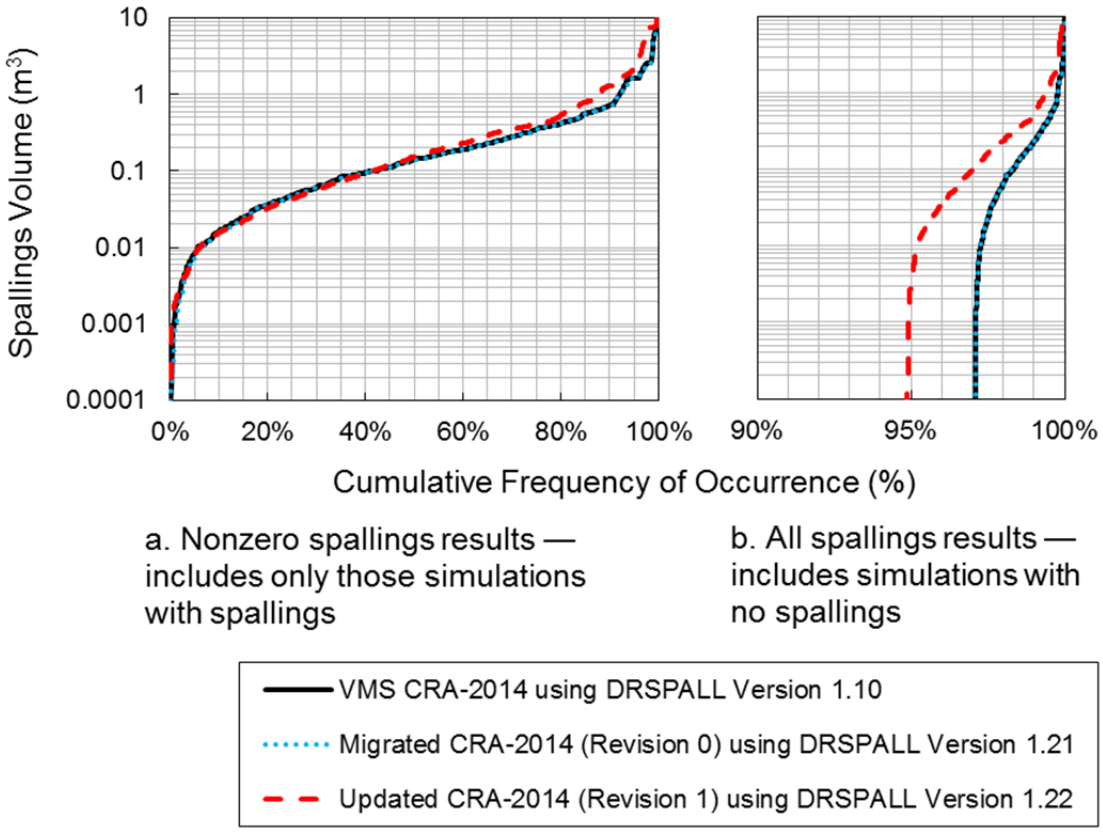


**Figure 6-21. Cumulative Distributons of Spallings Volumes in the CRA-2014 for Pooled Vectors (Replicates 1, 2, and 3 Combined).**

## 6.2. Normalized Radionuclide Releases

The impact of the changes in spallings volumes on the overall mean CCDF for normalized spallings releases obtained in the updated PABC-2009 developed using DRSPALL Version 1.22 output can be seen in Figure 6-22 for pooled vectors (replicates 1, 2, and 3 combined). As seen in that figure, the CCDF of spallings releases obtained in the updated PABC-2009 is higher

compared to both the VMS PABC-2009 (using DRSPALL Version 1.10) and the migrated PABC-2009 (using DRSPALL Version 1.21). The differences in spallings volumes and in the number of vectors that result in a nonzero spallings volume for the updated PABC-2009 correspond to an increase in spallings releases as all analyses use the same waste inventory.

The impact of the changes in spallings volumes on the overall mean CCDF for normalized spallings releases obtained in the updated CRA-2014 developed using DRSPALL Version 1.22 output can be seen in Figure 6-23 for pooled vectors (replicates 1, 2, and 3 combined). As seen in this figure, the CCDF of spallings releases obtained in the updated CRA-2014 is higher compared to both the VMS CRA-2014 (using DRSPALL Version 1.10) and the migrated CRA-2014 (using DRSPALL Version 1.21). The differences in spallings volumes and in the number of vectors that result in a nonzero spallings volume for the updated CRA-2014 correspond to an increase in spallings releases as all analyses use the same waste inventory.

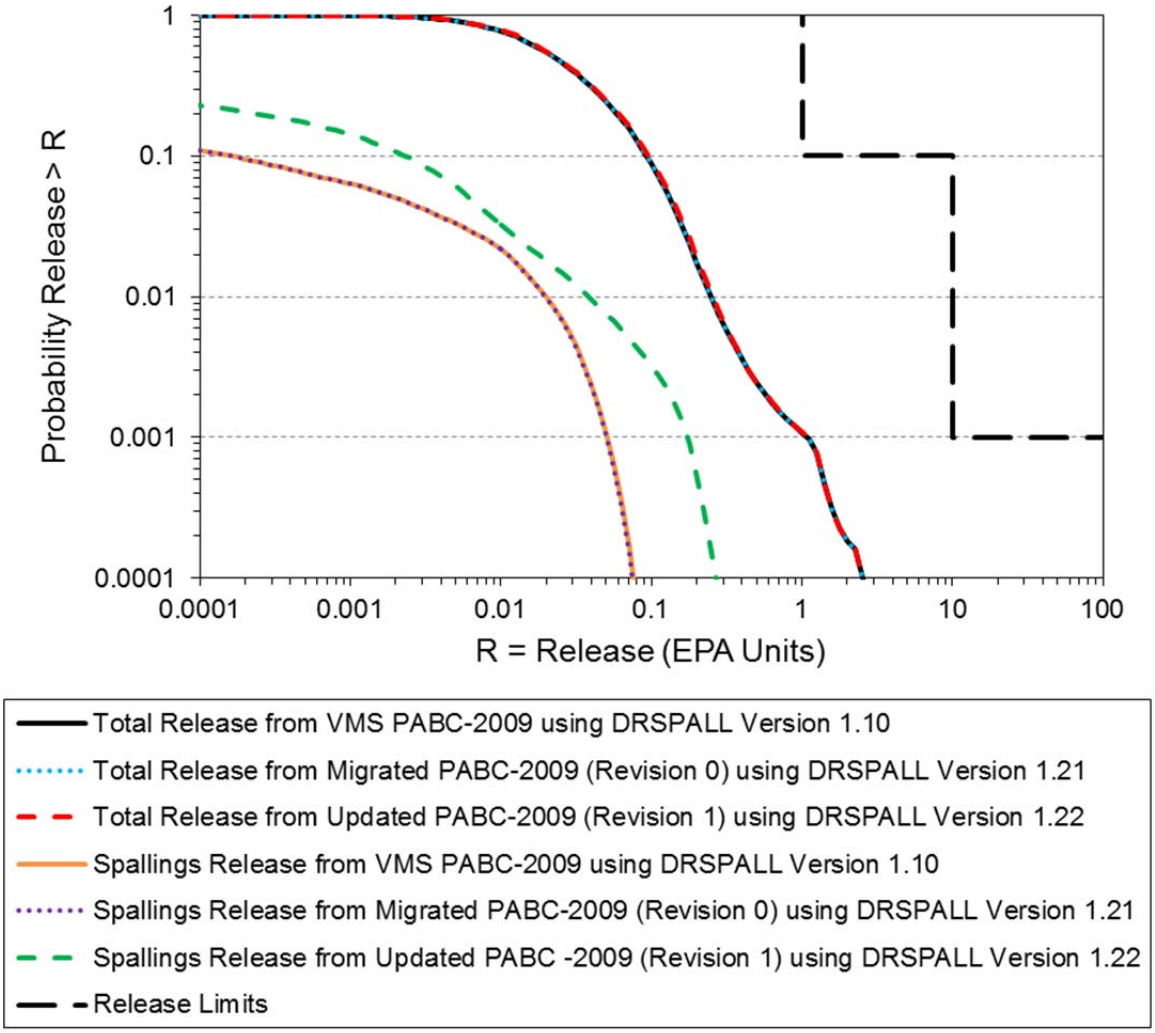


**Figure 6-22. Impact of DRSPALL Version 1.22 Output on the PABC-2009 Overall Mean CCDFs for Normalized Radionuclide Releases for Pooled Vectors.**

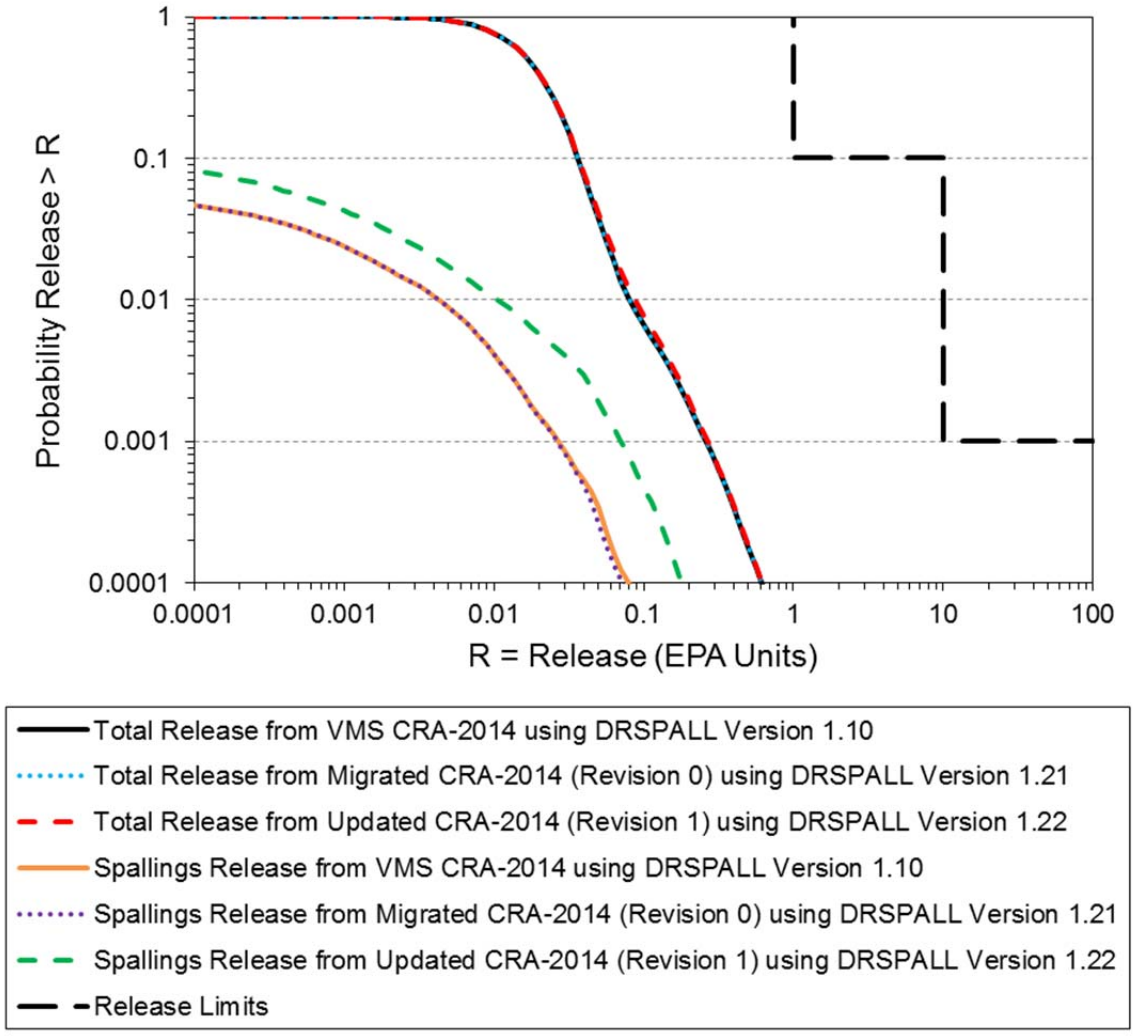


**Figure 6-23. Impact of DRSPALL Version 1.22 Output on the CRA-2014 Overall Mean CCDFs for Normalized Radionuclide Releases for Pooled Vectors.**

Total normalized releases using DRSPALL Version 1.22 output are also presented in Figures 6-22 and 6-23 for the PABC-2009 and CRA-2014, respectively for pooled vectors. Total releases are calculated by forming the summation of releases across each potential release pathway, namely cuttings and cavings releases, spallings releases, direct brine releases, and Culebra transport releases.

Both the VMS PABC-2009 and VMS CRA-2014 PAs have shown that spallings releases are a much less significant contributor to the total releases compared to the other potential release pathways (Clayton et al. 2010, Section 6.5; Camphouse et al. 2013, Section 6.9.5). Because spallings releases are not a primary contributor to the total releases, the updated PA (using DRSPALL Version 1.22), the migrated PA (using DRSPALL Version 1.21), and the VMS PA (using DRSPALL Version 1.10) overall mean CCDFs for total releases are virtually identical (Figures 6-22 and 6-23).

*This page is intentionally left blank.*

# 7. SUMMARY AND CONCLUSIONS

In response to SPR 13-001 (WIPP PA 2013a), modifications were implemented in DRSPALL Version 1.22 to correct finite difference equations contained in the source code file *wasteflowcalc.f90*. The errors identified in DRSPALL have been resolved, and SPR 13-001 has been closed (WIPP PA 2015d). Based on the assessment presented in this document, there is no impact to WIPP PA total radionuclide release calculations resulting from the modification to DRSPALL. Updated DRSPALL output is listed in Appendix C, which provides spallings data input for future PA calculations. The corresponding spallings data files are located in the CVS repository at /nfs/data/CVSLIB/WIPP_ANALYSES/PABC09/DRSPALL/Output.

The primary modifications to DRSPALL include:

- Forchterm

  The 'Forchterm' was corrected in three sections of the code as identified in SPR 13-001. In addition to the error identified in SPR 13-001, it was found that the derivation of the constant zone size equations were also incorrect. The derivation of Equation 4.6.1 in the design document (WIPP PA 2004a) was incorrect because $k'$ was treated as a constant in the denominator, despite it being a variable in the numerator.

  In correcting the calculation of 'Forchterm', the indexing of the second permeability() term was also corrected to be 'i-1' instead of 'i'. The coefficients for the last cell (i=numReposZones) have changed: aa(i) has been changed from '-alpha1' to '-alpha1-alpha2' and bb(i) has been changed from '1.0+alpha1' to '1.0+alpha1+alpha2'.

- Constant zone size

  Previously, a variable zone size implementation was described based on the DRSPALL design document (WIPP PA 2004a, Section 4.6; WIPP PA 2013b). However, this was done incorrectly, as a simple substitution of variable zone sizes into the equation derived for a constant zone size is not valid. The derivation of an equation similar to design document Equation 4.6.2 for a variable zone size would require a complete re-derivation, which was determined unnecessary because current computing resources allow for reasonably fast computational times even for a greater number of zones. It was decided to run DRSPALL exclusively with a constant zone size. The following zone size parameters have been selected as the standard configuration for DRSPALL calculations:
  - Repository zone size, $\Delta r = 0.004$ m
  - Characteristic length, $L_t = 0.04$ m
  - Wellbore zone size, $\Delta z = 2.0$ m.

- Boundary conditions

  The index of the "first cell coefficients" (i) has been changed from 'firstIntactZone' to 'firstIntactZone+1', since any values for the boundary ('firstIntactZone') would be constant and fixed by the specified pressure (Dirichlet) boundary condition in the cavity. That is, the boundary nodes are not included in the coefficient matrix, so there should be no aa(i), bb(i), cc(i) coefficients for 'firstIntactZone'. The effect of the

boundary node (firstIntactZone) is included in the b-vector of the linear system of equations. Consequently, the indexing for the "interior cell coefficients" now begins at 'firstIntactZone+2' instead of 'firstIntactZone+1'. Also, as a consequence of this, the indexing of the matrix inversion has changed. The boundary pressure is now assigned to 'reposPres(firstIntactZone)' instead of 'reposPres(0)'. Because of that, 'exitPoreVelocity' is now calculated using a centered-difference approximation, which leads to 'reposPres(firstIntactZone+1)' being used instead of 'reposPres(firstIntactZone)'.

Previously, the permeability of the 'firstIntactZone-1' zone was set to the value of the 'firstIntactZone'. This was changed because the permeability of the 'firstIntactZone-1' is no longer used. Also, where previously the array element 'psi(firstIntactZone-1)' was calculated from the gas viscosity and boundary pressure, this assignment has been made applicable to 'psi(firstIntactZone)', since the 'firstIntactZone' is the boundary.

- Fluidization limit

  Unrealistic values of 'fractionFluidized' could be calculated in the source code file *wellborecalc.f90*. Previously, 'fractionFluidized(i)' was set to 1.0 only if 'i' was for the 'firstIntactZone'. Otherwise, the 'fractionFluidized' could increase to values much higher than 1.0, which are not physically reasonable, and led to problems in calculating 'permeability' in *wasteflowcalc.f90*. An 'elseif' statement was added to set 'fractionFluidized(i)' to a number slightly larger than 1.0, such that the 'if' statement will be satisfied for zone 'i' in a later step.

Verification and validation testing has been completed for the modified DRSPALL code (Version 1.22). The porous flow and wellbore flow tests (Test Case #1 and Test Case #5, respectively) verified that the two major flow models in DRSPALL are operating properly by successfully comparing output from DRSPALL and alternative computational tools for well-defined test problems. Moreover, the internal logic checks test problem (Test Case #4) verified that selected sub-models such as stress/failure and fluidization are also operating correctly by comparison to spreadsheet calculations. Finally, the coalbed methane test problem (Test Case #2) demonstrated that DRSPALL reasonably simulates the coalbed methane cavitation process within the ranges of uncertainties of known data and values of parameters. Taken as a whole, these tests give sufficient assurance that the model is operating within design requirements that it may be considered qualified for use in WIPP compliance calculations according to NP 19-1 (Long 2014) standards.

The modifications to DRSPALL (Version 1.22) resulted in an increase in spallings volumes. The cumulative distributions of spallings volumes at repository pressures of 12.0, 14.0, and 14.8 MPa show higher spallings volumes compared to both the VMS DRSPALL (Version 1.10) and migrated DRSPALL (Version 1.21) (Figures 6-4, 6-8, and 6-12).

When considering only those simulations in which spallings occur, the cumulative distributions of spallings volumes from the updated PAs (run on Solaris using DRSPALL Version 1.22) are similar to the VMS and migrated PAs (Figures 6-20a and 6-21a). Figures 6-20b and 6-21b show the same plots except that all spallings results are used, including those simulations where no

spallings occur. In these cases, the cumulative distributions of spallings volumes from the updated results are quite different than those from the VMS and migrated PA results. The differences arise because the updated analyses yield more simulations with nonzero spallings.

The CCDF of spallings releases obtained in the PABC-2009 was updated using DRSPALL Version 1.22 output. Compared to both the VMS PABC-2009 (using DRSPALL Version 1.10) and the migrated PABC-2009 (using DRSPALL Version 1.21), there was an increase in the number of vectors that result in a nonzero spallings volume, which generally translates to an increase in spallings releases (Figure 6-22). The CCDF of spallings releases obtained in the CRA-2014 was also updated using DRSPALL Version 1.22 output. Similar to the PABC-2009, the update to CRA-2014 resulted in an increase in the number of vectors that result in a nonzero spallings volume, along with a corresponding increase in spallings releases (Figure 6-23).

Total normalized releases using DRSPALL Version 1.22 output were calculated for both the PABC-2009 and CRA-2014. The updated PA (using DRSPALL Version 1.22), the migrated PA (using DRSPALL Version 1.21), and the VMS PA (using DRSPALL Version 1.10) overall mean CCDFs for total releases are almost identical (Figures 6-22 and 6-23). Although spallings releases increased as a result of the modification to DRSPALL, spallings releases are not a primary contributor to the total releases, and the updated PA calculations of overall mean CCDFs for total releases are virtually unchanged. Therefore, the corrections to the spallings volume calculation (implemented in DRSPALL Version 1.22) did not impact WIPP PA calculation results.

*This page is intentionally left blank.*

# 8. REFERENCES


Camphouse, C. 2013a. *Analysis Plan for the 2014 Compliance Recertification Application Performance Assessment*. AP-164. Carlsbad, NM: Sandia National Laboratories. ERMS 559198.

Camphouse, R.C. 2013b. *Analysis Package for Salado Flow Modeling Done in the 2014 Compliance Recertification Application Performance Assessment (CRA-2014 PA)*. Carlsbad, NM: Sandia National Laboratories. ERMS 559980.

Camphouse, R.C., D.C. Kicker, S. Kim, T.B. Kirchner, J.J. Long, B. Malama, and T.R. Zeitler 2013. *Summary Report for the 2014 WIPP Compliance Recertification Application Performance Assessment*. Carlsbad, NM: Sandia National Laboratories. ERMS 560252.

Chan, D.Y.C., B.D. Hughes, and L. Paterson 1993. "Transient Gas Flow Around Boreholes," *Transport in Porous Media*. 10:137-152.

Clayton, D.J., R.C. Camphouse, J.W. Garner, A.E. Ismail, T.B. Kirchner, K.L. Kuhlman, and M.B. Nemer. 2010. *Summary Report of the CRA-2009 Performance Assessment Baseline Calculation*. Carlsbad, NM: Sandia National Laboratories. ERMS 553039.

Djordjevic, S. and M. Adams 2003. Memo to David Lord Re: Utility Code for Spallings Model Porous Flow Validation. June 5, 2003. Albuquerque, NM: Sandia National Laboratories. ERMS 524400.

EPA (U.S. Environmental Protection Agency) 1996. 40 CFR Part 194: Criteria for the Certification and Recertification of the Waste Isolation Pilot Plant's Compliance with the 40 CFR Part 191 Disposal Regulations; Final Rule. Federal Register, Vol. 61, 5223-5245.

EPA 2010. 40 CFR Part 194 Criteria for the Certification and Recertification of the Waste Isolation Pilot Plant's Compliance with the Disposal Regulations: Recertification Decision, Federal Register No. 222, Vol. 75, pp. 70584-70595, November 18, 2010.

Ergun, S. 1952. "Fluid Flow Through Packed Columns," *Chemical Engineering Progress*. 48:89-94.

FLUENT 2003. *FLUENT 6.1 User's Guide*. Lebanon, NH: Fluent, Inc. February 2003.

Hansen, F.D., T.W. Pfeifle, and D.L. Lord 2003. *Parameter Justification Report for DRSPALL*. SAND2003-2930. Carlsbad, NM: Sandia National Laboratories. ERMS 531057.

Ismail, A.E. 2010. *Analysis Package for Cuttings, Cavings, and Spallings: CRA-2009 Performance Assessment Baseline Calculation*. Carlsbad, NM: Sandia National Laboratories. ERMS 552893.

Khodaverdian, M.F., J.D. McLennan, I.D. Palmer, H.H. Vaziri, and X. Wang 1996. "Cavity Completions for Enhanced Coalbed Methane Recovery." GRI-95/0432, report by Terra Tek, Inc. to the Gas Research Institute, June 1996.

Kicker, D.C. 2013. *Analysis Package for Cuttings, Cavings, and Spallings: 2014 Compliance Recertification Application Performance Assessment (CRA-2014 PA)*, Revision 0. Carlsbad, NM: Sandia National Laboratories. ERMS 560060.

Kicker, D.C. 2015. *DRSPALL Zone Size Sensitivity Study*, Revision 0. Carlsbad, NM: Sandia National Laboratories. ERMS 564427.

Kicker, D.C. and C.G. Herrick 2013. *Parameter Summary Report for the 2014 Compliance Recertification Application*. Carlsbad, NM: Sandia National Laboratories. ERMS 560298.

Kicker, D.C., C.G. Herrick, and T.R. Zeitler 2015. *Impact of the DRSPALL Modification on Waste Isolation Pilot Plant Performance Assessment Calculations*, Revision 0. Carlsbad, NM: Sandia National Laboratories. ERMS 564863.

Kirchner, T.B. 2010. *Generation of the LHS Samples for the AP-145 (PABC09) PA Calculations*. Carlsbad, NM: Sandia National Laboratories. ERMS 552905.

Kirchner, T.B. 2013. *Generation of the LHS Samples for the CRA-2014 (AP-164) Revision 0 PA Calculations*. Carlsbad, NM: Sandia National Laboratories. ERMS 559950.

Kirchner, T., A. Gilkey, and J. Long 2013. *Summary Report on the Migration of the WIPP PA Codes from VMS to Solaris, AP-162*. Carlsbad, NM: Sandia National Laboratories. ERMS 561457.

Kirchner, T., A. Gilkey, and J. Long 2015. *Addendum to the Summary Report on the Migration of the WIPP PA Codes from VMS to Solaris, AP-162*. Carlsbad, NM: Sandia National Laboratories. ERMS 564675.

Long, J. J. 2014. Nuclear Waste Management Procedure NP 19-1 Software Requirements, Revision 16. Carlsbad, NM: Sandia National Laboratories. ERMS 562870.

Lord, D., D. Rudeen, and C. Hansen 2003. *Analysis Package for DRSPALL: Compliance Recertification Application, Part I – Calculation of Spall Volumes*. Carlsbad, NM: Sandia National Laboratories. ERMS 532766.

Lord, D.L., D.K. Rudeen, J.F. Schatz, A.P. Gilkey, and C.W. Hansen 2006. *DRSPALL: Spallings Model for the Waste Isolation Pilot Plant 2004 Recertification*. SAND2004-0730. Albuquerque, NM: Sandia National Laboratories.

Özişik, M.N. 1993. *Heat Conduction*. Second Edition. New York, NY: John Wiley & Sons.

Vugrin, E. 2005. *Analysis Package for DRSPALL, CRA-2004 Performance Assessment Baseline Calculation*. Carlsbad, NM: Sandia National Laboratories. ERMS 540415.

WIPP PA (Waste Isolation Pilot Plant Performance Assessment) 1996. *User's Manual for GROPECDB Version 2.12*. Albuquerque, NM: Sandia National Laboratories. ERMS 237496.

WIPP PA 2003a. *Requirements Document for DRSPALL Version 1.00* (document version 1.20). Carlsbad, NM: Sandia National Laboratories. ERMS 531278.

WIPP PA 2003b. *Verification and Validation Plan / Validation Document for DRSPALL Version 1.00*. Carlsbad, NM: Sandia National Laboratories. ERMS 524782.

WIPP PA 2004a. *Design Document for DRSPALL Version 1.10*. Carlsbad, NM: Sandia National Laboratories. ERMS 533149.

WIPP PA 2004b. *User's Manual for DRSPALL Version 1.10*. Carlsbad, NM: Sandia National Laboratories. ERMS 533151.

WIPP PA 2004c. *Design Document for CUTTINGS_S (Version 6.00)*. Carlsbad, NM: Sandia National Laboratories. ERMS 537038.

WIPP PA 2005. *User's Manual for SUMMARIZE Version 3.00*. Albuquerque, NM: Sandia National Laboratories. ERMS 540110.

WIPP PA 2012a. *Addendum to User's Manual for GROPECDB Version 2.13*. Carlsbad, NM: Sandia National Laboratories. ERMS 557792.

WIPP PA 2012b. *Addendum to User's Manual for SUMMARIZE Version 3.02*. Carlsbad, NM: Sandia National Laboratories. ERMS 557813.

WIPP PA 2013a. *Software Problem Report (SPR) 13-001 for DRSPALL Versions 1.10 and 1.21*. Carlsbad, NM: Sandia National Laboratories. ERMS 561524.

WIPP PA 2013b. *Addendum to Design Document (ERMS# 533149) for DRSPALL Version 1.21*. Carlsbad, NM: Sandia National Laboratories. ERMS 560045.

WIPP PA 2013c. *Addendum to User's Manual for DRSPALL Version 1.21*. Carlsbad, NM: Sandia National Laboratories. ERMS 560048.

WIPP PA 2015a. *Design Document for DRSPALL Version 1.22*. Carlsbad, NM: Sandia National Laboratories. ERMS 562640.

WIPP PA 2015b. *Addendum to User's Manual for DRSPALL Version 1.22*. Carlsbad, NM Sandia National Laboratories. ERMS 562642.

WIPP PA 2015c. *Verification and Validation Plan / Validation Document for DRSPALL Version 1.22*. Carlsbad, NM: Sandia National Laboratories. ERMS 562643.

WIPP PA 2015d. *Software Problem Closure Report (SPCR) 13-001 for DRSPALL Versions 1.10 and 1.21*. Carlsbad, NM: Sandia National Laboratories. ERMS 564912.

*This page is intentionally left blank.*

# APPENDIX A. FINITE DIFFERENCE SOLUTION TO DRSPALL WASTE FLOW EQUATION

The derivation provided in this appendix follows that given in the DRSPALL design document (WIPP PA 2015a, Section 4.6). Throughout this appendix, reference is made to both the DRSPALL design document and the related Sandia Report SAND2004-0730 (Lord et al. 2006). The nomenclature for the equations presented in this appendix is provided in Table A-1.

**Table A-1. Nomenclature for Equations in Appendix A.**

| Symbol | Definitions | Units |
|---|---|---|
| $j$, $N$ | Zone indices | — |
| $k'$ | Velocity-dependent permeability | $m^2$ |
| $m$ | Geometry exponent ($m$=2 for cylindrical, $m$=3 for spherical) | — |
| $p$ | Pressure in gas | Pa |
| $r$ | Radius | m |
| $t$ | Time | s |
| $n$ | Timestep index | — |
| $\eta$ | Viscosity of gas | Pa·s |
| $\phi$ | Current repository porosity | — |
| $\psi$ | Pseudopressure | Pa/s |

## A-1. Governing Equation Simplification

Start with DRSPALL design document Equation 4.3.10 (WIPP PA 2015a). This equation is not given in the Sandia Report (Lord et al. 2006).

$$\frac{\partial \psi}{\partial t} = \frac{D(\psi)}{r^{m-1}} \frac{\partial}{\partial r}\left( r^{m-1} \frac{\partial \psi}{\partial r} \right) + \frac{D(\psi)}{k'} \frac{\partial k'}{\partial r} \frac{\partial \psi}{\partial r} \tag{A-1}$$

where

$$D(\psi) = \frac{k'}{\phi} \sqrt{\frac{\psi}{\eta}} = \frac{k'p}{\phi \eta}$$

Note that

$$\frac{\partial \ln k'}{\partial r} = \frac{1}{k'} \frac{\partial k'}{\partial r} \tag{A-2}$$

Substituting Equation A-2 into Equation A-1 yields:

$$\frac{\partial \psi}{\partial t} = \frac{D(\psi)}{r^{m-1}} \frac{\partial}{\partial r}\left( r^{m-1} \frac{\partial \psi}{\partial r} \right) + D(\psi) \frac{\partial \ln(k')}{\partial r} \frac{\partial \psi}{\partial r} \tag{A-3}$$

Expand first term on right-hand side of Equation A-3:

$$\begin{aligned} \frac{D(\psi)}{r^{m-1}} \frac{\partial}{\partial r}\left( r^{m-1} \frac{\partial \psi}{\partial r} \right) &= D(\psi)\left[ \frac{1}{r^{m-1}} \frac{\partial}{\partial r}\left( r^{m-1} \frac{\partial \psi}{\partial r} \right) \right] \\ &= D(\psi)\left[ \frac{1}{r^{m-1}} r^{m-1} \frac{\partial}{\partial r}\left( \frac{\partial \psi}{\partial r} \right) + \frac{\partial \psi}{\partial r} \frac{1}{r^{m-1}} \frac{\partial \left( r^{m-1} \right)}{\partial r} \right] \\ &= D(\psi)\left[ \frac{\partial^2 \psi}{\partial r^2} + \frac{\partial \psi}{\partial r} \frac{1}{r^{m-1}} (m-1)\left( r^{m-2} \right) \frac{\partial r}{\partial r} \right] \\ &= D(\psi)\left[ \frac{\partial^2 \psi}{\partial r^2} + \frac{(m-1)}{r} \frac{\partial \psi}{\partial r} \right] \end{aligned} \tag{A-4}$$

Substituting Equation A-4 into Equation A-3 gives:

$$\frac{\partial \psi}{\partial t} = D(\psi)\left[ \frac{\partial^2 \psi}{\partial r^2} + \frac{(m-1)}{r} \frac{\partial \psi}{\partial r} + \frac{\partial \ln(k')}{\partial r} \frac{\partial \psi}{\partial r} \right] \tag{A-5}$$

Equation A-5 is nonlinear due to the dependence of the parameter $D$ on the state variable $\psi$. Hence, its numerical solution requires use of an iterative scheme such as the Newton-Raphson method. However, as explained in the next section, $D$ is assumed constant over a zone, which simplifies the numerical implementation, so an iterative Newton-Raphson scheme is not necessary here.

## A-2. Finite Difference Discretization

Using an implicit scheme, Equation A-5 can be represented in finite difference form by using the central difference method to discretize the right-hand side and the forward difference method to discretize the left-hand side (Özişik 1993, Chapter 12, "Implicit Method").

This gives:

$$\begin{aligned} \frac{\psi_j^{n+1} - \psi_j^n}{\Delta t} = D\left( \psi_j^{n+1} \right)\Bigg[ & \frac{\psi_{j+1}^{n+1} - 2\psi_j^{n+1} + \psi_{j-1}^{n+1}}{(\Delta r)^2} + \frac{(m-1)}{r_j} \frac{\left( \psi_{j+1}^{n+1} - \psi_{j-1}^{n+1} \right)}{2\Delta r} \\ & + \frac{\left( \ln\left( k_{j+1}'^{n+1} \right) - \ln\left( k_{j-1}'^{n+1} \right) \right)}{2\Delta r} \frac{\left( \psi_{j+1}^{n+1} - \psi_{j-1}^{n+1} \right)}{2\Delta r} \Bigg] \end{aligned} \tag{A-6}$$

As discussed in Lord et al. (2006), $D(\psi)$ is assumed constant over a zone, which simplifies the numerical implementation. Using its zone centered value at the current time, the linearizing approximation $D(\psi) \approx D\left(\psi_j^{n+1}\right) \approx D\left(\psi_j^{n}\right) \approx D_j^n$ is made. Equation A-6 becomes.

$$\frac{\psi_j^{n+1}-\psi_j^n}{\Delta t} = D_j^n\left[\frac{\psi_{j+1}^{n+1}-2\psi_j^{n+1}+\psi_{j-1}^{n+1}}{(\Delta r)^2}+\frac{\left(\psi_{j+1}^{n+1}-\psi_{j-1}^{n+1}\right)}{2\Delta r}\left(\frac{(m-1)}{r_j}+\frac{\left(\ln\left(k_{j+1}'^{n+1}\right)-\ln\left(k_{j-1}'^{n+1}\right)\right)}{2\Delta r}\right)\right]$$

Solve for $\psi_j^n$ and collect similar terms

$$\begin{aligned}
\psi_j^n &= \psi_j^{n+1} - D_j^n\Delta t\left[\frac{\psi_{j+1}^{n+1}-2\psi_j^{n+1}+\psi_{j-1}^{n+1}}{(\Delta r)^2}+\frac{\left(\psi_{j+1}^{n+1}-\psi_{j-1}^{n+1}\right)}{2\Delta r}\left(\frac{(m-1)}{r_j}+\frac{\left(\ln\left(k_{j+1}'^{n+1}\right)-\ln\left(k_{j-1}'^{n+1}\right)\right)}{2\Delta r}\right)\right] \\
&= -D_j^n\Delta t\left[\frac{1}{(\Delta r)^2}-\frac{1}{2\Delta r}\left(\frac{(m-1)}{r_j}+\frac{\left(\ln\left(k_{j+1}'^{n+1}\right)-\ln\left(k_{j-1}'^{n+1}\right)\right)}{2\Delta r}\right)\right]\psi_{j-1}^{n+1} + \left[1+\frac{2D_j^n\Delta t}{(\Delta r)^2}\right]\psi_j^{n+1} \\
&\quad -D_j^n\Delta t\left[\frac{1}{(\Delta r)^2}+\frac{1}{2\Delta r}\left(\frac{(m-1)}{r_j}+\frac{\left(\ln\left(k_{j+1}'^{n+1}\right)-\ln\left(k_{j-1}'^{n+1}\right)\right)}{2\Delta r}\right)\right]\psi_{j+1}^{n+1} \\
&= -\frac{D_j^n\Delta t}{\Delta r}\left[\frac{1}{\Delta r}-\frac{(m-1)}{2r_j}-\frac{\left(\ln\left(k_{j+1}'^{n+1}\right)-\ln\left(k_{j-1}'^{n+1}\right)\right)}{4\Delta r}\right]\psi_{j-1}^{n+1} + \left[1+\frac{2D_j^n\Delta t}{(\Delta r)^2}\right]\psi_j^{n+1} \\
&\quad -\frac{D_j^n\Delta t}{\Delta r}\left[\frac{1}{\Delta r}+\frac{(m-1)}{2r_j}+\frac{\left(\ln\left(k_{j+1}'^{n+1}\right)-\ln\left(k_{j-1}'^{n+1}\right)\right)}{4\Delta r}\right]\psi_{j+1}^{n+1}
\end{aligned}$$

Noting that $\ln\left(k_{j+1}'^{n+1}\right)-\ln\left(k_{j-1}'^{n+1}\right) = \ln\left(k_{j+1}'^{n+1}\Big/k_{j-1}'^{n+1}\right)$

$$\begin{aligned}
\psi_j^n &= -\frac{D_j^n\Delta t}{\Delta r}\left(\frac{1}{\Delta r}-\frac{(m-1)}{2r_j}-\frac{\ln\left(k_{j+1}'^{n+1}\Big/k_{j-1}'^{n+1}\right)}{4\Delta r}\right)\psi_{j-1}^{n+1} + \left(1+\frac{2D_j^n\Delta t}{(\Delta r)^2}\right)\psi_j^{n+1} \\
&\quad -\frac{D_j^n\Delta t}{\Delta r}\left(\frac{1}{\Delta r}+\frac{(m-1)}{2r_j}+\frac{\ln\left(k_{j+1}'^{n+1}\Big/k_{j-1}'^{n+1}\right)}{4\Delta r}\right)\psi_{j+1}^{n+1}
\end{aligned}$$

Rewriting the equation:

$$\psi_j^n = -\alpha_1 \psi_{j-1}^{n+1} + (1+2\alpha)\psi_j^{n+1} - \alpha_2 \psi_{j+1}^{n+1} \tag{A-7}$$

where

$$\alpha = \frac{D_j^n \Delta t}{(\Delta r)^2}$$

$$\alpha_1 = \frac{D_j^n \Delta t}{\Delta r}\left(\frac{1}{\Delta r} - \frac{(m-1)}{2r_j} - Forchterm\right)$$

$$\alpha_2 = \frac{D_j^n \Delta t}{\Delta r}\left(\frac{1}{\Delta r} + \frac{(m-1)}{2r_j} + Forchterm\right)$$

$$Forchterm = \frac{\ln\left(k'^{n+1}_{j+1} \big/ k'^{n+1}_{j-1}\right)}{4\Delta r}$$

and *j* and *n* are the cell and timestep indices, respectively. Equation A-7 is the same as Equation 4.6.3 in the previous version of the DRSPALL design document (WIPP PA 2004a) and Sandia Report Equation 4.3.4 (Lord et al. 2006) except that the coefficient terms $\alpha_1$ and $\alpha_2$ are different.

Also:

$$\alpha_1 + \alpha_2 = \frac{D_j^n \Delta t}{\Delta r}\left(\frac{1}{\Delta r} - \frac{(m-1)}{2r_j} - \frac{\ln\left(k'^{n+1}_{j+1} \big/ k'^{n+1}_{j-1}\right)}{4\Delta r}\right) + \frac{D_j^n \Delta t}{\Delta r}\left(\frac{1}{\Delta r} + \frac{(m-1)}{2r_j} + \frac{\ln\left(k'^{n+1}_{j+1} \big/ k'^{n+1}_{j-1}\right)}{4\Delta r}\right)$$

$$= \frac{D_j^n \Delta t}{\Delta r}\left(\frac{1}{\Delta r} + \frac{1}{\Delta r}\right)$$

$$= 2\frac{D_j^n \Delta t}{(\Delta r)^2}$$

$$\alpha_1 + \alpha_2 = 2\alpha.$$

## A-3. Boundary Conditions

For the boundary condition at the inner radius we use the method given in Thomas (1995, Section 1.6.3, "Cell Centered Grids") for cell centered grids. Using this method the difference equation is derived on the second cell in the usual, here central difference, manner. The first intact zone is the zone closest to the borehole and is indexed as 1. The boundary condition is implemented by noting that for the first intact cell ($j - 1 = 1$), $\psi_1^{n+1}$ is the cavity psuedo pressure, $\psi_{cav}^{n+1}$, which is known. Therefore, $\psi_1^{n+1} = \psi_{cav}^{n+1}$ can be moved to the left-hand side of Equation A-7.

Using $j = 2$, the second cell, Equation A-7 gives:

$$\psi_2^n + \alpha_1 \psi_{cav}^{n+1} = (1 + 2\alpha)\psi_2^{n+1} - \alpha_2 \psi_3^{n+1} \tag{A-8}$$

The far-field boundary condition is a zero gradient condition. Mathematically this is:

$$\left.\frac{\partial \psi}{\partial r}\right|_{r=\infty} = 0 \tag{A-9}$$

Discretizing using a second-order central difference formulation:

$$\begin{aligned} &\frac{\psi_{N+1}^{n+1} - \psi_{N-1}^{n+1}}{2\Delta r} = 0 \\ &\psi_{N+1}^{n+1} = \psi_{N-1}^{n+1} \end{aligned} \tag{A-10}$$

Using this to eliminate the fictitious point in the domain discretization Equation A-7, at node point $j = N$ (i.e., the final cell):

$$\begin{aligned} \psi_N^n &= -\alpha_1 \psi_{N-1}^{n+1} + (1 + 2\alpha)\psi_N^{n+1} - \alpha_2 \psi_{N+1}^{n+1} \\ &= -\alpha_1 \psi_{N-1}^{n+1} + (1 + 2\alpha)\psi_N^{n+1} - \alpha_2 \psi_{N-1}^{n+1} \\ &= -(\alpha_1 + \alpha_2)\psi_{N-1}^{n+1} + (1 + 2\alpha)\psi_N^{n+1} \end{aligned}$$

Using $\alpha_1 + \alpha_2 = 2\alpha$, the final condition can be simplified to:

$$\psi_N^n = -(2\alpha)\psi_{N-1}^{n+1} + (1 + 2\alpha)\psi_N^{n+1} \tag{A-11}$$

In the previous version of the DRSPALL design document (WIPP PA 2004a, which was prepared for DRSPALL Version 1.10), a forward difference formulation was applied to the boundary condition Equation A-9. Özişik (1993) shows that the error involved with the central difference representation is second-order accurate, i.e., $O\left((\Delta r)^2\right)$; whereas the error involved with the forward difference representation is first-order accurate, i.e., $O(\Delta r)$. Therefore, the

central difference formulation, Equation A-11, is used because it decreases numerical discretization errors and provides a more accurate numerical approximation to the exact solution.

## A-4. Summary of Recommended Finite Difference Equations

The recommended tri-diagonal linear system of equations is:

$$\begin{aligned}
\psi_j^n &= -\alpha_1 \psi_{cav}^{n+1} + (1+2\alpha)\psi_j^{n+1} - \alpha_2 \psi_{j+1}^{n+1} \quad \text{for } j = 2 \\
\psi_j^n &= -\alpha_1 \psi_{j-1}^{n+1} + (1+2\alpha)\psi_j^{n+1} - \alpha_2 \psi_{j+1}^{n+1} \quad \text{for } j = 3,..., N-1 \\
\psi_j^n &= -(2\alpha)\psi_{j-1}^{n+1} + (1+2\alpha)\psi_j^{n+1} \quad \text{for } j = N
\end{aligned} \tag{A-12}$$

where

$$\alpha = \frac{D_j^n \Delta t}{(\Delta r)^2}$$

$$\alpha_1 = \frac{D_j^n \Delta t}{\Delta r}\left(\frac{1}{\Delta r} - \frac{(m-1)}{2r_j} - Forchterm\right)$$

$$\alpha_2 = \frac{D_j^n \Delta t}{\Delta r}\left(\frac{1}{\Delta r} + \frac{(m-1)}{2r_j} + Forchterm\right)$$

$$Forchterm = \frac{\ln\left(k'^{n+1}_{j+1} \Big/ k'^{n+1}_{j-1}\right)}{4\Delta r}$$

Figure A-1 illustrates the expansion point ($j$, $n$+1) and the surrounding finite-difference molecules.

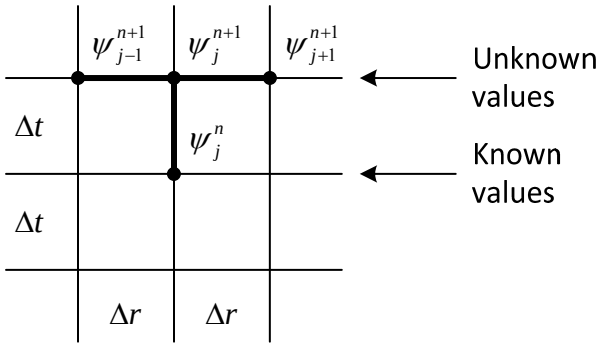


**Figure A-1. Finite Difference Molecules for the Implicit Scheme Using Constant Zone Sizes.**

# APPENDIX B. SUMMARY OF CODE CHANGES

A summary of DRSPALL code changes is provided in Table B-1, which shows excerpts of source code from DRSPALL Versions 1.21 and 1.22, highlighting the changes to DRSPALL Version 1.22. A description of the changes is also provided in Table B-1.

## Table B-1. Summary of DRSPALL Code Changes.

| DRSPALL Version 1.21 | DRSPALL Version 1.22 (changes shown in red) | Description of Change |
|---|---|---|
| Excerpts from source code file *A1main_drspall.f90* | | |
| fluidizationValidationFileID = 122<br>expulsionValidationFileID = 123<br><br><br>! test case #5,<br>wellboreValidationFileID = 125 | fluidizationValidationFileID = 122<br>expulsionValidationFileID = 123<br>fluidizationTimeValidationFileID = 124 !trz<br><br>! test case #5,<br>wellboreValidationFileID = 125 | An additional output file, *fluidization_time.dat*, was included as part of test case #4. This new output file provides the fluidization time for each zone to improve the ability to verify the DRSPALL fluidization time calculation. Specific changes to this source code file include:<br>– Added file id for *fluidization_time.dat*<br>– Added definition of filename of *fluidization_time.dat*<br>– Added opening of *fluidization_time.dat*<br>– Added writing of QA information to *fluidization_time.dat* |
| TC4EjectFileName =<br>trim(validationFilePrefix)//'_expulsion.dat' !apg<br><br><br><br>Open(fluidizationValidationFileID, FILE=<br>TC4Fluidfilename, RECL=2048, FORM='FORMATTED',<br>STATUS=status)<br>Open(expulsionValidationFileID, FILE= TC4Ejectfilename,<br>RECL=2048, FORM='FORMATTED', STATUS=status) | TC4EjectFileName =<br>trim(validationFilePrefix)//'_expulsion.dat' !apg<br>TC4FluidTimeFileName =<br>trim(validationFilePrefix)//'_fluidization_time.dat' !trz<br><br>Open(fluidizationValidationFileID, FILE=<br>TC4Fluidfilename, RECL=2048, FORM='FORMATTED',<br>STATUS=status)<br>Open(expulsionValidationFileID, FILE= TC4Ejectfilename,<br>RECL=2048, FORM='FORMATTED', STATUS=status)<br>Open(fluidizationTimeValidationFileID, FILE=<br>TC4FluidTimefilename, RECL=2048,<br>FORM='FORMATTED', &<br>STATUS=status) !trz | |
| ! expulsion file<br>CALL QAPAGE (expulsionValidationFileID,blank)<br>write(expulsionValidationFileID,'(1x,a)')<br>trim(TC4Ejectfilename) !apg new<br>!apg CALL<br>QABANNER(expulsionValidationFileID,blank,blank,blank)<br>!apg CALL QADOEDIS(expulsionValidationFileID,'*')<br><br><br><br><br>endif | ! expulsion file<br>CALL QAPAGE (expulsionValidationFileID,blank)<br>write(expulsionValidationFileID,'(1x,a)')<br>trim(TC4Ejectfilename) !apg new<br>!apg CALL<br>QABANNER(expulsionValidationFileID,blank,blank,blank)<br>!apg CALL QADOEDIS(expulsionValidationFileID,'*')<br><br>! fluidization time file<br>CALL QAPAGE (fluidizationTimeValidationFileID,blank)<br>write(fluidizationTimeValidationFileID,'(1x,a)')<br>trim(TC4FluidTimefilename) !trz<br><br>endif | |

## Table B-1. Summary of DRSPALL Code Changes. (Continued)

| DRSPALL Version 1.21 | DRSPALL Version 1.22 (changes shown in red) | Description of Change |
|---|---|---|
| Excerpts from source code file *A1main_drspall.f90* (continued) | | |
| string = READCFA(parameterFileID,'radius,growthRate')<br>read(string,*)reposRadius1, growthRate<br><br><br><br>initialWellZoneSize = READCF (parameterFileID,initialWellZoneSize,'initialWellZoneSize')<br>wellGrowthRate = READCF (parameterFileID,wellGRowthRate,'wellGRowthRate')<br><br><br><br>firstWellZone = READCF (parameterFileID,dble(firstWellZone),'firstWellZone') | string = READCFA(parameterFileID,'radius,growthRate')<br>read(string,*)reposRadius1, growthRate<br>if (growthRate < 1.0 .or. growthRate > 1.0) then !trz<br>call QAABORT ('Growth rate must be 1.0') !trz<br>endif !trz<br>initialWellZoneSize = READCF (parameterFileID,initialWellZoneSize,'initialWellZoneSize')<br>wellGrowthRate = READCF (parameterFileID,wellGRowthRate,'wellGRowthRate')<br>if (wellGrowthRate < 1.0 .or. wellGrowthRate > 1.0) then !trz<br>call QAABORT ('Well growth rate must be 1.0') !trz<br>endif !trz<br>firstWellZone = READCF (parameterFileID,dble(firstWellZone),'firstWellZone') | Checks of 'growthRate' and 'wellGrowthRate' were added to make sure they are set to '1.0' in the input file, since the code will now be run exclusively with constant zone sizes. If not, the code exits with an error. |
| Excerpts from source code file *globals.F90* | | |
| Character(255) TC1chanFileName, TC4couplefilename, TC4stressfilename, &<br>TC4Fluidfilename, TC4Ejectfilename, TC5Wellfilename | Character(255) TC1chanFileName, TC4couplefilename, TC4stressfilename, &<br>TC4Fluidfilename, TC4Ejectfilename, TC4FluidTimefilename, TC5Wellfilename | As a result of the new output file for test case #4, new definitions are required to pass values between subroutines. Specifically, *TC4FluidTimefilename* and *fluidizationTimeValidation FileID* variables were added. |
| !test case #4<br>couplingValidationFileID, stressValidationFileID, fluidizationvalidationFileID, &<br>expulsionValidationFileID, &<br><br>!test case #5 | !test case #4<br>couplingValidationFileID, stressValidationFileID, fluidizationvalidationFileID, &<br>expulsionValidationFileID, fluidizationTimeValidationFileID, &<br>!test case #5 | |

## Table B-1. Summary of DRSPALL Code Changes. (Continued)

| DRSPALL Version 1.21 | DRSPALL Version 1.22 (changes shown in red) | Description of Change |
|---|---|---|
| Excerpts from source code file *maincalc.f90* | | |
| gasFac = DSqrt(invGasViscosity)<br><br><br><br><br><br>i = firstIntactZone<br>dCoeff(i) = permeability(i)*invPorosity(i)*gasFac*DSqrt(psi(i))<br>reposAllowedDeltaTime = reposDR(i)**2/DCoeff(i)<br>cellControl(2) = i<br><br><br><br>do i = firstIntactZone+1, numReposZones | gasFac = DSqrt(invGasViscosity)<br><br>!trz<br>reposAllowedDeltaTime = maxTime !initialize with large time<br><br>if (cavityPres /= 0.0) then !skip for test case #1<br>i = firstIntactZone<br>dCoeff(i) = permeability(i)*invPorosity(i)*gasFac*DSqrt(psi(i))<br>reposAllowedDeltaTime = reposDR(i)**2/DCoeff(i)<br>cellControl(2) = i<br>endif<br>!trz<br><br>do i = firstIntactZone+1, numReposZones | A check of the timestep calculation was added for the 'firstIntactZone' that will skip the calculation if 'cavityPres' is zero. Because of the changes to the boundary condition, this change was needed to run validation test case 1. |
| Excerpts from source code file *parameters.f90* | | |
| ie = ie+ boundcheck('tensileStrength', tensileStrength, 1.0D4, 6.91D6)<br>ie = ie+ boundcheck('Lt', Lt, -0.0001D0, 0.1D0)<br>!dkr changed for QE0110<br>ie = ie+ boundcheck('particleDiameter',particleDiameter, 1.0D-3, 1.0D0) | ie = ie+ boundcheck('tensileStrength', tensileStrength, 1.0D4, 6.91D6)<br>ie = ie+ boundcheck('Lt', Lt, -0.0001D0, 0.1D2)<br>!dkr changed for QE0110<br>ie = ie+ boundcheck('particleDiameter',particleDiameter, 1.0D-3, 1.0D0) | The upper bound for characteristic length, $L_t$, was increased to 10 for zone size sensitivity testing. |
| Excerpts from source code file *setupcalc.f90* | | |
| if(numwellzones2 > 0)Then<br>wellArea(collarIndex-1) = .6667*collarAnnulusArea+0.3333*pipeAnnulusArea<br><br>wellArea(collarIndex) = .3333*collarAnnulusArea+0.6667*pipeAnnulusArea<br><br>wellVol (collarIndex-1) = wellArea(collarIndex-1)*wellZoneSize(collarIndex-1) | if(numwellzones2 > 0)Then<br>wellArea(collarIndex-1) = (2d0/3d0)*collarAnnulusArea+(1d0/3d0)*pipeAnnulusArea<br>!dkr v1.22, was .3333/.6667<br>wellArea(collarIndex) = (1d0/3d0)*collarAnnulusArea+(2d0/3d0)*pipeAnnulusArea<br>!dkr v1.22, was .6667/.3333<br>wellVol (collarIndex-1) = wellArea(collarIndex-1)*wellZoneSize(collarIndex-1) | – The 'wellArea' array definition was updated to calculate fractions 2/3 and 1/3 instead of the given decimal values of 0.6667 and 0.3333.<br>– The 'reposVol' array definition was updated to calculate fraction 2/3 |

## Table B-1. Summary of DRSPALL Code Changes. (Continued)

| DRSPALL Version 1.21 | DRSPALL Version 1.22 (changes shown in red) | Description of Change |
|---|---|---|
| Excerpts from source code file *setupcalc.f90* (continued) | | |
| if (geometry == 'S') then<br>reposVol(i) = 0.666667d0*Pi*(reposRadiusH(i+1)**3 &<br>-reposRadiusH(i)**3)<br><br>else | if (geometry == 'S') then<br>reposVol(i) = (2d0/3d0)*Pi*(reposRadiusH(i+1)**3 &<br>-reposRadiusH(i)**3) !dkr v1.22, was .666667<br>else | instead of the given decimal value of 0.666667.<br>– The 'numReposZones' definition was updated to work correctly with a constant zone size (added 1).<br>– Updated the 'reposZoneSize' definition to work correctly with a constant zone size (subtracted 1 from denominator). The original code version failed when a constant zone size was selected.<br>– Added call to QAABORT that exits out of the section of code that previously recalculated the number of zones based on a growth rate greater than 1.0.<br>– In the definition of 'reposDR', the option to calculate its values using the cell growth rate was commented out, which ensures that 'reposDR' array values will all be the same (constant zone size). |
| numReposZones = repositoryOuterRadius/initialReposZoneSize<br>reposZoneSize = (repositoryOuterRadius-initialCavityRadius)/numReposZones | numReposZones = repositoryOuterRadius/initialReposZoneSize + 1 !trz<br>reposZoneSize = (repositoryOuterRadius-initialCavityRadius)/(numReposZones - 1) !trz | |
| IF( reposRadius1 < (repositoryOuterRadius-initialCavityRadius) .and. GrowthRate > 1.00001) then<br><br>!dkr 7/23 use brute force | IF( reposRadius1 < (repositoryOuterRadius-initialCavityRadius) .and. GrowthRate > 1.00001) then<br>call QAABORT ('Growth Rate should be 1.0 ')<br>!dkr 7/23 use brute force | |
| endif<br><br>if(reposRadius(i-1) > reposRadius1a)then<br>reposDR (i) = reposDR(i-1)*GrowthRate<br>if(reposRadius(i-1) < reposRadius2) Then<br>reposDR(i)= MIN(LT/minNumCells, reposDR (i))<br>endif<br><br>else<br>reposDR (i) = reposDR(i-1)<br>endif<br>reposDRH(i) = 0.5*(reposDR(i) + reposDR(i-1)) | endif<br><br>!trz if(reposRadius(i-1) > reposRadius1a)then<br>!trz reposDR (i) = reposDR(i-1)*GrowthRate<br>!trz if(reposRadius(i-1) < reposRadius2) Then<br>!trz reposDR(i)= MIN(LT/minNumCells, reposDR (i))<br>!trz endif<br>!trz<br>!trz else<br>reposDR (i) = reposDR(i-1)<br>!trz endif<br>reposDRH(i) = 0.5*(reposDR(i) + reposDR(i-1)) | |

## Table B-1. Summary of DRSPALL Code Changes. (Continued)

| DRSPALL Version 1.21 | DRSPALL Version 1.22 (changes shown in red) | Description of Change |
|---|---|---|
| Excerpts from source code file *vmsfilewrite.f90* | | |
| Close(expulsionValidationFileID)<br><br>! test case #5 | Close(expulsionValidationFileID)<br>Close(fluidizationTimeValidationFileID) !trz<br><br>! test case #5 | – Added closing of *fluidization_time.dat*.<br>– Added writing of header data to *fluidization_time.dat*.<br>– Increased output for stress validation file to indices less than 250.<br>– Redefined when information is written to the fluidization.dat file. Previously, data was only written when the first intact zone was less than or equal to zone 20 (or between 100 and 150). Based on the other changes made to the code, the relevant output is now needed when the first intact zone is less than or equal to zone 70 (or between 100 and 150), so the 'if' statement has been modified. |
| write(expulsionValidationFileID, '(10A15)') '(sec)', 'Penetrated(T/F)', 'Removed(-)', 'Removed(kg)', &<br>'Store (kg)', 'In Well (kg)', 'Ejected (kg)', 'In Well (m)', 'Error (-)'<br><br>endif | write(expulsionValidationFileID, '(10A15)') '(sec)', 'Penetrated(T/F)', 'Removed(-)', 'Removed(kg)', &<br>'Store (kg)', 'In Well (kg)', 'Ejected (kg)', 'In Well (m)', 'Error (-)'<br><br>! fluidization time file !trz<br>Write(fluidizationTimeValidationFileID, '(A)') 'Program DR_SPALL - WIPP PA 2003'<br>Write(fluidizationTimeValidationFileID, '(A)') 'ASCII Output file for Test Case #4'<br>Write(fluidizationTimeValidationFileID, '(A)') "<br>Write(fluidizationTimeValidationFileID, '(A)') 'Zone Fluidization Time'<br><br>endif | |
| if (maxTensileFailedIndex <= 20 .or. &<br>(maxTensileFailedIndex > 100 .and. maxTensileFailedIndex <150)) then<br><br>write(stressValidationFileID, '(A15)') " | if (maxTensileFailedIndex <= 20 .or. &<br>(maxTensileFailedIndex > 100 .and. maxTensileFailedIndex <250)) then<br><br>write(stressValidationFileID, '(A15)') " | |
| if (firstIntactZone <=20 .or. &<br>(firstIntactZone >100 .and. firstIntactzone < 150)) then<br>i = 0 | if (firstIntactZone <=70 .or. & !trz<br>(firstIntactZone >100 .and. firstIntactzone < 150)) then<br>i = 0 | |

## Table B-1. Summary of DRSPALL Code Changes. (Continued)

| DRSPALL Version 1.21 | DRSPALL Version 1.22 (changes shown in red) | Description of Change |
|---|---|---|
| Excerpts from source code file *vmsfilewrite.f90* (continued) | | |
| end<br><br>!----------<br>! test case #4<br>Subroutine WriteToCouplingValidationFile | end<br><br>!----------<br>! test case #4 !trz<br>Subroutine WriteToFluidizationTimeValidationFile(izone)<br><br>Use Globals<br>Implicit None<br><br>Integer izone<br><br>write (fluidizationTimeValidationFileID, 200) izone, fluidizationTime(izone)<br><br>200 FORMAT (I8, 1pE21.13)<br><br>return<br>end<br><br>!----------<br>! test case #4<br>Subroutine WriteToCouplingValidationFile | Added subroutine WriteToFluidizationTime ValidationFile() that writes fluidization times to *fluidization_time.dat*. |
| Excerpts from source code file *wasteflowcalc.f90* | | |
| Real(8) exitGasDen, exitGasArealFlux, boundaryPres, exitGasFlowRate, &<br>deltaP, curGasDen, ForchNumber, temp, c1, c2, c3, c4, dr2<br><br>!if (repositoryPenetrated == .FALSE.) then<br>boundaryPres = cavityPres | Real(8) exitGasDen, exitGasArealFlux, boundaryPres, exitGasFlowRate, &<br>deltaP, curGasDen, ForchNumber, temp, c1, c2, c3, c4, dr2<br>Real(8) permEnhanceFactor !dkr<br><br>!if (repositoryPenetrated == .FALSE.) then<br>boundaryPres = cavityPres | – Added definition of 'permEnhanceFactor' and set value to 4.0; this results in no change, since the factor of 4.0 was already used, just not defined as a variable. |

## Table B-1. Summary of DRSPALL Code Changes. (Continued)

| DRSPALL Version 1.21 | DRSPALL Version 1.22 (changes shown in red) | Description of Change |
|---|---|---|
| Excerpts from source code file *wasteflowcalc.f90* (continued) | | |
| !JFS3 add velocity dependent k (Forchheimer)<br><br>do i = firstIntactZone, (numReposZones-1)<br>curGasDen = 0.5d0*gasBaseDensity*reposPres(i)*invAtmosphericPressure<br>ForchNumber = ABS(ForchBeta)*curGasDen*abs(superficialVelocity(i))* invGasViscosity*invPorosity(i)<br>permeability(i) = repositoryInitialPerm*(1.0+4.0*fractionFluidized(i))/(1.0+ ForchNumber)<br>enddo<br>permeability(firstIntactZone-1) = permeability(firstIntactZone)<br>!********** | !JFS3 add velocity dependent k (Forchheimer)<br>permEnhanceFactor = 4.0 !dkr V1.22, was 4.0<br>do i = firstIntactZone, numReposZones !trz<br>curGasDen = gasBaseDensity*reposPres(i)*invAtmosphericPressure !trz<br>ForchNumber = ABS(ForchBeta)*curGasDen*abs(superficialVelocity(i))* invGasViscosity*invPorosity(i)<br>permeability(i) = repositoryInitialPerm*(1.0+permEnhanceFactor* fractionFluidized(i))/(1.0+ForchNumber)<br>enddo<br>!permeability(firstIntactZone-1) = permeability(firstIntactZone) !trz<br>!********** | – The factor of 0.5 was eliminated in the definition of 'curGasDen' to be consistent with the ideal gas law.<br>– The definition of 'permeability(i)' was updated to include the variable 'permEnhanceFactor'.<br>– The definition of 'permeability(firstIntact Zone-1)' was removed (commented out). |
| deltaP = reposPres(firstIntactZone) - boundaryPres<br><br>psi(firstIntactZone-1) = invGasViscosity*(boundaryPres)**2<br><br>! flow calculations | deltaP = reposPres(firstIntactZone) - boundaryPres<br>psi(firstIntactZone) = invGasViscosity*(boundaryPres)**2 !trz<br>!psi(firstIntactZone-1) = invGasViscosity*(boundaryPres)**2 !orig<br><br>! flow calculations | The index of 'psi()' was changed from 'firstIntactZone-1' to 'firstIntactZone'. |
| do i = firstIntactZone, numReposZones<br><br>reposPres(i) = DSqrt(gasViscosity*psi(i))<br><br>end do | do i = firstIntactZone, numReposZones<br>temp = gasViscosity*psi(i) !apg V1.22 temp for negative check<br>IF(temp < 0.0) then !apg V1.22<br>call QAABORT ('SQRT(-x) reposPres') !apg V1.22<br>ENDIF !apg V1.22<br>reposPres(i) = DSqrt(temp) !apg was DSqrt(gasViscosity*psi(i))<br>end do | The variable 'temp' (equal to 'gasViscosity*psi(i)') was created to use in a test to prevent the square root of a negative number. Inserted a QAABORT call if the code is about to take the square root of a negative number. |

## Table B-1. Summary of DRSPALL Code Changes. (Continued)

| DRSPALL Version 1.21 | DRSPALL Version 1.22 (changes shown in red) | Description of Change |
|---|---|---|
| Excerpts from source code file *wasteflowcalc.f90* (continued) | | |
| !dkr used for zone in cavity on CDB<br><br>reposPres(0) = boundaryPres | !dkr used for zone in cavity on CDB<br>reposPres(firstIntactZone) = boundaryPres !trz<br>!reposPres(0) = boundaryPres !orig | The boundary pressure ('boundaryPres') is set equal to 'reposPres(firstIntact Zone)' instead of 'reposPres(0)'. |
| !dkr changed to improve centering => improved mass balance<br>!exitPoreVelocity = 2.0d0*(reposPres(firstIntactZone)-boundaryPres) &<br>exitPoreVelocity = (reposPres(firstIntactZone)-boundaryPres) & | !dkr changed to improve centering => improved mass balance<br>!exitPoreVelocity = 2.0d0*(reposPres(firstIntactZone)-boundaryPres) &<br>exitPoreVelocity = (reposPres(firstIntactZone+1)-boundaryPres) & !trz | The variable 'exitPoreVelocity' is defined using '(reposPres(firstIntact Zone+1)-boundaryPres)' instead of '(reposPres(firstIntact Zone)-boundaryPres)'. |
| ! First cell coefficients<br>i = firstIntactZone<br>compressibility = 1.0d0/reposPres(i) | ! First cell coefficients<br>i = firstIntactZone + 1 !trz<br>compressibility = 1.0d0/reposPres(i) | Definition of 'i' is 'firstIntactZone+1', instead of 'firstIntactZone'. |
| IF(forchBeta > 0.0)THEN<br>Forchterm = (permeability(i+1)-permeability(i)) &<br>/ (permeability(i)*4.0*reposDR(i))<br>ELSE<br>ForchTerm = 0.0 | IF(forchBeta > 0.0)THEN<br>Forchterm = log(permeability(i+1)/permeability(i-1)) & !trz<br>/ (4.0*reposDR(i)) !trz<br>ELSE<br>ForchTerm = 0.0 | The definition of 'Forchterm' is now<br>'Forchterm = log(permeability(i+1)/permeability(i-1))/(4.0*reposDR(i))'<br>This is due to a re-derivation of an equation in the design document (WIPP PA 2015a; see the definition of the coefficient terms $\alpha_1$ and $\alpha_2$ in Section A-2) and is done in three sections of the code. |
| ! Interior cell coefficients<br>do i = (firstIntactZone+1), (numReposZones-1)<br>compressibility = 1.0d0/reposPres(i) | ! Interior cell coefficients<br>do i = (firstIntactZone+2), (numReposZones-1) !trz<br>compressibility = 1.0d0/reposPres(i) | Index of 'i' starts at 'firstIntactZone+2', instead of 'firstIntactZone+1'. |

## Table B-1. Summary of DRSPALL Code Changes. (Continued)

| DRSPALL Version 1.21 | DRSPALL Version 1.22 (changes shown in red) | Description of Change |
|---|---|---|
| Excerpts from source code file *wasteflowcalc.f90* (continued) | | |
| IF(forchbeta > 0.0)THEN<br>  Forchterm = (permeability(i+1)-permeability(i)) &<br>  / (permeability(i)*4.0*reposDR(i))<br>ELSE<br>  ForchTerm = 0.0 | IF(forchbeta > 0.0)THEN<br>  Forchterm = log(permeability(i+1)/permeability(i-1)) & !trz<br>  / (4.0*reposDR(i)) !trz<br>ELSE<br>  ForchTerm = 0.0 | The 'Forchterm' occurs at three locations in the source code. This is the second occurrence. |
| IF(forchbeta > 0.0)THEN<br>  Forchterm = (permeability(i+1)-permeability(i)) &<br>  / (permeability(i)*4.0*reposDR(i))<br>ELSE<br>  ForchTerm = 0.0 | IF(forchbeta > 0.0)THEN<br>  Forchterm = log(permeability(i)/permeability(i-1)) & !trz<br>  / (4.0*reposDR(i)) !trz<br>ELSE<br>  ForchTerm = 0.0 | The 'Forchterm' occurs at three locations in the source code. This is the third occurrence. |
| alpha1 = (DarcyTerm1 -Forchterm)<br>*dPrime*deltaTime/reposDR(i)<br>alpha2 = (DarcyTerm2 +Forchterm)<br>*dPrime*deltaTime/reposDR(i)<br>aa(i) = -alpha1<br>bb(i) = 1.0d0 + alpha1<br>rr(i) = psi(i)<br><br>! Perform inversion.<br>bet = bb(firstIntactZone)<br>psi(firstIntactZone) = rr(firstIntactZone)/bet<br>do i = (firstIntactZone+1), numReposZones<br>  gam(i) = cc(i-1)/bet<br>  bet  = bb(i)-aa(i)*gam(i)<br>  psi(i) = (rr(i)-aa(i)*psi(i-1))/bet<br>end do<br><br>!dkr changed from contant pressure to zero gradient<br>!psi(numReposZones) =<br>repositoryInitialPressure**2/gasViscosity<br>!New BC - Comment next line**********<br>!psi(numReposZones) = reposPres(numReposZones-<br>1)**2/gasViscosity<br>do i = (numReposZones-1), firstIntactZone, -1<br>  psi(i) = psi(i)-gam(i+1)*psi(i+1) | alpha1 = (DarcyTerm1 -Forchterm)<br>*dPrime*deltaTime/reposDR(i)<br>alpha2 = (DarcyTerm2 +Forchterm)<br>*dPrime*deltaTime/reposDR(i)<br>aa(i) = -alpha1 - alpha2 !trz<br>bb(i) = 1.0d0 + alpha1 + alpha2 !trz<br>rr(i) = psi(i)<br><br>! Perform inversion.<br>bet = bb(firstIntactZone+1) !trz<br>psi(firstIntactZone+1) = rr(firstIntactZone+1)/bet !trz<br>do i = (firstIntactZone+2), numReposZones !trz<br>  gam(i) = cc(i-1)/bet<br>  bet  = bb(i)-aa(i)*gam(i)<br>  psi(i) = (rr(i)-aa(i)*psi(i-1))/bet<br>end do<br><br>!dkr changed from contant pressure to zero gradient<br>!psi(numReposZones) =<br>repositoryInitialPressure**2/gasViscosity<br>!New BC - Comment next line**********<br>!psi(numReposZones) = reposPres(numReposZones-<br>1)**2/gasViscosity<br>do i = (numReposZones-1), firstIntactZone+1, -1 !trz<br>  psi(i) = psi(i)-gam(i+1)*psi(i+1) | – Definition of 'aa(i)' is now '-alpha1-alpha2'.<br>– Definition of 'bb(i)' is now '1.0d0 + alpha1 + alpha2'.<br>– Definition of 'bet' is now 'bb(firstIntactZone+1)' instead of 'bb(firstIntactZone).'<br>– The definition 'psi(firstIntactZone) = rr(firstIntactZone)/bet' has been replaced by 'psi(firstIntactZone+1) = rr(firstIntactZone+1)/bet'<br>– Index of 'i' starts at 'firstIntactZone+2', instead of 'firstIntactZone+1'.<br>– Index of 'i' ends at 'firstIntactZone+1', instead of 'firstIntactZone'. |

## Table B-1. Summary of DRSPALL Code Changes. (Continued)

| DRSPALL Version 1.21 | DRSPALL Version 1.22 (changes shown in red) | Description of Change |
|---|---|---|
| Excerpts from source code file *wastestresscalc.f90* | | |
| do i = firstIntactZone, numReposZones<br>! Elastic Stresses<br>temp1 = (reposRadius(firstIntactZone-1)/ reposRadius(i))**geomExponent<br>radElasticStress(i) = (cavityPres-farfieldStress)*temp1 +farfieldStress | do i = firstIntactZone, numReposZones<br>! Elastic Stresses<br>temp1 = (reposRadius(firstIntactZone)/ reposRadius(i))**geomExponent<br>radElasticStress(i) = (cavityPres-farfieldStress)*temp1 +farfieldStress | In the definition of temp1, the index of reposRadius() was changed from: (firstIntactZone-1) to (firstIntactZone). |
| Excerpts from source code file *wellborecalc.f90* | | |
| ! used by test case #4<br>fluidizationSaveTime = runTime<br><br><br><br>end if | ! used by test case #4<br>fluidizationSaveTime = runTime<br>!trz<br>if(validationTestCase == 4)then<br>CALL WriteToFluidizationTimeValidationFile(i)<br>endif<br>!trz<br>end if | Added call to a new subroutine WriteToFluidizationTimeValidation File(). This subroutine writes fluidization times to *fludization_time.dat*, which is an output file added for test case #4 to facilitate the verification of fluidization times. |
| firstIntactZone = i+1<br><br><br><br>end if<br><br>end if<br>i = i + 1<br>end do | firstIntactZone = i+1<br><br>elseif (fractionFluidized(i) > 1.0001) then !trz<br>fractionFluidized (i) = 1.0001 !trz<br><br>end if<br><br>end if<br>i = i + 1<br>end do | Added 'elseif' possibility for 'fractionFluidized(i)' calculation. Previously, 'fractionFluidized(i)' was set to 1.0 only if 'i' was for the 'firstIntactZone'. Otherwise, the 'fractionFluidized' could increase to values much higher than 1.0, which are not physically reasonable, and led to problems in calculating 'permeability' in *wasteflowcalc.f90*. The 'elseif' statement was added to set 'fractionFluidized(i)' to a number slightly larger than 1.0 (1.0001), such that the 'if' statement will be satisfied for zone 'i' in a later step. |

*This page is intentionally left blank.*

# APPENDIX C. DRSPALL CALCULATED SPALL VOLUMES

Tables C-1, C-2 and C-3 list the spall volumes calculated by the modified DRSPALL code (Version 1.22) for all four pressure scenarios and for replicates 1, 2, and 3, respectively. These data are located in the CVS repository at /nfs/data/CVSLIB/WIPP_ANALYSES/PABC09/DRSPALL/Output (files *mspall_drs_PABC09_r1.out*, *mspall_drs_PABC09_r2.out*, and *mspall_drs_PABC09_r3.out*).

**Table C-1. Modified Spall Volumes from DRSPALL Version 1.22: Replicate 1.**

| Vector | DPS1 10.0 MPa | DPS2 12.0 MPa | DPS3 14.0 MPa | DPS4 14.8 MPa |
|---|---|---|---|---|
| 1 | 0.000 | 0.143 | 1.147 | 1.727 |
| 2 | 0.000 | 0.769 | 7.300 | 10.811 |
| 3 | 0.000 | 0.320 | 0.874 | 1.236 |
| 4 | 0.000 | 0.351 | 0.472 | 0.660 |
| 5 | 0.000 | 0.000 | 0.000 | 0.000 |
| 6 | 0.000 | 0.000 | 0.000 | 0.000 |
| 7 | 0.000 | 0.000 | 0.000 | 0.000 |
| 8 | 0.000 | 0.154 | 1.002 | 1.290 |
| 9 | 0.000 | 0.055 | 0.425 | 0.794 |
| 10 | 0.000 | 0.000 | 0.000 | 0.000 |
| 11 | 0.000 | 0.163 | 1.031 | 1.855 |
| 12 | 0.000 | 0.000 | 0.000 | 0.000 |
| 13 | 0.000 | 0.363 | 0.533 | 0.608 |
| 14 | 0.000 | 0.439 | 1.024 | 1.114 |
| 15 | 0.000 | 0.000 | 0.328 | 0.772 |
| 16 | 0.000 | 0.303 | 0.497 | 0.597 |
| 17 | 0.000 | 0.342 | 1.524 | 2.524 |
| 18 | 0.000 | 0.051 | 0.427 | 0.877 |
| 19 | 0.000 | 0.044 | 0.750 | 0.753 |
| 20 | 0.000 | 0.000 | 0.000 | 0.000 |
| 21 | 0.000 | 0.000 | 0.125 | 0.201 |
| 22 | 0.000 | 0.000 | 0.000 | 0.000 |
| 23 | 0.000 | 0.197 | 1.200 | 2.590 |
| 24 | 0.000 | 0.182 | 0.949 | 1.770 |
| 25 | 0.000 | 0.131 | 0.785 | 1.432 |
| 26 | 0.000 | 0.205 | 0.960 | 0.856 |
| 27 | 0.000 | 0.183 | 0.358 | 0.422 |
| 28 | 0.000 | 0.470 | 4.268 | 7.473 |
| 29 | 0.000 | 0.533 | 1.932 | 3.473 |
| 30 | 0.000 | 0.054 | 0.539 | 0.817 |
| 31 | 0.000 | 0.263 | 1.027 | 1.224 |
| 32 | 0.000 | 9.676 | 9.996 | 10.229 |
| 33 | 0.000 | 1.625 | 7.964 | 7.502 |

**Table C-1. Modified Spall Volumes from DRSPALL Version 1.22: Replicate 1. (Continued)**

| Vector | DPS1 10.0 MPa | DPS2 12.0 MPa | DPS3 14.0 MPa | DPS4 14.8 MPa |
|---|---|---|---|---|
| 34 | 0.000 | 0.426 | 3.292 | 5.283 |
| 35 | 0.000 | 0.540 | 2.289 | 3.558 |
| 36 | 0.000 | 3.509 | 4.819 | 5.864 |
| 37 | 0.000 | 0.175 | 0.462 | 0.701 |
| 38 | 0.000 | 0.104 | 0.618 | 0.639 |
| 39 | 0.000 | 0.000 | 0.000 | 0.000 |
| 40 | 0.000 | 0.425 | 0.901 | 1.005 |
| 41 | 0.000 | 0.186 | 1.139 | 1.856 |
| 42 | 0.000 | 0.745 | 2.199 | 1.482 |
| 43 | 0.000 | 0.133 | 0.835 | 1.360 |
| 44 | 0.000 | 0.305 | 1.143 | 2.231 |
| 45 | 0.000 | 0.549 | 0.793 | 1.020 |
| 46 | 0.000 | 0.000 | 0.000 | 0.000 |
| 47 | 0.000 | 0.378 | 2.485 | 4.502 |
| 48 | 0.000 | 0.145 | 0.691 | 1.261 |
| 49 | 0.000 | 0.000 | 0.000 | 0.000 |
| 50 | 0.000 | 0.048 | 0.618 | 0.655 |
| 51 | 0.000 | 0.000 | 0.000 | 0.142 |
| 52 | 0.000 | 0.176 | 0.896 | 2.073 |
| 53 | 0.000 | 0.379 | 1.632 | 2.809 |
| 54 | 0.000 | 0.159 | 0.884 | 1.251 |
| 55 | 0.000 | 0.207 | 0.350 | 0.436 |
| 56 | 0.000 | 0.644 | 0.673 | 0.931 |
| 57 | 0.000 | 0.395 | 0.536 | 0.709 |
| 58 | 0.000 | 0.000 | 0.000 | 0.000 |
| 59 | 0.000 | 2.651 | 9.262 | 9.426 |
| 60 | 0.000 | 0.000 | 0.000 | 0.000 |
| 61 | 0.000 | 0.000 | 0.000 | 0.000 |
| 62 | 0.000 | 0.000 | 0.000 | 0.000 |
| 63 | 0.000 | 0.000 | 0.000 | 0.000 |
| 64 | 0.000 | 0.328 | 1.127 | 1.368 |
| 65 | 0.000 | 0.503 | 6.320 | 7.880 |
| 66 | 0.000 | 0.360 | 1.510 | 1.812 |
| 67 | 0.000 | 0.000 | 0.142 | 0.223 |
| 68 | 0.000 | 0.000 | 0.000 | 0.000 |
| 69 | 0.000 | 0.000 | 0.000 | 0.000 |
| 70 | 0.000 | 0.000 | 0.000 | 0.000 |
| 71 | 0.000 | 0.150 | 0.942 | 1.421 |
| 72 | 0.000 | 0.000 | 0.047 | 0.090 |
| 73 | 0.000 | 0.000 | 0.000 | 0.000 |

**Table C-1. Modified Spall Volumes from DRSPALL Version 1.22: Replicate 1. (Continued)**

| Vector | DPS1 10.0 MPa | DPS2 12.0 MPa | DPS3 14.0 MPa | DPS4 14.8 MPa |
|---|---|---|---|---|
| 74 | 0.000 | 0.144 | 0.977 | 1.469 |
| 75 | 0.000 | 0.376 | 0.555 | 0.622 |
| 76 | 0.000 | 0.546 | 5.939 | 9.995 |
| 77 | 0.000 | 0.214 | 0.974 | 1.788 |
| 78 | 0.000 | 0.188 | 0.949 | 1.718 |
| 79 | 0.000 | 1.013 | 9.647 | 10.268 |
| 80 | 0.000 | 0.457 | 1.197 | 1.257 |
| 81 | 0.000 | 0.139 | 0.776 | 1.385 |
| 82 | 0.000 | 0.138 | 0.602 | 0.889 |
| 83 | 0.000 | 0.141 | 0.827 | 1.223 |
| 84 | 0.000 | 0.000 | 0.000 | 0.000 |
| 85 | 0.000 | 0.307 | 0.462 | 0.743 |
| 86 | 0.000 | 0.407 | 0.597 | 0.631 |
| 87 | 0.000 | 0.403 | 2.231 | 3.185 |
| 88 | 0.000 | 0.124 | 0.624 | 0.676 |
| 89 | 0.000 | 0.139 | 0.662 | 0.773 |
| 90 | 0.000 | 0.000 | 0.000 | 0.000 |
| 91 | 0.000 | 0.036 | 0.665 | 0.805 |
| 92 | 0.000 | 0.419 | 0.994 | 1.798 |
| 93 | 0.000 | 0.000 | 0.175 | 0.220 |
| 94 | 0.000 | 0.000 | 0.069 | 0.103 |
| 95 | 0.000 | 0.061 | 0.592 | 0.631 |
| 96 | 0.000 | 0.000 | 0.000 | 0.000 |
| 97 | 0.000 | 0.000 | 0.000 | 0.000 |
| 98 | 0.000 | 0.000 | 0.000 | 0.000 |
| 99 | 0.000 | 0.000 | 0.000 | 0.000 |
| 100 | 0.000 | 0.069 | 0.702 | 1.393 |

**Table C-2. Modified Spall Volumes from DRSPALL Version 1.22: Replicate 2.**

| Vector | DPS1 10.0 MPa | DPS2 12.0 MPa | DPS3 14.0 MPa | DPS4 14.8 MPa |
|---|---|---|---|---|
| 1 | 0.000 | 0.416 | 2.239 | 2.012 |
| 2 | 0.000 | 0.106 | 0.792 | 0.813 |
| 3 | 0.000 | 0.157 | 0.318 | 0.420 |
| 4 | 0.000 | 0.387 | 0.501 | 0.597 |
| 5 | 0.000 | 0.461 | 0.493 | 0.548 |
| 6 | 0.000 | 0.399 | 2.444 | 4.066 |
| 7 | 0.000 | 0.000 | 0.000 | 0.000 |

**Table C-2. Modified Spall Volumes from DRSPALL Version 1.22: Replicate 2. (Continued)**

| Vector | DPS1 10.0 MPa | DPS2 12.0 MPa | DPS3 14.0 MPa | DPS4 14.8 MPa |
|---|---|---|---|---|
| 8 | 0.000 | 0.000 | 0.142 | 0.254 |
| 9 | 0.000 | 0.381 | 0.701 | 0.792 |
| 10 | 0.000 | 0.000 | 0.000 | 0.000 |
| 11 | 0.000 | 0.327 | 1.835 | 2.887 |
| 12 | 0.000 | 0.000 | 0.189 | 0.253 |
| 13 | 0.000 | 0.000 | 0.169 | 0.184 |
| 14 | 0.000 | 0.000 | 0.000 | 0.000 |
| 15 | 0.000 | 0.000 | 0.000 | 0.000 |
| 16 | 0.000 | 0.366 | 1.991 | 3.121 |
| 17 | 0.000 | 0.414 | 1.077 | 1.110 |
| 18 | 0.000 | 0.000 | 0.125 | 0.190 |
| 19 | 0.000 | 0.000 | 0.000 | 0.000 |
| 20 | 0.000 | 0.000 | 0.000 | 0.000 |
| 21 | 0.000 | 0.000 | 0.000 | 0.000 |
| 22 | 0.000 | 0.609 | 0.627 | 0.877 |
| 23 | 0.000 | 0.000 | 0.178 | 0.208 |
| 24 | 0.000 | 0.098 | 0.683 | 1.143 |
| 25 | 0.000 | 1.103 | 9.431 | 10.183 |
| 26 | 0.000 | 0.146 | 1.254 | 1.491 |
| 27 | 0.000 | 0.397 | 2.603 | 4.953 |
| 28 | 0.000 | 0.000 | 0.000 | 0.000 |
| 29 | 0.000 | 0.000 | 0.000 | 0.000 |
| 30 | 0.000 | 0.199 | 1.191 | 2.148 |
| 31 | 0.000 | 0.000 | 0.000 | 0.000 |
| 32 | 0.000 | 0.369 | 1.869 | 3.851 |
| 33 | 0.000 | 0.123 | 0.834 | 1.629 |
| 34 | 0.000 | 0.680 | 2.521 | 2.104 |
| 35 | 0.000 | 0.150 | 0.711 | 1.477 |
| 36 | 0.000 | 0.094 | 0.273 | 0.365 |
| 37 | 0.000 | 0.000 | 0.000 | 0.089 |
| 38 | 0.000 | 0.000 | 0.000 | 0.000 |
| 39 | 0.000 | 0.182 | 0.855 | 1.525 |
| 40 | 0.000 | 0.157 | 0.909 | 1.344 |
| 41 | 0.000 | 7.070 | 6.749 | 15.817 |
| 42 | 0.000 | 0.093 | 0.253 | 0.362 |
| 43 | 0.000 | 0.309 | 0.433 | 0.551 |
| 44 | 0.000 | 0.030 | 0.337 | 0.645 |
| 45 | 0.000 | 0.536 | 1.276 | 1.749 |
| 46 | 0.000 | 0.408 | 1.806 | 2.244 |
| 47 | 0.000 | 0.373 | 0.878 | 1.264 |

**Table C-2. Modified Spall Volumes from DRSPALL Version 1.22: Replicate 2. (Continued)**

| Vector | DPS1 10.0 MPa | DPS2 12.0 MPa | DPS3 14.0 MPa | DPS4 14.8 MPa |
|---|---|---|---|---|
| 48 | 0.000 | 0.000 | 0.000 | 0.000 |
| 49 | 0.000 | 0.000 | 0.000 | 0.000 |
| 50 | 0.000 | 0.392 | 0.686 | 0.640 |
| 51 | 0.000 | 0.000 | 0.000 | 0.000 |
| 52 | 0.000 | 0.000 | 0.000 | 0.000 |
| 53 | 0.000 | 0.000 | 0.000 | 0.000 |
| 54 | 0.000 | 0.040 | 0.772 | 0.815 |
| 55 | 0.000 | 0.352 | 1.512 | 2.552 |
| 56 | 0.000 | 0.173 | 0.877 | 1.635 |
| 57 | 0.000 | 0.000 | 0.000 | 0.000 |
| 58 | 0.000 | 0.084 | 1.728 | 1.850 |
| 59 | 0.000 | 0.067 | 0.611 | 1.193 |
| 60 | 0.000 | 0.161 | 0.885 | 1.308 |
| 61 | 0.000 | 0.081 | 0.255 | 0.369 |
| 62 | 0.000 | 0.133 | 0.909 | 1.605 |
| 63 | 0.000 | 0.192 | 0.416 | 0.534 |
| 64 | 0.000 | 0.000 | 0.000 | 0.000 |
| 65 | 0.000 | 0.345 | 0.440 | 0.519 |
| 66 | 0.000 | 0.073 | 0.758 | 1.171 |
| 67 | 0.000 | 0.152 | 0.771 | 1.439 |
| 68 | 0.000 | 0.111 | 0.728 | 0.773 |
| 69 | 0.000 | 0.000 | 0.000 | 0.000 |
| 70 | 0.000 | 0.583 | 1.094 | 1.098 |
| 71 | 0.000 | 0.845 | 7.027 | 7.051 |
| 72 | 0.000 | 0.000 | 0.000 | 0.000 |
| 73 | 0.000 | 0.000 | 0.000 | 0.000 |
| 74 | 0.000 | 0.502 | 1.298 | 1.166 |
| 75 | 0.000 | 0.169 | 0.806 | 1.470 |
| 76 | 0.000 | 0.085 | 0.562 | 0.777 |
| 77 | 0.000 | 0.370 | 1.636 | 2.860 |
| 78 | 0.000 | 0.420 | 0.619 | 0.698 |
| 79 | 0.000 | 0.046 | 0.529 | 0.767 |
| 80 | 0.000 | 0.044 | 0.505 | 0.607 |
| 81 | 0.000 | 0.176 | 0.926 | 1.339 |
| 82 | 0.000 | 0.000 | 0.000 | 0.000 |
| 83 | 0.000 | 0.332 | 1.517 | 2.754 |
| 84 | 0.000 | 0.162 | 0.883 | 1.277 |
| 85 | 0.000 | 0.325 | 0.644 | 1.022 |
| 86 | 0.000 | 1.246 | 7.663 | 9.055 |
| 87 | 0.000 | 0.000 | 0.234 | 0.268 |

**Table C-2. Modified Spall Volumes from DRSPALL Version 1.22: Replicate 2. (Continued)**

| Vector | DPS1 10.0 MPa | DPS2 12.0 MPa | DPS3 14.0 MPa | DPS4 14.8 MPa |
|---|---|---|---|---|
| 88 | 0.000 | 0.151 | 0.821 | 0.923 |
| 89 | 0.000 | 0.158 | 0.327 | 0.427 |
| 90 | 0.000 | 0.000 | 0.000 | 0.000 |
| 91 | 0.000 | 0.064 | 0.634 | 1.559 |
| 92 | 0.000 | 0.271 | 0.551 | 0.678 |
| 93 | 0.000 | 0.154 | 0.712 | 0.730 |
| 94 | 0.000 | 0.046 | 0.540 | 0.755 |
| 95 | 0.000 | 0.338 | 1.529 | 2.921 |
| 96 | 0.000 | 0.042 | 0.574 | 0.732 |
| 97 | 0.000 | 0.302 | 0.610 | 0.886 |
| 98 | 0.000 | 0.000 | 0.000 | 0.000 |
| 99 | 0.000 | 0.422 | 0.499 | 0.564 |
| 100 | 0.000 | 0.000 | 0.000 | 0.000 |

**Table C-3. Modified Spall Volumes from DRSPALL Version 1.22: Replicate 3.**

| Vector | DPS1 10.0 MPa | DPS2 12.0 MPa | DPS3 14.0 MPa | DPS4 14.8 MPa |
|---|---|---|---|---|
| 1 | 0.000 | 3.009 | 8.482 | 8.694 |
| 2 | 0.000 | 0.409 | 3.209 | 5.072 |
| 3 | 0.000 | 0.046 | 0.386 | 0.758 |
| 4 | 0.000 | 0.000 | 0.350 | 0.560 |
| 5 | 0.000 | 1.174 | 3.262 | 4.298 |
| 6 | 0.000 | 0.279 | 1.614 | 1.523 |
| 7 | 0.000 | 0.000 | 0.000 | 0.000 |
| 8 | 0.000 | 0.389 | 0.822 | 0.970 |
| 9 | 0.000 | 0.397 | 3.136 | 5.032 |
| 10 | 0.000 | 0.000 | 0.000 | 0.000 |
| 11 | 0.000 | 0.571 | 0.784 | 0.950 |
| 12 | 0.000 | 0.186 | 0.976 | 0.848 |
| 13 | 0.000 | 0.440 | 2.772 | 2.241 |
| 14 | 0.000 | 0.302 | 0.417 | 0.549 |
| 15 | 0.000 | 0.513 | 1.393 | 1.104 |
| 16 | 0.000 | 0.114 | 0.625 | 0.819 |
| 17 | 0.000 | 0.054 | 0.554 | 0.920 |
| 18 | 0.000 | 0.000 | 0.000 | 0.000 |
| 19 | 0.000 | 0.342 | 0.487 | 0.521 |
| 20 | 0.000 | 0.052 | 0.487 | 0.703 |
| 21 | 0.000 | 0.476 | 1.081 | 1.492 |

**Table C-3. Modified Spall Volumes from DRSPALL Version 1.22: Replicate 3. (Continued)**

| Vector | DPS1 10.0 MPa | DPS2 12.0 MPa | DPS3 14.0 MPa | DPS4 14.8 MPa |
|---|---|---|---|---|
| 22 | 0.000 | 0.483 | 0.752 | 1.304 |
| 23 | 0.000 | 0.000 | 0.122 | 0.188 |
| 24 | 0.000 | 0.000 | 0.000 | 0.000 |
| 25 | 0.000 | 7.958 | 8.018 | 8.036 |
| 26 | 0.000 | 0.000 | 0.000 | 0.000 |
| 27 | 0.000 | 0.000 | 0.000 | 0.000 |
| 28 | 0.000 | 0.665 | 1.582 | 1.475 |
| 29 | 0.000 | 0.065 | 0.613 | 0.687 |
| 30 | 0.000 | 0.365 | 0.528 | 0.564 |
| 31 | 0.000 | 0.000 | 0.000 | 0.000 |
| 32 | 0.000 | 0.180 | 0.646 | 0.571 |
| 33 | 0.000 | 0.134 | 0.662 | 0.644 |
| 34 | 0.000 | 0.000 | 0.000 | 0.000 |
| 35 | 0.000 | 0.000 | 0.000 | 0.000 |
| 36 | 0.000 | 4.516 | 5.382 | 4.678 |
| 37 | 0.000 | 0.403 | 0.990 | 1.097 |
| 38 | 0.000 | 0.372 | 1.665 | 2.299 |
| 39 | 0.000 | 0.057 | 0.582 | 1.397 |
| 40 | 0.000 | 0.189 | 1.162 | 2.561 |
| 41 | 0.000 | 0.000 | 0.000 | 0.000 |
| 42 | 0.000 | 0.284 | 1.374 | 2.319 |
| 43 | 0.000 | 0.408 | 0.958 | 0.800 |
| 44 | 0.000 | 0.000 | 0.000 | 0.000 |
| 45 | 0.000 | 0.056 | 0.580 | 1.013 |
| 46 | 0.000 | 0.102 | 0.528 | 1.005 |
| 47 | 0.000 | 0.159 | 0.730 | 0.749 |
| 48 | 0.000 | 0.000 | 0.000 | 0.000 |
| 49 | 0.000 | 0.118 | 0.850 | 1.052 |
| 50 | 0.000 | 0.000 | 0.000 | 0.000 |
| 51 | 0.000 | 0.517 | 4.722 | 3.999 |
| 52 | 0.000 | 0.000 | 0.000 | 0.000 |
| 53 | 0.000 | 0.379 | 2.026 | 3.233 |
| 54 | 0.000 | 0.046 | 0.623 | 0.809 |
| 55 | 0.000 | 0.045 | 0.441 | 0.885 |
| 56 | 0.000 | 0.180 | 1.091 | 1.887 |
| 57 | 0.000 | 0.388 | 0.505 | 0.827 |
| 58 | 0.000 | 0.382 | 0.571 | 0.674 |
| 59 | 0.000 | 0.189 | 1.177 | 2.489 |
| 60 | 0.000 | 0.000 | 0.000 | 0.000 |
| 61 | 0.000 | 0.468 | 4.277 | 4.572 |

**Table C-3. Modified Spall Volumes from DRSPALL Version 1.22: Replicate 3. (Continued)**

| Vector | DPS1<br>10.0 MPa | DPS2<br>12.0 MPa | DPS3<br>14.0 MPa | DPS4<br>14.8 MPa |
|---|---|---|---|---|
| 62 | 0.000 | 0.071 | 0.723 | 1.143 |
| 63 | 0.000 | 0.054 | 0.539 | 0.780 |
| 64 | 0.000 | 0.000 | 0.099 | 0.158 |
| 65 | 0.000 | 0.089 | 0.288 | 0.395 |
| 66 | 0.000 | 0.000 | 0.000 | 0.000 |
| 67 | 0.000 | 1.048 | 10.177 | 13.326 |
| 68 | 0.000 | 0.523 | 5.610 | 7.668 |
| 69 | 0.000 | 0.417 | 2.723 | 4.726 |
| 70 | 0.000 | 0.000 | 0.000 | 0.000 |
| 71 | 0.000 | 0.000 | 0.000 | 0.000 |
| 72 | 0.000 | 0.000 | 0.126 | 0.273 |
| 73 | 0.000 | 0.000 | 0.000 | 0.000 |
| 74 | 0.000 | 0.400 | 0.845 | 0.834 |
| 75 | 0.000 | 0.156 | 0.319 | 0.452 |
| 76 | 0.000 | 0.000 | 0.000 | 0.000 |
| 77 | 0.000 | 0.052 | 0.543 | 0.986 |
| 78 | 0.000 | 0.331 | 1.249 | 2.991 |
| 79 | 0.000 | 0.149 | 0.756 | 0.736 |
| 80 | 0.000 | 0.000 | 0.000 | 0.000 |
| 81 | 0.000 | 0.055 | 0.175 | 0.281 |
| 82 | 0.000 | 0.219 | 0.422 | 0.818 |
| 83 | 0.000 | 0.055 | 0.674 | 0.718 |
| 84 | 0.000 | 0.000 | 0.000 | 0.000 |
| 85 | 0.000 | 0.000 | 0.050 | 0.110 |
| 86 | 0.000 | 0.339 | 0.520 | 0.581 |
| 87 | 0.000 | 0.290 | 1.116 | 2.045 |
| 88 | 0.000 | 0.000 | 0.000 | 0.000 |
| 89 | 0.000 | 0.000 | 0.000 | 0.000 |
| 90 | 0.000 | 0.000 | 0.181 | 0.216 |
| 91 | 0.000 | 0.129 | 0.682 | 0.735 |
| 92 | 0.000 | 0.000 | 0.000 | 0.000 |
| 93 | 0.000 | 0.342 | 1.534 | 2.843 |
| 94 | 0.000 | 0.321 | 1.508 | 3.194 |
| 95 | 0.000 | 0.000 | 0.090 | 0.165 |
| 96 | 0.000 | 0.420 | 1.478 | 1.989 |
| 97 | 0.000 | 0.000 | 0.185 | 0.213 |
| 98 | 0.000 | 0.000 | 0.000 | 0.000 |
| 99 | 0.000 | 0.037 | 0.477 | 0.888 |
| 100 | 0.000 | 0.396 | 2.573 | 3.848 |

# DISTRIBUTION

2 California Polytechnic State University
Natural Resources Management & Environmental Sciences (180-209)
Attn: Bwalya Malama
San Luis Obispo, CA 93407

2 GRAM, Inc.
Attn: Krishan Wahi
8500 Menaul Boulevard NE
Suite B-335
Albuquerque, NM 87112

2 Stoller Newport News Nuclear, Inc.
Attn: Donald L. George
400-2 Cascades Ave., Suite 202
Carlsbad, NM 88220

3 Waste Isolation Pilot Plant
U.S. Department of Energy
Attn: Roger A. Nelson
Abraham E. Van Luik
Russell L. Patterson
4021 National Parks Highway
Carlsbad, NM 88220

1 Golder Associates, Inc.
Attn: Bill Thompson
44 Union Boulevard
Suite 300
Lakewood, CO 80228

1 Michael B. Gross
415 Riviera Drive
San Rafael, CA 94901

2 WIPP Technical Library GSA-214
P.O. Box 2078
Carlsbad, NM 88221

| | | | |
|---|---|---|---|
| 1 | MS0706 | David K. Rudeen | 6931 |
| 1 | MS0721 | Peter B. Davies | 6900 |
| 1 | MS0776 | Amy P. Gilkey | 6931 |
| 1 | MS1395 | R. Chris Camphouse | 6931 |
| 1 | MS1395 | Courtney G. Herrick | 6931 |
| 2 | MS1395 | Dwayne C. Kicker | 6931 |

## DISTRIBUTION (Continued)

| | | | |
|---|---|---|---|
| 1 | MS1395 | Paul E. Shoemaker | 6930 |
| 1 | MS1395 | Todd R. Zeitler | 6931 |
| 2 | MS1395 | WIPP Library | 6930 |
| | | | |
| 1 | MS0899 | Technical Library | 9536 (electronic copy) |


Sandia National Laboratories